DOCTOR OF PHILOSOPHY

The hypothalamic role of BACE1 in energy homeostasis

Jalicy, Susan M.

Award date:
2016

The hypothalamic role of BACE1 in energy homeostasis

Susan M. Jalicy

Thesis submitted for the degree of Doctor of Philosophy

January 2016

Table of contents

List of figures

List of tables

Acknowledgements

Firstly, I would like to thank my supervisor, Professor Mike Ashford, for allowing me to carry out my PhD in his lab and, more importantly, for all his guidance and support throughout the project.

I have worked with some great people during my PhD, who have all helped me in some way and for that I am very grateful. Thanks are directed at those in the CVDM division and in particular, all past and present members of the Ashford Lab for helping me throughout my project. I have been very lucky to receive valuable post doc guidance during my PhD and want to thank Paul, Lee, K-Dog, Gemma and Alison in particular for that. Lee - for always motivating me and getting me pumped about science even from afar, and Paul - for teaching me most of what I learned during my project. A huge thanks goes to Alison for being a constant source of advice, a shoulder to cry on, helping me spread my wings in the unit and for not only being a great post doc but becoming a dear friend. A 'BLF' to be more precise.

I am thankful to Alison Milne for training me on the confocal, and being a source of advice and support throughout my long confocalling days! Also, thanks to John and all the staff in the MSRU for their help throughout my project.

Greatest thanks must go to my PhD family; the fellow CVDM students. I want to thank you all for providing excellent chat (mostly regarding lunches), bringing fun to the lab and for raising spirits on the bad days. In particular I want to thank my final year lab buddies; firstly, Daniella for all our non-scientific chat which made the days far more enjoyable as well as huge thanks for the fun, but hugely helpful, revision sessions. Secondly, to my sisters (sorry David!) Claire and David, who made my final year the best it could have been, full of hilarious memories. Also, thanks to Arun for travelling with me during the write up period (I'll never forget our time across the continents!) and Moneeza, Abi and Polly, for providing me with great food, conversation and laughs. Special thanks must go to Lauren and Lyndsey for being such great friends to me, especially during my final year. Thank you for keeping me going throughout the write up period (especially all the proofreading and formatting!), for always providing advice and of course the pay day dinners! Finally, I want to thank Nandos club; Lizzie, John, Geoff and Fiona. I couldn't have asked for better friends than you guys and truly can't thank you enough, you have provided me with constant support throughout my PhD and I can say with certainty I couldn't have done it without you guys!

I want to thank all my friends for putting up with me during the last four years, in particular, Peyt and the Glasgow Core; Lesley, Lindsay and Katie. A huge thanks must go to you guys for all the laughs and endless fun at the motel - forever my happy place. A special thank you must also go to Catherine, for being a great support to me and for relentlessly correcting my grammar over the years so I was able to write a coherent thesis. You are a wonderful friend.

I want to say a huge thank you to my Dundee badminton family for filling the last four years with such happy memories. You guys have truly made my time in Dundee the most fun it could have been. Especially, thank you to Gill, Anna, Nicola and Lisa for putting up with me during my final year, listening to me moan and constantly being great, supportive friends. Come on DABA woo!

Last, but certainly not least, I want to thank my brilliant family. Sara, Steve and especially Sam - thank you for pretending to understand what I do and for keeping me going with your endless mocking! Most importantly, I want to thank Mum and Dad for always being there, listening and advising. Thanks to Dad for reminding me every day that I'm a scientist (you can stop now!) and to you both for supporting me, especially during the final stages of my PhD. I appreciate everything you do.

Declarations

Student declaration

I hereby declare that all results described in this thesis, unless otherwise stated, are entirely my own work. I further state that the composition of this thesis was performed by myself and none of the material has been submitted for any other degree. Lastly, I verify that all sources have been appropriately cited. The work was carried out in the Medical Research Institute, University of Dundee, under the supervision of Professor M. L. J. Ashford.

Susan M. Jalicy

Supervisor declaration

I certify that Susan M. Jalicy has completed 8 terms of experimental research and has fulfilled the conditions of Ordinance 39, University of Dundee, such that she is eligible to submit the following thesis in application for the degree of Doctor of Philosophy.

Professor M. L. J. Ashford

Abbreviations

ACTH	Adrenocorticotrophin hormone
AD	Alzheimer's disease
ADAM	A-disintegrin and metalloproteinase
ADAM10i	ADAM10 inhibitor
AgRP	Agouti-related peptide
AICD	Cytoplasmic amyloid precursor protein intracellular domain
ANOVA	Analysis of variance
Aph-1	Anterior pharynx-defective 1
APP	Amyloid precursor protein
ARC	Arcuate nucleus
Arg-1	Arginase 1
Aβ	Amyloid β protein
BACE1	The β-site amyloid precursor protein-cleaving enzyme 1 (aka the β-secretase)
BAT	Brown adipose tissue
BBB	Blood brain barrier
BDNF	Brain-derived neurotrophic factor
BMI	Body mass index
BSA	Bovine serum albumin
CART	Cocaine and amphetamine regulated transcript
CCK	Cholecystokinin
CCL2	Chemokine (C-C motif) ligand 2 (MCP1)
CCL3	Chemokine (C-C motif) ligand 3 (aka MIP-1α)
CCL4	Chemokine (C-C motif) ligand 4 (aka MIP-1β)
CCL5	Chemokine (C-C motif) ligand 5 (aka RANTES)
cDNA	Complimentary deoxyribonucleic acid
CNS	Central nervous system
CRH	Corticotropin-releasing hormone
CRR	Counter-regulatory response
CSF	Cerebrospinal fluid
DAPI	4',6-diamidino-2-phenylindole

DIG	Digoxigenin
DIO	Diet-induced obese
DIO2	Type II iodothyronine deiodinase
DMH	Dorsomedial hypothalamus
DMSO	Dimethyl sulphoxide
DNA	Deoxyribonucleic acid
DS	Down's syndrome
DVM	Dorsal vagal motor nucleus
EDTA	Ethylene diamine tetraacetic acid
EGTA	Ethylene glycol tetraacetic acid
Emr1	EGF-like module-containing mucin-like hormone receptor-like 1 (aka F4/80)
ER	Endoplasmic reticulum
ERK	Extracellular signal-related kinase
EtoH	Ethanol
FAD	Familial Alzheimer's disease
FISH	Fluorescent *in-situ* hybridization
FOXO	Forkhead box O
GABA	γ-aminobutyric acid
GAD	Glutamic acid decarboxylase
GFAP	Glial fibrillary acidic protein
GFP	Green fluorescent protein
GGA	Golgi-localised γ-adaptin ear containing ARF-binding
GLP-1	Glucagon-like peptide 1
GTT	Glucose tolerance test
H_2O_2	Hydrogen peroxide
HFD	High fat diet
HIF	Hypoxia-inducible factor
HRP	Horseradish Peroxidase
JAK	Janus associated kinase
ICV	Intracerebroventricular
IDE	Insulin degrading enzyme
IF	Immunofluorescence

IFN-γ	Interferon-γ
IGF1	Insulin/Insulin-like growth factor 1
IHC	Immunohistochemistry
IL1β	Interleukin 1 β
IL-1R2	Interleukin 1 receptor type II
IL-6	Interleukin 6
IL-10	Interleukin 10
i.p	Intraperitoneal
IRS	Insulin receptor substrate
ITT	Insulin tolerance test
IVT	In vitro transcription
KO	Knock-out
LacZ	β-galactosidase reporter gene
LH	Lateral hypothalamus
LRa/c/d	Short leptin receptor isoforms
LRe	Secreted leptin receptor isoform
MAPK	Mitogen-activated protein kinases
MCH	Melanin-concentrating hormone
MCP1	Monocyte chemotactic protein-1 (aka CCL2)
MCR	Melanocortin receptor
ME	Median eminence
Min	Minute(s)
MIP-1α	Macrophage inflammatory protein-1α (aka CCL3)
MSH	Melanocyte stimulating hormone
MW	Molecular weight
NaPPi	Sodium pyrophosphate
NC	Normal chow
NeuN	Neuronal nuclear antigen
NFT	Neurofibrillary tangle
NFκB	Nuclear factor κ-light-chain-enhancer of activated B cells
NLRP3	NOD-like receptor family, pyrin domain containing 3
NOS2	Nitric oxide synthase 2
NPY	Neuropeptide Y

NPYR	Neuropeptide Y receptor
NTS	Nucleus tractus solitarius
ObRb	Long leptin receptor isoform (aka LRb)
OXR	Orexin receptor
PAGE	Polyacrylamide gel electrophoresis
PBS	Phosphate buffered saline
PBST	Phosphate buffered saline Triton^{TM}-X
PCR	Polymerase chain reaction
PFA	Paraformaldehyde
PGC1α	Peroxisome proliferator-activated receptor-γ, coactivator 1-α
PHF	Paired helical filament
PI3K	Phosphoinositide 3-kinase
PIP2	Phosphatidylinositol (4,5) bisphosphate
PIP3	Phosphatidylinositol (3,4,5) triphosphate
PKB	Protein kinase B
PMSF	Phenylmethylsulphonyl fluoride
POMC	Proopiomelanocortin
Prdm16	The zinc finger transcription factor
PS1/2	Presenilin 1/2
PSGL-1	P-selectin glycoprotein ligand-1
PTP1B	Protein-tyrosine phosphatase 1B
PVN	Paraventricular nucleus
PYY	Peptide YY
RANTES	Regulated on activation, normal T cell expressed and secreted (aka CCL5)
RIP	Rat insulin II promoter
RT	Real-Time
RNA	Ribonucleic acid
SCN	Suprachiasmatic nucleus
SDS	Sodium dodecyl sulphate
Sec	Second(s)
SF-1	Steroidogenic factor 1
SH2	Src homology 2
SIRT1	Sirtuin 1

SOCS3	Suppressor of cytokine signalling 3
ST6Gal-1	TGN-resident β-galactosidase α2,6-sialytransferase
STAT3	Signal transducer and activator of transcription 3
TACE	Tumour necrosis factor-α convertase
TAE	Tris-acetate-EDTA
TBS	Tris-buffered-saline
TBST	Tris-buffered-saline-Tween®-20
TCPTP	T cell protein-tyrosine phosphatase
TEMED	Tetramethylenediamine
Tg	Transgenic
TGF-β1	Transforming growth factor-β1
TH	Tyrosine hydroxylase
TNF	Tumour necrosis factor
TRH	Thyrotropin-releasing factor
Tris	Tris(hydroxymethyl)aminomethane
T2DM	Type 2 diabetes mellitus
UCP	Uncoupling protein
VGlut	Vesicular glutamate transporter
VMH	Ventromedial hypothalamus
WAT	White adipose tissue
WT	Wild-type

Summary

Obesity is a global problem, with significant rises in obesity levels observed in recent years. This is owing to our modern lifestyles, associated with diminished physical activity and increased calorific intake. The increase in obesity is closely linked with type 2 diabetes mellitus (T2DM), leptin and insulin resistance, impaired glucose homeostasis and often inflammation and endoplasmic reticulum stress. Worryingly, obesity and T2DM are also risk factors for Alzheimer's disease (AD).

The β-site amyloid precursor protein-cleaving enzyme 1 (BACE1) is critically involved in AD development, cleaving the amyloid precursor protein (APP) to generate amyloid-β (Aβ), which drives progression of the hallmark pathologies of AD. Consequently, higher BACE1 levels/activity is considered a primary causative factor for AD. Increased BACE1 is driven by chronic stress (e.g. hypoxia, oxidative and metabolic) also associated with obesity and T2DM. Thus, impaired glucose homeostasis and insulin resistance is common to all three disease states, suggesting that BACE1 and Aβ may contribute to the progression of metabolic disease. Consequently, BACE1 knock-out mice have been demonstrated to be protected against diet-induced obesity (DIO) and have improved insulin and leptin sensitivity.

Here we show that pharmacological inhibition of BACE1 improves metabolic syndrome in mice, and that elevations in BACE1, through altered APP processing, may exacerbate obesity and the metabolic syndrome. Furthermore, we show that BACE1 is present in hypothalamic nuclei and neuronal populations that control energy balance. Taken together, these data suggest BACE1 activity alters energy metabolism through actions on the neuronal circuitry regulating energy balance, and chronically raised BACE1 levels/activity may result in dysregulation of these circuits and consequent metabolic disorder. Accordingly, a better understanding of the role of APP processing and BACE1 activity under physiological and pathophysiological conditions may provide evidence for repurposing BACE1 inhibitors, currently in clinical trials for AD, towards treatment of obesity and T2DM.

Chapter 1

Introduction

1.1 Obesity

Obesity is a metabolic disease defined by an imbalance between energy intake to the body and energy expenditure of the body, whereby intake becomes greater than expenditure. This results in excessive levels of fat. The standard measure of obesity in the population is the body mass index (BMI), which is defined by an individual's weight in kilograms divided by the square of their height in metres (kg/m^2). A BMI of 25 or greater classifies an individual as overweight and a BMI of 30 or greater is classified as obese. In 2008 it was recorded that over 1.4 billion adults worldwide were overweight and over 0.5 billion obese, with the incidence having doubled since the 1980's (www.who.int). This rise in obesity is likely attributed to the more 'modern' lifestyle many now live, which is one of a more sedentary nature involving less physical activity and a higher calorific diet. Worryingly obesity carries major health implications, increasing the risk for a number of co-morbidities including diabetes, cardiovascular disease and Alzheimer's disease.

1.2 The hypothalamus

The central control centre for whole body energy homeostasis is the hypothalamus, in particular the basomedial hypothalamus. The presence of distinct neuronal populations within this region, particularly first order neurons in the arcuate nucleus (ARC), form a network which control energy regulation via their inputs and connectivity to other higher brain regions. The first evidence indicating a key role of the hypothalamus in regulating energy homeostasis came from lesion studies in rodents (King 2006). These studies crudely demonstrated that damage to the ventromedial hypothalamus (VMH) resulted in obesity, whilst lesions to the lateral hypothalamus (LH) resulted in a lean phenotype. This led to the 'dual-centre' model, which became the accepted model regarding hypothalamic control over energy balance (Stellar 1994). This model terms the VMH as a satiety centre, where lesions not only cause obesity, as mentioned, but also hyperphagia, and the LH is classically referred to as a feeding centre. The 'dual-centre' model demonstrated a clear role for these hypothalamic regions in the control of body weight and feeding behaviour, however subsequent research argued the validity of this model. Studies by Gold and colleagues failed to replicate the obese phenotype observed with VMH destruction and found only when areas which extended out with the VMH, such as the paraventricular nucleus (PVN), were damaged did obesity occur (Gold 1973). Subsequently, many groups have since established that VMH damage does result in body weight gain and there has been failure to replicate Gold's work, supporting the original model whereby

VMH is crucial for feeding behaviour (King 2006). Nonetheless, as Gold and colleagues alluded to other hypothalamic areas may also be important. In keeping with this, studies using monosodium glutamate as a toxin found selective destruction of the arcuate nucleus (ARC) also evoked an obese phenotype (Olney 1969). Taken together it seems, although the VMH and LH are key centres involved in regulating energy homeostasis, that the 'dual-centre' model is rather simplified and the hypothalamic network controlling body weight and food intake is extended further than these nuclei. Furthermore, the pathways innervating these nuclei may be more important than the specific nuclei themselves in regulating these behaviours (King 2006).

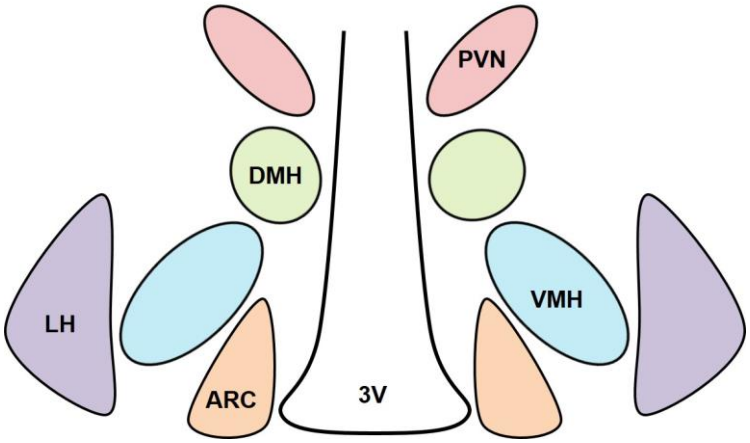

Figure 1.1 Schematic diagram of the basic anatomy of the hypothalamus.

The basomedial hypothalamus contains distinct nuclei contributing to the control centre for energy homeostasis. ARC, arcuate nucleus. LH, lateral hypothalamus. VMH, ventromedial hypothalamus. DMH, dorsomedial hypothalamus. PVN, paraventricular nucleus.

The major hypothalamic regions which have subsequently been defined to contribute to the control of whole body energy homeostasis along with the VMH and LH, are the ARC, dorsomedial hypothalamus (DMH) and PVN (Figure 1.1). These regions contain distinct populations of neurons forming the neuronal circuitry which controls energy balance, allowing the hypothalamus to act as the central metabolic control centre. The ARC, like the LH, is also described as a 'feeding centre' (Funahashi et al. 2000). Importantly, the positioning of the ARC is key for its role within the hypothalamus, as it is ideally located just above the median eminence (ME) which is situated at the base of the hypothalamus. The ME allows for the integration of peripheral signals and hormones released from the

circulation (Elmquist et al. 1999), therefore the ARC neurons are the first point of contact for responding to these signals. Thus, as previously mentioned, the neuronal populations within the ARC are defined as 'first order' neurons. The first order neurons innervate other hypothalamic sites which are populated by second order neurons to relay the circulating signals. As briefly mentioned, the VMH is referred to as a 'satiety' centre and contains a dense population of glucose sensing neurons (Routh 2010), thus plays an important role in glucose homeostasis and the response to hypoglycaemia. The LH contains second order neurons that receive information from the ARC first order neurons, modifies this information, and relays these signals via anabolic pathways to the hindbrain, particularly the nucleus tractus solitarius (NTS) (Schwartz et al. 2000). The LH has also been described to contain glucose sensing neurons (Arora & Anubhuti 2006) which, along with other second order neuronal populations, contribute to its role as a 'feeding centre'. The second order neurons in the LH also project back to the ARC as well as processing and receiving information from other hypothalamic nuclei such as the DMH. The DMH is situated dorsal to the VMH and plays an important role in regulating feeding and body weight, as well as circadian rhythms (Chou et al. 2003). The DMH also connects the other hypothalamic nuclei, by receiving information to and from nuclei, particularly the PVN (Elmquist et al. 1998). Lastly the PVN, situated in the anterior hypothalamus, is another crucial point of connectivity within the hypothalamus receiving heavy input from first order ARC neurons. Many pathways both project to and converge here, in particular afferents from first order ARC neurons which innervate second order neurons within the PVN, as well as neurons from the LH (Arora & Anubhuti 2006). Signals from the thyroid and hypo-pituitary axis are also integrated in the PVN (Neary et al. 2004) and neurons, from the parvicellular region of this nuclei in particular, innervate the ME as well as preganglionic neurons in the medulla and spinal cord, thus playing a role in autonomic output (Elmquist et al. 1998; Swanson & Sawchenko 1983). Alike the second order neurons in the LH, second order PVN neurons also relay signals back to the ARC as well as innervating the NTS via catabolic pathways (Schwartz et al. 2000). The current knowledge of these hypothalamic nuclei has demonstrated that the hypothalamus acts as an integrative centre vital for controlling energy regulation and metabolic status, via a network of neuronal circuitry between these distinct nuclei. More recent research has focused on the specific neuronal populations present within these nuclei and the pathways they are part of which form this hypothalamic network, in order to respond to endocrine, neural and metabolic signals to control energy balance (Spiegelman & Flier 2001).

1.3 Arcuate first-order neurons

1.3.1 Anorexigenic neuropeptides

1.3.1.1 Pro-opriomelanocortin

The α-melanocyte stimulating hormone (α-MSH) is a potent anorexigenic neuropeptide derived from the pro-opiomelanocortin (POMC) peptide which is part of the central melanocortin system regulating energy homeostasis. α-MSH is generated from POMC through a series of post-translational modifications by pro-hormone covertases; PC1 and PC2 (Nillni 2007), with any abnormalities in their processing resulting in obesity. The POMC gene is selectively present in the pituitary, the skin, the immune system and the hypothalamus; abundantly expressed in the ARC (Arora & Anubhuti 2006). POMC ARC neurons produce and release α-MSH, which acts as an agonist at the melanocortin receptors; MC3R and MC4R, to elicit anorexigenic effects (Sohn et al. 2013). POMC ARC neurons further project to multiple hypothalamic and extra-hypothalamic sites where there are high levels of MC4R neurons, such as the PVN, LH, NTS and the spinal cord (Figure 1.2). Noteworthy is that α-MSH is not the only product of POMC. POMC processing results in various products via PC1 and PC2 cleavage, including adrenocorticotrophin hormone (ACTH), β-endorphin and other intermediate peptides (Millington 2007). The POMC products have various roles including involvement in skin pigmentation and adrenal steroidogenesis, however other physiological roles particularly of the intermediate products are not fully known (Millington 2007; Pritchard et al. 2002). Further cleavage of ACTH within the hypothalamus releases α-MSH, and, as referred too, this is the predominant POMC product believed to play a functional role in body weight and feeding behaviour, via MC3R and MC4R (Pritchard et al. 2002). Thus, MC3R and MC4R are vital for allowing the anorexigenic effects of POMC, however three other melanocortin receptor subtypes do exist; MC1R, MC2R and MC5R. MC1R and MC5R are expressed in low levels centrally, in comparison to MC3R and MC4R, and these subtypes along with MC2R are responsible for the skin pigmentation and adrenal functions of POMC (Pritchard et al. 2002). MC1R is the predominant receptor for α-MSH and responsible for controlling skin colour, and MC2R is the main receptor for ACTH and responsible for adrenal functions (Millington 2007).

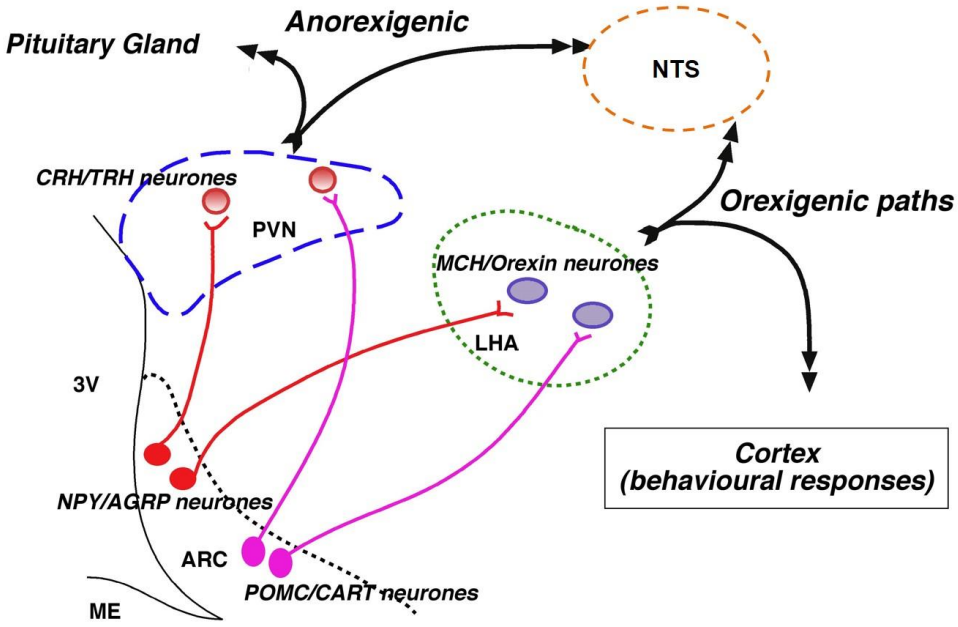

Figure 1.2 Basic schematic diagram of the main neuronal pathways controlling energy homeostasis.

First order neurons (POMC/CART and NPY/AgRP neurons) project to second order neurons in the LH and the PVN. MCH and orexin neurons in the LH send orexigenic signals to the NTS and cortical regions to control behavioural functions. CRH/TRH neurons in the PVN send anorexigenic signals to the pituitary and the NTS. These pathways form the main neuronal pathways controlling energy balance. 3V, third ventricle.
Figure adapted from Ashford Lab teaching material.

Central α-MSH acts to reduce food intake (Rossi et al. 1998) and this is reflected by mRNA changes in POMC expression during fasted or fed conditions. Following fasting in lean mice POMC mRNA expression is markedly reduced, an effect which is exacerbated further in genetically obese mice models (Mizuno et al. 1998). However, the fasting-induced reduction in POMC expression is restored following a period of re-feeding in mice (Swart et al. 2002). Furthermore, when there is an absence of POMC entirely, for example in POMC-deficient mice, an obese and hyperphagic phenotype is observed (Yaswen et al. 1999). Obesity is also observed in humans with a POMC deficiency, which also reportedly results in the appearance of red hair, via a lack of activity at MC1R, and adrenal insufficiency most likely due to a lack of activity at MC2R (Krude et al. 1998). Furthermore, MC3R and MC4R null mice, in particular, show a metabolic phenotype, with both mice displaying increased fat mass (Butler et al. 2000; Sutton et al. 2006; Huszar et al. 1997). MC4R null mice are also hyperphagic,

hyperglycaemic and display hyperinsulinemia (Sutton et al. 2006; Huszar et al. 1997). Interestingly, MC4R mutations are found in humans and represent the most common cause of monogenic obesity, with homozygote mutations resulting in severe early-onset obesity and hyperphagia (Farooqi et al. 2000). This genetic defect clearly demonstrates the role of the MC4R in regulating POMC neurons anorexigenic effects, and that this role cannot be compensated for by other forms of the receptor. The POMC gene itself is predominantly limited to the ARC and the pituitary, with some expression in the NTS and retrochiasmatic area, which is situated at the base of the hypothalamus in front of the ARC and VMH. However, the ARC neurons project to many other central areas, such as the PVN, which send further projections via autonomic pre-ganglionic neurons to the medulla and spinal cord (Elmquist et al. 1999). These projections to other central regions carry out differential roles in the regulation of energy homeostasis, with the MC4R neurons expressed in the PVN acting to reduce food intake and conversely those expressed in autonomic pre-ganglionic neurons function to increase energy expenditure and control glucose homeostasis (Balthasar et al. 2005; Rossi et al. 2011). POMC neurons within the ARC form part of a neural circuitry, in which they receive input from neurons containing orexigenic neuropeptides, as well as receiving both inhibitory and excitatory inputs. The regulation of this circuitry allows for the control of feeding, energy expenditure and glucose homeostasis.

1.3.1.2 Cocaine and Amphetamine Regulated Transcript

The cocaine and amphetamine regulated transcript (CART) was identified in rodents following treatment with cocaine and amphetamine (Douglass et al. 1995). This led to the finding of another anorexigenic neuropeptide. The CART gene is highly conserved in both rodents and humans, and, like POMC, is strongly associated with feeding (Elmquist et al. 1999; Arora & Anubhuti 2006). CART expression is found throughout the hypothalamus, in the PVN, DMH, the perfornica areas of the hypothalamus, the LH and the ARC. Studies performed in rats revealed that central injections of CART result in reduced food intake, demonstrating its ability to elicit anorexigenic effects (Stanley et al. 2001). Conversely, in obese rodent models CART transcript expression is reduced, which is also observed during periods of fasting, demonstrating a role for CART in regulating energy balance. Although CART is expressed throughout hypothalamic sites, within the ARC all CART neurons co-express POMC (Elmquist et al. 1999), producing a strong anorexigenic neuronal output.

1.3.2 Orexigenic neuropeptides

1.3.2.1 Neuropeptide Y

Neuropeptide Y (NPY) is a potent orexigenic neuropeptide 36 amino acids in length (Williams et al. 2000). NPY is found abundantly in the hypothalamus, particularly within first order ARC neurons which project to the DMH, LH and PVN to regulate feeding (Figure 1.2) (Sawchenko 1998). Functionally, NPY is known to stimulate feeding and acts to restore energy balance when necessary. In a state of starvation expression of NPY mRNA is upregulated (Hahn et al. 1998; Swart et al. 2002), and this is partially restored during re-feeding in mice (Swart et al. 2002). The strong orexigenic effects of NPY are observed following central administration of the neuropeptide in rats which stimulates feeding (Billington et al. 1991), and furthermore chronic administration results in obesity. Subsequent studies have revealed that injection of NPY directly into the PVN, where the most abundant NPY fibres are present, results in increased food intake, fat mass and reduced energy expenditure (Billington et al. 1994). These data suggest that the PVN is particularly important in the downstream mediation of NPYs effects, not only on feeding but also on regulating energy expenditure via brown adipose tissue (BAT) thermogenesis (Billington et al. 1994). This proposed role for NPY in regulating thermogenesis is also observed when NPY is overexpressed in the ARC and these changes are shown to be mediated via sympathetic activity (Shi et al. 2013). Additionally, ARC NPY neurons innervating the PVN project to areas of the hindbrain, which control the autonomic nervous system, such as the NTS (Figure 1.2) and are involved in controlling sympathetic output (Arora & Anubhuti 2006).

NPY has five G-protein coupled receptors; NPY1-5R, with NPY1R and NPY5R believed to mediate NPYs feeding affects (Yulyaningsih et al. 2011; Arora & Anubhuti 2006). NPY5R, in particular, is found in abundance in the LH and PVN. Interestingly, deletion of NPY in mice does not result in any changes to body weight or feeding phenotypes (Erickson et al. 1996). Yet NPY1R and NPY5R deficient animals display increased body weight (Kushi et al. 1998; Sohn et al. 2013). Notably, these mouse models display different phenotypes in regards to feeding, with NPY1R null mice showing reduced food intake whereas NPY5R null mice show increased food intake. In contrast, NPY4R null mice show a completely altered phenotype of reduced body weight and fat mass (Sainsbury et al. 2002). These studies clearly demonstrate differential roles for the NPY receptors and thus their regulation of NPY action may work via different networks, with

NPY5R mediating feeding behaviour and NPY1R regulating energy expenditure (Shi et al. 2013). Additionally, these studies also suggest that NPY receptors are not solely responsible for NPYs orexigenic actions and separate contributors, such as gamma-aminobutryic acid (GABA), may play a role.

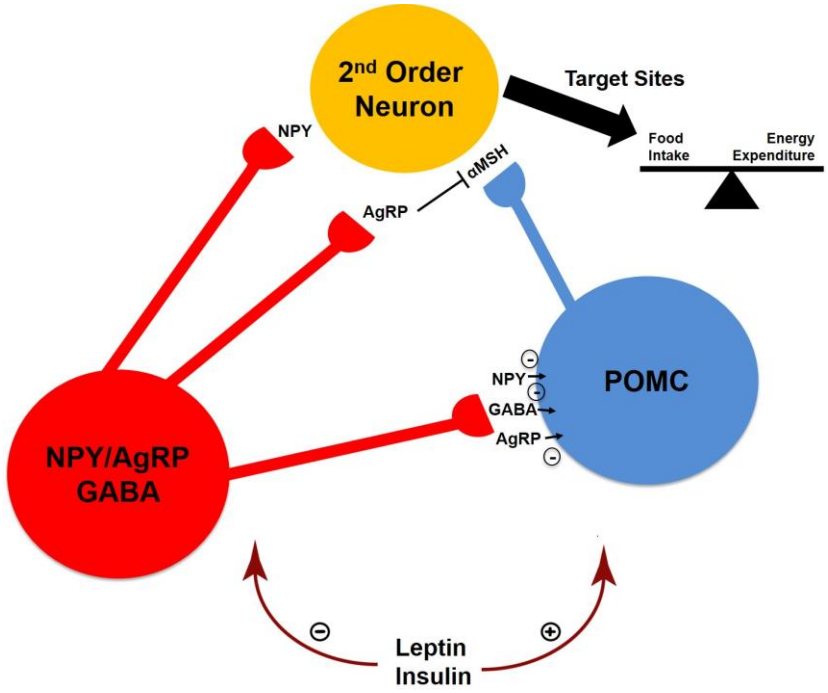

Figure 1.3 Schematic diagram of the basic neuronal model of the ARC circuitry controlling energy homeostasis.

Adiposity signals insulin and leptin act on first order ARC neurons to inhibit NPY/AgRP neurons and activate POMC neurons. POMC neurons release α-MSH which acts on second order neurons and AgRP inhibits this action. GABAergic NPY/AgRP neurons can also innervate POMC neurons through synaptic GABA, NPY and AgRP release, directly inhibiting POMC neurons. First order ARC neurons project to second order neurons to influence food intake and energy expenditure, maintaining energy balance.
Figure adapted from Ashford Lab teaching material.

GABA is the main inhibitory neurotransmitter utilised by the CNS (Delgado 2013) and is released by NPY neurons in the ARC which has been shown to mediate, in part, the orexigenic actions of NPY (Figure 1.3). In contrast only a proportion of POMC/CART-expressing neurons release GABA as their main neurotransmitter, with some utilising the excitatory neurotransmitter glutamate (Wittmann et al. 2013), supporting the role of GABA in mediating orexigenic effects. The contribution of GABA neurotransmission on feeding behaviour in regards to NPY-expressing neurons occurs independently of the

NPY receptors (Atasoy et al. 2012). NPY therefore acts to stimulate feeding via NPY1R and NPY5R in conjunction with other orexigenic mediators such as GABA, whilst inhibiting anorexigenic neuropeptides. Both the synthesis and secretion of NPY are increased when energy stores are low, suggesting a physiological role for these neurons in the regulation of energy homeostasis by restoring energy balance during periods of energy deficiency (Arora & Anubhuti 2006).

1.3.2.2 Agouti-related Peptide

The identification of another neuropeptide affecting food intake and body weight arose from work on the *lethal yellow* A^y/a mouse. The A^y/a mouse is an obese mouse model, which also exhibits a yellow coat colour, increased linear growth, insulin resistance and hyperglycaemia (Flier & Maratos-Flier 1998). The phenotype of the A^y/a mouse arises due to disruption in the expression of the agouti gene which is normally localised to the skin in mice and alters hair pigmentation via α-MSH by acting as antagonist at MC1R. The agouti gene is also found in the human genome with high homology to mouse agouti, however interestingly in humans it is also expressed in adipose tissue (Kwon et al. 1994). In the A^y/a mouse agouti expression is unregulated and expressed throughout the body, which led to the finding that in the brain agouti also acts as an antagonist at MC4R (Flier & Maratos-Flier 1998). Subsequently, this led to the discovery of an alternative neuropeptide responsible for this antagonism at MC4R; the agouti-related peptide (AgRP).

AgRP is a 132 amino acid peptide which has since been shown to mediate strong orexigenic actions. As mentioned, AgRP is a potent antagonist of α-MSH via MC4R and also MC3R (Lu et al. 1994) and therefore elicits orexigenic effects through inhibition of the melanocortin system. AgRP specifically antagonises MC3R and MC4R only, and unlike agouti itself, does not inhibit the melanocortin system through MC1R (Flier & Maratos-Flier 1998). AgRP acts to stimulate food intake, acting in a similar manner to NPY, whereby central administration of AgRP in rats causes increased food intake (Rossi et al. 1998) and following prolonged administration in mice a hyperphagic phenotype is observed with a concomitant increase in body weight, resulting in obesity (Small et al. 2001). Interestingly, when AgRP is knocked-out in mice, like NPY, there is no body weight or feeding behaviour phenotype (Qian et al. 2002). Furthermore, Qian and colleagues demonstrated this was also the case in NPY/AgRP double knock-out mice (Qian et al. 2002). This alludes to the potential for different circuits to also be involved

in feeding behaviour that could compensate for the normal pathways mediating energy balance when necessary for survival.

Under normal circumstances AgRP acts along with NPY to induce orexigenic effects. Within the ARC, AgRP is co-expressed in neurons with NPY (Broberger et al. 1998) and these neurons utilise GABA as their main neurotransmitter to elicit inhibitory effects. NPY/AgRP ARC neurons respond to both peripheral signals, such as leptin, insulin and ghrelin, and central signals, sending this information to other hypothalamic and extra-hypothalamic centres, including the PVN and hindbrain (Figure 1.2, Figure 1.3).

1.3.3 Additional first-order arcuate neurons

As discussed the predominant neuronal populations in the ARC are POMC/CART-expressing neurons and NPY/AgRP-expressing neurons. However, there are neurons within the ARC that are distinct from these neuronal populations, yet owing to their location are thought to play a role in the regulation of whole body energy homeostasis. One population are RIPCre neurons which are defined by having cre expression driven by the rat insulin II promoter. This specific population was discovered when utilising this cre expression to study the pancreatic β-cell, where it was noted that there was expression present in areas of the brain. Cre expression was found to be largely restricted to the hypothalamus, where it is concentrated in the ARC and also the suprachiasmatic nucleus (SCN), VMH and DMH, as well as distributed in regions of the cortex and striatum (Song et al. 2010). It has subsequently been found that these neurons lie in very close apposition to POMC/CART-expressing neurons and NPY/AgRP-expressing neurons in the ARC, however are completely distinct (Choudhury et al. 2005). Due to this close proximity it is believed that RIPCre neurons may be targets for POMC neurons and communication between the two populations may occur. This proposal is supported by the finding that RIPCre neurons become depolarised in response to melanotan-II (MTII); an agonist of the melanocortin receptor (Choudhury et al. 2005). Furthermore, when the leptin receptor is knocked-out of these neurons an obese phenotype similar to that observed in POMC-leptin receptor deficient mice is observed, accompanied with impaired glucose homeostasis (Covey et al. 2006). This is suggestive of a role in glucose homeostasis as well as an involvement in the regulation of the body weight actions of leptin. Still, the precise function of RIPCre neurons and what they release is unknown, although it is believed that they have important functions regarding the regulation of whole body energy balance, and further research is required to determine this.

Although RIPCre may be key in the regulation of energy balance, along with POMC and NPY/AgRP neurons, noteworthy is the presence of additional ARC neuronal populations. In brief, other ARC populations exist including neurotensin-releasing neurons and galanin-releasing neurons, both of which are implicated in regulating feeding behaviours. Neurotensin is produced and released in the ARC, however is also present in the PVN and DMH, where it is believed to interact with leptin to stimulate anorectic effects (Sobrino Crespo et al. 2014). Galanin is found in the ARC and thought to be involved in feeding regulation, however within the hypothalamus it is predominantly found in the PVN, as well as existing peripherally in the gut (Sobrino Crespo et al. 2014; Arora & Anubhuti 2006). Centrally, galanin is co-expressed with GABA, noradrenaline and serotonin (5-HT), and may be involved in many other autonomic functions as the majority of galanin terminals are situated in the NTS (Sobrino Crespo et al. 2014). 5-HT is also important in the regulation of feeding behaviour in relation to first order ARC neurons although it actually originates from the dorsal raphe nucleus in the midbrain (Sobrino Crespo et al. 2014). 5-HT neurons project heavily to areas of the hypothalamus, including the DMH and VMH, however importantly 5-HT receptors are expressed on POMC and NPY/AgRP ARC neurons, thus these first order ARC neurons also sense 5-HT signals and regulate responses (Sohn et al. 2013). The outputs of these neurons have many functions including sleep, temperature regulation and importantly feeding behaviour where 5-HT acts as a satiety signal and reduces food intake as well as regulating glucose homeostasis (Sohn et al. 2013). Furthermore, 5-HT along with dopamine present themselves as additional neurotransmitters utilised by first order ARC neurons in the regulation of energy balance (Flier & Maratos-Flier 1998).

1.4 Extra-arcuate neurons

1.4.1 Steroidogenic Factor-1 neurons

The VMH is a key hypothalamic site involved in regulating body weight and food intake, as well as a role in glucose homeostasis. The VMH contains many populations of neurons, although steroidogenic factor-1-expressing (SF-1) neurons are considered the most abundant. SF-1 is an orphan member of a nuclear hormone family and regulates a number of endocrine functions, specifically the hypothalamic-pituitary-gonadal axis and adrenal function (Parker & Schimmer 1997). SF-1 neurons are a representative population in the VMH, as they are exclusively expressed in this nucleus and although they do not make up the entire nucleus they form a dense population within it. SF-1 neurons have been

implicated in the control of food intake and whole body energy homeostasis, with SF-1 deficient mice characterised with hyperphagia and develop obesity in adulthood (Majdic et al. 2002). SF-1 deficient mice also display abnormalities of the VMH itself, however the ARC and DMH remain intact (Majdic et al. 2002). This phenotype demonstrates the importance of SF-1 in the development of the VMH and the regulation of metabolism. SF-1 neurons have also been shown to be responsive to leptin, which may mediate its role in body weight control. Dhillon and colleagues demonstrated SF-1 neurons depolarised following treatment with leptin, a response similar to that observed with POMC neurons (Dhillon et al. 2006). Subsequent studies within the same laboratory demonstrated SF-1 neurons lacking the leptin receptor have increased body weight, particularly adiposity, again matching the POMC neuronal response (Dhillon et al. 2006). Additionally, SF-1 neurons may also mediate a large component of the regulation of glucose homeostasis the VMH controls. Tong *et al* demonstrated that when the vesicular glutamate transporter; VGLUT2, is knocked out of SF-1 neurons, not only is body weight increased, impairments in glucose homeostasis are observed accompanied with an impaired response to hypoglycaemia (Tong et al. 2007). As a result, these studies implicate SF-1 neurons to play a role, not only in the regulation of body weight and food intake, but also presents them as glucose-sensing neurons playing an important role in the response to hypoglycaemia.

1.4.2 Orexin neurons

Orexin neurons have emerged as a population important in the regulation of energy homeostasis. Orexins were first described as hypocretins and have two isoforms; orexin A and orexin B, with corresponding receptors OX_1R and OX_2R (Sakurai et al. 1998). Orexins are excitatory neuropeptides found in neurons within the LH. Examination of orexin receptor mRNA expression reveal they are distributed throughout the brain, with OX_1R most abundant in the VMH and OX_2R most abundant in the PVN (Trivedi et al. 1998). However, orexin A and B themselves are not expressed within neurons in these areas. Although expression is mainly found in the LH, peripheral mRNA expression is observed in the small intestine of rats and orexin neuronal immunoreactivity is observed in the gut (Kirchgessner & Liu 1999). Expression of both isoforms of orexin are found to be elevated during periods of fasting, furthermore central administration of both isoforms results in increased food intake (Sakurai et al. 1998). This mechanism of control over food intake may act in part through NPY neurons, as NPY neurons innervating the LH (Figure 1.2) have been shown to make close contact with all orexin neurons (Broberger

et al. 1998). This proposal has been further supported by central administration of orexin A causing an increase in food intake, an effect comparable to those observed with NPY treatment (Yamanaka et al. 2000). Additionally, Yamanaka and colleagues found pre-treatment with an NPY antagonist inhibits the orexin-induced increase in food intake and that following treatment with orexin A c-FOS expression in NPY ARC neurons was detected, indicating neuronal activation (Yamanaka et al. 2000). These data suggest that orexin neurons also innervate ARC NPY neurons, forming another connection between the LH and the ARC. Signals from peripheral peptides, such as leptin and ghrelin, are also thought to regulate these neurons, with orexin fibres specifically making synaptic contact with neurons within the VMH and ARC which express the leptin receptor (Funahashi et al. 2000). Outwith their role in energy regulation orexin neurons are also thought to carry out many physiological functions, including a role in sleep and wakefulness with these neurons heavily projecting to the SCN (Arora & Anubhuti 2006).

1.4.3 Melanin-Concentrating Hormone neurons

A separate population of neurons in the LH are those releasing melanin-concentrating hormone (MCH), which are distinct from orexin neurons. MCH is a 19 amino acid peptide which was first established for its role in the regulation of skin colour, however has since been implicated in the regulation of energy homeostasis (Flier & Maratos-Flier 1998). Areas of the LH abundant in MCH expression receive input from the ARC, with NPY/AgRP and α-MSH projecting to these sites (Figure 1.2) (Elias et al. 1998), however MCH has been shown to have opposing actions to α-MSH, with elevated expression observed during fasting. MCH has no interaction with the known melanocortin receptors, thus its actions are via an unidentified receptor, yet it may still be implicated in body weight and food intake control through the melanocortin system, with this pathway linking the ARC and the LH to allow regulation of energy balance. (Qu et al. 1996; Flier & Maratos-Flier 1998). This was demonstrated in rodent studies by Broberger *et al* who showed that NPY neurons project to the LH and almost all MCH neurons were surrounded by and in very close contact to the NPY neurons, suggesting MCH neurons are innervated by NPY (Broberger et al. 1998). In an obese state MCH expression is elevated, as demonstrated in the genetically obese *ob/ob* mouse, and central administration of this peptide in lean rats causes increased food intake and reduced energy expenditure (Qu et al. 1996). Furthermore, MCH deficient mice have reduced body weight, food intake and circulating leptin levels (Shimada et al. 1998). The specific metabolic role of MCH neurons is yet to be fully elucidated, however it has been

implicated in the control of complex behaviours due to these neurons projecting throughout the brain, in particular to cortical regions.

1.4.4 Paraventricular second order neurons

Second order neurons located in the PVN are also important in regulating anorexigenic affects and controlling energy balance. These neurons release corticotropin-releasing factor (CRH) and thyrotropin-releasing factor (TRH) which are involved in the release of hormones from the pituitary and both act as catabolic mediators (Figure 1.2). Neurons releasing these factors have been shown to be involved in regulating food intake and body weight (Sobrino Crespo et al. 2014).

CRH is involved in regulating the hypothalamic-pituitary-adrenal axis. Neurons releasing CRH have been shown to have an important role in the control of food intake with processes found in the ME, hypothalamus and NTS; areas largely implicated in the circuitry controlling food intake. Moreover, central administration of CRH in rats has been shown to reduce food intake and body weight (Sobrino Crespo et al. 2014). This regulation is possibly mediated via the NPY system and CRH may be a direct target of NPY action (Li et al. 2000). Studies by Li and colleagues showed NPY fibres surround CRH neurons, providing synaptic input. It can be assumed these NPY projections are from the ARC, however as NPY neurons are present elsewhere in the brain contact may come from other regions. Additionally, CRH neurons do not express NPY1R receptor (Li et al. 2000), suggesting NPY does not directly act upon these neurons, however NPY may mediate the action of CRH neurons through another receptor isoform. NPY may also indirectly act upon CRH neurons, as ARC NPY neurons innervate GABA interneurons present in the PVN altering GABA release on PVN second order neurons. Thus, NPY and GABA may elicit food intake actions in conjunction with and/or by acting upon CRH neurons.

TRH is involved in the regulation of the hypothalamic-pituitary-thyroid axis, releasing thyroid-stimulating hormone from the pituitary. TRH is also involved in the control of feeding, with treatment in rats causing a reduction in food intake (Choi et al. 2002). This action is also thought to occur via NPY pathways as well as the melanocortin system, as TRH neurons in the PVN lie in close apposition to α-MSH and NPY/AgRP fibres (Fekete et al. 2000). When NPY is administered centrally to rats there is a reduction in pro-TRH mRNA staining in the PVN and a reduction in thyroid hormone release corresponding to a state of hyperthyroidism (Fekete et al. 2001). The reduction in TRH observed during

periods of fasting may be directly due to the increase of NPY in this state. However, the fasting-induced reduction in TRH is attenuated following central administration of α-MSH treatment (Fekete et al. 2000), suggesting TRH neurons may be regulated by α-MSH neurons.

1.5 Peripheral peptides regulating energy homeostasis

1.5.1 Leptin

Since the discovery of the obese gene (*ob*) and its product leptin (Zhang et al. 1994), leptin has been established in having a key role in regulating whole body energy homeostasis. Leptin is secreted from adipocytes and circulating levels are directly correlated with the degree of adiposity, whereby increased adipose tissue mass causes elevations in leptin levels (Maffei et al. 1995). Leptin therefore reflects the energy status of the body and availability of energy stores, predominantly acting to reduce appetite, by signalling via central receptors in the hypothalamus and regulating body weight. Alternatively, during periods of fasting where energy stores are low, there is a reduction in leptin levels (Ahima et al. 1996) which signals to stimulate feeding and reduce energy usage, maintaining body weight. A single point mutation in the *ob* gene, resulting in leptin-deficiency, reported in both rodents and humans, results in obesity; observed in the *ob/ob* mouse model (Zhang et al. 1994). The *ob/ob* mouse does not produce the mature form of leptin as a result of the *ob* mutation and this causes an excessive accumulation of fat, hyperphagia, lowered basal metabolic rate and oxygen consumption, and reduced energy expenditure and body temperature (Bray & York 1979; Bates & Myers 2003). *ob/ob* mice are also infertile and have reduced linear growth (Bates & Myers 2003). The obese phenotype can be completely reversed by recombinant leptin therapy shown, in both rodents (Campfield et al. 1995; Halaas et al. 1995) and humans (Farooqi et al. 1999). Leptin treatment results in reduced food intake and body weight, particularly a reduction in adiposity (Farooqi et al. 1999). This is not only the case in *ob/ob* mice, but in wild-type (WT) lean rodents as shown by induction of chronic hyperleptinemia using recombinant adenovirus delivery, which causes reduced food intake and body fat mass in WT rats (Chen et al. 1996). In all cases the observed reduction in body weight is primarily due to a reduction in adiposity, and arises largely due to the suppression of food intake, although leptin also acts to increase energy expenditure. Additionally, the resulting weight loss is correlated to the amount of leptin administered, with greater weight loss occurring with increasing dosage of leptin (Heymsfield et al. 1999), highlighting leptins weight-reducing

effects. Importantly the same results can be observed when leptin is administered centrally (Campfield et al. 1995), in which injection of leptin into the lateral ventricle also causes a reduction in food intake and body weight. Cumulatively, these studies suggest the weight-reducing effects of leptin are through direct action on the CNS. However, work in humans produces mixed results with studies demonstrating that recombinant leptin treatment in obese individuals who are not leptin deficient does not alter body weight (Mittendorfer et al. 2011; Zelissen et al. 2005). The discrepancy between rodent and human models in regards to the effectiveness of leptin therapy is unknown, however such studies suggest that leptin treatment will not provide a therapeutic intervention for obese humans that lack an *ob* mutation and exhibit high circulating levels of the hormone.

1.5.1.1 Leptin signalling

Following the discovery of leptin, the specific receptor was identified by Tartaglia and colleagues in 1995 utilising cloning techniques. They were classified as members of the interleukin 6 receptor family of class I cytokines with five isoforms existing; ObRa-ObRe (Tartaglia et al. 1995). These isoforms can be separated into three distinct categories; the secreted form, the short forms and the long form of the receptor (Bates & Myers 2003). The secreted form, ObRe, differs to the long and short forms in that it only has extracellular domains which bind to leptin, therefore it has been proposed that this form may play a role in regulating circulating leptin levels (Li et al. 1998; Bates & Myers 2003). The function of the short forms; ObRa, ObRc and ObRd, is not well defined. However, ObRa is the most highly expressed isoform and is particularly abundant in the choroid plexus, suggesting a role in the transportation of leptin across the BBB, from the blood to the CSF (Tartaglia 1997).

1.5.1.1.1 The signalling form of the leptin receptor

The long form of the receptor (ObRb) is considered the signalling form and is critical for leptin body weight actions. This is demonstrated by the genetically obese *db/db* mouse which lack functional leptin receptor signalling. *db/db* mice have all the leptin receptors, however within the region where ObRb and ObRa diverge there is a disruption resulting in termination of the intracellular domain of ObRb (Chen et al. 1996). This ultimately results in a dysfunctional ObRb which is more like ObRa, and results in a phenotype alike the *ob/ob* mouse; morbidly obese, hyperphagic and with reduced energy expenditure (Bray & York 1979; Bates & Myers 2003).

ObRb signals via a noncovalently associated family of janus associated kinases (JAK), of which four members exist, and ObRb preferentially uses JAK2 (Kloek et al. 2002). When leptin binds ObRb there is a conformational change in its structure which allows for binding and activation of JAK2, forming an ObRb-JAK2 complex. When JAK2 becomes activated this allows for phosphorylation of tyrosine residues present on ObRb and in turn activation of downstream signalling events (Kloek et al. 2002; Bates & Myers 2003). Three conserved tyrosine residues are present on the intracellular domain of ObRb; Tyrosine positions 985, 1138 and 1077 (Tyr_{985}, Tyr_{1138} and Tyr_{1077}) (A S Banks et al. 2000; Bates & Myers 2003; Leshan et al. 2006). Tyr_{985} and Tyr_{1138} are required for ObRb signalling (A S Banks et al. 2000). Tyr_{1138} is a docking site for a member the signal transducer and activator of transcriptions (STAT); STAT3, which is activated as part of the main signalling cascade leptin utilises (Münzberg & Myers 2005). Phosphorylation of Tyr_{985} recruits the tyrosine phosphatase SHP-2 which allows for the activation of the extracellular signal-related kinases (ERK) and mitogen-activated protein kinases (MAPK) signalling pathways, which are also utilised by leptin however are more important for growth and differentiation, rather than energy homeostasis (Münzberg & Myers 2005). Conversely, the phosphorylation Tyr_{1077} is not believed to be necessary for leptin signalling, although subsequent studies have shown that it may contribute to leptin signalling, just less so than Tyr_{985} and Tyr_{1138}. Patterson *et al* generated knock-in (KI) mice with a mutated form of Tyr_{1077} present on ObRb and found that these mice display moderate obesity and a mild increase in food intake (Patterson et al. 2012), suggesting Tyr_{1077} may play a minor role in the body weight and food intake actions of leptin. JAK2 can also signal independently without phosphorylation of these tyrosine residues, however the sites at which this occurs are yet to be identified and therefore little is known about these signals.

1.5.1.1.2 The JAK-STAT signalling pathway

As mentioned, the main signalling pathway utilised by leptin is the JAK-STAT pathway, which is dependent on phosphorylation at Tyr_{1138} (Figure 1.4). It is accepted that signalling occurs at this site as KI mice which have a mutation at the 1138 position (*s/s* mice) have a similar phenotype to *db/db* mice (Bates et al. 2003). Interestingly, as mentioned, *db/db* mice are also infertile and have reduced linear growth, however *s/s* mice do not exhibit these traits, with increased hyperphagia and reduced basal metabolic rate being the only shared features. When JAK2 phosphorylates Tyr_{1138} it binds STAT3 which becomes activated and translocates to the nucleus to initiate gene transcription (A

S Banks et al. 2000; Leshan et al. 2006; Bates & Myers 2003) Although ObRa has the ability to bind JAKs, unlike ObRb, they cannot activate STAT3, hence ObRb alone controls leptin signalling (Sweeney 2002). Upon translocation to the nucleus STAT3 has the ability to switch on transcription of certain genes, such as suppressors of cytokine signalling (SOCS) which promotes a negative feedback loops, and POMC.

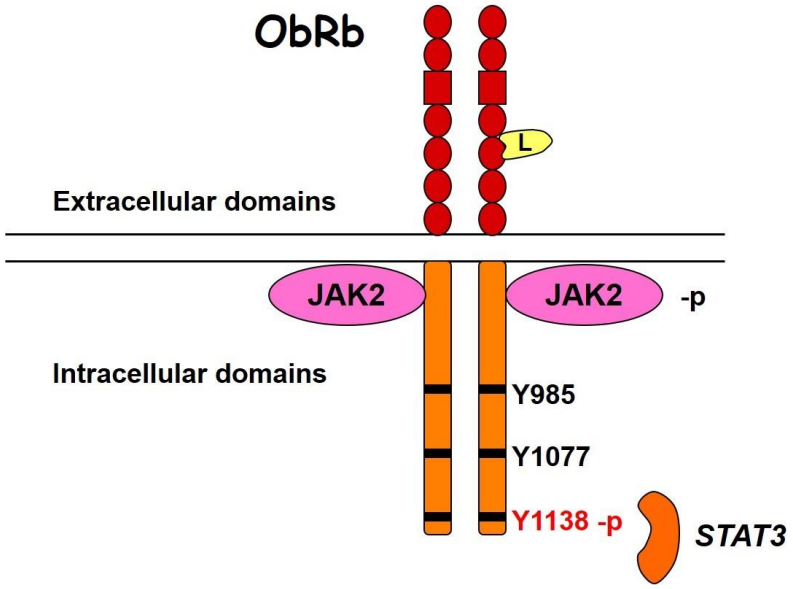

Figure 1.4 Schematic diagram of the leptin receptor and JAK2/STAT3 signalling.

Leptin binds the long form of the leptin receptor, ObRb, which activates a Janus associated kinase, JAK2. JAK2 allows for phosphorylation of Tyrosine residues, with phosphorylation of Y1138 binding the signal transducer and activator of signalling, STAT3, to initiate leptin signalling.
Figure adapted from Ashford Lab teaching material.

ObRb is expressed in many tissues, with highest expression found centrally in the hypothalamus, in particular the basomedial hypothalamic areas including the ARC, DMH and VMH (Fei et al. 1997; Lee et al. 1996). As mentioned, these are the key sites of leptin action, and studies have shown that physically or chemically damaging these nuclei result in a phenotype resembling the *ob/ob* and *db/db* mice (Bates & Myers 2003). Within these areas the highest ObRb expression is present in the ARC, specifically in neurons regulating food intake and body weight; POMC-expressing neurons (Cowley et al. 2001) and NPY/AgRP-expressing neurons (Hâkansson et al. 1998). The product of the POMC gene; α-MSH is implicated in mediating anorectic effects of leptin and conversely AgRP is an antagonist of α-MSH, therefore ObRb-STAT3 signalling causes STAT3 activation

of POMC, whilst inhibiting NPY and AgRP, in order to suppress appetite (Figure 1.5), with the reverse occurring during fasting (Schwartz et al. 2000; Bates & Myers 2003). The specific neurons and neuronal circuitry involved in the actions of leptin is not clearly defined and ARC leptin signalling needs to be further examined, however leptin action on POMC is proposed to be the predominant action. Leptin increases POMC expression (Schwartz et al. 1997) and electrophysiology studies demonstrate that application of leptin readily depolarises POMC neurons (Choudhury et al. 2005; Cowley et al. 2001), accompanied by the speculation that leptin will hyperpolarise NPY/AgRP neurons. The obese *db/db* mice have reduced POMC levels (Balthasar et al. 2004; Mizuno et al. 1998), and furthermore daily leptin injections to *ob/ob* mice result in reduced body weight with elevated POMC expression (Schwartz et al. 1997; Mizuno et al. 1998). This shows leptin receptor signalling on POMC neurons is necessary for the body weight action of leptin; however it is important to highlight that POMC may not be the sole mediator. In addition, not all leptin action on POMC neurons is direct, with synaptic innervation directly from NPY neurons and GABA-releasing neurons inhibiting POMC neurons (Cowley et al. 2001). This is accompanied by work suggesting synaptic plasticity in the hypothalamus and synaptic alterations on ARC POMC neurons may play a role in regulating body weight and food intake (Horvath 2005), independently from leptin action on ObRb-expressing neurons, further supporting the notion that POMC neurons are not the only ARC population implicated in the control of energy balance. Furthermore, Balthasar and colleagues found that when ObRb is knocked out of POMC neurons there is only modest obesity (Balthasar et al. 2004) and Coppari *et al* found rescuing ObRb in *db/db* mice only reverses their obese phenotype in part (Coppari et al. 2005). Therefore, other neurons must be targets of leptin signalling, and indeed other ObRb-expressing neurons exist in the basomedial hypothalamus, particularly the ARC, such as the aforementioned RIPCre neurons (Cui et al. 2004) as well as MCH neurons in the LH (Hâkansson et al. 1998), however less is known regarding these neurons and their role in energy balance. Nonetheless, ObRb-STAT3 signalling is clearly necessary for the hypothalamic anorectic effects of leptin, and maintaining overall energy homeostasis. Importantly, the JAK-STAT signalling pathway is not required for other functions of leptin, including growth and reproduction, therefore although this signalling cascade is the principle pathway utilised by leptin, it is not the sole signalling pathway mediating its functions.

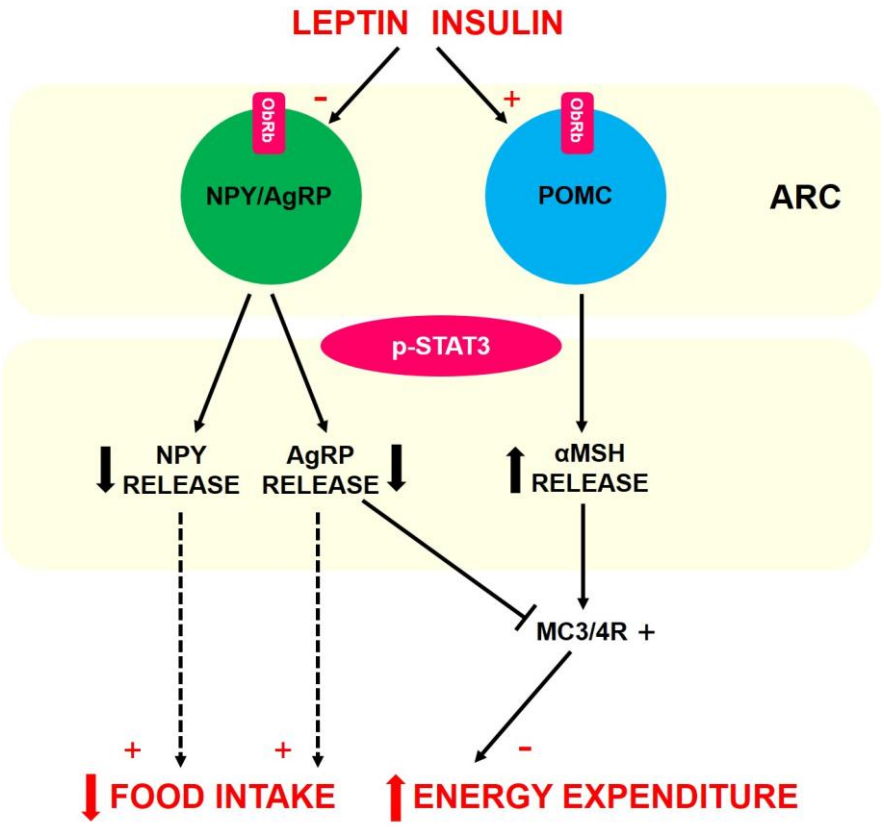

Figure 1.5 Schematic diagram of the first order ARC neuronal model controlling energy balance.

Leptin binds its receptor, ObRb, on first order ARC neurons resulting in phosphorylation of STAT3 activating POMC and the release of the POMC product α-MSH, which acts as an agonist at the melanocortin receptors (MC3R and MC4R), whilst AgRP acts as an antagonist at these receptors. In addition, STAT3 inhibits NPY/AgRP. Leptin action on these first order ARC neurons causes reduced food intake and increased energy expenditure, maintaining energy balance.
Figure adapted from Ashford Lab teaching material.

1.5.1.1.3 The PI3-kinase signalling pathway

A separate signalling pathway leptin activates is the phosphatidylinositol 3-kinase (PI3K) pathway. PI3Ks are heterodimers which control many functions, including metabolism (Donato et al. 2010; Sweeney 2002). The most common form of PI3K includes an 85kDa peptide (p85), which forms a regulatory subunit of PI3K, and a 100kDa catalytic subunit (p110) (Niswender & Schwartz 2003). This pathway involves insulin receptor substrate (IRS) proteins, of which four have been identified (IRS1-4) and are defined as docking proteins, which act as intracellular signalling molecules. The docking proteins can be phosphorylated by different tyrosine kinases, such as the insulin receptor and other cytokine receptors (Bates & Myers 2003), and importantly enable the formation of

signalling complexes to form and bring multiple signalling proteins in close proximity with each other. IRS2 has been shown to be particularly important in this pathway as leptin has the ability to activate PI3K via IRS2 in the hypothalamus, furthermore pharmacological inhibition of PI3K results in leptin no longer able to suppress food intake (Niswender et al. 2001). The hormone insulin also activates this pathway in the hypothalamus, and is in fact required with leptin to induce its anorectic effects (Niswender & Schwartz 2003). This STAT3-independent pathway is crucial for the majority of insulin action alone, however is also believed to be necessary for regulating leptin action on food intake, for example through POMC-expressing neurons. Hill *et al* demonstrated that when PI3K is disrupted in POMC neurons they are no longer activated in response to leptin (Hill et al. 2008), thus these neurons require PI3K signalling to respond appropriately to leptin. However, in this model mice do not have a body weight phenotype, demonstrating that PI3K is clearly involved in mediating leptin actions in part, but is not solely responsible for its effects. Conversely, subsequent studies demonstrated that mice lacking the β-subunit of p110 (p110β) on POMC neurons show increased fat mass and food intake, with reduced leptin sensitivity (Al-Qassab et al. 2009). Interestingly, Al-Qassab and colleagues also found a phenotype when p110β was removed from AgRP neurons, with AgRP-p110β null mice displaying a lean phenotype, hypophagia and resistance to diet-induced obesity (Al-Qassab et al. 2009). Although the precise functions of the PI3K signalling cascade in regards to leptin function remain unknown, these data indicate it may be important in regulating leptin signalling in POMC neurons, as well as AgRP neurons for the control of energy balance.

1.5.1.1.4 Negative regulators of leptin signalling

The phosphorylation at $Tyr_{985,}$ following initiation of leptin signalling, is also implicated in the negative regulation of leptin signalling as SOCs, in particular SOCS3, binds and is activated at Tyr_{985} inhibiting ObRb-STAT3 signalling (Figure 1.6) (Bjorbak et al. 2000). SOCS3 also binds JAK2 directly resulting in further down-regulation of leptin signalling (Münzberg & Myers 2005). As SOCS3 binds Tyr_{985} it has the ability to inhibit both leptin-stimulated JAK2 phosphorylation and activation of ERK signalling. This was demonstrated in studies on obese and lean rats by Wang and colleagues whereby overexpression of SOCS3 in islets causes a 75% reduction in the ability of leptin to reduce body weight (Wang et al. 2000). It has also been shown that following leptin administration in mice SOCS3 mRNA levels rise in areas of the hypothalamus which

express ObRb. This results in blockage of leptin signalling (Bjorbaek et al. 1998) and thus demonstrates a key role for SOCS3 in the negative regulation of leptin signalling.

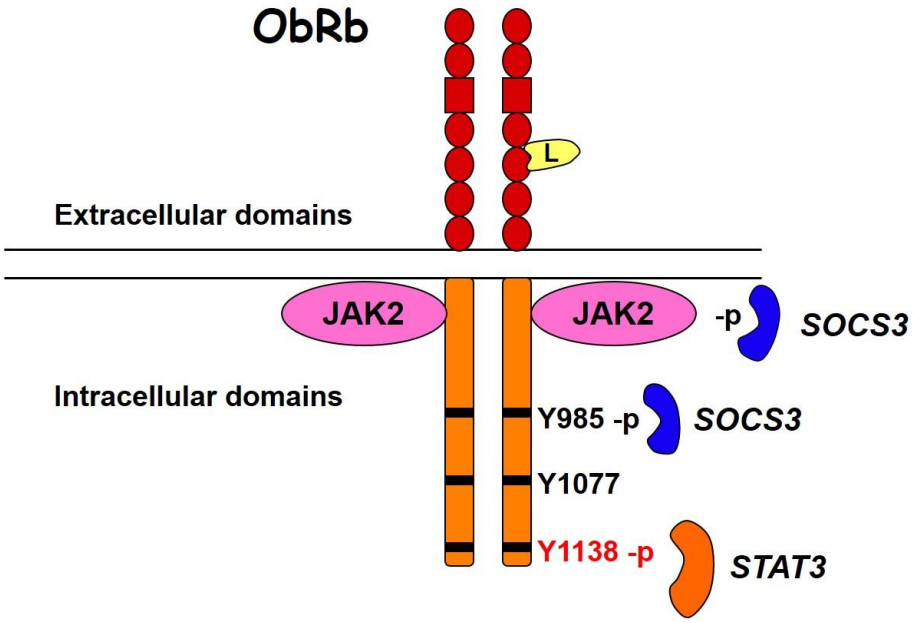

Figure 1.6 Schematic diagram of the negative regulation of leptin signalling by SOCS3.

The activation and phosphorylation of JAK2 and the tyrosine residue Y985 directly binds the suppressor of cytokine signalling SOCS3. This activation of SOCS3 inhibits further STAT3 signalling.
Figure adapted from Ashford Lab teaching material.

The protein-tyrosine phosphatase 1B (PTP1B) is another negative regulator of leptin signalling. In vitro studies demonstrate when fibroblast-like cells and human embryonic kidney (HEK) 293 cells are transfected with PTP1B a reduction in leptin signalling is observed via JAK2/STAT3 blockage (Zabolotny et al. 2002). PTP1B acts directly on JAK2, causing dephosphorylation and inhibition (Figure 1.7), demonstrating, like SOCS3, that PTP1B negatively regulates leptin signalling. Other protein-tyrosine phosphatases also exist and are implicated in the negative regulation of leptin signalling, such as T cell protein-tyrosine phosphatase (TCPTP). TCPTP, like PTP1B, also dephosphorylates STAT3 inhibiting JAK2/STAT3 signalling (Figure 1.7) and furthermore STAT3 phosphorylation is enhanced in brain deficient TCPTP mice (Loh et al. 2011). Thus, the presence of additional negative regulators to SOCS3, play an important role in the regulation of leptin signalling.

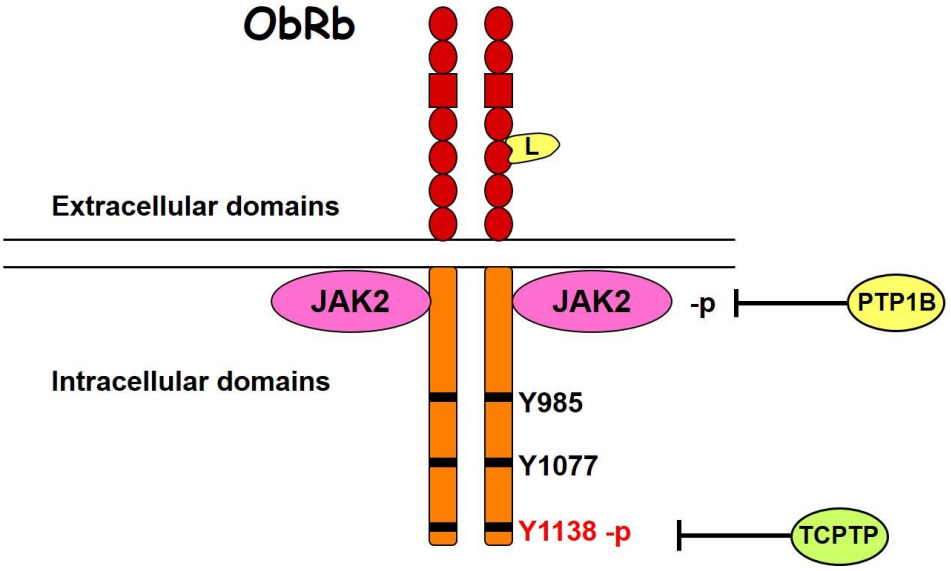

Figure 1.7 Schematic diagram of the negative regulation of leptin signalling by PTP1B and TCPTP.

Negative regulation of leptin signalling occurs through directly inhibition of JAK2/STAT3 signalling by negative regulators PTP1B and TCPTP. PTP1B dephosphorylates JAK2 and TCPTP dephosphorylates STAT3 resulting in blockage of JAK2/STAT3 signalling.
Figure adapted from Ashford Lab teaching material.

1.5.1.2 Leptin resistance

A problem arises in obesity, where the majority of individuals have high circulating levels of leptin, leading to the notion of leptin resistance (Considine et al. 1996). This is supported by the diminished response to leptin observed in diet-induced obese (DIO) mice compared to genetically obese *ob/ob* mice (Halaas et al. 1995; Halaas et al. 1997). The precise mechanisms underlying the development of leptin resistance are unknown, however there are two proposed mechanisms associated with, and likely responsible for, leptin resistance; defects in leptin transport across the BBB and/or impaired leptin receptor signalling in the hypothalamus.

A proposed state of peripheral versus central leptin resistance supports the concept that a reduction in transport of leptin across the BBB is causative in the development of leptin resistance. A longitudinal study examined this and showed that following 8 weeks on a high-fat diet (HFD) mice develop leptin resistance and are unresponsive to peripherally administered leptin, however at the same time point centrally administered leptin stimulated a reduction in food intake (Van Heek et al. 1997). Similarly, El-Haschimi *et*

al demonstrated leptin levels increase in response to HFD and that following 4 weeks on a HFD peripheral leptin treatment evokes an increase in STAT3 (El-Haschimi et al. 2000). However, at 15 weeks on a HFD this response was diminished unless leptin was administered centrally where activation of STAT3 still occurred, which supports the notion there is reduced leptin entering the CNS. Furthermore, it has been found that the ratio of CSF to leptin levels is reduced in obesity (Banks 2001).

Although, El-Haschimi and colleagues demonstrated that DIO mice remain sensitive to centrally administered leptin, they found this response was still diminished in comparison to mice fed a normal chow (NC) diet (El-Haschimi et al. 2000). This supports the idea that reduced transport of leptin into the CNS is not solely responsible for the development of leptin resistance and is suggestive a second signalling mechanism may be involved. A defect in leptin signalling is thought to occur via STAT3, but how this arises is largely unknown. One proposed mechanism is through the leptin receptor, as leptin receptor mRNA and protein levels are reduced in rodent models of leptin resistance (Martin et al. 2000) suggesting leptin resistance may be due to downregulation of leptin signalling at the receptor level. This proposed mechanism was supported by Wilsey and Scarpace, who found DIO rats have reduced leptin receptor expression, as well as elevated basal STAT3 levels, and central administration of leptin was unable to recover these effects (Wilsey & Scarpace 2004). Interestingly, the ARC appears to be the only hypothalamic site to become leptin resistant, with a reduced leptin-activated STAT3 response only observed in the ARC of mice challenged with a HFD, with expression remaining normal in other sites (Münzberg et al. 2004). This is in line with a signalling defect contributing to leptin resistance as the ARC is the main site of leptin action and STAT3 activation.

As mentioned, one of the negative regulators of leptin signalling; SOCS3, inhibits JAK-STAT3 signalling and in turn blocks the body weight effects of leptin, therefore enhanced SOCS-3 expression presents a possible mechanism for leptin reisstance. As leptin levels rise, or in a state of leptin resistance, SOCS3 expression is elevated (Bjørbæk et al. 1999) and this is observed in genetically obese (Shi et al. 2004) and DIO mice models (Münzberg et al. 2004). The elevated SOCS3 expression observed in DIO mice is more specifically associated with higher basal mRNA levels in the ARC (Enriori et al. 2007), which appears to affect AgRP neurons in the first instance, preceding leptin resistance in POMC neurons, which ultimately occurs after chronic high-fat feeding (Olofsson et al. 2013). Importantly, supporting the association between SOCS3 and leptin resistance, Enriori *et al* show that DIO mice with elevated basal SOCS3 expression do not respond

to leptin treatment, whereas SOCS3 mRNA expression is upregulated in the ARC of control mice (Enriori et al. 2007). Chronic low-grade inflammation is also associated with obesity, resulting in increased levels of pro-inflammatory cytokines. Importantly, inflammation also increases SOCS3 expression, which may further exacerbate an obese/leptin-resistant state (Zeyda & Stulnig 2009b). *In vitro*, Chinese hamster ovary (CHO) cells exposed to chronic leptin treatment to induce leptin resistance, show elevated SOCS3 expression and additionally cells transfected with SOCS3 have a direct blockage of leptin signalling via JAK2 (Bjørbæk et al. 1999). Furthermore, mice deficient in SOCS3 display increased STAT3 activation in response to leptin with a concomitant elevation in POMC expression, resulting in reduced body weight gain when compared to WT littermates on a HFD (Mori et al. 2004). Moreover, SOCS3-deficient mice are protected against diet-induced obesity and resulting leptin resistance, providing further evidence for SOCS3 as a potential contributor of defective leptin signalling.

PTP1B is also believed to be key in the development of leptin resistance, due to it also negatively regulating leptin signalling. Following chronic leptin treatment in rats, or models of DIO, PTP1B protein levels become elevated in the hypothalamus, exacerbating and contributing to leptin resistance (White et al. 2009). In addition, PTP1B null mice have an elevated STAT3 response following leptin and are also resistant to diet-induced obesity (Zabolotny et al. 2002). Subsequent studies demonstrated mice with a PTP1B deficiency, specifically in the brain, have reduced body weight and adiposity, increased leptin sensitivity and energy expenditure, as well as improved glucose homeostasis (Bence et al. 2006), which provides further evidence for PTP1B to be implicated in the development of central leptin resistance. Interestingly, when PTP1B is deleted solely from POMC neurons, the same phenotype is observed; reduced fat mass, increased energy expenditure and heightened leptin sensitivity (Banno et al. 2010), suggesting PTP1B may specifically alter leptin signalling on the melanocortin system. Furthermore, additional negative regulators of leptin signalling may also be implicated in the development of leptin resistance, as shown by increased levels of TCPTP in obese mice (Loh et al. 2011). Loh and colleagues also demonstrated that both *in vitro* in CHO cells and *in vivo* in mice that leptin increases TCPTP levels and the observed elevation in TCPTP is associated with obesity and is likely driven by hyperleptineamia (Loh et al. 2011). Thus, targeting of negative regulators of leptin signalling may provide a therapeutic strategy for the reversal of leptin resistance in obesity.

1.5.2 Insulin

The hormone insulin is also key in the regulation of energy homeostasis and was the first adiposity signal described (Porte et al. 2002; Niswender & Schwartz 2003) Insulin is a small protein produced and secreted from pancreatic β-cells acting predominantly to control glucose homeostasis by stimulating glucose uptake into peripheral tissues (adipose tissue, liver, skeletal muscle) allowing for glucose to be stored or utilised as a fuel when required (Heide et al. 2006). To do this, insulin reduces the breakdown of lipids in adipose tissue, particularly white adipose tissue (WAT), blocks gluconeogenesis in the liver, and increases glucose uptake in skeletal muscle (Zeyda & Stulnig 2009a). These actions occur when insulin binds its receptor and stimulates translocation of the glucose transporter, Glut4, from the cytoplasm to the plasma membrane. Although insulin is predominantly found in the pancreas, both the protein and its receptor are also found in the CNS, thus insulin has the ability to infiltrate the CNS across the BBB (Arora & Anubhuti 2006). Although insulin is transported into the CNS there is little evidence of it being produced there, and it may act through its receptors in the brain once transported across the BBB. Like leptin, within the brain insulin is thought to mediate anorexigenic effects. In fact, it is believed that both leptin and insulin are required in conjunction to mediate whole body energy homeostasis and that the signals generated by both hormones interact and are likely coupled by PI3K. Evidence for this includes investigations in the *ob/ob* mouse, where administration of leptin results in a marked decrease in insulin levels and glucose concentrations (Harris et al. 1998). In addition, insulin administration in rats causes an increase in STAT3 phosphorylation which mediates the main action of leptin (Kim et al. 2000). It has also been demonstrated that leptin can mimic insulin actions *in vitro*, again via the PI3K pathway. Kellerer and colleagues found stimulating C_2C_{12} muscle myotubes with insulin and leptin both induced PI3K activity (Kellerer et al. 1997), thus this may link the insulin and leptin signalling pathways to one another in order to control energy homeostasis.

Insulin, like leptin, is thought to mediate its anorectic effects via the melanocortin system. When insulin is administered centrally in fasted mice there is an increase in POMC and a concomitant reduction in food intake (Air et al. 2002; Benoit et al. 2002). Work by Benoit and colleagues found the majority of POMC neurons within the ARC are co-localised with a subunit of the insulin receptor, however notably not all neurons containing the insulin receptor were POMC neurons (Benoit et al. 2002). Furthermore, Air *et al* found the increased POMC following central insulin treatment also caused

reduced body weight gain and adiposity in mice when challenged with a HFD (Air et al. 2002). When insulin binds its receptor there is recruitment of the IRS proteins, which are fundamental for insulin signalling. In particular IRS1 and IRS2 play an important role in insulin signalling and are expressed centrally in neurons (Arora & Anubhuti 2006). The anorectic effects of insulin may be mediated in particular by IRS2, as Burks *et al* found IRS2 null mice display increased food intake, increased body weight and adiposity, and elevated circulating leptin levels (Burks et al. 2000). Due to the effects observed on feeding behaviour and insulin action in response to fasting, it is unsurprising that NPY is also a target of insulin. When insulin mimetics are administered, following fasting, NPY is reduced, attenuating the fasting-induced increase in NPY and AgRP in the hypothalamus (Air et al. 2002). Additionally, in diabetic and obese rodent models centrally administered insulin improves the phenotype by reducing NPY and AgRP expression (Sipols et al. 1995; Dunbar et al. 2005). Therefore, not only is the melanocortin system a target of insulin action but it may also mediate NPY/AgRP pathways in the ARC to regulate catabolic affects.

1.5.2.1 Insulin signalling

Insulin carries out its functions via two signalling cascades; the aforementioned PI3K pathway and the MAPK pathway. The MAPK pathway principally regulates cell growth, differentiation and cell death mechanisms, whereas the PI3K pathway is the predominant pathway regulating glucose uptake affects and, as mentioned in conjunction with leptin, mediates food intake. Thus, the PI3K pathway is intricately involved in the regulation of energy homeostasis.

The insulin receptor is a tetramer which consists of two extracellular α-subunits and two intracellular β-subunits (Heide et al. 2006). Insulin binds the α-subunits which results in phosphorylation of tyrosine residues on the β-subunits, and in turn recruits IRS proteins. It is the recruitment of the IRS proteins and their subsequent phosphorylation which allows for the binding and activation of PI3K (Figure 1.8). This activation involves the most common form of PI3K, including p85 and p110 (Niswender & Schwartz 2003). The phosphorylated sites on the IRS proteins bind to a SH2 domain on p85 which allows for the activation of p110 and thus PI3K stimulation. When PI3K is activated this causes the conversion of phosphatidylinositol (4,5) bisphosphate (PIP2) to phosphatidylinositol (3,4,5) triphosphate (PIP3) allowing for the phosphorylation of the main downstream target of PI3K signalling; protein kinase B (PKB) (Niswender & Schwartz 2003). PKB

allows for insulin induction of glucose transporters and thus increased glucose uptake, therefore activation of the IRS-PI3K cascade is crucial for the majority of insulin action. However, within the hypothalamus relatively little is known about the specifics of insulin signalling. Activation of PKB results in phosphorylation of a member of the forkhead transcriptional factor subfamily; forkhead box O1 (FoxO1), which is implicated in the regulation of the food intake actions of insulin (Nakae et al. 2008). FoxO1 signalling is required for leptin and insulin anorectic actions, as increased expression in the hypothalamus inhibits anorexigenic effects by increasing food intake and body weight (Kim et al. 2006). Kim *et al* demonstrated that FoxO1 drives NPY and AgRP expression, whilst inhibiting action of POMC neurons by directly anatagonising STAT3 (Figure 1.8) (Kim et al. 2006). The precise neurons FoxO1 acts upon is yet to be defined, however the melanocortin system may be the predominant target, as FoxO1 ablation in POMC neurons only results in reduced food intake and body weight (Plum et al. 2009). This further supports that both insulin and leptin are required, likely via P13K-FoxO1 signalling, to mediate feeding behaviour.

Although insulin stimulates PI3K activity via IRS1 and IRS2, leptin only stimulates PI3K via IRS2, as well as JAK2 (Kellerer et al. 1997). Therefore, JAK2 and IRS2 may be responsible for the coupling of leptin and insulin, and thus the combined effects on metabolism. Due to the convergence between insulin and leptin in the hypothalamus the development of insulin and leptin resistance may also be coupled by a common mechanism, which could be due, in part, to reductions or defects in PI3K signalling (Niswender & Schwartz 2003).

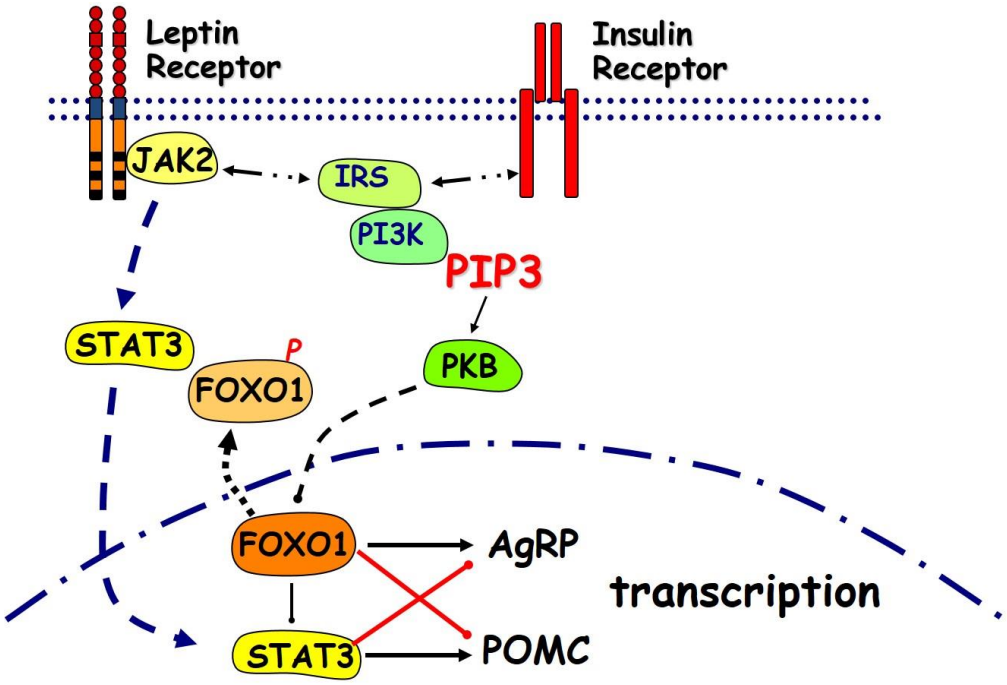

Figure 1.8 Schematic diagram showing the convergence of insulin and leptin signalling controlling neuropeptide expression.

Leptin and insulin both activate PI3K signalling through activation of IRS1. PI3K activates PIP3 and subsequent phosphorylation of PKB, further phosphorylating FOXO1. FOXO1 directly inhibits the anorexigenic action of JAK2/STAT3 leptin signalling.
Figure provided from Ashford Lab teaching material.

1.5.2.2 Insulin resistance

In obesity target tissues become insensitive to the effects of insulin, leading to insulin resistance. Obesity is the main risk factor for insulin resistance, as insulin levels correlate with body weight and are elevated in an obese state (Bagdade et al. 1967). When there is an impairment in insulin sensitivity, causing insulin resistance, free-fatty acids (FFAs) increase and glucose uptake is obstructed exacerbating an obese phenotype through impaired glucose homeostasis. This phenotype is observed in IRS1 null mice which display insulin resistance and are in a state of hyperglycaemia (Araki et al. 1994). Additionally, mice lacking IRS2, specifically in neurons, also display impaired glucose homeostasis (Choudhury et al. 2005). Furthermore, HFD induces insulin resistance (Dresner et al. 1999), which again exacerbates obesity, and is associated with other co-morbidities such as diabetes. The precise mechanism causing central insulin resistance is not fully defined, however like leptin resistance, it is proposed that it develops due to reduced transport into the CNS and/or defects in brain, specifically hypothalamic, signalling.

Little is known regarding insulin transport into the CNS, however as insulin receptors are present in the hypothalamus it is likely that a reduction in insulin binding to central receptors may account for reduced insulin sensitivity. More is understood regarding defects in insulin signalling. Opposed to tyrosine phosphorylation, serine phosphorylation of IRS proteins can occur, which leads to blockage of insulin signalling. Such kinases that cause this serine phosphorylation are I kappa B kinase-β (IKK-β), C-jun N-terminal kinase (JNK1) and MAPK (Zeyda & Stulnig 2009b), which are all activated by insulin. This forms a negative feedback loop, whereby increasing levels of insulin occurring in obesity may elevate the activity of these kinases and further attenuate insulin signalling. Chronic inflammation, associated with obesity, also contributes to insulin resistance as pro-inflammatory cytokines such as tumour necrosis factor alpha (TNFα) and interleukin-6 (IL-6) can also interfere with insulin signalling. This is supported by the finding that TNFα knock-out mice display protection from insulin resistance (Uysal et al. 1997). This inflammation particularly affects peripheral tissues; primarily the adipose tissue and liver. The adipose tissue produces a large number of pro-inflammatory cytokines and chemokines, and in mice it has been shown that body mass correlates with macrophage expression, therefore in obesity there is increased adipose tissue derived macrophages (ATMs) (Weisberg et al. 2003). This rise in ATMs are potentially crucial in obesity-induced inflammation and in turn will contribute to insulin resistance. As mentioned, inflammatory processing also affects the liver. Hepatic steatosis is another factor associated with obesity, and this drives inflammatory processing through nuclear factor-kappa B (NF-κB) which further exacerbates insulin resistance (Zeyda & Stulnig 2009b). In support of this, Wunderlich *et al* demonstrated that in mice where NF-κB is inactivated specifically in the liver there is improved glucose homeostasis and increased insulin sensitivity, even when challenged with a HFD (Wunderlich et al. 2008). However, the definitive role of liver macrophages in the development of insulin resistant is not fully defined yet, although the contribution to obesity-induced inflammation is a major contributing factor. The precise cause for this obesity-induced inflammation is unknown, although one proposed mechanism is through the development of endoplasmic reticulum (ER) stress. Obesity increases ER stress, as shown by an upregulation of ER stress markers in the adipose tissue and liversof obese mice (Ozcan et al. 2004). This elevation in ER stress markers induces inflammatory signalling via JNK and NF-κB, which inhibits insulin signalling through the serine phosphorylation of IRS1. Furthermore, Miller and colleagues found that ER stress reduces Glut4 mRNA expression in an adipocyte cell line

(Miller et al. 2007), thus blocking insulin action. Subsequent studies showed this inhibition of insulin signalling could be reversed, as Ozcan *et al* showed that the application of chaperones that reduce ER stress, in obese mice, cause increased insulin signalling and sensitivity in the liver and adipose tissue through increased tyrosine phosphorylation of IRS1 (Ozcan et al. 2006). In addition, in a separate study Ozcan and colleagues inhibited JNK activity in obese mice and found this reversed the ER stress-induced serine phosphorylation of IRS1 (Ozcan et al. 2004). Therefore, ER stress may be causative in obesity-induced inflammation and thus drive the progression of insulin resistance.

Due to the combined actions of leptin and insulin it is likely a mutual mechanism between both peptides may exist. This common mechanism potentially involves the negative regulators of leptin signalling, SOCS3 and PTP1B. Pro-inflammatory cytokines, as well as insulin itself, increase SOCS3 levels (Shi et al. 2004), and this may in turn contribute to insulin resistance. Additionally, elevated SOCS3 in response to inflammation leads to degradation of IRS proteins (Zeyda & Stulnig 2009b) and furthermore SOCS3-deficient adipocytes have increased PI3K activity is observed via inhibition of IRS degradation (Shi et al. 2004). PTP1B, on the other hand, is not only a negative regulator of leptin signalling but is known to attenuate insulin signalling. PTP1B dephosphorylates IRS proteins, in the same way JAK2 is dephosphorylated in leptin signalling, resulting in inhibition of insulin signalling (Yip et al. 2010; Chernoff 1999). Furthermore, PTP1B is also driven, like SOCS3, by inflammation and, as previously mentioned, is elevated in an obese state (White et al. 2009), thus this may contribute to the progression of insulin resistance. In addition, PTP1B deficient mice show enhanced phosphorylation of the IRS proteins in response to insulin and have heightened sensitivity to insulin, reversing an insulin resistant phenotype (Elchebly et al. 1999). These data provide evidence indicating that SOCS3 and PTP1B are potential targets for not only leptin resistance, but also insulin resistance, with these two outcomes of obesity sharing common mechanisms.

1.5.3 Additional peripheral peptides

Although leptin and insulin are key in the regulation of energy homeostasis other peripheral peptides exist which also play essential roles. Key examples include the orexigenic acting hormone ghrelin and the satiety signal peptide YY (PYY), which are both released from the gut (Figure 1.9). PYY belongs to the same family of peptides as NPY, acting to control food intake through negative regulation of NPY (Arora &

Anubhuti 2006; Sobrino Crespo et al. 2014). Peripheral administration of PYY in both mice (Challis et al. 2003) and humans (Batterham et al. 2003) reduces food intake and furthermore levels of PYY are low in obese individuals (Batterham et al. 2003). Similarly, ghrelin acts to inrease appetite via direct action on NPY and AgRP neurons, antagonising the actions of leptin (Arora & Anubhuti 2006). Ghrelin levels fall during feeding and elevate during periods of fasting (Ariyasu et al. 2001) and central administration of the hormone causes increased food intake and consequently body weight (Tschöp et al. 2000).

Other satiety signals exist which signal the feeling of fullness during a meal and marks the period of time between meals. Thus, these peptides are involved in short-term processes mediating food intake rather than altering adiposity signalling which results in obesity. Examples include glucagon-like peptide 1 (GLP-1), oxyntomodulin (OXM) and cholecystokinin (CCK) that are found in the gut, and others include amylin from the pancreas, and bombesin.

1.6 Type 2 Diabetes Mellitus

Type 2 diabetes mellitus (T2DM) is a disease characterised by the body's inability to make sufficient amounts of insulin or when insulin that is produced does not function normally. This results in a constant state of hyperglycaemia and an inability to handle glucose efficiently. T2DM accounts for 85-95% of all diabetes, mostly occurring in people over the age of forty; however the number of children diagnosed is rising (www.diabetes.org.uk). As mentioned, a principle factor responsible for T2DM is insulin resistance, and therefore the increasing prevalence is closely associated with obesity. The underlying mechanisms associated with obesity such as chronic low-grade inflammation, particularly in adipose tissue and liver, and ER stress thus contribute to the progression of insulin resistance and T2DM. In regards to obesity, the rise in T2DM particularly in the younger population can likely be attributed to lifestyle factors such as less physical activity and consumption of a HFD. Combatting such factors by leading a healthier lifestyle can aid prevention of T2DM and obesity or delay the onset of T2DM, however often diagnosis is at a later stage when damage has already ensued. Therefore, effective treatments of T2DM and contributing metabolic disease are required.

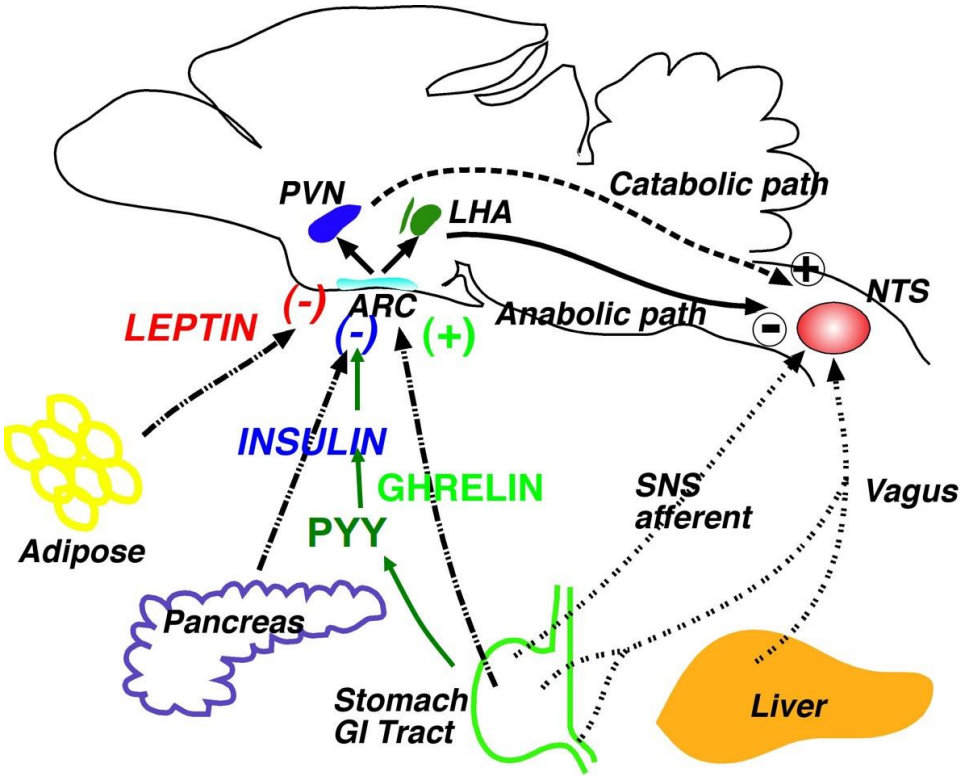

Figure 1.9 Schematic diagram of the main pathways between the CNS and the periphery.

First order neurons in the ARC sense signals from peripheral tissues and organs through peripheral peptide release. Major signals include adiposity signals leptin and insulin, from adipose tissue and the pancreas, and satiety signal peptide YY (PYY) and orexigenic signal ghrelin from the stomach. First order ARC neurons receive these signals project to second order neurons which form anabolic and catabolic pathways projecting to the NTS, in the brainstem. The NTS also receives signals from the vagus nerve and the sympathetic nervous system forming part of the circuitry controlling energy balance.
Figure provided from Ashford Lab teaching material.

1.7 Alzheimer's disease

Alzheimer's disease (AD) is the most prevalent neurodegenerative disease, accounting for the majority of dementia cases worldwide. Dementia currently affects 850,000 people in the UK, which is expected to rise over 1 million by 2025, and double by 2050. This places a huge burden on society as at present, in the UK, it is estimated to cost the economy over 24 billion pounds per year (www.alzheimersresearchuk.org).

AD is characterised by progressive memory loss and cognitive decline, with a number of associated pathologies including neuronal dysfunction and death particularly in the hippocampus and the cortex. Neuronal loss in these brain regions is thought to occur long

before classical symptoms are observed (O'Brien & Wong 2011). Alois Alzheimer noted two pathologies post-mortem associated with the disease in 1907; intracellular neurofibrillary tangles (NFTs) and neuritic plaques (Alzheimer et al. 1995). Consequently, these are recognised as the hallmark pathologies associated with AD, and both are required for definitive diagnosis of the disease, however are only achievable post-mortem. As a result, a great deal of research has focused on the contribution of these pathologies on the progression of AD, and research into methods to detect early diagnosis of AD.

1.7.1 Neurofibrillary tangle pathology

NFTs are tangles of paired helical filaments (PHFs) and are a pathology found not only in AD but many neurodegenerative diseases. In AD, the PHFs collect as bundles of tangles and surround the neuritic plaques; the other hallmark pathology of the disease. The main component of the PHFs was found to be the microtubule associated protein; tau (Grundke-Iqbal et al. 1986). Tau is predominantly localised to neurons and is involved in the assembly and stability of the microtubules present in neurons, and does so through phosphorylation (Iqbal et al. 2005). The NFTs in AD are due to accumulation of hyperphosphorylated tau, and this tau pathology is also observed in other neurodegenerative diseases which, in all cases, causes degeneration and dementia symptoms. It has also been found that abnormal phosphorylation of tau can occur in the cytosol in AD, and thus may occur prior to PHF accumulation and presence in the tangles (Kopke et al. 1993).

1.7.2 Amyloid plaque pathology

The neuritic plaques observed in AD brains consist of neuronal processes surrounding a distinct protein within its core, which was discovered to be amyloid-β (Aβ); a 4.2kDa peptide (Glenner & Wong 1984). Glenner and Wong utilised microscopy with congo red staining which allowed visualisation of amyloid fibres within these neuritic plaques. The Aβ protein was further purified and characterised from the plaques by other groups, and found to be approximately 40 amino acids in length and present in AD and Down's syndrome (DS) brains (Masters et al. 1985). According to the 'Amyloid Cascade Hypothesis' proposed by Hardy and Higgins in 1992, the presence of this Aβ protein is the predominant cause for AD pathology and progression (J. Hardy & Higgins 1992). This model states that Aβ is toxic and its generation leads to the formation of NFTs and subsequent neuronal death. Following its identification as the component of the

extracellular plaques Alois Alzheimer described in 1907, Aβ was shown to be the product of the amyloid precursor protein (APP) gene which is found on chromosome 21 (Kang et al. 1987).

1.7.3 Amyloid precursor protein

As mentioned, Aβ is a product of the proteolysis of APP (Kang et al. 1987). APP is a transmembrane protein, which is a member of a family of related proteins including APP like protein 1 and 2 (APL1 and APL2) (O'Brien & Wong 2011), however only APP itself generates the formation of Aβ. Alternative splicing of APP results in eight isoforms of the protein, with the three most common being a 695, 751 and a 770 amino acid forms (APP695, APP751 and APP770) (O'Brien & Wong 2011). These isoforms are expressed throughout many tissues, APP751 and APP770 in particular are ubiquitously expressed whereas APP695 is predominantly found within neural tissue in the CNS (Sinha & Lieberburg 1999).

1.7.3.1 APP processing

Owing to the fact APP generates Aβ, which is considered the causative factor in the pathogenesis of AD, the processing of APP has been well studied (Sathya et al. 2012; Stockley & O'Neill 2008; Sun et al. 2012; Vassar et al. 2009b). APP can be processed down two distinct pathways; the non-amyloidogenic pathway and the amyloidogenic pathway, under the control of three protein secretases; α, β and γ (Figure 1.10). The preferential pathway, utilised under normal circumstances, is the non-amyloidogenic pathway, which is under the control of the α-secretase(s). APP is cleaved by the α-secretase at amino acid positions 16 and 17 resulting in the production of a secreted APP derivative (sAPPα) and a short C-terminal fragment 83 amino acids in length (C83). A sequential cleavage then occurs of C83 by a γ-secretase which generates a non-toxic 3kDa peptide (p3) and a cytoplasmic APP intracellular domain (AICD). The initial α-secretase cleavage of APP occurs within the Aβ domain, thus under normal circumstances this precludes Aβ production.

Through the amyloidogenic pathway APP is first cleaved by the β-secretase at two sites; methionine position 671 and aspartic acid position 672. This cleavage generates a secreted APP derivative (sAPPβ) and a longer membrane C-terminal fragment; 99 amino acids in length (C99). A subsequent cleavage of C99, again via the γ-secretase releases the mature form of Aβ predominantly 40 amino acids long ($A\beta_{40}$), as well generating AICD in the cytosol. This final cleavage step by the γ-secretase is heterogeneous and as a result forms

Aβ of varying lengths, which in some cases results in a form 42 amino acids in length ($A\beta_{42}$). The production of $A\beta_{42}$ is considered to be toxic and leads to the pathologies associated with AD (J. A. Hardy & Higgins 1992).

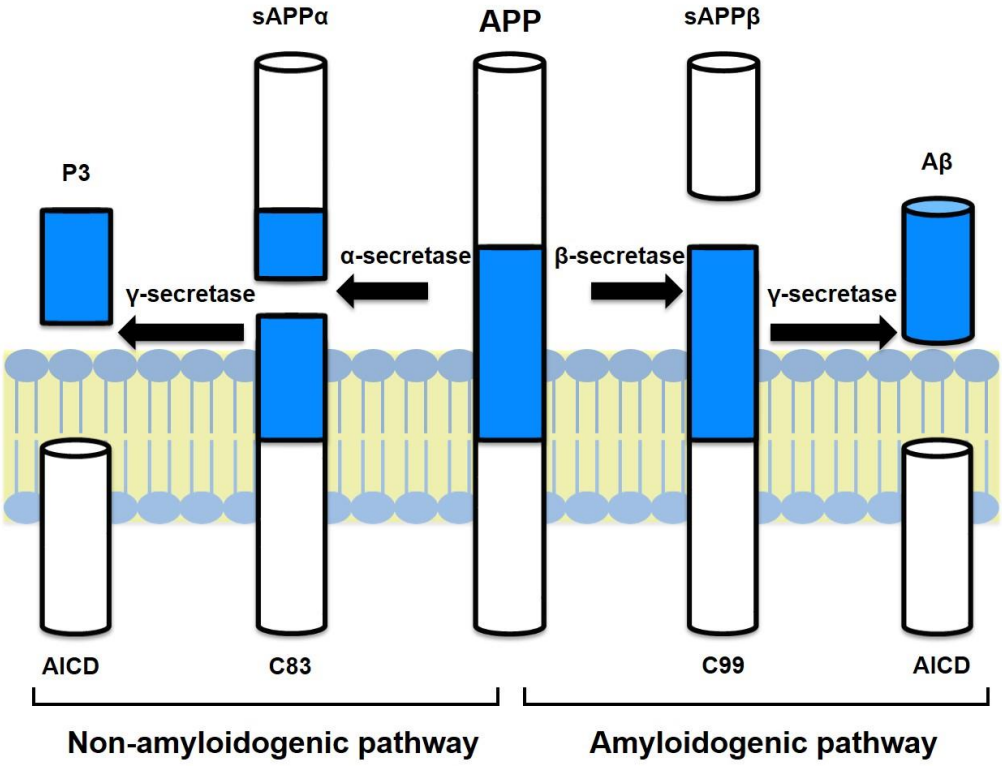

Figure 1.10 Scehmatic diagram showing the non-amyloidogenic and amyloiogenic pathways of APP processing.

Preferentially APP is processed down the non-amyloiodgenic pathway involving α-secretase cleavage giving rise to soluble APP derivative (sAPPα) and an 83 amino acid C-terminal fragment (C83). Subsequent cleavage by γ-secretase produces a non-toxic peptide (p3) and a cytoplasmic APP intracellular domain (AICD). Amyloiodgenic processing occurs through β-secretase cleavage forming a soluble APPβ derivative (sAPPβ) and a 99 amino acid C-terminal fragment (C99) and subsequent γ-secretase cleavage forms an AICD as well as the mature form of Aβ. The production of Aβ through this pathway is considered the causative factor for the symptoms observed in Alzheimer's disease.

1.7.3.2 Identification of the α–secretase

The α-secretase is considered a zinc metalloproteinase and its activity has been attributed to a group of enzymes forming the a-disintegrin and metalloproteinase (ADAM) family. The ADAM family are type 1 integral membrane proteins which have multi-domain

structures consisting of a N-terminal signal peptide, a propeptide, a cleavage site, a catalytic domain, a cysteine rich domain, a hydrophobic domain and a short cytoplasmic domain (Allinson et al. 2003). In particular the activity of three members of the ADAM family are considered to mediate α-secretase activity; ADAM17, ADAM9 and ADAM10.

ADAM17 is also referred to as TACE (tumour necrosis factor-α convertase) which is involved in the release of TNFα from TNF (Black et al. 1997). TACE is a glycoprotein which is found in areas of the brain affected by AD, expressed in neurons and co-localised with Aβ (Skovronsky et al. 2001). TACE inhibitors have been utilised to confirm its role as the α-secretase, demonstrating inhibition in primary neuronal cultures reduces α-secretase activity (Blacker et al. 2002). ADAM9 was first isolated from mouse lung cDNA by Weskamp and colleagues (Weskamp et al. 1996) and is also considered to contribute to α-secretase activity. ADAM10 was isolated and sequenced by Howard and colleagues (Howard et al. 1996) and it has been shown that overexpression of this enzyme in HEK 293 cells results in increased α-secretase activity (Lammich et al. 1999). Conversely, transfection of a dominant negative form of ADAM10 causes a reduction in α-secretase cleavage (Lammich et al. 1999). ADAM10 is also expressed in neurons and *in situ* hybridisation (ISH) studies reveal that within these neurons there is co-expression with APP (Marcinkiewicz & Seidah 2000). Furthermore, this enzyme, in particular, is found to be reduced, as well as the sAPPα product, in AD platelets and CSF (Colciaghi et al. 2002). ADAM10 is considered to be the predominant α-secretase responsible for constitutive activity. This was supported by work from Kuhn and colleagues who knocked-down ADAM17, 9 and 10 in HEK293 cells and SH-SY5Y cells (a human neuroblastoma cell line) (Kuhn et al. 2010). They found that knocking-down ADAM9 had no effect, ADAM17 caused a small reduction in APP processing in HEK293 cells but no affect in SH-SY5Y cells, whereas ADAM10 knock-down resulted in a reduction in APP processing and the production of sAPPα. This demonstrated ADAM10 is necessary for α-secretase activity in neurons and that ADAM9 and 17 cannot compensate for its loss. Interestingly, however, ADAM10 knock-out mice are embryonic lethal, due to a defect in notch signalling, however ADAM 9 and 17 are not affected and α-secretase activity is maintained (Hartmann et al. 2002). Similarly ADAM9 knock-out mice, although they show no developmental abnormalities, the α-secretase cleavage products are unchanged (Weskamp et al. 2002). This illustrates the necessity for not only one ADAM to act as the α-secretase, but rather multiple (9, 17 and 10) will act together to mediate α-secretase cleavage of APP.

1.7.3.3 Identification of the β-secretase

As cleavage of APP by the β-secretase is considered the rate-limiting step in the production of Aβ a great deal of research focused on characterising this enzyme over the identification of the α- and γ-secretases. Many groups identified the transmembrane aspartic protease BACE1 (the β-site APP cleaving enzyme 1) as the β-secretase mainly due to it sharing the same characteristics. Vassar and colleagues were amongst the first groups to identify BACE1 (also known as Asp2) as the β-secretase utilising an expression cloning strategy whereby they found increased Aβ and C99 in HEK293 cells transfected with a BACE1 vector and overexpression of APP with the Swedish mutation ($hAPP_{swe}$) (Vassar et al. 1999). Vassar and colleagues also showed high expression of BACE1 in the brain, predominantly in neurons and only low levels in glia, which is consistent with the β-secretase, a finding supported by other groups (Vassar et al. 1999; Zhao et al. 2007; Hussain et al. 1999). Others also confirmed BACE1 to share the same characteristics as the β-secretase and cleave APP at the same site using cloning and purification techniques (Sinha et al. 1999) and genomic screening of aspartic proteases (Hussain et al. 1999; Lin et al. 2000). Such characteristics include the structure and localisation of BACE1, as it is a type 1 transmembrane protein with an active site on the luminal side, which is where β-secretase cleaves APP, and it is localised mainly to the golgi and the endosomes which is characteristic of the β-secretase (Vassar et al. 1999). In support of BACE1 being identified as the β-secretase it has further been shown that inhibition of BACE1 using antisense oligomers reduces Aβ release, levels of sAPPβ and C99, whilst increasing sAPPα levels (Yan et al. 1999). This reduction in β-secretase activity with a concomitant increase in α-secretase activity demonstrates the relationship between the two enzymes in which they compete for APP as a substrate and have opposing actions to one another. This is also observed when ADAM10 is overexpressed in neurons which results in enhanced α-secretase activity and reduced BACE1 cleavage (Postina et al. 2004). Interestingly, however, enzymes other than the α-secretase and BACE1 may account for a degree of APP processing as Kuhn *et al* found when both ADAM10 and BACE1 are inhibited in SH-SY5Y cells there is still APP secretion into the media (approximately 10-15%) (Kuhn et al. 2010). Furthermore, BACE1 knock-out studies in mice have shown a deficiency in BACE1 results in reduced sAPPβ levels, increased sAPPα levels and Aβ secretion is abolished (Luo et al. 2001; Roberds et al. 2001; Cai et al. 2001). Such work validates BACE1 as the β-secretase and provides a potential target for therapeutic intervention in AD.

Soon after the identification of BACE1 as the β-secretase, a second aspartic protease BACE2 was discovered (Lin et al. 2000). The sequence and expression pattern of BACE2 was analysed, revealing it shared a similar structure and 64% amino acid similarity to BACE1 (Bennett et al. 2000). Although BACE1 and BACE2 share similar homology they only share 40-44% similarity with other members of the pepsin family, presenting these two enzymes as a novel family of aspartic proteases. BACE2 also has the ability to cleave APP at the β-secretase site (Hussain et al. 2000), which raised the possibility of it also being the β-secretase. However, Bennett and colleagues found utilising northern blot analysis that BACE2 is expressed in most tissues with highest mRNA expression in adult tissues including the pancreas, kidney and stomach, however unlike BACE1, in the brain BACE2 expression is low (Bennett et al. 2000). Owing to the expression pattern in the brain is it unlikely that BACE2 acts as the β-secretase.

1.7.3.4 Identification of the γ-secretase

The γ-secretase has also been identified and studied as a potential therapeutic target in AD. However, the γ-secretase has many substrates other than just C99, including the notch receptor which controls cellular differentiation events, therefore modulation of this enzyme rather than inhibition provides a better therapeutic strategy. The γ-secretase has been identified as an enzymatic complex made up of four membrane proteins; presenilin 1 or 2 (PS1/2), nicastrin, anterior pharynx-defective 1(Aph-1) and presenilin enhancer 2 (Pen-2) (Wolfe 2008). Initially it was accepted that PS1 was responsible for γ-secretase activity, acting as the catalytic component, as Wolfe *et al* showed mutations of aspartate residues in PS1 reduce Aβ release (Wolfe et al. 1999). Similarly, Zhang and colleagues found knock-down of PS1 and PS2 in cells reduced Aβ levels (Zhang et al. 2000), arguing the presenilins are vital for γ-secretase mediated processing of APP. It was further found that other proteins interact with the presenilins to mediate γ-secretase cleavage, such as nicastrin which is a type 1 transmembrane glycoprotein which interacts with PS1 and plays a role in its mediation of APP processing (Yu et al. 2000). Latterly, Aph-1 and Pen-2 were isolated and identified as novel presenilin enhancers which, like nicastrin, are necessary for γ-secretase activity (Francis et al. 2002). Although the identification of this protein complex as the γ-secretase has been found the precise structure and function is still relatively unknown and yet to be defined.

1.7.4 BACE1 characterisation

Since its discovery as the β-secretase a large body of research has focussed on the characterisation of BACE1, in terms of its structure and regulation. BACE1 structurally consists of an N-terminal signal peptide sequence, a propeptide, a catalytic domain, a transmembrane domain and a cytoplasmic carboxy-terminal (Vassar et al. 1999). BACE1 is a type 1 transmembrane protein of 501 amino acids, which is highly expressed in the pancreas and the brain. Studies utilising RT-PCR indicates 3 alternatively spliced BACE1 transcripts are also present and expressed in the brain and pancreas involving deletions of 25, 44 or 69 amino acids; creating BACE-457, BACE1-476 and BACE1-432 (Tanahashi & Tabira 2001). BACE1-501 is the mature form and has the greatest activity.

It is well accepted within the literature that BACE1 responds to various cellular stresses and owing to this it is regulated predominately by posttranslational modifications. Consequently, substantial research has focussed on the trafficking of BACE1 and its regulation through these modifications. An immature form of BACE1; pro-BACE1, with a molecular weight of approximately 58kDa is synthesised in the ER, which rapidly undergoes maturation in the golgi apparatus (Vassar 2001). This stable and mature form of BACE1 runs on a gel at approximately 70kDa, which is a greater mass than predicted for the protein suggesting BACE1 undergoes glycosylation (Haniu et al. 2000; Capell et al. 2000). The maturation process of BACE1 involves cleavage of the propeptide once the protein exits the ER and is transported to the golgi and endosomes (Huse et al. 2000; Haniu et al. 2000). Usually aspartic proteases will shed the propeptide domain themselves via autocatalysis, however BACE1 contains a propeptide convertase (PC) cleavage site, in which a separate protease can remove the propetide domain (Benjannet et al. 2001). The main PC which promotes this reaction is Furin, which is localised in the golgi and has been to shown to be necessary for removal of the propeptide (Benjannet et al. 2001; Bennett, Denis, et al. 2000). Work by Benjannet and colleagues found by transfecting HEK 293 cells with a mutated form of BACE1 which lacks the propetide domain, that BACE1 remains in the ER, therefore the propeptide is essential for the exit from the ER and the beginning of the maturation process. Interestingly, this immature form has been shown to also have β-secretase activity, as Creemers *et al* found even upon removal of furin BACE1 activity was unaffected, showing the propeptide domain has some β-secretase activity and Aβ could be produced in the ER (Creemers et al. 2001).

BACE1 contains four N-linked glycosylation sites, three of which undergo glycosylation, which has shown to be necessary for BACE1 activity (Huse et al. 2000; Haniu et al. 2000). This modification occurs within the ER and BACE1 is subsequently transported to the endosomal system. The requirement for glycosylation of BACE1 activity was demonstrated by Charlwood *et al* who utilised site directed mutagenesis to mutate the 4 glycosylation sites in CHO cells and found reduced activity, confirming glycosylation is required for BACE1 activity (Charlwood et al. 2001). After glycosylation, BACE1 is recycled between the cell surface and the endosomes which, based on its long half-life (approximately 9 hours), is believed to occur many times. This was supported by work from Huse and colleagues who carried out staining on HeLa cells (a human epithelial cell line) transfected with BACE1 constructs and found BACE1 co-localised with endosomes and also present at the membrane (Huse et al. 2000). It is accepted that this trafficking of BACE1 to the endosomes occurs via internalisation at the cell surface. The process of this trafficking from the cell surface to the endosomes is, at least in part, under the control of Golgi-localised γ-adaptin ear containing ARF-binding (GGA) proteins (Tan & Evin 2012). GGA3 in particular, which is processed during apoptosis, regulates BACE1 activity by increased cleavage of GGA3 resulting in elevated BACE1 activity (Tesco et al. 2007). Furthermore, GGA3 as well as other GGA proteins have found to be reduced in AD brains, in turn correlating with increased BACE1 levels, highlighting the importance of the trafficking of BACE1 in AD progression (Tesco et al. 2007).

The cytoplasmic tail of BACE1 is also crucial for its trafficking. Work by Capell and colleagues found that if BACE1 lacks this component of its structure it cannot be transported from the ER (Capell et al. 2000). Within the C-tail BACE1 contains six extracellular cysteine resides which form three disulphide bonds and a dileucine motif contributing to its unique structure and lack of homology with other pepsins (Vassar et al. 1999). Huse *et al* showed that deletions of the dielucine motif resulted in BACE1 remaining at the membrane, therefore blocking endosomal trafficking (Huse et al. 2000), potentially via reduced internalisation. The C-tail is also targeted for posttranslational modifications. The cysteine residues present on BACE1 have been shown to be palmitoylated, in particular three of these sites (Benjannet et al. 2001), and it is believed that this process is necessary for trafficking. The generation of cysteine residue mutants, transfected in HEK 293 cells shows reduced palmitoylation (Benjannet et al. 2001). A small part of BACE can undergo ectodomain shedding, resulting in some soluble BACE and this is thought to be involved in amyloidogensis as overexpression of a soluble form

of BACE1 increased Aβ generation (Benjannet et al. 2001). Benjannet and colleagues also found that this generation of a soluble form of BACE is inhibited by palmitoylation, and the amount of shedded ectodomain released is reliant on the degree of palmitoylation.

Another posttranslational modification involved in the regulation of BACE1, particularly at the C-tail, is phosphorylation. Walter *et al* found BACE1 undergoes phosphorylation exclusively at the C-tail end, and only to the mature form of BACE1 (Walter et al. 2001) Their studies also revealed that phosphorylation affected both the trafficking and localisation of BACE1, with phosphorylation occurring in the golgi, but a non-phosphorylated form present at the endosomes. In close proximity to the dileucine motif is a serine 498 (ser498) site which has also been shown to undergo phosphorylation (Pastorino et al. 2002). Phosphorylation at this site also enhances GGA binding, mediating BACE1 for degradation (Wahle et al. 2005; Tesco et al. 2007). However, Pastorino and colleagues showed, using site directed mutagenesis, that this site doesn't affect degradation, and BACE1 activity, whereas mutations of the dileucine motif increases BACE1 at the membrane suggesting this component of BACE1 regulates its internalisation.

Lastly, BACE1 also undergoes acetylation during its regulation, specifically in the lumen of the ER (Costantini et al. 2007), which also affects its trafficking. Constantini and colleagues found BACE1 is acetylated on seven lysine residues within its N-terminal domain. Using CHO cells they also demonstrated that mutating these lysine residues, resulting in no acetylation, reduced transport from the ER, and observed the opposite with a constititutively acetylated form. As mentioned, this is exclusive to pro-BACE1 and is thought that deacetylation occurs in the golgi.

The structure, trafficking and regulation of BACE1 mentioned above highlights its existence as a novel member of the pepsin family. Differences in structure to other members of the pepsin family is an important feature as such differences may affect substrate specificity of the enzyme. The role of posttranslational modifications in the trafficking and regulation of BACE1 are also important in allowing rapid responses to stress conditions and changes in this regulation may affect BACE1-mediated APP processing, resulting in elevated BACE1 levels and activity, and a concomitant increase in Aβ.

1.7.5 BACE1 in AD

Owing to BACE1-mediated APP processing resulting in the release of Aβ, BACE1 is considered the rate-limiting step in Aβ production. Consequently, any elevations in BACE1 levels or activity is considered the primary causative factor for the symptoms associated with AD progression.

In support of this, BACE1 mRNA, protein and activity have all been shown to be elevated in AD brains, in both human samples (Yang et al. 2003; Fukumoto & Cheung 2002; Li et al. 2004) and mouse models (Zhao et al. 2007). Importantly, this increase in BACE1 correlates with increased $A\beta_{42}$, and is thus considered causative of increased Aβ (Li et al. 2004). Familial Alzheimer's disease (FAD) also provides evidence for increased BACE1 driving AD pathology as this form of AD is associated with the Swedish, $APP_{swe,}$ mutation which results in increased APP levels and elevated BACE1 cleavage (Vassar et al. 2009b). In addition, Tyler and colleagues found that a large proportion of sporadic AD brains have increased BACE1 activity, with a corresponding reduction of α-secretase activity below the normal level (Tyler et al. 2002). Interestingly, Harada *et al* showed BACE1 is specifically increased in surviving neurons in AD brains (Harada et al. 2006). In this study they found a reduction in staining of the neuronal marker MAP2 in AD brains, corresponding to the neuronal loss associated with AD, however observed an increase in the ratio of BACE1 to MAP2 suggesting increased BACE1 within individual neurons. Therefore increased BACE1 in surviving neurons may further drive AD progression.

BACE1 appears to act as a cellular stress response protein, and elevations can occur due to many stress-related factors, which are in turn associated with AD. For example, oxidative stress is known to play a role in AD with oxidative species accumulating in AD brains. Furthermore it has been shown that oxidative stress products can modulate BACE1 (Tamagno et al. 2002). Tamagno and colleagues showed that neurons exposed to pro-oxidant stimuli increased BACE1 protein levels, particularly the mature form in which they found strong staining localised to the golgi. BACE1 may also be mediated by hypoxia, as the induction of hypoxic conditions in a neuroblastoma cell line expressing APP695 causes increased BACE1 protein and activity, with no change in α-secretase activity or APP levels (Zhang et al. 2007). In particular HIF-1 (hypoxia-inducible factor 1), which is a transcription factor activated in response to hypoxia, may modulate BACE1 activity. Zhang *et al* found neuron specific HIF-1 null mice showed reduced BACE1 in

the hippocampus and cortex; the two regions most affected by AD, and conversely reduced BACE1 levels were observed when cells where transfected with HIF-1 (Zhang et al. 2007). This study further revealed that there is a functional HIF-1 site within the mouse BACE1 promoter, suggesting HIF-1 has the ability to directly regulate BACE1 activity. As well as oxidative stress and hypoxia, defective energy metabolism may also contribute to elevated BACE1 activity, as impaired glucose homeostasis is considered to be associated with AD (Vassar et al. 2009b). Work by Velliquette *et al* further supported this by demonstrating reduced energy metabolism in mice leads to increased BACE1 and Aβ levels (R. a Velliquette et al. 2005). Therefore disruptions in energy metabolism may also regulate BACE1 levels and contribute to AD pathogenesis.

Events associated with a higher risk of developing AD such as stroke and traumatic brain injury (TBI) may also contribute to BACE1-mediated production of Aβ. Wen and colleagues generated a stroke model of transient cerebral ischaemia in rats and found that these animals showed a large elevation in BACE1 protein and activity (Wen et al. 2004). This study also demonstrated co-localisation between BACE1 and a TUNEL stain- utilised as a marker of apoptosis, in regions directly affected by the ischaemia. It has also been found that apoptosis alone, independent of stroke models, drives an increase in BACE1 activity (Tesco et al. 2007). Stroke is also associated with oxidative stress, thus this may also drive the large increase in BACE1 levels associated. Similarly following TBI, in rats, BACE1 mRNA is increased in the hippocampus and the cortex, and this increase is associated with BACE1 present in astrocytes rather than predominantly neurons (Blasko et al. 2004). Therefore, these types of chronic stress or traumatic events drive increases in BACE1 and thus this may account for their association in AD.

Further evidence for BACE1 causing AD symptoms stems from work on DS tissue, which also shows a large increase in BACE1 protein levels in cortical regions (Sun et al. 2006). This is of particular interest as most DS patients develop AD due to abnormal APP processing. DS patients have two copies of the APP gene, as well as other alterations, on chromosome 21 resulting in increased sAPPβ and Aβ deposition giving rise to a phenotype alike that observed in FAD (Selkoe 1991). Sun and colleagues found that the ratio of mature to immature form of BACE1 is increased in DS brains and the mature form remains for an extended time in the golgi (Sun et al. 2006). This is suggestive that the increased Aβ detected in DS cortical regions and the association with AD may be in particular due to abnormal BACE1 trafficking.

This work provides evidence that BACE1 cleavage of APP is the causative factor for the symptoms observed in AD. The factors associated with increasing BACE1 levels, and thus contributing to AD progression, are also those associated with many other non-communicable chronic disease states (e.g. obesity, T2DM and cardiovascular disease) and therefore creates greater risk of developing AD as a result of other co-morbidities.

1.8 AD links with T2DM/obesity

Obesity and T2DM are now widely considered to be risk factors for AD, with the diseases sharing many common features such as inflammation and insulin resistance (Yang & Song 2013).

Population-based studies investigating BMI and dementia have demonstrated obesity as a risk factor for AD, with patients developing dementia presenting increased BMI (Gorospe & Dave 2007; Investigation 2015). Interestingly, however this has been shown to vary with age, with mid-life obesity increasing the risk of dementia, yet in late-life (>65 years) reduced BMI is actually a risk factor for AD (Fitzpatrick et al. 2009). This is supported by recent research suggesting obesity may actually be protective in regards to AD progression (Qizilbash et al. 2015). However, the precise reasons behind this are unknown, and could be due to changes in BMI occurring with age. Significantly, symptoms associated with obesity may be linked to AD years before the onset of clinical symptoms and a great deal of research still links obesity to AD. Diet-induced obesity has been shown to result in elevated $A\beta_{40}$ and $A\beta_{42}$ in triple transgenic AD mouse models (Julien et al. 2010). Additionally, APP has been found in abundance in adipose tissue, and is upregulated with obesity, along with the presence of $A\beta_{40}$ and $A\beta_{42}$ not only in the adipose tissue but also in ATMs (Lee et al. 2008). This expression correlates with pro-inflammatory cytokines produced by the adipose tissue, as well as chemokines, which all contribute to the development of insulin resistance (Luchsinger & Gustafson 2009), and moreover, inflammation is an associated factor of AD. Wang and colleagues have shown that calorie restriction, utilised to reverse obesity and insulin resistance in Tg2576 mice, which develop amyloid pathology, prevents amyloid depositions in the brain and enhances α-secretase APP processing through increased ADAM10 levels (Wang et al. 2005). Furthermore, a consequence of obesity is leptin resistance which may also be implicated in increasing BACE1 levels as under normal conditions leptin has been shown to reduce BACE1 expression (Marwarha, Dasari, Prabhakara, et al. 2010; G Marwarha et

al. 2014). Thus, in an obese-leptin resistant state this action of leptin may become impaired and BACE1 expression increase.

People with AD are also at greater risk of having T2DM (Janson et al. 2004), with the two diseases sharing defects in insulin signalling, which can lead to cognitive impairment and neuronal death (Li & Hölscher 2007). Furthermore, insulin resistance associated with HFD in Tg2576 mice show increased Aβ levels and further cognitive impairments (Ho et al. 2004) Population-based studies in humans also demonstrate the link between AD and T2DM, with an increased prevalence of T2DM in patients with dementia (Biessels et al. 2006). Insulin resistance is also associated with reductions in the insulin degrading enzyme (IDE) (Ho et al. 2004), which has been described to also target Aβ for degradation. This may be another potential mechanism linking T2DM to AD, as IDE deficient mice show reduced degradation of Aβ and a related increase in Aβ levels (Farris et al. 2003). Again, calorie restriction has been shown to attenuate this reduction in IDE associated with insulin resistance and enhance its expression (Wang et al. 2005).

As mentioned, BACE1 is considered the primary causative factor in the progression of AD and elevations can occur via a number of stresses, including age, hypoxia, oxidative stress as well as factors associated with obesity and T2DM such as impaired glucose homeostasis and insulin resistance. Therefore these factors may elevate BACE1 leading to increased risk of AD, and specifically highlights the role of BACE1 in connecting obesity/T2DM with AD. Recent work from our lab supports this notion demonstrating that BACE1 deficient (*BACE1*$^{-/-}$) mice have an improved metabolic phenotype (Meakin et al. 2012). Meakin *et al* found *BACE1*$^{-/-}$ mice are protected against DIO and have improved glucose homeostasis and insulin sensitivity. Furthermore, pharmacological inhibition of BACE1 on a skeletal muscle cell line has shown to enhance glucose uptake and insulin signalling (Meakin et al. 2012; Hamilton et al. 2014). This work provides the potential for BACE1 to be a novel therapeutic target for not only AD, but obesity and T2DM. However, the precise role of BACE1 in energy metabolism remains yet to be defined.

The current literature highlights a clear link between AD and factors associated with metabolic disease. Worryingly the prevalence of such diseases as obesity and T2DM are increasing rapidly due to the more modern lifestyle many now live, and therefore there is a drastic need to investigate potential therapies for metabolic disease to prevent people entering old age with poorer health.

1.9 Project aims and hypotheses

Taken together, there is a clear role of BACE1 not only in the processing of APP and progression of AD, but also in energy metabolism. Our hypothesis is that BACE1 may be acting as a sensor of metabolic stress in particular and once elevated acts to modify metabolic processes to enable the cell/tissue to recover to or withstand the initiating stress. Unfortunately, under chronic stress conditions the permanently raised BACE1 activity results in prolonged higher levels of Aβ, driving further increases in the initiating and other adverse stress events, such as oxidative and inflammatory stress, creating a vicious cycle. Thus, it is therefore crucial to investigate the role of BACE1 in whole body energy homeostasis, to define a potential physiological role outwith the actions of BACE1 directly relating to AD.

The main objective of this project was to therefore investigate the role of BACE1 in metabolic disease by studying the effects of pharmacological inhibition of BACE1 as a potential treatment strategy for obesity and T2DM. With this in mind, additionally the characterisation of BACE1 in the hypothalamus and its role in the neural circuitry regulating energy balance was investigated with regards to a role for BACE1 in whole body energy homeostasis.

The knowledge from this research may allow for advancements in the treatment of obesity and T2DM, and provide the potential for BACE1 inhibitors to play a role in the therapeutic intervention of metabolic disease.

1.10 Objectives

- Examine the effects of pharmacologically inhibiting BACE1 on obesity and T2DM
    - Treat diet-induced obese wild-type mice with BACE1 inhibitors and measure metabolic outcomes (body weight, food intake, body composition, glucose tolerance and insulin sensitivity).
    - Examine various tissues (hypothalamus, white adipose tissue, brown adipose tissue and skeletal muscle) using real-time PCR to investigate changes in gene expression of markers of leptin signalling, inflammation, and thermogenic programming following treatment with BACE1 inhibitors.
- Examine the effects of altering APP processing on metabolic disease
    - Challenge mice overexpressing a human APP mutation, which enhances BACE1-mediated processing, and wild-type littermates with a high-fat diet for 16 weeks and measure metabolic outcomes.
    - Treat wild-type mice, when challenged with a high-fat diet, with an α-secretase (ADAM10) inhibitor and measure metabolic outcomes.
- Characterise BACE1 expression in the hypothalamus
    - Use immunofluorescence staining to examine BACE1 expression in different regions of the hypothalamus.
    - Examine co-expression of BACE1 and known hypothalamic neuronal populations using immunofluorescence staining to determine the neuronal circuitry BACE1 is part of.

Chapter 2

Materials and Methods

2.1 General

2.1.1 Chemicals

Ammonium persulfate (APS), bovine serum albumin (BSA), dimethyl sulphoxide (DMSO), ethylene glycol tetraacetic acid (EGTA), ethidium bromide, gluconic acid, glycerol, hydrogen peroxide (H_20_2), methyl cellulose, β-mercaptoethanol, paraformaldehyde, phenylmethylsulphonyl fluoride (PMSF), sodium dodecyl sulphate (SDS), sodium orthovanadate, tetramethylethylenediamine (TEMED), TrisAcetate, Triton X-100 and Tween®20 were purchased from Sigma Aldrich. Chloroform, ethanol, glycine, hydrochloric acid, methanol, sodium chloride, sodium hyrodxide and sucrose were purchased from VWR. Bromophenol blue, D-glucose, isopropanol, n-butanol and tris(hydroxymethyl)aminomethane (TRIS) were purchased from Fisher. Citric acid was purchased from Fluka.

2.1.2 Statistical analysis

All data was expressed as mean ± standard error of the mean. To make comparisons between groups standard unpaired two-tailed Student's *t*-tests, one-sample Student's t-tests or repeated-measures two-way ANOVAs with Bonferroni post-tests were carried out, using GraphPad software (Prism5). A $p \leq 0.05$ value was considered statistically significant. Degree of significance was expressed as follows: *$p<0.05$, **$p<0.01$ and ***$p<0.001$.

2.2 Animals

2.2.1 Maintenance of animal lines

All animal procedures were performed in accordance to Home Office guidelines under the project license PPL 60/4280 held by Michael Ashford and personal license PIL 60/13320. Animals were maintained under a 12 hour light/dark cycle and at a controlled temperature (21°C), with free access to normal chow (NC) diet (7.5% fat, 75% carbohydrate and 17.5% protein by energy) (RM1 diet, Special Diet Services) and water. During high-fat feeding studies animals had free access to water and were fed a 45% high-fat diet (HFD) (45% fat, 35% carbohydrate and 20% protein by energy) (824053; Special Diet Services) or a 60% HFD (58% fat, 25.5% carbohydrate and 16.4% protein by energy) (824054; Special Diet Service).

2.2.2 BACE1 knock-out mouse

BACE1$^{-/-}$ mice were generated by GlaxoSmithKline and maintained on a C57BL/6J background in-house (Ninewells Hospital & Medical School, University of Dundee). Mice were generated where the β-galactosidase reporter gene (*LacZ*) is inserted within the BACE1 locus where it precludes BACE1 gene expression allowing identification and visualisation of BACE1 gene expression (Harrison et al. 2003).

2.2.3 *hAPP*$_{swe}$ transgenic mouse

Transgenic mice were generated to express all isoforms of the human amyloid precursor protein (APP) containing the Familial Alzheimer Disease (FAD) associated Swedish mutation K67ON/M671L (strain name: B6.129-Tg(APPsw)40Btla/Mmjax, stock number: 034831; Jackson Laboratories). Hemizygous mice have a two to three fold increase in endogenous *APP* levels. Mice were maintained on C57Bl/6J background.

2.2.4 RIP-cre transgenic mouse

Transgenic mice carrying the RIP-cre transgene which contains a 668bp fragment of the rat insulin II promoter, cre recombinase and a 2.1kb fragment from the human growth gene were generated (strain name: B6. Cg-Tg(Ins2-cre)25Mgn/J, stock number: 003573; Jackson Laboratories). The resulting transgene is expressed in the pancreatic beta cell and in areas of the hypothalamus. Mice were maintained on a C57BL/6J background in-house. RIP-Cre transgenic mice were crossed with Z/EG mice, expressing GFP upon cre-mediated excision, allowing visualisation of RIP-cre expression. Whole brains were kindly provided by Dr. Mark Smith, Imperial College London.

2.2.5 POMC-GFP transgenic mouse

Mice were generated to express enhanced green fluorescent protein (EGFP) in the mouse *POMC* promoter/enhancer regions (strain name: C57BL/6J-Tg (POMC-EGFP)1Low/J, stock number: 009593; Jackson Laboratories). Fluorescence is detected in neurons within the hypothalamus, pituitary, medulla and in a proportion of cells in the dentate gyrus of the hippocampus. Mice were maintained on a C57Bl/6J background. Whole brains were kindly provided by Professor Lora Heisler, University of Aberdeen.

2.2.6 Neuropeptide Y-GFP transgenic mouse

Mice were generated expressing the tau (MAPT)-sapphire green fluorescent protein (GFP) under transcriptional control of the mouse *NPY* promoter (strain name: B6.Cg-Tg

(NPY-MAPT/Sapphire)1Rck/J, stock number: 008321; Jackson Laboratories). Fluorescence is detected in neuronal populations within the arcuate nucleus of the hypothalamus. Mice were maintained on a C57BL/6J. Coronal brain sections were kindly provided by Professor Lora Heisler, University of Aberdeen.

2.2.7 GAD67 transgenic mouse

Knock-in mice expressing EGFP under control of the glutamic acid decarboxylase 67 (GAD67) promoter were generated (Tamamaki et al. 2003), with GAD67 utilised as a marker of γ-aminobutyric acid (GABA). GFP expression is found throughout the adult brain in GABAergic neurons. Heterozygous mice with the GAD67-GFP allele were maintained on a C57BL/6J background. Mice were kindly provided by Dr. Delia Belelli, Division of Neuroscience, University of Dundee.

2.2.8 Vglut2-ires-cre transgenic mouse

Knock-in mice were generated expressing cre recombinase in excitatory glutamatergic neuronal cell bodies (strain name: Slc17a6$^{tm2(cre)Lowl}$/J, stock number: 016963; Jackson Laboratories). Cre expression is detected in areas including the thalamus, paraventricular nucleus and ventromedial hypothalamus. Mice were maintained on a C57BL/6J background. Vglut2-ires-cre mice were crossed with Z/EG mice, expressing GFP upon cre-mediated excision, allowing visualisation of Vglut2 expression. Whole brains were kindly provided by Dr. Mark Smith, Imperial College London.

2.2.9 SF-1-cre transgenic mouse

Transgenic mice were generated to express cre recombinase in steroidogenic factor-1 neurons (strain name: Tg (Nr5a1-cre)7Lowl/J, stock number: 012462; Jackson Laboratories). Cre expression is detected in the ventromedial hypothalamus, the pituitary, gonad and adrenal tissue. Mice were maintained on a C57BL/6J background. SF-1-cre transgenic mice were crossed with Z/EG mice, expressing GFP upon cre-mediated exicision, allowing visualisation of SF-1 expression. Whole brains were kindly provided by Dr. Mark Smith, Imperial College London.

2.2.10 Genotyping of animals by PCR

Polymerase-chain reaction (PCR) amplification of DNA and relevant primers (Table 2.1 and Table 2.3) was performed in order to genotype mouse lines. Once weaned mice were ear-notched for identification and the ear-notch collected for DNA extraction. DNA extraction was achieved by pre-mixing 100µl of extraction buffer (E7526; Sigma) with

25µl of tissue preparation solution (T3073; Sigma), with care taken to ensure the sample was fully submerged. Samples were vortexed and incubated for 10 minutes at room temperature, followed by a 3 minute incubation at 95°C. 100µl of neutralisation buffer (N3910; Sigma) was added, the sample vortexed and placed on ice. Extracted DNA was stored at -20°C until required for PCR. DNA was amplified using Novagen® KOD Hot Start Polymerase kit (71086; Merck Millipore), with relevant primers for the mouse line being genotyped (as detailed in Table 2.1 and Table 2.3).

Primer	**Sequence 5'→3'**
LacZ forward	GAC CAG CCC TTC CCG GCT GTG CCG
LacZ reverse	GCC GAC CAC GGG TTG CCG TTT TCA
BACE1$^{-/-}$ forward	CGC TGC ACT GGC TCC TGC TAT GGG
BACE1$^{-/-}$ reverse	TCT CCA CAT AGT CCT GGC CGG

Table 2.1 Primer sequences used for genotyping *BACE1*$^{-/-}$ mice.

2.2.10.1 Genotyping of *BACE1*$^{-/-}$ mice

Primer sequences (Sigma Aldrich) required for genotyping of *BACE1*$^{-/-}$ mice are shown in Table 2.1. Two PCR master-mixtures were prepared (Table 2.2) using the Novagen® KOD Hot Start Polymerase kit, one containing *LacZ* primers and one containing BACE1 primers (Table 2.1). 5µl of extracted DNA and 45µl of PCR master-mix was added to two PCR tubes (Star Lab) and placed in a Veriti® 96-well Thermal Cycler machine (Applied Biosystems) using an approximately 45 minute cycle protocol shown in Table 2.4. PCR products were mixed with loading dye (G2101; Promega) and ran on an ethidium bromide infused 1% agarose gel, with a DNA ladder (G1881; Promega) for reference. PCR products were ran at 120V for approximately 35-40 minutes in Tris-acetate-EDTA (TAE) buffer (T9650; Sigma). The gel was imaged with a GeneFlash Imager (Syngene Bioimaging) by exciting the ethidium bromide stained DNA under a UV light. These two reactions allow detection of the *LacZ* gene (299 kDa band) and the *BACE1* gene (200 kDa band) respectively, and the genotype of the animals is determined by the presence or absence of these bands. A wild-type (WT) mouse was identified by the absence of a *LacZ* band, a *BACE1*$^{-/-}$ mouse identified by the absence of a *BACE1* band (*BACE1* has been replaced by *LacZ*) and a heterozygote mouse identified by the presence of both bands present (only one *BACE1* allele has been replaced by *LacZ*).

Component	**Volume (*BACE1*$^{-/-}$ mice)**		**Volume (*hAPPswe* mice)**	
KOD 10x buffer	5µl		5µl	
25 mM $MgSO_4$	3µl		3µl	
dNTPS (2mM each)	5µl		5µl	
Nuclease-free water	29.5µl		26µl	
KOD Taq	1µl		1µl	
Primers	BACE1 fwd	0.75µl	Tg fwd	1.5µl
	LacZ fwd	0.75µl	Tg rev	1.5µl
	BACE1 rev	0.75µl	WT fwd	1µl
	LacZ rev	0.75µl	WT rev	1µl

Table 2.2 PCR master-mix components and volumes required for genotyping of *BACE1*$^{-/-}$ and *hAPPswe* mouse lines.

2.2.10.2 Genotyping of *hAPP$_{swe}$* mice

Primer sequences required for genotyping *hAPPswe* mice (Jackson Laboratories) are shown in Table 2.3. A PCR master-mix was prepared (Table 2.2) using the Novagen® KOD Hot Start Polymerase kit, containing WT and transgenic (Tg) primers (Table 2.3). Using a similar methodology as described above, 5µl of extracted DNA and 45µl of PCR master-mix was added to PCR tubes and placed in a PCR machine. PCR protocol cycle performed is shown in Table 2.4. Obtained PCR products were ran on an agarose gel and visualised. The reaction detects a WT band at approximately 200kDa and a Tg band at approximately 84kDa molecular weight. The WT band serves as a control and the presence of a Tg band indicates a transgenic *hAPP$_{swe}$* mouse.

Primer	**Sequence 5'→3'**
oIMR6938 (Tg fwd)	CTT CAC TCG TTC TCA TTC TCT TCC A
oIMR6939 (Tg rev)	GCG TTT TTA TCC GCA TTT CGT TTT T
oIMR8744 (WT fwd)	CCA ATG TTG CTT GTC TGG TG
oIMR8745 (WT rev)	GTC AGT CGA GTG CAC AGT TT

Table 2.3 Primer sequences used for genotyping *hAPP$_{swe}$* mice.

	***BACE1*$^{-/-}$ Mice**			***hAPPswe* Mice**		
Step	**Temperature**	**Duration**		**Temperature**	**Duration**	
Polymerase activation	95°C	2 min		95°C	180 sec	
Denaturation	95°C	20 sec	x35	95°C	30 sec	x35
Annealing	62°C	15 sec		67°C	30 sec	
Elongation	70°C	7 sec		72°C	30 sec	
Terminal Elongation	/	/		72°C	300 sec	
Hold	4°C	∞		4°C	∞	

Table 2.4 PCR cycle details for genotyping of *BACE1*$^{-/-}$ and *hAPPswe* mouse lines.

2.2.11 Intracerebroventricular (ICV) surgery

Osmotic minipumps connected to brain infusion kits (Alzet®) were utilised to centrally deliver inhibitors in diet-induced obese (DIO) WT C57BL/6J mice. Minipumps were primed by filling the pump using a syringe and blunt ended needle (provided in pump kit) with compound or vehicle at 37°C for 40 hours, to allow the pump to equilibrate and reach a steady pumping rate. The pump was then connected to the brain infusion assembly (a cannula connected to the pump via a catheter), ready for implantation.

Mice were anaesthetised using a combination of 5% isoflurane (Abbott Laboratories) and medical oxygen (BOC gases) delivered at a flow rate of 1.5-2L/minute via standard Boyle's Apparatus (Fluovac, Harvard Apparatus). The correct level of anaesthetic was confirmed by an absence of foot reflexes. Mice were fitted into a nose cone delivering a 1.5-2% concentration of isoflurane in oxygen to maintain anaesthesia during surgery. Mice were shaved and placed in a stereotaxic frame (Harvard Apparatus), with bars inserted into the external auditory meatus to prevent lateral head movements. Once secured in the frame the mouse was wiped with ethanol for sterility and a mid-line incision was made through the scalp, the area exposed and the skull thoroughly dried. The canula was lowered and pushed directly through the skull using the stereotaxic apparatus to target the lateral ventricle and secured into place using glue. The original incision was cut to the back of the skull and hemostats were inserted, gently opening and closing, to create a pocket in the back of the mouse. The minipump was inserted into the pocket, leaving

room for the catheter to move slightly and the incision closed using sutures. Mice were monitored regularly following surgery.

All ICV surgery was performed by Dr. Paul J Meakin.

2.3 Metabolic studies

2.3.1 Inhibitor studies

Unless otherwise stated, studies testing compounds were performed on WT C57BL/6J male mice (aged 8-10 weeks) fed a HFD for a period of 20 weeks to induce obesity. Compounds (Table 2.5) were administered via oral gavage, using gavage needles, or delivered by osmotic minipump connected to a brain infusion kit, as previously described (section 2.2.11). All studies were performed for a period of 28 days, during which time body weight and food intake measurements were taken daily. Where possible further measurements were carried out, including glucose and insulin tolerance tests and assessments of body composition. Mice were maintained on a HFD during the course of these studies and had free access to water at all times.

Compound	**Compound Type**	**Vehicle**	**Dose**	**Route of Administration**
AZ4217 (AstraZenaca)	BACE1 inhibitor	Gluconic Acid	50mg/kg	Oral gavage (daily)
Merck-3 (In-house)	BACE1 inhibitor	DMSO	10mg/kg,	Osmotic minipump (ICV surgery)
AZ3839 (In-house)	BACE1 inhibitor	Gluconic Acid	43mg/kg	Oral gavage (daily)
GI254023X (In-house)	ADAM10 inhibitor	DMSO	10mg/kg	Osmotic minipump (ICV surgery)

Table 2.5 Compounds, corresponding vehicles, dose and route of administration used during *in-vivo* metabolic studies.

2.3.2 Glucose tolerance test

Mice were fasted overnight prior to glucose tolerance testing. Fasted blood glucose levels were measured using a glucometer by extracting blood from the tail vein onto a glucose

measuring strip (Contour®, Bayer). D-glucose was administered at either 2mg/kg or 1mg/kg (in PBS) via intraperitoneal (i.p) injection and blood glucose levels measured at 15, 30, 45, 60 and 120 minutes post-injection using a glucometer.

2.3.3 Insulin tolerance test

Mice were fasted for four hours prior to testing and fasted blood glucose levels were measured using a glucometer, as previously described. Human insulin (Actrapid®, Novo Nordisk) was administered at 0.75IU/kg (in PBS) via i.p injection and blood glucose levels measured at 15, 30, 60, 90 and 120 minutes post-injection using a glucometer.

2.3.4 Echo MRI scanning

Body composition was assessed using a magnetic resonance analyser (Echo MRI™, Echo Medical Systems). Mice were weighed and placed in a cylinder tube to be inserted into the machine. Three repeat scans were taken resulting in a measurement of fat and lean mass. Raw fat and lean mass levels were analysed, and measurements were calculated as a percentage of total body weight.

2.3.5 Blood biochemistry

Animals were sacrificed by cervical dislocation, the head removed and blood collected in EDTA-coated tubes (Startedt AG & Co.). Whole blood was centrifuged at 3500 rpm for 15 minutes at 4°C to separate plasma. Plasma samples were stored at -80°C until required.

2.3.5.1 Leptin ELISA

To measure the leptin concentration in serum samples a Mouse Leptin Quantikine® ELISA (R&D Systems) was used according to the manufacturer's instructions. In brief, all components of the kit were allowed to equilibrate to room temperature prior to carrying out the assay. Assay diluent RD1W (50µl) and 50µl of sample (each ran in duplicate) were added to the 96-well microplate. Working leptin standards provided were also ran in duplicate. Solutions were mixed by gently tapping the frame of the plate for approximately 1 minute prior to incubation for 2 hours at room temperature. Wells were washed (5x) in 400µl of wash buffer, ensuring all liquid was removed each time. Mouse leptin conjugate (100µl) was added to each well and incubated for 2 hours at room temperature followed by repeating the washing step. Substrate solution (100µl) was added to each well and incubated for 30 minutes at room temperature, covered to protect from light exposure. The reaction was stopped by adding 100µl of stop solution, initiating a colour change from blue to yellow, and mixed by gentle tapping. The absorbance was

measured within 30 minutes on an EnVision® 2104 Multilabel Plate Reader (Perkin Elmer), measuring the absorbance at 450nm and subtracting the absorbance at 540nm/570nm. The means of the absorbance of each sample was calculated and using the leptin standards a standard curve was plotted of mean absorbance against concentration, which allowed the concentration of leptin in samples to be calculated.

2.3.5.2 Insulin ELISA

To measure the insulin concentrations in serum samples an Ultra Sensitive Rat Insulin ELISA Kit (90060; Crystal Chem Inc.) was used according to the manufacturer's instructions. In brief, the 96-well antibody-coated microplate was allowed to equilibrate to room temperature and 95µl of sample diluent and 5µl of samples added to wells, with all samples ran in duplicate. Working insulin standards provided were also ran in duplicate. The plate was covered and incubated for 2 hours at 4°C followed by washing (5x) in 300µl of wash buffer, ensuring all liquid was removed each time. Anti-insulin enzyme conjugate (100µl) was added to each well and incubated for 30 minutes at room temperature, followed by washing (5x) as before. Enzyme substrate solution (100µl) was added to each well and incubated for 40 minutes at room temperature, covered to protect from light exposure. The reaction was stopped by adding 100µl of enzyme stop solution to each well and the absorbance measured within 30 minutes on an EnVision® 2104 Multilabel Plate Reader (Perkin Elmer). The absorbance at 450nm was measured and the absorbance at 630nm subtracted. The means of the absorbance of each sample was calculated and using the insulin standards a standard curve was plotted of mean absorbance against concentration, which allowed the concentration of insulin in serum samples to be calculated.

2.3.6 *In vivo* leptin treatment

Age-matched adult animals, fed a NC chow diet, were dosed with 4mg/kg leptin (498-OB; R & D Systems) via i.p injection following an overnight fast. Animals were sacrificed by CO_2 1 hour post leptin injection, and perfused fixed with 4% paraformaldehyde (PFA) in PBS. For perfuse fixation mice were deeply sacrificed by CO_2, dissected to expose the heart and slowly flushed with 10ml PBS via the apex of the heart, until all blood ran clear, followed by 10ml 4% PFA. Whole brains were removed and processed for imaging studies, or the brains dissected and snap frozen for Western blot analysis.

2.4 Gene expression studies

2.4.1 Tissue preparation

Mice were sacrificed by cervical dislocation and tissues harvested. Tissue was snap frozen in liquid nitrogen and stored at -80°C until further use. Frozen tissue was transferred from -80°C to a tight-fit glass homogenizer and homogenised in 1ml of TRI Reagent (T9424; Sigma Aldrich). Tissue was homogenized on ice until a solution formed, which was subsequently transferred to a 1.5ml eppendorf and kept on ice Samples were stored at -80°C until further use.

2.4.2 RNA extraction

Homogenised samples were transferred from -80°C to a 1.5ml eppendorf and allowed to stand at room temperature for five minutes. For white adipose tissue, samples were additionally centrifuged at 13000 rpm for 15 minutes to remove any fatty layer present before continuing. For phase separation 0.2ml of chloroform was added to each sample and shaken vigorously by hand. Samples were allowed to stand at room temperature for 15 minutes before centrifugation at 12000 rpm for 15 minutes. This step separates the RNA into an aqueous phase which can be isolated by transferring the clear phase to a fresh eppendorf and adding 0.5ml isopropanol, mixing by inverting the tube. This was allowed to stand at room temperature for 10 minutes before centrifugation at 12000 rpm for 10 minutes, resulting in the RNA forming a pellet. The supernatant was removed and the pellet washed in 1ml of 75% ethanol. Samples were vortexed and centrifuged at 12000 rpm for 5 minutes and the pellets air-dried for 7 minutes in a fume hood. Pellets were dissolved in 30µl of nuclease-free water (Ambion) by repeated pipetting at 55-60°C for 15 minutes. Once dissolved the purity and concentration of RNA was measured using a NanoDrop ND-8000 Spectrophotometer and NanoDrop 8000 V.2.3.2 Software. Nuclease-free water was used to blank the machine and to measure samples 1.5µl of total RNA was loaded. The concentration of RNA was measured in ng/µl at an absorbance of 260nm and a purity ratio of ≥1.7 from a reading of 260/280nm was considered useable. RNA was stored at -80°C until further use.

2.4.3 cDNA synthesis

RNA samples were converted to first-strand cDNA using a SuperScript™ II RT kit (Invitrogen by Life Technologies; 10864-014). In brief, a mixture of random primers (1µl), total RNA (1µg), 10mM dNTP mix (1µl) and nuclease-free water (to a final volume

of 13µl) was incubated for 5 minutes at 65°C, briefly chilled on ice and vortexed. 4µl of 5x first-strand buffer and 2µl of 0.1M DTT were added to the mixture and mixed gently before adding 1µl of SuperScript™ II RT, gently mixing by pipetting. The mixture was incubated for 1 minute at room temperature, followed by a 50 minute incubation at 42°C and the reaction stopped by heating the mixture to 70°C for 15 minutes. cDNA was diluted (1:10) with nuclease-free water to give a final concentration of 1µg in 200µl and stored at -20°C until required.

2.4.4 Real-time PCR

Real-time PCR was performed using Taqman® gene expression assays (Applied Biosystems) which uses reverse transcription-PCR (RT-PCR) to detect specific genes and measure relative expression. A fluorescent FAM™ reporter dye is connected to the Taqman® probe which becomes released during the RT-PCR reaction and the resulting fluorescence is detected, ultimately measuring relative levels of the probe. A PCR reaction mixture (Table 2.6) for each DNA sample and gene of interest was added to a 1.5ml eppendorf and mixed. 17.5µl of the reaction mixture was added to a 96-well plate (Nunc) and 2.5µl of DNA. The plate was spun briefly in a Centrifuge 5810R (Eppendorf) to collect the contents of the wells at the bottom and placed in a real-time PCR machine (7900HT; Applied Biosystems). The PCR cycle protocol used is shown in Table 2.7. The PCR machine generates a copy number which is used to calculate mRNA expression levels and this is normalised against *actin* as an endogenous control. Details of all probes used to identify genes of interest are shown in Table 2.8.

Component	**Volume**
cDNA	2.5µl
Mastermix (Applied Biosystems)	10µl
Primer/Probe (Life Technologies)	1µl
Nuclease-free water	6.5µl

Table 2.6 Components of PCR reaction mixtures.

Step	Temperature	Duration	
Initial	95°C	10 min	
Denaturation	95°C	15 sec	x40
Annealing	60°C	1 min	
Elongation	60°C	1 min	

Table 2.7 Real-time PCR cycle details.

Probe Name	Specificity	Code
Actin	Mouse	4352663
Arg-1	Mouse	Mm00475988m1
Cartpt (CART)	Mouse	Mm0048906_m1
Dio2	Mouse	Mm00515664_m1
Emr1 (F4/80)	Mouse	Mm00802529_m1
IFN-ϒ	Mouse	Mm01168134_m1
IL-10	Mouse	Mm00439614_m1
IL-6	Mouse	Mm00446190_m1
IL1β	Mouse	Mm00434228_m1
Leptin	Mouse	Mm00434759_m1
Leptin Receptor	Mouse	Mm00440181_m1
MCP-1	Mouse	Mm00441242_m1
MIP-1α	Mouse	Mm00441259_g1
MIP-1β	Mouse	Mm00443111_m1
NOS2	Mouse	Mm00440488_m1
NPY	Mouse	Mm03048253_m1
POMC	Mouse	Mm00435874_m1
Ppargc1 (PGC1α)	Mouse	Mm01208835_m1
Prdm16	Mouse	Mm00712556_m1
PTP1β	Mouse	Mm00448431_m1
RANTES	Mouse	Mm01302427_m1
SOCS3	Mouse	Mm00545913_s1
TGFβ-1	Mouse	Mm01178820_m1

TNFα	Mouse	Mm00443260_g1
UCP1	Mouse	Mm01244861_m1
UCP2	Mouse	Mm00627597_m1
UCP3	Mouse	Mm00494077_m1
YM-1	Mouse	Mm00657889_mH

Table 2.8 Summary of all Taqman® probes used in present studies.

2.5 Western blotting

2.5.1 Tissue preparation

Mice were sacrificed by cervical dislocation and tissues harvested. Tissue was snap frozen in liquid nitrogen and stored at -80°C until further use. Frozen tissue was transferred from -80°C to a tight-fit glass homogenizer (Fisher) and homogenized, as previously described (section 2.4.1), in 100-500µl (depending on tissue size) of lysis buffer (Table 2.12) added. The lysate was vortexed and centrifuged at 4°C for 15 minutes at 13000 rpm. The resulting supernatant was removed and transferred to a fresh eppendorf and stored at -20°C.

2.5.2 Determining protein content

The protein content of samples was measured using a Bradford Assay (Bradford 1976). This involves Coomassie Blue G-250 forming a complex with proteins which causes a shift in the absorbance maximum of the dye from 465nm to 595nm. The resulting absorbance can be measured and indicates the amount of protein present in a sample. In brief, 1µl of sample and 9µl of distilled water are added to a 96-well plate (Nunc), followed by the addition of 250µl of Bradford Reagent (B6916; Sigma Aldrich). The colour was allowed to develop for approximately 15 minutes at room temperature and the plate ran on an EnVision® 2104 Multilabel Plate Reader (Perkin Elmer), measuring the absorbance at 595nm. Serial dilutions of BSA standards were also ran so a standard curve of absorbance against protein content could be plotted allowing the lysate concentration to be calculated.

2.5.3 SDS-Page gel system

Proteins within lysates were separated according to their molecular weight using Sodium Dodecyl Sulphate Polyacrylamide Gel electrophoresis (SDS-PAGE). Lysates (containing

10-20µg of protein) were prepared by adding distilled water and sample buffer (Table 2.12) containing SDS, to add negative charges to the proteins, and Bromophenol blue, to allow visualisation of proteins as they move through the gel. A molecular weight marker (SeeBlue Plus2 pre-stained protein standard; Life Technologies) run alongside samples to identify the weight of proteins of interest.

Proteins were separated using self-poured gels with BioRad gel casting equipment. Lower gel (Table 2.9) was poured into the casting equipment, which comprised of two glass plates held together tightly with plastic clips (BioRad), and topped with a layer of 50:50 (v/v) solution of distilled water and n-butanol to straighten the top of the lower gel. This was allowed to set for approximately 15-30 minutes and once set the water:butanol solution was discarded, the gels rinsed with water and a stacking gel (Table 2.9) poured on top. 10- or 15-well plastic combs were placed within the stacking buffer, which contained a pinch of bromophenol blue for visualisation, and allowed to set for approximately 15-30 minutes. When set the combs were removed and electrophoresis performed in gel running tanks (BioRad) filled with 10x Tris-Glycine running buffer (National Diagnostics) in distilled water. Electrophoresis ran for approximately 1-2 hours at 150V.

	Lower Gel	**Stacking Gel**
Component	**Volume (10% gel)**	**Volume (4% gel)**
dH_2O	6.2ml	4.2ml
0.5M Tris (pH 6.8)	4.7ml	1.9ml
30% Acrylamide	5.6ml	1.25ml
10% SDS	165µl	75µl
TEMED	16.5µl	8µl
20% APS	83µl	75µl

Table 2.9 Components of SDS-PAGE gels.

2.5.4 Transfer of proteins onto nitrocellulose membrane for immunoblotting

Once electrophoresis was complete the gel casts were removed and prised apart leaving the gel remaining on one of the glass plates. A blotting ‘sandwich’ was assembled

comprising of blotting sponges, filter paper (Whatman), the protein gel and a nitrocellulose membrane (GE Healthcare Life Sciences), which were all pre-soaked in transfer buffer (Table 2.12) prior to the assembly of the transfer module. The transfer cassette was assembled by placing blotting sponges on the white facing of the blotting cassette, followed by soaked filter paper. The nitrocellulose membrane was carefully placed on top of the gel avoiding the introduction of air bubbles, which was then flipped over and placed onto the filter paper and the glass plate removed. This was topped with another piece of soaked filter paper, rolled to remove any bubbles and another blotting sponge placed on top. The black facing of the cassette was then closed and the assembled cassette placed in a transfer tank (BioRad), along with an ice pack, filled with transfer buffer. Electrophoresis was run for 1 hour at 100V. Once the transfer was complete the cassette was removed and the membrane placed in a blotting dish and rinsed with tris-buffered saline-tween (TBST). The membrane was stained with Ponceau S Stain (Sigma Aldrich) to ensure complete transfer of proteins onto the membrane. Membranes were then washed in TBST to remove ponceau staining.

2.5.5 Immunoblotting

To reduce non-specific antibody binding membranes were blocked, prior to immuno-blotting, with 10% dried milk (Marvel™) in TBST for 1 hour at room temperature on a rocking platform. Membranes were briefly washed in TBST to remove any remaining milk and incubated in primary antibody (Table 2.10) made up in 5% BSA in TBST overnight at 4°C on a rocking platform. Following primary antibody incubation the membrane was washed (5x 5 minutes) in TBST on a rocking platform and blocked, again, in 4% BSA in TBST for 20 minutes at room temperature. Membranes were incubated in secondary antibody (Table 2.11) made up in TBST for 1 hour at room temperature on a rocking platform, followed by washing (5x 5 minutes) in TBST on a rocking platform. Membranes were placed in fresh TBST and stored at 4°C until imaging.

2.5.6 Analysis

Membranes were imaged on a Licor Odyssey Infrared Scanner and densitometry analysis perfomed on Image Studie Lite Version 4.0 (Licor). All protein expression was normalised against actin as an endogenous control.

2.6 Imaging studies

2.6.1 Tissue preparation

Mice were sacrificed by CO_2 and perfused fixed, as previously described (section 2.3.6). Tissues were removed and post-fixed overnight in 4% PFA at 4°C and for immunofluorescence (IF) this was followed by 30% sucrose in PBS until the tissue sank or for immunohistochemistry (IHC) transferred to 10% neutral buffered formalin (v/v) (4% Formaldehyde) (NHS Tayside Tissue Bank) until required. For IF brain studies, once fixed, tissue was placed in a plastic mould with M-1 embedding matrix (Thermo Scientific) and frozen on a bed of dry ice and isopropanol. Once frozen, moulds were wrapped in parafilm and stored at -80°C. For fluorescent *in situ* hybridization (FISH) mice were sacrificed by CO_2 and perfused fixed with 4% PFA (with 2mM EGTA). Brains were post fixed as previously described, and whole brains washed (2x10 minutes) in PBS (with 2mM EGTA) with gentle agitation on an orbital shaker at room temperature. Brains were then frozen and stored as previously described.

2.6.2 Tissue sectioning

For IF and FISH whole brains were sectioned using a cryostat 5040 Microtome (Bright). Frozen embedded brains were removed from moulds and glued onto a cryostat chuck using cryo-embedding compound (Bright). The chuck was placed in the cryostat, sprayed with cryo-spray (Bright) to quick freeze the cryo-embedding compound and left for approximately 20 minutes to equilibrate to the cryostat temperature (approximately -20°C). For IF, sections were cut using microtome blades (Feather) 15-30µm in thickness and collected serially, using a paintbrush, in PBS. Sections were stored at 4°C in PBS until used, and for long-term storage were kept at -20°C in cryo-protectant solution (Table 2.12). For FISH, sections were cut as previously described, 30µm in thickness, and collected serially in 50% EtOH in PBS. Sections were washed (1x 10 minutes) in fresh 50% EtoH followed by washes (2x 10 minutes) in 100% EtoH. Sections were stored at -20°C in 100% EtoH until used. Brains for all studies were sectioned coronally (unless stated) in accordance with The Mouse Brain in Stereotaxic Coordinates (Paxinos & Franklin, Second Edition) focussing on bregmas (approximately -1.22mm to -1.96mm) from the hypothalamic region. For IHC on peripheral tissue (white adipose tissue), samples were removed from neutral buffered formalin and processed overnight on a Leica Peloris II processor using an 8 hour xylene standard protocol (NHS Tayside Standard Protocol). Tissue was embedded in paraffin wax using a Tissue-Tek embedding centre

(Sakura), ready for sectioning into 4µm thick sections using a microtome (Leica RM 2135). Sections were collected onto Superfrost® glass microscopic pulse slides (VWR) and dried for 1 hour at room temperature, before staining.

For IHC samples were processed by Tayside Tissue Bank.

2.6.3 Immunofluorescence on free-floating sections

Where necessary antigen retrieval was performed to un-mask epitopes hidden during protein cross-linking (occurring due to PFA fixation). This involved pre-heating 10mM citric acid (pH 6.0) in 24-well plates (Nunc) to 80-100°C in an oven (Genlab) and placing tissue sections (1 section/well) in the heated citric acid for 30 minutes. Sections were cooled to room temperature in the acid. Following a quick wash in PBS sections were permeabilised, to allow antibody penetration through the tissue in 0.1% triton X-100 in PBS (PBST) for 1 hour on an orbital shaker. Sections remained on an orbital shaker for gentle agitation for the remainder of the protocol. To prevent non-specific binding of antibodies sections were blocked in 5% BSA in PBST for 1 hour prior to primary antibody incubation. Primary antibodies (Table 2.10) were diluted in blocking solution and incubated with sections overnight at 4°C. Following removal of primary antibodies sections were washed (5x 5 minutes in PBST) and, for single-labelling experiments, incubated in secondary antibody (Table 2.11) in PBST for 1 hour at room temperature. Sections were washed again (5x 5 minutes in PBST), followed by a final wash in PBS, to remove any remaining detergent, before mounting. Tissue sections were mounted onto glass microscopes slides (VWR International) with Vectashield anti-fade medium containing the nuclear marker 4',6-diamidino-2-phenylindole (DAPI) (H-1200; Vector Laboratories). Glass coverslips were placed over the sections and sealed with nail varnish. For dual-labelling experiments sequential staining was performed whereby following removal of the primary antibody and washes a second primary antibody of a different host species was applied for another overnight incubation. The same method was adopted for secondary antibody incubation steps, whereby following removal of the first secondary antibody and washes a second secondary antibody was applied. Sections were mounted as described above and slides stored at 4° in the dark until imaged.

For pSTAT3 staining a 3,3' diaminobenzidine (DAB) staining protocol was performed using a Vectastain®Elite®ABC kit (PK-6100 Series, Vector Laboratories), an avidin/biotin blocking kit (SP-2001; Vector Laboratories) and a liquid DAB and substrate chromogen system (K3468; DAKO), prior to IF. First, antigen retrieval and

permeabilisation were performed, as previously described (section 2.6.3). Sections were incubated in 0.6% H_20_2 in PBST, to block endogenous peroxidases, for 30 minutes and washed again (5x 5 minutes in PBST) before blocking. Sections were blocked in PBST with avidin solution (100µl/ml) and serum (15µl/ml) (provided in kit) for one hour prior to primary antibody incubation. pSTAT3 antibody (Table 2.10) was diluted in a blocking solution containing biotin solution (100µl/ml) and serum (15µl/ml) in PBST and incubated with sections overnight at 4°C. Following removal of primary antibody sections were washed (5x 5 minutes in PBST) and incubated with a biotinylated secondary antibody (5µl/ml) (provided in kit) in PBST with serum (15µl/ml) for 1hour. Sections were washed (5x 5minutes in PBST) and incubated in an Avidin/Biotinylated enzyme complex, prepared by mixing 2 drops from both solutions A and B (provided in kit) per 5ml of PBST, 30 minutes prior to use to allow the solutions to form a complex, for 2 hours at room temperature. Following removal of the complex sections were washed (5x5 minutes + 1x 10 minute in PBST) and developed in DAB stain prepared at a concentration of 1:50 of DAB + chromogen (provided in kit) in DAB + substrate buffer (provided in kit) for 4 minutes. The DAB stain was removed and sections washed (5x 5 minutes + 1x 10 minutes in PBST). For dual-labelling, IF was performed on the sections as previously described from the blocking stage.

2.6.4 Immunofluorescence on paraffin-embedded sections

Sections were heated at 60°C, in an oven, for 45 minutes, to remove paraffin then cooled to room temperature for 10 minutes. Sections were submerged in Histo-Clear™ III histological clearing agent (HS-204; National Diagnostics) for 20 minutes, followed by 100% ethanol for 10 minutes and subsequently fresh 100% ethanol for 5 minutes. Sections were washed in distilled water for 10minutes before undergoing antigen retrieval, which was performed as previously described (section 2.6.3). Sections were permeabilised in 0.5% PBST for 1 hour and blocked in 5% BSA in 0.5% PBST for 1 hour, both at room temperature before primary antibody incubation. Primary antibodies (Table 2.10) were prepared in blocking solution and sections incubated overnight in a humidified chamber at 4°C. The humidified chamber was removed and sections were allowed to equilibrate to room temperature for 10 minutes, before washing (2 x 10 minutes) in PBS. Excess buffer was drained from the sections and incubated in secondary antibody (Table 2.11) prepared in 0.1% PBST for 1 hour at room temperature. Sections were washed (2 x 10 minutes) in PBS followed by a distilled water wash for 10 minutes, before dehydrated through a series of ethanol steps; 70% for 2 minutes, 90% for 2 minutes

and 2 x 5 minutes in 100%. Sections were air dried for approximately 30 minutes at room temperature before mounting as previously described (2.6.3).

2.6.5 Fluorescent *in situ* hybridization (FISH)

All FISH protocols were provided by and performed under the supervision of Dr Kim Dale's Lab (School of Life Sciences, University of Dundee).

2.6.5.1 Probe generation

Primer sequences for POMC (151-850bp, Genbank: NM_008895.4) and NPY (101-501bp, Genbank: NM_023456.2) were chosen, amplified and cloned in a pBluescript II Sk(-) plasmid by Dundee Cell Products. To generate antisense cRNA probes the plasmid was linearised using a BamHI restriction enzyme for 1.5 hours at 37°C. To confirm the digestion was successful and the product was the correct size, linearised DNA was ran on a 1% agarose gel in TBE electrophoresis buffer (1X). Linearised DNA was purified using a QIAquick® PCR Purification kit (28104; Qiagen) according to the manufacturer's instructions. In brief, samples were diluted 1:5 with buffer (provided in kit) and added to columns in 2ml collections tubes (provided in kit) Samples were centrifuged for approximately 1 minute and the flow-through discarded. DNA was washed in 750µl of buffer and centrifuged and the flow-through discarded again, to ensure all wash buffer was removed. DNA was eluted by adding 50µl of buffer EB (provided in kit) and centrifuged as described. To ensure the purification was successful DNA was ran on a 1% agarose gel, as previously described. The concentration of DNA was measured using a Nanodrop spectrophotometer and an in vitro transcription (IVT) carried out to synthesis the RNA. In brief, the IVT involved mixing 1µg of DNA, 4µl of transcription optimised 5X buffer (P118B; Promega) , 2µl DTT (P117B; Promega), 2µl digoxigenin (DIG)-labelling mix (11277073910; Roche), 2µl T7 RNA polymerase (P207B; Promega), and 1µl RNase inhibitor, made up to a final volume of 20µl with nuclease-free water, and incubating this for 2 hours at 37°C. After the IVT the template DNA was cut using DNase and RNase (04716728001; Roche) and incubated for 1 hour at 37°C. The RNA was purified using a Purelink™ RNA Mini Kit (12183018A; Ambion) according to the manufacturer's instructions. In brief, lysis buffer was added to samples to protect the RNA from degradation prior to the protocol. EtoH (70%) was added to each sample and vortexed. Samples were transferred to collection tubes (provided in kit) and centrifuged at 12000 rpm for 15 seconds. Flow-through was removed and the initial steps repeated before washing in 700µl of wash buffer I (provided in kit) and centrifuged again. Samples

were washed in 500µl of wash buffer II (provided in kit) with ethanol and centrifuged. The flow-through was discarded and wash steps repeated. The collection tube was then centrifuged at 12000 rpm for 1 minute to dry the RNA, before adding nuclease-free water and incubating at room temperature for 1 minute. Finally, samples were centrifuged at 12000 rpm for 2 minutes to elute the RNA. To ensure the IVT and purification was successful the RNA was run on a 1% agarose gel as previously described. RNA was stored at -80°C until further use.

2.6.5.2 FISH

Tissue sections were removed from -20°C and rehydrated in 50% EtoH/PBS-0.1% Tween®20 for 10 minutes on a rocking platform, followed by washing (2x 10 minutes) in PBS-0.1% Tween®20. Sections were dissected under a dissecting microscope (Leica) to cut out the arcuate nucleus of the hypothalamic region, and the remaining section disregarded. Hypothalamic sections were treated with proteinase K (Roche) in PBST (20mg/ml) for precisely 8 minutes, carefully removed and rinsed in PBS-0.1% Tween®20 before post-fixing in 4% HCHO + 0.1% glutaraldehyde in PBS-0.1% Tween®20 for 30 minutes. After post-fixation sections were washed (2x 10 minutes) in PBST on a rocking platform, followed by a 10 minute wash in 1:1 PBST/exonic hybridisation mix (Table 2.12) at 65°C. Sections were rinsed twice with exonic hybridisation mix before incubation in fresh exonic hybridisation mix for 2 hours at 65°C. This solution was then replaced with pre-warmed (65°C) exonic hybridisation mix with DIG-labeled RNA probes (80µl/ml) and incubated overnight at 65°C. The plate containing sections was taped around the edges to avoid evaporation during the incubation period. All probes were recovered and stored at -20°C for re-use and sections were rinsed twice in pre-warmed (65°C) exonic hybridisation mix and transferred to 12-well plates (Nunc) to increase washing volume. Sections were washed (3x 1 hour) with pre-warmed (65°C) exonic hybridisation mix followed by a 15 minute wash in 1:1 exonic hybridisation mix/ TBST (1x TBS + 0.1% Tween®20) at 65°C. Sections were rinsed twice in TBST at room temperature on a rocking platform, followed by a 30 minute wash in fresh TBST before incubation in blocking solution. Blocking solution contained 2% blocking buffer reagent (11096176001; Roche) and 20% heat treated goat serum (Life Technologies) in TBST, and sections were blocked for 2 hours at room temperature on a rocking platform. Following blocking, sections were incubated in anti-Dig-HRP antibody (11207733910; Roche) diluted in blocking solution (1:200) overnight at 4°C on a rocking platform. Antibody was removed and sections were rinsed in TBST (3x) at room temperature

followed by washing (3x 1 hour) in TBST on a rocking platform. Fluorescence was achieved using a TSA™ Plus Cyanine 3 System (NEL744001KT; PerkinElmer) which involved transferring sections to 1.5ml eppendorf tubes and incubating in 0.25ml 1x amplification buffer (provided in kit) for 1 minute. Amplification buffer was removed and recovered to make Fluorescein-TSA solution (1:50) (provided in kit), which was added to sections (250µl/tube) and incubated for 90 minutes on a rocking platform, covered in foil to protect from light. The TSA-solution was removed and sections were transferred back into 12-well plates and washed (3x5 minutes) in TBST on a rocking platform. Sections were incubated in 1% H_20_2 in TBST for 45 minutes and washed (3x 5 minutes in TBST, and 2x 5 minutes in PBST) on a rocking platform. For dual-labelling, IF was carried out as previously described from the permeabilisation stage.

2.6.6 Immunohistochemistry

Antigen retrieval and de-paraffinisation were performed on sections using a DAKO EnVision™ Flex Target Retrieval solution (high pH) in a DAKO PT Link machine. Staining was subsequently performed on a DAKO Autostainer Link48 machine using DAB staining and a Vectastain® ABC Elite IgG kit (Vector Laboratories). Staining with the ABC kit was performed as previously described (section 2.6.3). Sections were blocked in 10% avidin solution in normal rabbit serum for 20 minutes at room temperature followed by primary antibody incubation. Primary antibodies (Table 2.10) were made up in 10% biotin solution in normal rabbit serum and incubated for 30 minutes at room temperature. Sections were then incubated in a biotinylated secondary antibody for 30 minutes at room temperature prior to a 30 minute incubation in Vectastain® Elite ABC solution. Sections were then incubated with a DAKO substrate working solution as a chromogenic agent (as previously described) twice for 5 minutes at room temperature then counterstained with EnVision™ Flex hematoxylin stain. Between all steps slides were washed briefly in tris-buffered saline (TBS). Sections were stored at room temperature until imaging.

Immunhistochemistry was performed by Tayside Tissue Bank.

Primary Antibody	Species	Dilution	Source
Actin	Rabbit	1:1000	Sigma Aldrich
BACE1	Rabbit	1:250 (IF), 1:1000 (WB)	Sigma Aldrich
BACE1	Rabbit	1:250 (IF)	Genetex
CD68	Rat	1:100 (IHC)	AbD Serotec
Insulin	Guinea-pig	1:100 (IF)	Abcam
F4/80	Rat	1:100 (IHC)	AbD Serotec
GFAP	Chicken	1:500 (IF)	Millipore
GFP	Rabbit	1:200 (IF)	Abcam
GFP	Mouse	1:200 (IF)	Abcam
GFP	Chicken	1:200 (IF)	Abcam
Glucagon	Mouse	1:100 (IF)	Sigma Aldrich
Leptin Receptor	Sheep	1:10 (IF)	In-house
NeuN	Guinea-pig	1:500 (IF)	Millipore
Perilipin	Goat	1:200 (IF)	Abcam
pSTAT3	Rabbit	1:8000 (IF)	Cell Signalling

Table 2.10 Summary of all primary antibodies and concentrations used in the present studies.

Secondary Antibody	Dilution	Source
Alexa 488	1:500 (IF)	Life Technologies
Alexa 568	1:500 (IF)	Life Technologies
Alexa 594	1:500 (IF)	Life Technologies
Alexa 647	1:500 (IF)	Life Technologies
Alexa Fluor 680 (IR dye 700)	1:10000 (WB)	Life Technologies
Alexa Fluor 790 (IR dye 800)	1:10000 (WB)	Rockland Inc.
Cy3	1:250 (IF)	Jackson ImmunoResearch

Table 2.11 Summary of all secondary antibodies and concentrations used in the present studies.

2.6.7 Confocal Microscopy

Fluorescent images were acquired using a laser scanning confocal microscope (Leica TCS SP5 II). Sections were scanned sequentially using 405 diode, Argon, HeNe 543 and/or HeNe 633 lasers. Scanning was performed bi-directionally at 400Hz, with resolution set at 1024 x 1024 pixels for all images. Unless stated, Z-stack images were taken, scanning 0.4μm steps, at either x40 or x63 magnification using an oil-objective lens on Leica Application Software (LAS). Necessary controls where included, where primary antibodies where omitted and minimal fluorescence was observed to take into account non-specific binding.

2.6.8 Light Microscopy

IHC images were acquired using a light microscope (Leica AF600). Images were taken at x10 magnification using a dry-objective lens on LAS. Necessary controls were included, where primary antibodies were omitted and minimal staining was observed to take into account non-specific binding.

2.6.9 Analysis

Images were processed on Volocity (Perkin Elmer) and Photoshop CS4 (Adobe). In Volocity single plane images from Z-stacks were merged to give maximally projected images (as representatives) and scale bars added. In some instances the 'remove noise' Volocity function was applied to images with a high background, and the contrast enhancement tool utilised to adjust brightness and contrast. Snapshots of final images were acquired and additional brightness and contrast adjustments made on Photoshop. For cell counting, Z-stack images were analysed in Fiji Imaging Software. Cells were counted manually using the multi-pointer tool, and a cell was considered 'co-localised' where staining from both fluorophores was present in the same pixels or same cell in the individual plane. The maximum resolution of the confocal microscope is 200nm in the X and Y planes and 700nm in the Z plane, therefore in cell counting experiments co-localisation is defined as an association between the two stains, whereby the sources of the staining are within this maximal resolution range, for example less than 200nm apart. Cell counting was carried out from multiple sections from different animals and the mean of the total cell count for each population, from all animals, was calculated.

Cell counting analysis was performed by Christopher McGinley (DCAT Summer Project Studentship).

Solution	Components	Volume
Cryoprotectant solution (protocol from www.ihcworld.com)	Sucrose	300g
	Polyvinyl-pyrrolidone (PVP-40)	10g
	Ethylene glycol	300ml
	0.1M Phosphate buffer	Fill to 1L
Exonix hybridisation mix (solutions supplied and made by Dr. J Kim Dale's Laboratory)	Formamide	500ml
	20X Saline Sodium Citrate (pH 5.0)	65ml
	0.5M EDTA (pH 8.0)	10ml
	tRNA (20mg/ml)	2.5ml
	Tween-20	2ml
	20% SDS	5ml
	Heparin (50mg/ml)	2ml
	Milli Q water	Fill to 1L
Lysis Buffer (5x stock)	Tris HCL (pH 7.4)	125mM
	NaF	250mM
	NaCl	0.5M
	EDTA	5mM
	EGTA	25mM
	NaPPi	50mM
	Triton X-100	5% (v/v)
Lysis Buffer (1x) (supplements added at time of use)	Sucrose	92mg/ml
	β-mercaptoethanol	1µl/ml
	1mM Sodium orthovanadate (pre-heated at 95°C for 5 minutes)	2µl/ml
	1mM Benzamidine	1µl/ml
	0.1mM PMSF	1µl/ml
Sample Buffer (4x)	0.5M Tris (pH6.8)	4ml
	Glycerol	3.2ml
	20% SDS	3.2ml

	β-mercaptoethanol	1.6ml
	Bromophenol blue	Pinch
TBE Electophoresis Buffer (10X) (solutions supplied and made by Dr. J Kim Dale's Laboratory)	Tris Base	121.1g
	Boric Acid	61.8g
	EDTA	7.4g
	RNAse-free water	Fill to 1L
Transfer Buffer	Tris Base	11.62g
	Glycine	5.86g
	Methanol	400ml
	dH_2O	1600ml
Tris-buffered Saline-Tween (TBST)	1M Tris HCL (pH 7.4)	40ml
	4M NaCl	74ml
	Tween-20	1ml
	dH_2O	Fill to 2L

Table 2.12 Components of commonly used solutions in the present studies

Chapter 3

Pharmacological reduction of BACE1 improves an obese and diabetic phenotype in mice

3.1 Introduction

BACE1-mediated APP processing is considered the primary causative factor for the symptoms associated with AD. There are numerous APP mutations which lead to familial AD (FAD) in particular, all of which occur close to or within the β-secretase cleavage site and increase Aβ levels. However, the Icelandic (A673T) mutation, which occurs adjacent to the BACE1-cleavage site, and in very close proximity to a mutation responsible for FAD, is proven to be protective against the development of AD (Jonsson et al. 2012). Jonsson *et al* found carriers of the A673T mutation had improved cognitive function and reduced BACE1-mediated processing of APP. Owing to this BACE1 has become a key target in the investigation of therapeutic strategies for AD.

Consequently, a large body of research has focused on blocking (or reducing) BACE1 activity, and in turn preventing Aβ production, as a therapeutic approach for AD. BACE1-deficient rodent models have been widely used to investigate this and many mouse lines have been developed, which demonstrate complete ablation or drastic reductions in Aβ levels. *BACE1*$^{-/-}$ mice are generally reported to be healthy, viable, fertile and display no phenotypic or genetic abnormalities (Roberds et al. 2001; Luo et al. 2001). Owing to this, the investigation into the development of small molecule BACE1 inhibitors has become a focus for AD treatment. However, as yet, the production of effective compounds is proving challenging due to low stability, oral availability, and difficulty in developing molecules small enough to cross the BBB (Citron 2004; Vassar 2014). A major concern related to BACE1 inhibitors currently in clinical trials is the lack of knowledge of potential side effects and whether complete removal or inhibition may be linked to mechanism based toxicities, corresponding with more recent reports of adverse effect in *BACE1*$^{-/-}$ rodent models. *BACE1*$^{-/-}$ mice have since been described to exhibit mild behaviour and cognitive problems, including deficits in learning and memory tasks (Laird et al. 2005), showing a less explorative and more anxious behaviour than WT littermates (Harrison et al. 2003), and sharing many common symptoms associated with schizophrenia (Savonenko et al. 2008). As well as the reported cognitive impairments in *BACE1*$^{-/-}$ mice there has been studies describing biological changes. These include reports of altered synaptic plasticity and reduced synaptic function (Laird et al. 2005), as well as observed hypomyelination and markedly thinner myelin sheath in comparison to WT littermates (Hu et al. 2006). This proposes a potential role for BACE1, not only in behaviour, but in myelination and synaptic functions- which are tightly controlled biological events. More worryingly, one report has demonstrated that *BACE1*$^{-/-}$ mice have

increased mortality rates (Dominguez et al. 2005), however not all *BACE1*$^{-/-}$ mouse models report this, and therefore not all variants will encounter this problem. Nevertheless, taken together current knowledge suggests complete inhibition could cause detrimental side effects and may not be a successful therapeutic intervention. Conversely, partial inhibition may be a positive approach, as it has been shown that only a 50% reduction in BACE1 activity leads to a small, but effective, decrease in Aβ (McConlogue et al. 2007) and that reduced BACE1 expression via lentiviral knock-down also demonstrates dampened APP processing and Aβ production (Singer et al. 2005). Notably, individuals carrying one copy of the Icelandic A673T mutation also show reduced Aβ levels (approximately 20% reduction) and have lifelong protection against AD (Vassar 2014). Therefore, a partial reduction in BACE1 activity appears a more beneficial therapeutic strategy for the treatment of AD.

BACE1 levels and activity can become elevated due to a number of stresses including age, hypoxia (Zhang et al. 2007), oxidative stress (Tamagno et al. 2002) and apoptosis (Tesco et al. 2007), as well as metabolic stress, where disruptions in energy metabolism have been shown to raise BACE1 levels (Velliquette et al. 2005). Consequently, the factors associated with obesity and T2DM such as impaired glucose homeostasis and insulin resistance, may increase BACE1 levels/activity and furthermore metabolic disease could be linked to, and potentially drive, the pathological processes underlying AD. This is supported by the growing body of research describing obesity and T2DM as risk factors for AD (Gorospe & Dave 2007; Janson et al. 2004; Biessels et al. 2006), with these diseases linked by many common features such as inflammation and insulin resistance (Yang & Song 2013).

Despite having established a link between AD, obesity and T2DM, the precise role of BACE1 in energy metabolism is unknown. Work from our lab investigating the *BACE1*$^{-/-}$ mouse from a metabolic perspective have shown that these animals are lean and more insulin sensitive than WT littermates. Importantly, when challenged with a HFD *BACE1*$^{-/-}$ mice display resistance to diet-induced obesity, improved glucose homeostasis and increased energy expenditure compared to high-fat fed WT littermates (Meakin et al. 2012). Furthermore, pharmacological inhibition of BACE1 has also been shown to improve glucose homeostasis. *In vitro* BACE1 inhibition increased muscle glucose uptake and insulin signalling, with over-expression of BACE1 producing the opposite effect (Meakin et al. 2012; Hamilton et al. 2014). Meakin *et al* also demonstrated that *BACE1*$^{+/-}$ mice share the same beneficial effects as *BACE1*$^{-/-}$ mice (Meakin et al. 2012).

Additionally, recent work from our lab has tested a BACE1 inhibitor (Merck-3), *in vivo*, through peripheral administration in DIO mice over a 28 day period. This work showed Merck-3 reduces body weight and improves glucose homeostasis, although does not alter insulin sensitivity, over the course of treatment (unpublished data). Interestingly, these effects are only observed in DIO mice and not in mice fed a regular chow diet. Furthermore, peripheral treatment with Merck-3 also results in an elevated resting metabolic rate in DIO mice, increased expression of genes involved in thermogenic programming in both brown and white adipose tissue, and reduced high-fat diet driven inflammation. Taken together, this provides the potential for BACE1 inhibition to be a novel therapeutic strategy for not only AD, but obesity and T2DM. However, the precise role of BACE1 in energy homeostasis and the mechanism(s) responsible for its removal or reduction causing improvements in the metabolic disturbances associated with obesity and T2DM is unknown.

The present studies aimed to investigate the effects of pharmacological inhibition of BACE1 in DIO mice. Different compounds and administration routes were investigated, examining various metabolic measurements, comparing the effects to those observed in *BACE1*$^{-/-}$ mice and peripheral Merck-3 treated mice. This chapter will also consider the potential mechanisms underlying the role of BACE1 in energy homeostasis, by examining peripheral and central tissues using real-time PCR to examine changes in gene expression that may allude to the potential mechanism(s) occurring. The knowledge from this research may provide insight into the role of BACE1 in energy homeostasis whilst providing potential for a novel therapeutic target for the treatment of obesity and T2DM.

3.1.1 Objectives

- Test BACE1 inhibitors *in vivo* in DIO mice and measure the following metabolic outcomes:
    - Changes in body weight and body composition
    - Changes in food intake
    - Changes in glucose homeostasis
    - Changes in insulin sensitivity
- Test structurally different, peripherally acting, BACE1 inhibitors; AZ4217 and AZ3839 in DIO mice via oral gavage
    - AZ4217 is tested to directly compare to previous Merck-3 studies as both compounds have been reported to target BACE1 however are structurally different. AZ4217 is an orally active BACE1 inhibitor which has been shown to reduce Aβ levels in the plasma after a single dose and amyloid burden in the brain following repeated dosing in mice, with no reported adverse side effects (Eketjäll et al. 2013).
    - AZ3839 is tested as this compound completed a Phase 1 clinical trial for AD. AZ3839 is an orally active BACE1 inhibitor which reportedly crosses the BBB and reduces Aβ (Jeppsson et al. 2012).
- Examine the effects of centrally inhibiting BACE1 in DIO mice using Merck-3 (previously tested via peripheral administration) via central infusion through an osmotic minipump and brain infusion kit
    - Merck-3 is tested to investigate if BACE1 is acting via a central mechanism and it has been shown to cross the blood brain barrier (unpublished data). Merck-3 reportedly inhibits sAPPβ, increases sAPPα and reduces $A\beta_{40/42}$ following central infusion (Sankaranarayananet al. 2008).
- Examine peripheral and central tissues following treatment with BACE1 inhibitors to investigate changes in gene expression associated with:
    - White adipose tissue leptin expression
    - Hypothalamic leptin signalling
    - Thermogenic programming in brown and white adipose tissue and skeletal muscle

- Central (hypothalamic) and peripheral (white adipose tissue) inflammatory programming

3.2 Methods Summary

Wild-type adult mice (8 weeks of age) were fed a 45% HFD for a period of 20 weeks to be considered DIO. Animals were then administered BACE1 inhibitor (via oral gavage or central infusion directly into the lateral ventricle) for a period of 28 days. Throughout the study body weight and food intake measurements were taken daily. A glucose tolerance test was performed on day 14 of the study, following an overnight fast, and an insulin tolerance test was performed on day 21 following a four hour fast. An assessment of fat and lean mass was conducted at the beginning and end of the study. Throughout the study animals were maintained on the 45% HFD. Following 28 days of treatment mice were fasted overnight and tissue harvested for gene and protein expression studies and blood collected for leptin and insulin measurements.

3.3 Results

3.3.1 Peripheral inhibition of BACE1 *in vivo* reduces body weight and improves glucose homeostasis

Initially the effects of the orally active BACE1 inhibitor, AZ4217 (AstraZeneca), were investigated. DIO mice were treated with either AZ4217 (50mg/kg; Starting body weight: 43.79 ± 1.37g; n=10) or vehicle (Gluconic acid; Starting body weight: 45.23 ± 1.04g; n=9) (control mice) daily, via oral gavage, for up to 28 days.

3.3.1.1 Treatment with AZ4217 reduces body weight in diet-induced obese mice

Over the course of treatment AZ4217 resulted in a reduction in body weight, which was significant after day 16, compared to control mice (Day 25: Control; -2.4% vs. AZ4217; -9.3%, $p<0.01$, n=9-10, Figure 3.1A). The percentage change in body weight corresponded to a significant reduction in actual mass, measured in grams (Control; -1.17 ± 0.51g vs. AZ4217; -3.60 ± 0.76g, $p<0.01$, n=9-10, Figure 3.1B). The observed loss of body weight is more specifically a reduction in adiposity, as AZ4217 treated mice display a reduction in fat mass (Control; -0.99 ± 0.77% vs. AZ4217; -6.78 ± 1.80%, $p<0.01$, n=9-10, Figure 3.1C), with lean mass between the two groups unaltered. To determine if the reduced fat mass was associated with circulating leptin levels, leptin was measured in the

serum of these mice upon termination of the study (day 28). AZ4217 treatment caused a reduction in circulating leptin levels compared to control mice (Control; 73.51 ±9.46ng/ml vs. AZ4217; 44.60 ± 7.18ng/ml, $p<0.05$, n=9-10, Figure 3.1D), which correlates with the observed reduction in fat mass. Taken together these data show BACE1 inhibition with AZ4217 reduces adiposity in DIO mice, which is associated with decreased circulating leptin levels.

To determine if these effects were attributable to changes in food consumption, daily food intake was measured over the course of the study. There was no difference in cumulative food intake between AZ4217 treated mice and control mice (Figure 3.2A), with both groups consuming the same amount throughout the study. As total food intake was unchanged relative food intake in relation to body weight was measured as a ratio of the amount of food consumed and body weight. At days 1 and 16 of treatment there was no difference in relative food intake between AZ4217 treated mice and control mice (Figure 3.2B), however by day 24 AZ4217 treatment caused an increase in relative food intake compared to control mice (Day 24: Control; 0.08 ± 0.002 vs. AZ4217; 0.09 ± 0.007, $p<0.05$, n=9-10, Figure 3.2B). This increase in relative food intake in AZ4217 treated mice indicates these animals have relative hyperphagia in relation to body weight.

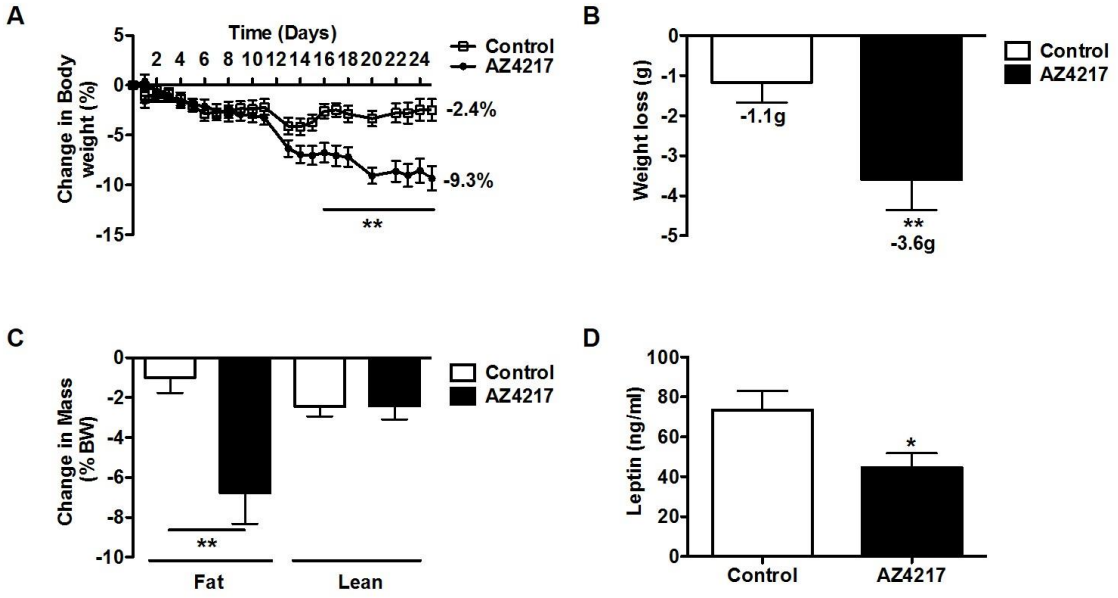

Figure 3.1 Treatment of diet-induced obese mice with AZ4217 for 28 days reduces body weight and circulating leptin levels.

(A) Treatment with AZ4217 causes a significant reduction in percentage body weight from day 16 of treatment ($p<0.01$, n=9-10). (B) Actual weight loss, at the end of the study, is significantly reduced in mice treated with AZ4217 ($p<0.01$, n=9-10). (C) Echo MRI data demonstrating a significant reduction in fat mass in mice treated with AZ4217, with no change in lean mass ($p<0.01$, n=9-10). (D) Reduction in fat mass is associated with a significant reduction in circulating serum leptin levels in AZ4217 treated mice ($p<0.05$, n=9-10).

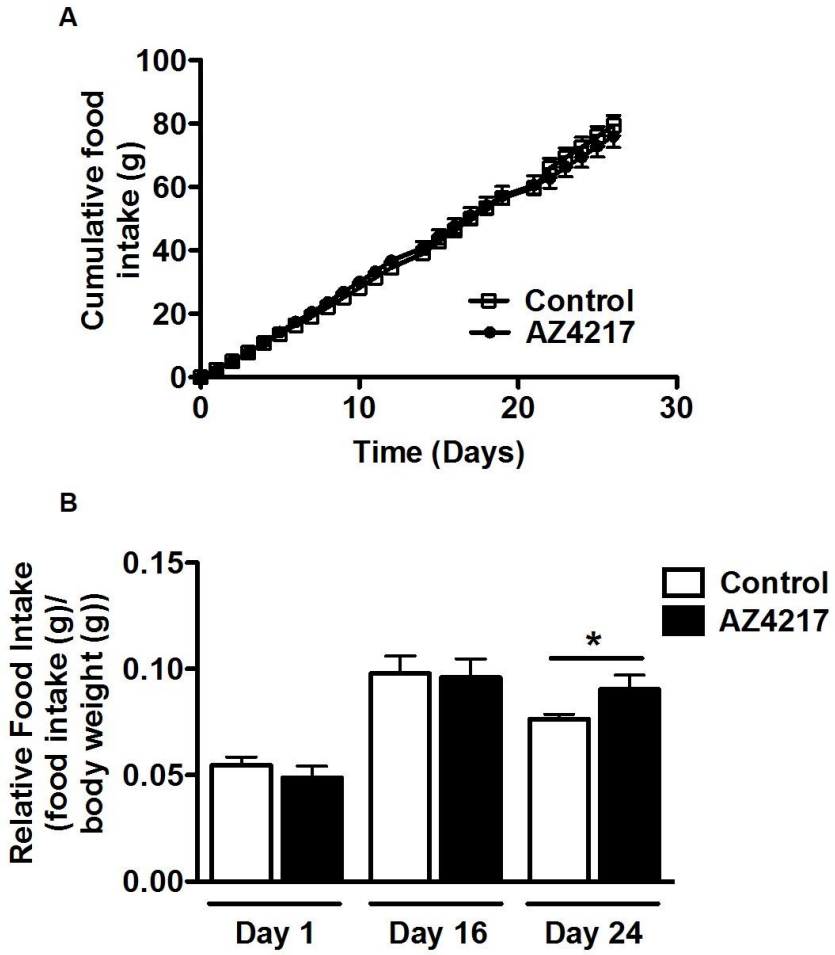

Figure 3.2 Treatment of diet-induced obese mice with AZ4217 for 28 does not affect total food intake, however increases relative food intake.

(A) Cumulative food intake was unchanged with AZ4217 treated (n=9-10). (B) Relative food intake, described as the ratio between food intake and body weight, was significantly increased at the end of the study (day 24) with AZ4217 treatment, but showed no difference at day 1 and 16 ($p<0.05$, n=9-10).

3.3.1.2 Treatment with AZ4217 improves glucose homeostasis in diet-induced obese mice

To examine the diabetic phenotype of DIO mice treated with AZ4217 and vehicle, glucose and insulin tolerance tests were carried out on day 14 and 21 of treatment respectively. Following an overnight fast AZ4217 treated mice displayed increased glucose clearance compared to control mice (AUC: control; 2196 ± 150.5 vs. AZ4217; 1848 ± 119.2, $p<0.05$, n=9-10, Figure 3.3A and B). AZ4217 treated mice also showed a reduction in fasting blood glucose levels compared to control mice (Control; 4.78 ± 0.25mmol/l vs. AZ4217; 4.16 ± 0.17mmol/l, $p<0.05$, n=9-10, Figure 3.3C). These data demonstrate that AZ4217 treatment causes an overall improvement in glucose tolerance.

Following a four hour fast an insulin tolerance test was carried out and no difference in blood glucose levels throughout the course of the test (15-120 minutes) was observed between AZ4217 treated mice and control mice (Figure 3.4A). Circulating insulin levels were also examined, following an overnight fast at the end of the study, and there was a trend towards a reduction in insulin levels in the serum of AZ4217 treated mice compared to control mice, however this was not a significant effect (Figure 3.4B). Taken together these results show AZ4217 treated mice have improved glucose homeostasis, compared to control mice, however insulin sensitivity is unaltered.

3.3.2 Treatment with AZ4217 modifies white adipose tissue leptin expression in diet-induced obese mice

Having shown that inhibition of BACE1 causes a reduction in circulating leptin levels we asked the question whether this was due to a direct effect on white adipose tissue (WAT). Initially, BACE1 expression in WAT was examined and if this expression was affected by HFD. Using immunofluorescence (IF) WAT from WT mice fed a NC or HFD were double-stained for BACE1 (red) and perilipin (green), which is a protein associated with lipid droplets and utilised to indicate adipocytes. Representative confocal images show BACE1 is co-localised with perilipin, indicating BACE is present in adipocytes, and BACE1 staining is stronger in high-fat fed animals (Figure 3.5). These data show BACE1 is present in WAT and is elevated following a HFD.

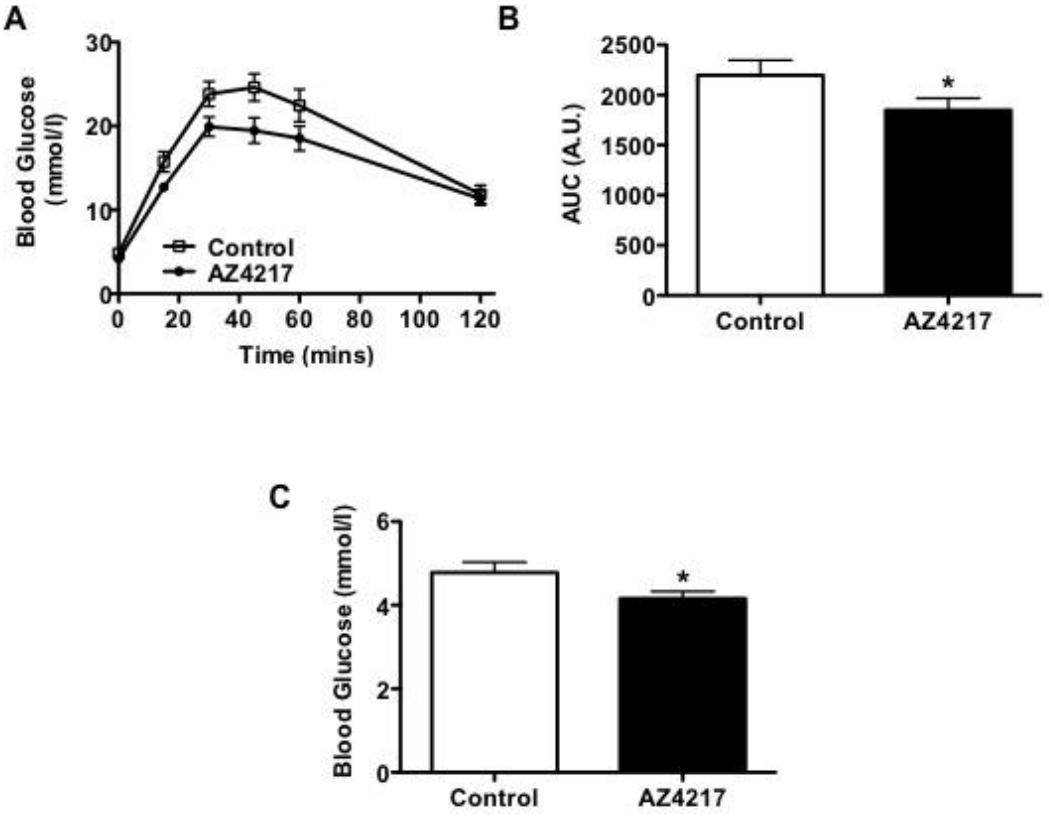

Figure 3.3 Treatment of diet-induced obese mice with AZ4217 significantly improves glucose homeostasis.

(A) Glucose tolerance test profile showing AZ4217 treatment improves glucose disposal. (B) Quantification of area under the curve (AUC) for glucose response shown in (A), demonstrating significant improvement in glucose disposal with AZ4217 treatment ($p<0.05$, n=9-10). (C) Treatment with AZ4217 significantly reduces fasting blood glucose levels ($p<0.05$, n=9-10).

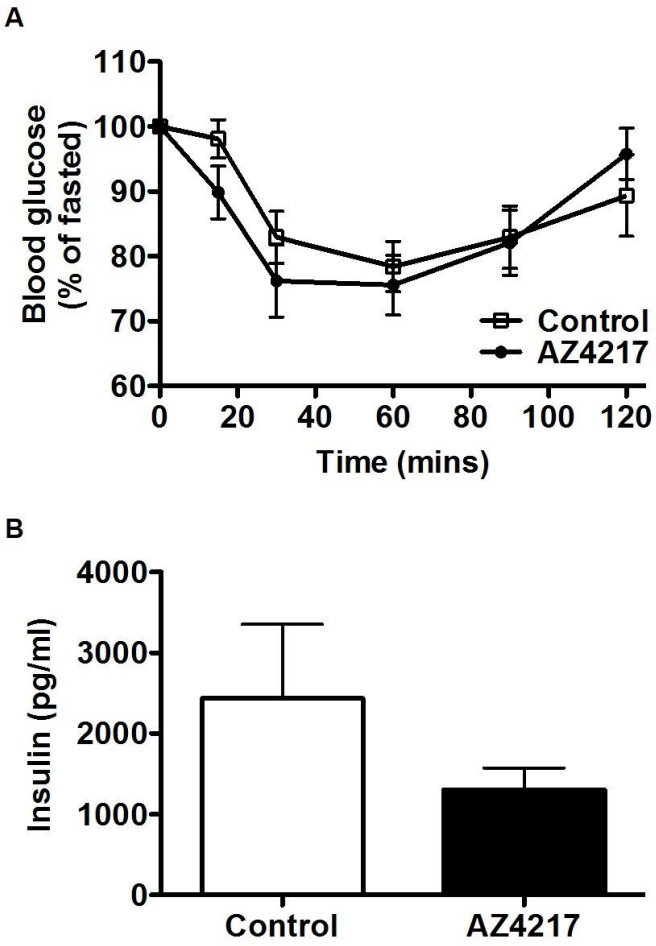

Figure 3.4 Treatment of diet-induced obese mice with AZ4217 for 28 days does not alter insulin sensitivity.

(A) Insulin tolerance test profile displaying no significant effect of AZ4217 treatment on insulin sensitivity (n=9-10). (B) AZ4217 treatment caused no significant effect on circulating serum insulin levels (n=9-10).

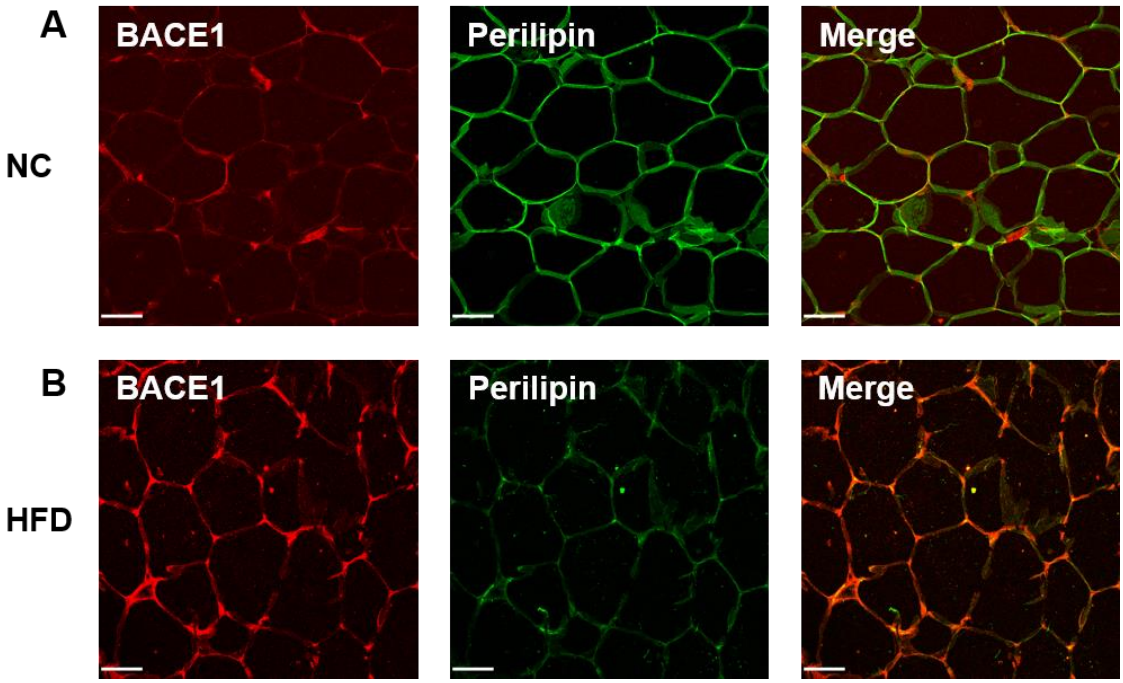

Figure 3.5 BACE1 expression is elevated in white adipose tissue when mice are fed a high-fat diet for 20 weeks.

Confocal images taken at x40 magnification, showing BACE1 (red), adipocyte marker perilipin (green) and merged channels within white adipose tissue. Representative images from (A) mice fed a normal chow (NC) diet and (B) mice fed a high-fat diet (HFD) for a period of 20 weeks. All scale bars 50µm.

Having observed BACE1 is increased following a HFD in WAT, it was investigated if BACE1 inhibition affects WAT directly and whether this may be responsible for the observed reduction in circulating leptin levels. The expression of *leptin* in WAT was examined, using real-time PCR, and AZ4217 treated mice displayed reduced *leptin* expression in comparison to control mice (Control; 1.00 ± 0.23 vs. AZ4217; 0.54 ± 0.07, $p<0.001$, n=9-10, Figure 3.6A). AZ4217 treated mice also showed reduced levels of the long form of the leptin receptor, *ObRb*, in WAT compared to control mice (Control; 1.00 ± 0.18 vs. AZ4217; 0.77 ± 0.10, $p<0.05$, n=6-10, Figure 3.6B). Taken together these data suggest BACE1 may be involved in the high circulating levels of leptin present in obesity, and that increased BACE1 levels/activity may be required for the resulting leptin resistance, which primarily targets the hypothalamus. Consequently, reducing BACE1 levels/activity may be associated with reduced WAT leptin and circulating leptin levels, thus improving leptin sensitivity in DIO mice, and reversing hypothalamic leptin resistance.

3.3.3 Treatment with AZ4217 alters hypothalamic leptin signalling in diet-induced obese mice

Having found BACE1 inhibition causes a large reduction in circulating leptin levels, whether this and the associated reduction in body weight is driven by a direct effect on leptin signalling was investigated. The hypothalamic expression of key anorexigenic and orexigenic neuropeptides involved in leptin signalling were measured in AZ4217 treated and control mice. The hypothalamus was extracted and analysed following an overnight fast, examining the expression of the anorexigenic neuropeptides, *pro-opiomelanocortin* (*POMC*) and *cocaine- and amphetamine- regulated transcript* (*CART*) and the orexigenic neuropeptides, *neuropeptide Y* (*NPY*) and *agouti- related protein* (*AgRP*). Treatment with AZ4217 caused a reduction in *POMC* expression compared to control mice (Control; 1.00 ± 0.32 vs AZ4217; 0.53 ± 0.12, $p<0.01$, n=9-10, Figure 3.7A), however the compound had no effect on *CART* expression (Figure 3.7B). Treatment with AZ4217 also had no effect on orexigenic hypothalamic peptide expression, with no difference between groups observed for *NPY* or *AgRP* expression (Figure 3.7C and D). To assess if the expression of orexigenic neuropeptides changed in relation to anorexigenic expression the ratios of *NPY/POMC* and *AgRP /POMC* were calculated. AZ4217 treatment resulted in a slight, but non-significant, increase in the ratios of *NPY/POMC* and *AgRP/POMC* (Figure 3.7E and F), suggesting AZ4217 may promote orexigenic signalling. Owing to AZ4217 having

little effect on the key neuropeptides involved in leptin signalling, the expression of negative regulators of leptin signalling, which are thought to elicit leptin resistance, were measured in the hypothalamus. *SOCS3* and *PTP1B* levels were examined as they have been reported to contribute to leptin resistance (Münzberg & Myers 2005; Bjorbaek et al. 1998; Zabolotny et al. 2002). Hypothalamic *SOCS3* mRNA was reduced in AZ4217 treated mice relative to control mice (Control; 1.00 ± 0.16 vs. AZ4217; 0.80 ± 0.08, $p<0.05$, n=9-10, Figure 3.8A). As SOCS3 blocks leptin signalling the observed reduction may indicate improved hypothalamic leptin sensitivity/signalling. However, *PTP1B* levels were unchanged between AZ4217 treated mice and controls (Figure 3.8B and C), indicating reduced PTP1B levels may not be responsible for the observed improvement in leptin sensitivity.

3.3.4 Treatment with AZ4217 does not alter thermogenic programming in diet-induced obese mice

Having shown an improvement in the metabolic state of DIO mice treated with AZ4217, a possible mechanism explaining this outcome is increased energy expenditure through increased thermogenesis. It has previously been shown that *BACE1*$^{-/-}$ mice have increased energy expenditure and elevated levels of uncoupling proteins in brown adipose tissue (BAT) and skeletal muscle (Meakin et al. 2012), indicating increased thermogenesis. Thus, thermogenic programming was examined in BAT and skeletal muscle of AZ4217 treated and control mice. In BAT the thermogenic factors uncoupling protein 1 (*UCP1*), peroxisome proliferator-activated receptor-γ, coactivator 1-α *(PGC1α)*, type 2 deiodinase *(DIO2)* and the zinc finger transcription factor *Prdm16* mRNA levels were measured as markers of the switching on of thermogenic programming. AZ4217 treatment had no effect on *UCP1*, *DIO2* or *Prdm16* mRNA levels in BAT relative to control mice (Figure 3.9A, C and D), and reduced *PGC1α* levels compared to control mice (Control; 1.00 ± 0.2 vs. AZ4217; 0.70 ± 0.06, $p<0.01$, n=9, Figure 3.9B). These data show AZ4217 does not impact thermogenic programming in BAT, and increased energy expenditure via this tissue is unlikely to be responsible for the improved metabolic phenotype observed.

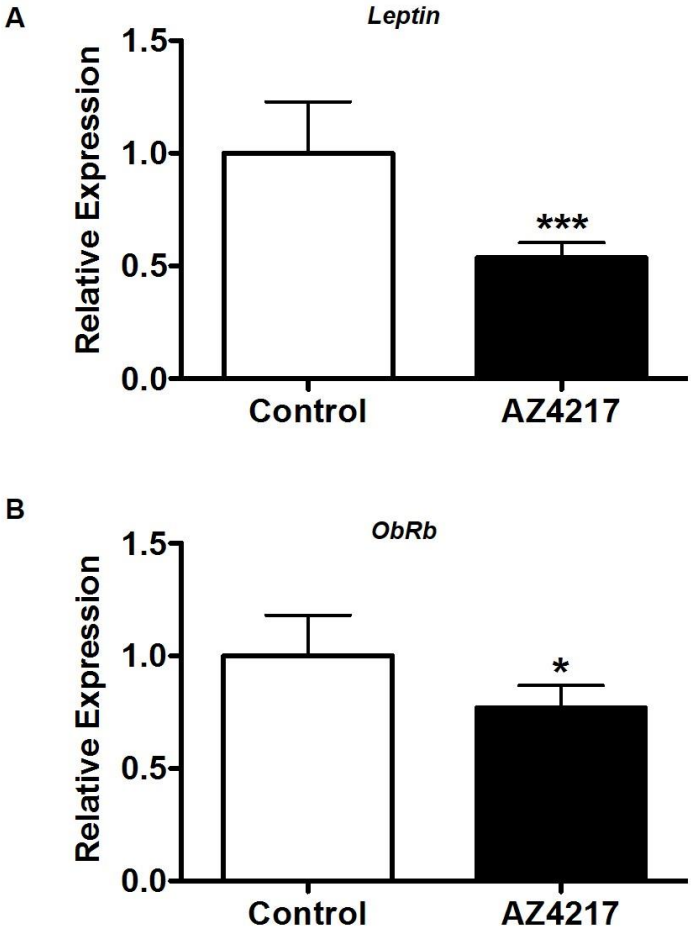

Figure 3.6 AZ4217 treatment significantly reduces *leptin* mRNA expression in white adipose tissue.

Histograms showing relative mRNA expression of (A) *leptin* and (B) the long form of the leptin receptor (*ObRb*) in white adipose tissue. (A) AZ4217 treatment causes a significant reduction in *leptin* ($p<0.001$, n=9-10) and (B) *ObRb* ($p<0.05$, n=6-10).

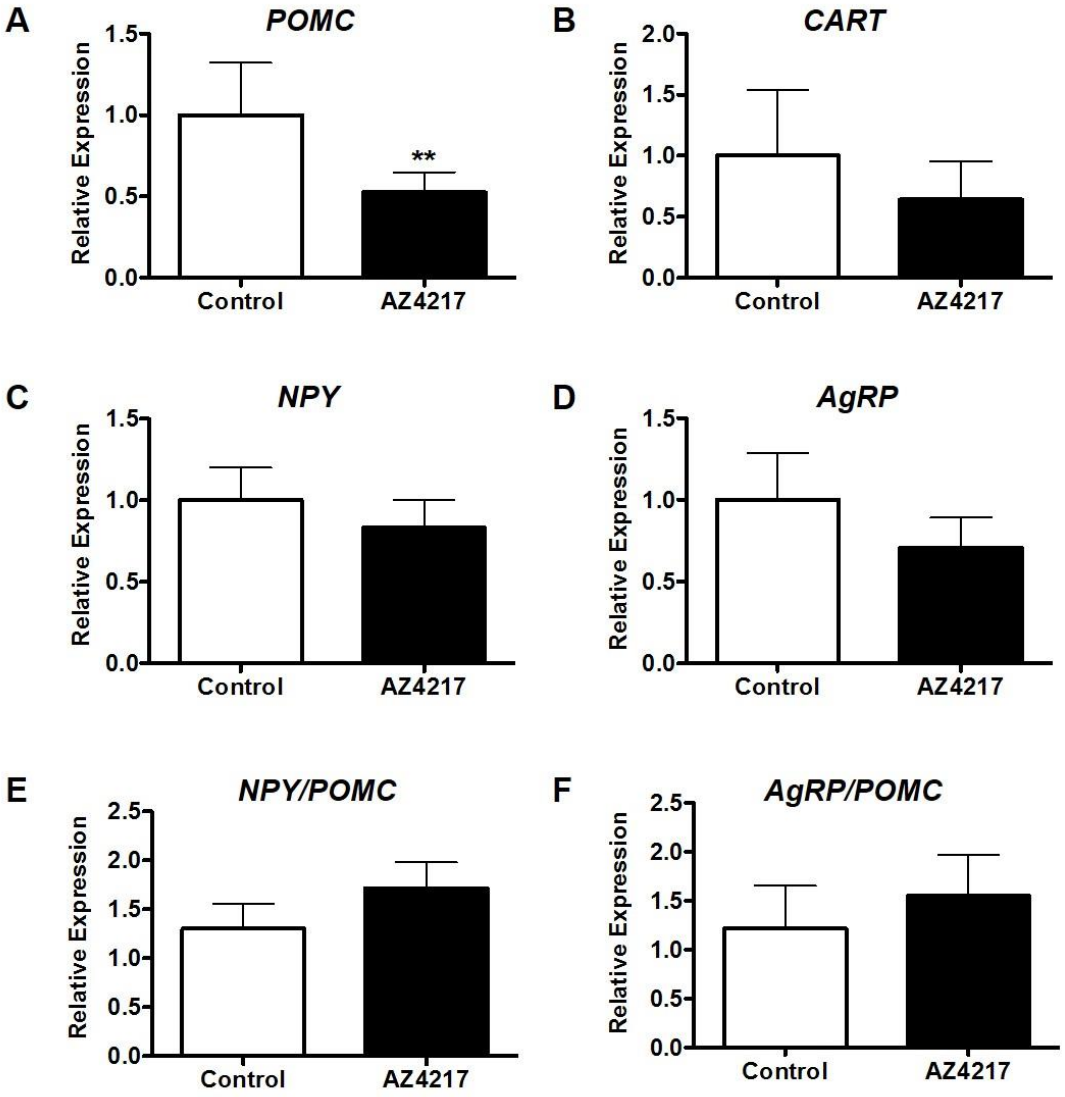

Figure 3.7 AZ4217 treatment reduces anorexigenic, but does not affect orexigenic, neuropeptide hypothalamic gene expression.

Histograms showing relative mRNA expression of (A) *POMC*, (B) *CART*, (C) *NPY*, (D) *AgRP*, (E) *NPY/POMC* and (F) *AgRP/POMC* in the hypothalamus. (A) AZ4217 treatment causes a significant reduction in hypothalamic *POMC* mRNA expression ($p<0.01$, n=9-10) but no significant effect on *CART* mRNA expression (n=7-8). (C and D) AZ4217 had no significant effect on orexigenic neuropeptides *NPY* or *AgRP* (n=9-10). (E and F) Representative hypothalamic ratios of *NPY/POMC* (n=9) and *AgRP*/*POMC* (n=9-10) display no significant difference with AZ4217 treatment.

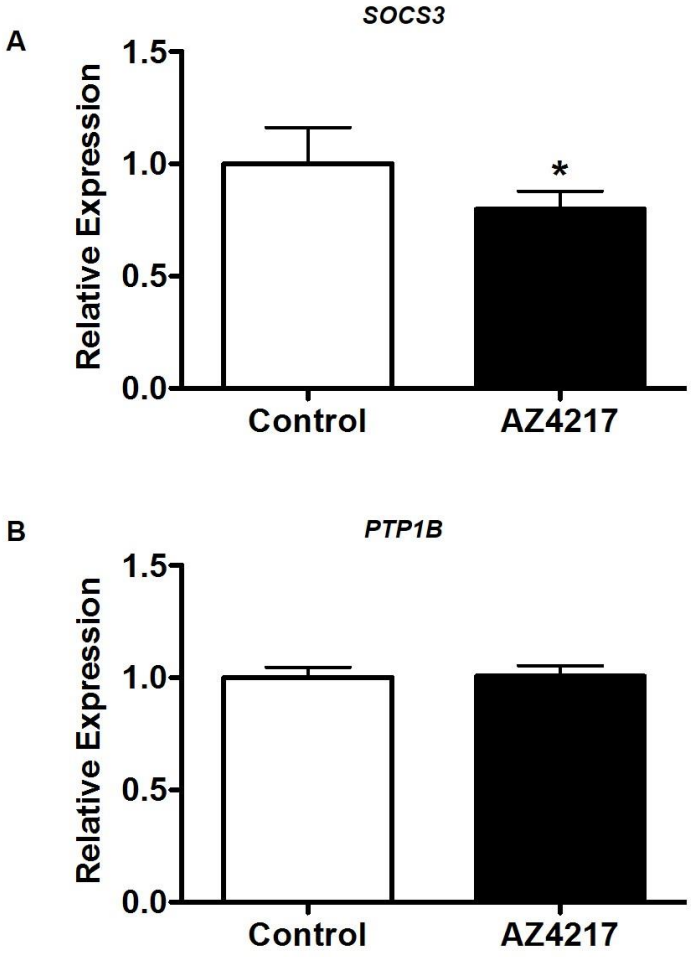

Figure 3.8 AZ4217 treatment significantly reduces SOCS3 gene expression, but does not alter PTP1B gene expression in the hypothalamus.

Histograms showing relative mRNA expression of (A) *SOCS3* and (B) *PTP1B* in the hypothalamus. (A) AZ4217 treatment causes a significant reduction in hypothalamic *SOCS3* expression ($p<0.05$, n=9-10). (B) AZ4217 treatment has no significant effect on *PTP1B* (n=8-9).

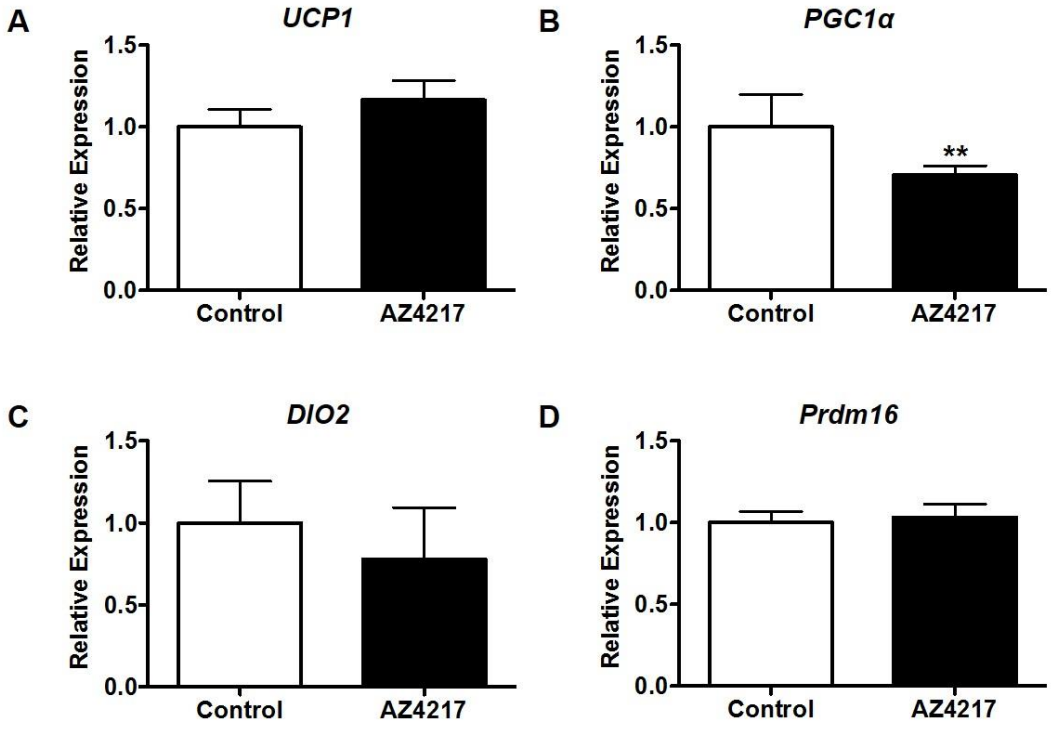

Figure 3.9 AZ4217 treatment significantly reduces *PGC1α* but does not affect other markers of thermogenic programming in brown adipose tissue.

Histograms showing relative mRNA expression of (A) *UCP1*, (B) *PGC1α*, (C) *DIO2* and (D) *Prdm16* in brown adipose tissue.(B) AZ4217 treatment causes a significant reduction in *PGC1α* ($p<0.01$, n=9), but causes no significant effect on (A) *UCP1*, (C) *DIO2* or (D) *Prdm16* (n=9).

Skeletal muscle in mice was also examined. It is reported that UCP1 expression is low in skeletal muscle, which was found in the *BACE1*$^{-/-}$ mouse, however increased levels of the uncoupling proteins 2 and 3 (UCP2/3) could be measured (Meakin et al. 2012). Thus, *UCP2* and *UCP3* levels were examined in skeletal muscle of AZ4217 treated and control mice. AZ4217 treatment caused no change in *UCP2* and *UCP3* mRNA levels in skeletal muscle relative to control mice (Figure 3.10A and B), which is consistent with no change in thermogenic programming detected in BAT.

Markers of BAT cell-selective genes, such as Prdm16, have also been shown to be present in WAT, with this gene in particular driving the 'browning' of white adipocytes to brown or 'brite' adipocytes (Seale et al. 2011). This is also indicative of raised thermogenesis and decreased metabolic efficiency. To examine whether any such changes occurred in WAT of AZ4217 treated and control mice the thermogenic genes analysed in BAT were measured. In WAT, AZ4217 treatment caused a reduction in *PGC1α* (Control; 1.00 ± 0.26 vs. AZ4217; 0.75 ± 0.11, $p<0.01$, n=9, Figure 3.11B) and *Prdm16* (Control; 1.00 ± 0.22 vs. AZ4217; 0.56 ± 0.08, $p<0.001$, n=9, Figure 3.11D) levels relative to controls, suggesting a reduction in 'browning' of WAT. However, *UCP1* and *DIO2* were unchanged between AZ4217 treated and control mice (Figure 3.11A and C). Taken together these data show there is no effect on thermogenic programming in WAT, consistent with the BAT and skeletal muscle data, and AZ4217 is unlikely to be increasing energy expenditure via raised thermogenesis to result in the improved metabolic phenotype observed.

3.3.5 Treatment with AZ4217 modifies high-fat diet-mediated inflammatory programming in diet-induced obese mice

HFD drives increased pro-inflammatory cytokine expression both centrally, in the hypothalamus (De Souza et al. 2005), and peripherally (Gregor & Hotamisligil 2011), as well as increasing the accumulation of macrophages in peripheral tissues such as WAT (Caruso et al. 2010). Furthermore, work in our lab has recently shown that *BACE1*$^{-/-}$ mice have a reduced number of inflammatory cells in WAT and liver (unpublished data) and therefore may be resistant to HFD-induced inflammation. To examine this further WAT of WT and *BACE1*$^{-/-}$ mice, fed a HFD for a period of 20 weeks, were stained for macrophage markers F4/80 and Cd68. Representative light microscopy images show there is an increase in macrophage staining in WAT of WT mice in comparison to *BACE1*$^{-/-}$ mice, with the adipocytes displaying a more irregular and larger morphology (Figure

3.12). These data show there is increased inflammation associated with diet-induced obesity, however in the absence of BACE1 there is no inflammatory response.

As we observed reduced numbers of macrophages in WAT of *BACE1*$^{-/-}$ mice, in AZ4217 treated mice we next investigated markers of the inflammasome, which are elevated in obesity (Vandanmagsar et al. 2011) and activate inflammatory processing (Guo et al. 2015), as well as levels of pro- and anti-inflammatory cytokines. The expression of inflammatory markers were examined in the hypothalamus and WAT of AZ4217 treated and control mice. In the hypothalamus pro-inflammatory cytokines; *TNFα* and *IL-6*, markers of the inflammasome; *IL-1β*, *NLRP3* and *caspase 1*, and *F4/80*, as a marker of total macrophage number, were studied. AZ4217 treatment reduced *TNFα* levels compared to controls (Control; 1.00 ± 0.41 vs. AZ4217; 0.35 ± 0.17, $p<0.001$, n=6-9, Figure 3.13A), however AZ4217 had no effect on *IL-6* levels (Figure 3.13B). Unexpectedly, AZ4217 treatment drives a non-significant increase in *IL-1β* levels (Figure 3.13C) and causes no change in *NLRP3* or *caspase 1* levels (Figure 3.13D and E). Total macrophage number is also unaltered in AZ4217 treated mice compared to control mice indicated by no change in *F4/80* levels (Figure 3.13F). Taken together these data suggest AZ4217 causes a reduction in hypothalamic inflammation through reduced *TNFα* expression, however markers of the inflammasome and total macrophage levels are unchanged, therefore AZ4217 treatment does not appear to greatly alter HFD-mediated hypothalamic inflammation.

In WAT, pro-inflammatory cytokines; inducible nitric oxide synthase (*NOS2*), *INFγ*, *IL-1β*, *TNFα* and *IL-6*, anti-inflammatory cytokines; *IL-10*, *YM-1* and *Arg-1*, and *F4/80* were studied. Alike the hypothalamus, AZ4217 treatment induced a large reduction in *TNFα* levels relative to controls (Control; 1.00 ± 0.62 vs. AZ4217; 0.39 ± 0.06, $p<0.001$, n=7-10, Figure 3.14D), however did not alter *NOS2*, *IFNγ*, *IL-1β* or *IL-6* compared to controls (Figure 3.14A, B and C). Anti-inflammatory cytokines *IL-10*, *YM-1* and *Arg-1* were also unaltered following AZ4217 treatment (Figure 3.14F, G and H), although *F4/80* levels were reduced following AZ4217 treatment in comparison to controls (Control; 1.00 ± 0.47 vs. AZ4217; 0.66 ± 0.09, $p<0.01$, n=7-10, Figure 3.14I), indicating a reduced number of macrophages in WAT following BACE1 inhibition. Taken together these data suggest AZ4217 treatment reduces HFD-mediated WAT inflammation, however this is not a large change and may not be the main driver for the improved metabolic phenotype observed with reduced BACE1.

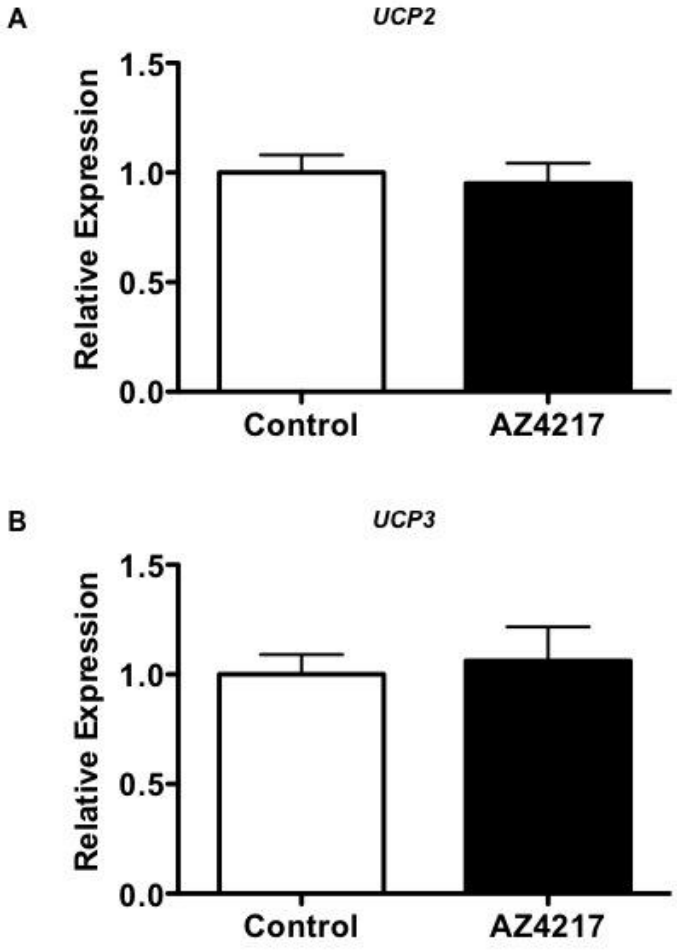

Figure 3.10 AZ4217 treatment does not alter uncoupling proteins expression in skeletal muscle.

Histograms showing relative mRNA expression of (A) *UCP2* and (B) *UCP2* in skeletal muscle. AZ4217 treatment causes no significant effect on (A) *UCP2* or (B) *UCP3* expression (n=9-10).

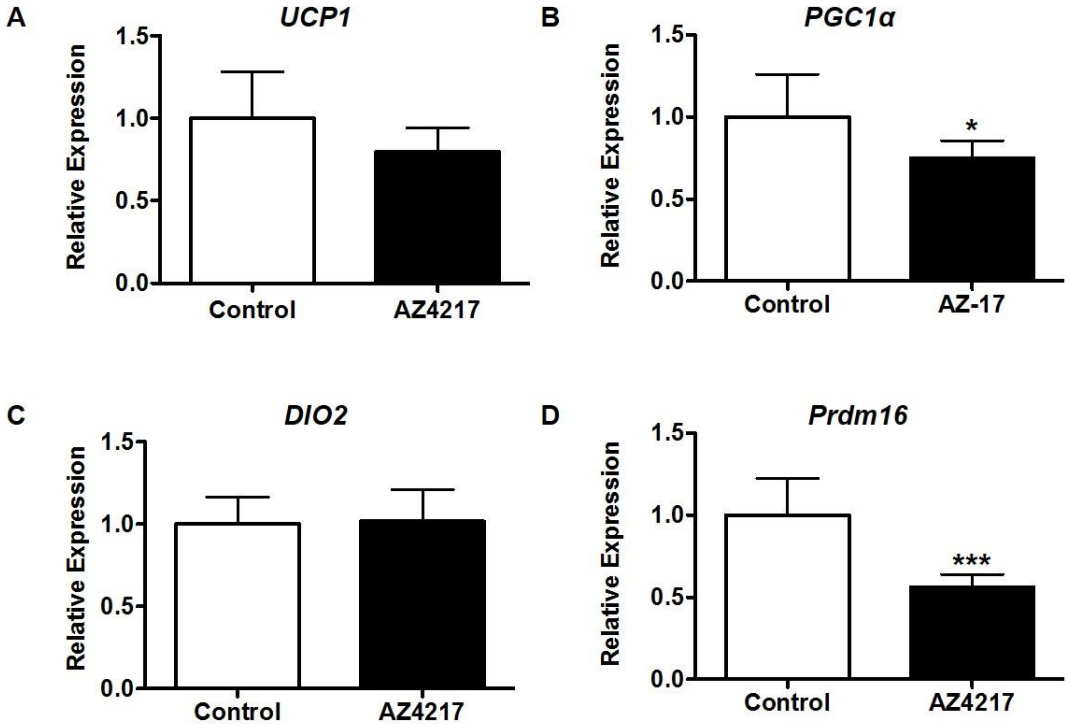

Figure 3.11 AZ4217 treatment significantly reduces *PGC1α* and *Prdm16*, but does not affect other markers of thermogenic programming in white adipose tissue.

Histograms showing relative mRNA expression of (A) *UCP1*, (B) *PGC1α*, (C) *DIO2* and (D) *Prdm16* in white adipose tissue. (A and C) AZ4217 treatment causes no significant effect on *UCP1* (n=9) or *DIO2* (n=7-10). (B and D) AZ4217 treatment causes a significant reduction in *PGC1α* ($p<0.05$, n=6-10) and *Prdm16* ($p<0.001$, n=7-10).

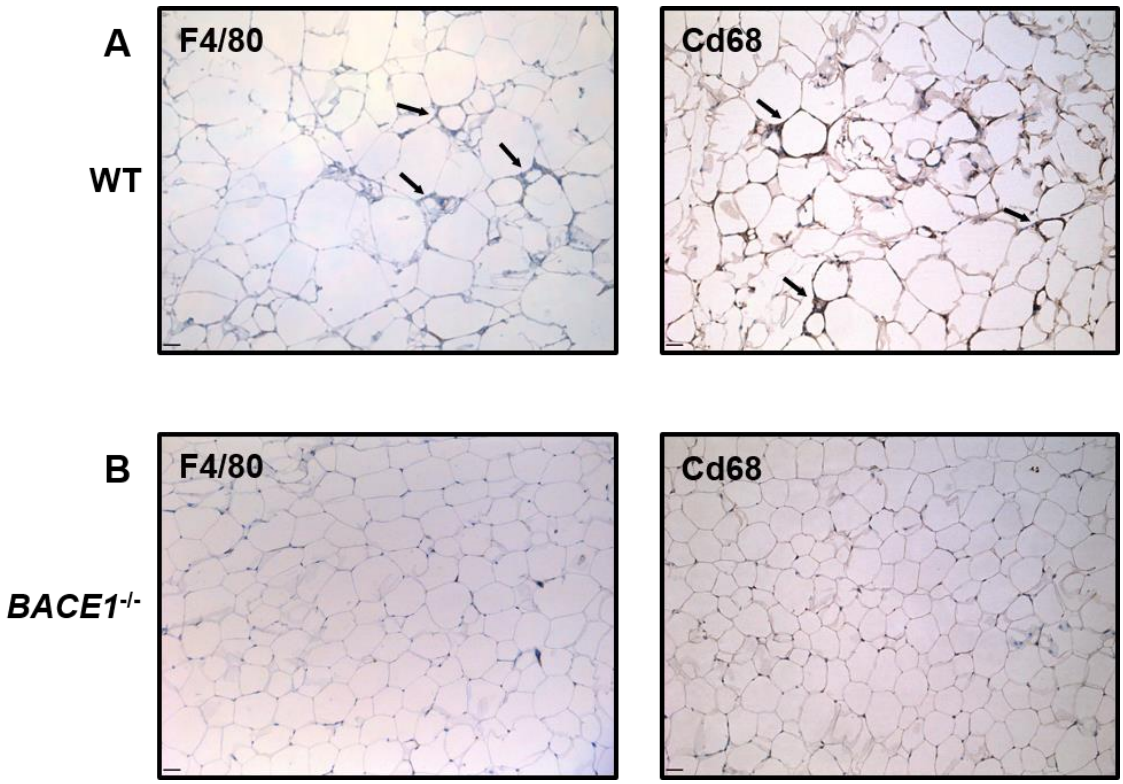

Figure 3.12 *BACE1*$^{-/-}$ mice do not display diet-induced inflammation in white adipose tissue following 20 weeks on a high-fat diet.

Light microscopy images taken at x10 magnification showing macrophage markers F4/80 and Cd68 staining in white adipose tissue. Representative images from (A) wild-type (WT) mice and (B) *BACE1*$^{-/-}$ mice fed a high-fat diet for a period of 20 weeks. Arrows indicate areas of macrophage infiltration. All scale bars 100µm.

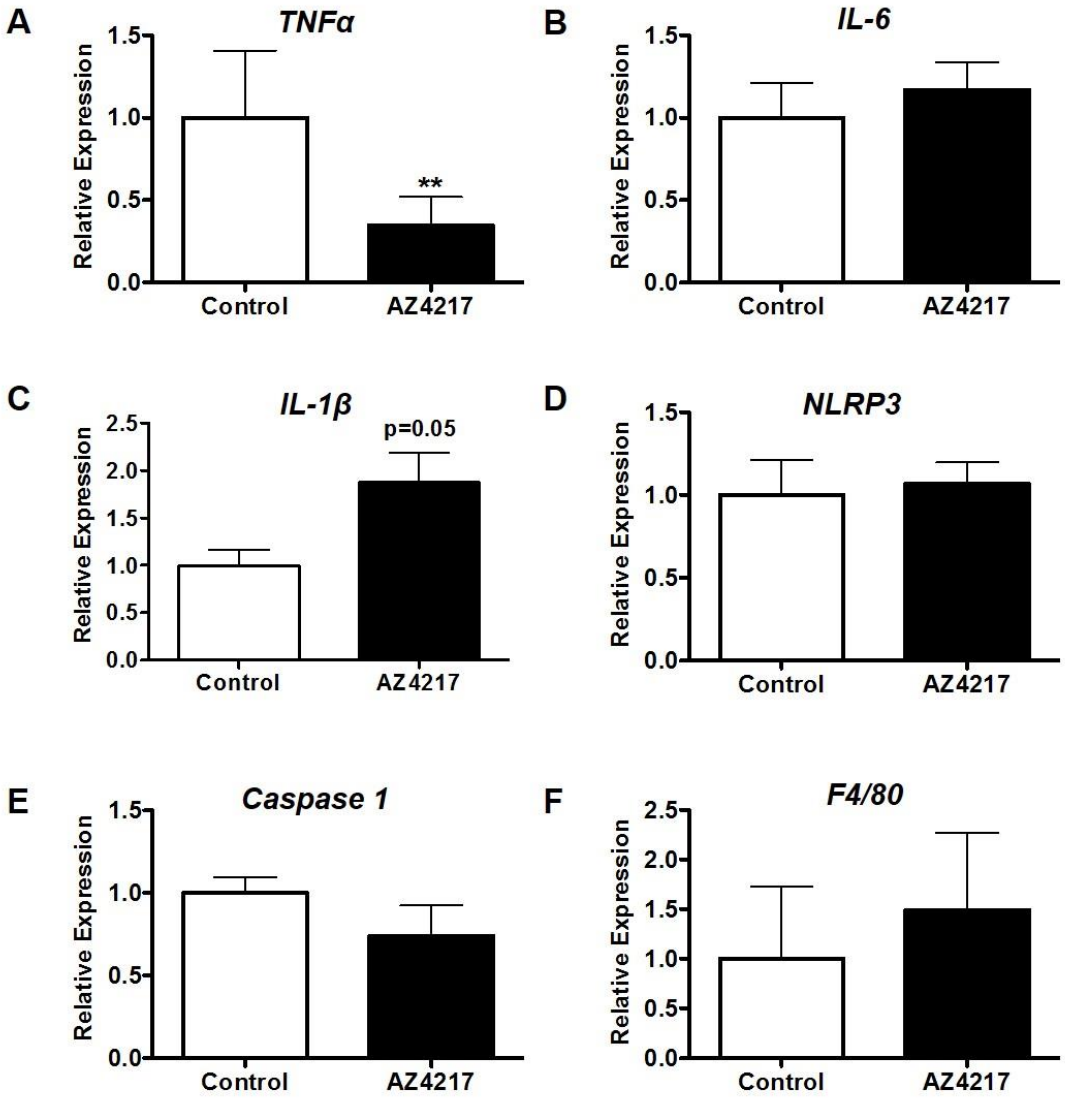

Figure 3.13 AZ4217 treatment significantly reduces central *TNFα* expression, but does not alter other inflammatory markers in the hypothalamus.

Histograms showing relative mRNA expression of pro-inflammatory cytokines (A) *TNFα* , (B) *IL-6*, (C) *IL-1β*, markers of the inflammasome (D) *NLRP3*, (E) *Caspase 1* and macrophage marker (F) F4/80 in the hypothalamus.(A) AZ4217 treatment causes a significant reduction in (A) *TNFα* ($p<0.01$, n=6-9), however has no significant effect on (B) *IL-6* (n=6). (C) AZ4217 treatment causes a trend towards a significant increase in (C) *IL-1β* ($p=0.05$, n=5) but has no significant effect on (D) *NLRP3* or (E) *Caspase 1* (n=5). (F) AZ4217 treatment has no significant effect on total macrophage number indicated by (F) *F4/80* expression (n=7-10).

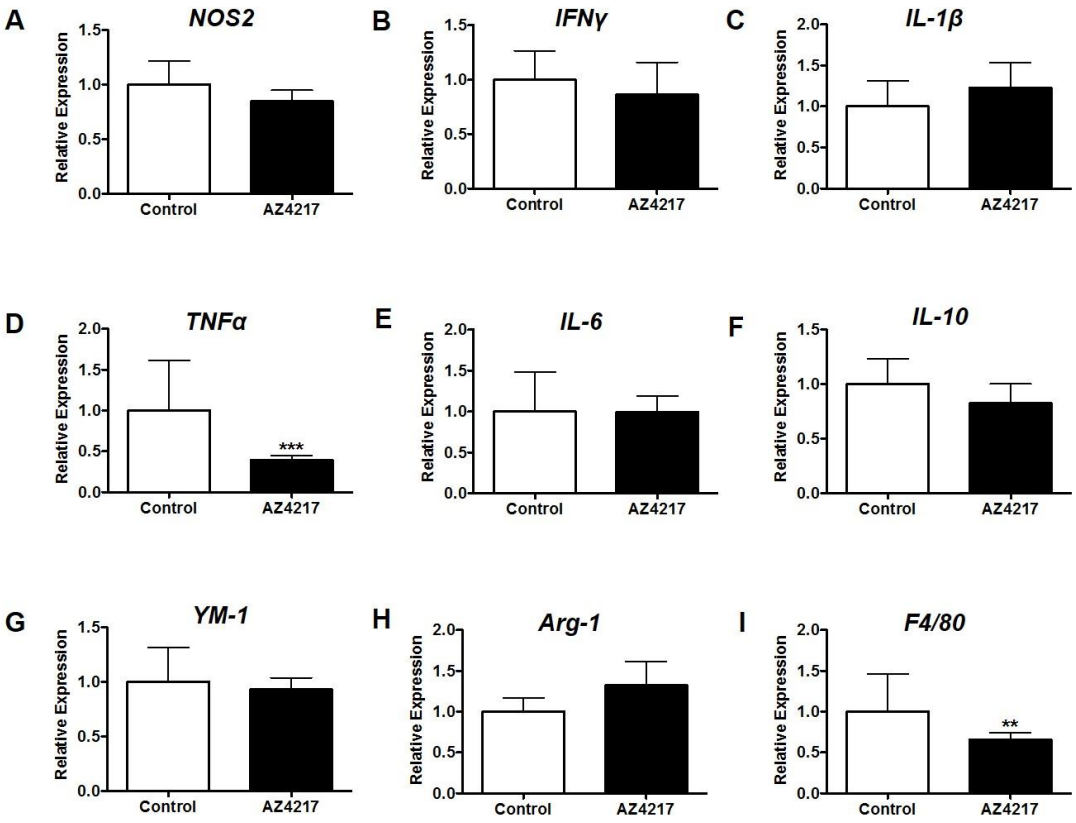

Figure 3.14 AZ4217 treatment significantly reduces *TNFα* and *F4/80* expression, but does not alter other inflammatory markers in white adipose tissue.

Histograms showing relative mRNA expression of pro-inflammatory cytokines (A) *NOS2*, (B) *IFNγ*, (C) *IL-1β*, (D) *TNFα*, (E) *IL-6*, anti-inflammatory cytokines (F) *IL-10*, (G) *YM-1*, (H) *Arg-1* and macrophage marker (I) *F4/80* in white adipose tissue. (D) AZ4217 treatment causes a significant reduction in *TNFα* expression ($p<0.001$, n=7-10), but has no significant effect on other pro-inflammatory cytokines (A) *NOS2* (n=7-10), (B) *IFNγ* (n=7-9), (C) *IL-1β* (n=7-9) or (D) *IL-6* (n=5-9).(F-H) AZ4217 treatment has no significant effect on anti-inflammatory cytokines (F) *IL-10* (n=7-10), (G) *YM-1* (n=7-10) and (H) *Arg-1* (n=5-9). (I) AZ4217 treatment significantly reduces total number of macrophages, measured by *F4/80* expression ($p<0.01$, n=7-10).

An important response to chronic inflammation is the recruitment of macrophages by chemokines, particularly to WAT, which is associated with insulin resistance and obesity. As we observe a reduced number of macrophages in WAT we examined whether altered chemokine expression may account for this. In WAT levels of chemotactic cytokines; monocyte chemoattractant protein-1 (*MCP-1*), macrophage inflammatory proteins 1α and 1β (*MIP-1α* and *MIP-1β*), and regulated upon activation, normal T cell expressed and secreted (*RANTES*), which are responsible for the migration of inflammatory cells into sites of inflammation, in particular monocytes and lymphocytes, and in some instance neutrophils, were measured (Surmi & Hasty 2010). AZ4217 treatment resulted in a reduction in *MCP-1*, *MIP-1α* and *MIP-1β* levels in comparison to control mice (*MCP-1*: Control; 1.00 ± 0.13 vs. AZ4217; 0.83 ± 0.09, p=0.08, *MIP-1α*: Control; 1.00 ± 0.18 vs. AZ4217; 0.66 ± 0.09, p<0.01, *MIP-1β*: Control; 1.00 ± 0.16 vs. AZ4217; 0.58 ± 0.11, p<0.05, n=5-9, Figure 3.15A, B and C), suggesting BACE1 inhibition reduces the number of immune cells being attracted to WAT, due to reduced HFD-mediated inflammation. However, AZ4217 treatment had no effect on *RANTES* expression compared to control mice (Figure 3.15D). Transforming growth factor β1 (*TGFβ-1*), which is secreted by activated macrophages and has been shown to act as a chemoattractant for neutrophils (Reibmant et al. 1991), was also examined in WAT. This growth factor is associated with obesity, with increased levels found in adipose tissue of obese mice (Samad et al. 1997), however AZ4217 did not alter the expression of this cytokine (Figure 3.15E).

Taken together these data show BACE1 may be involved in HFD-mediated inflammatory programming and inhibition of BACE1 reduces a degree of inflammation in WAT as well as the accumulation of macrophages at this site and this could drive, in part, the improved obese/diabetic phenotype of DIO mice observed following reduction of BACE1.

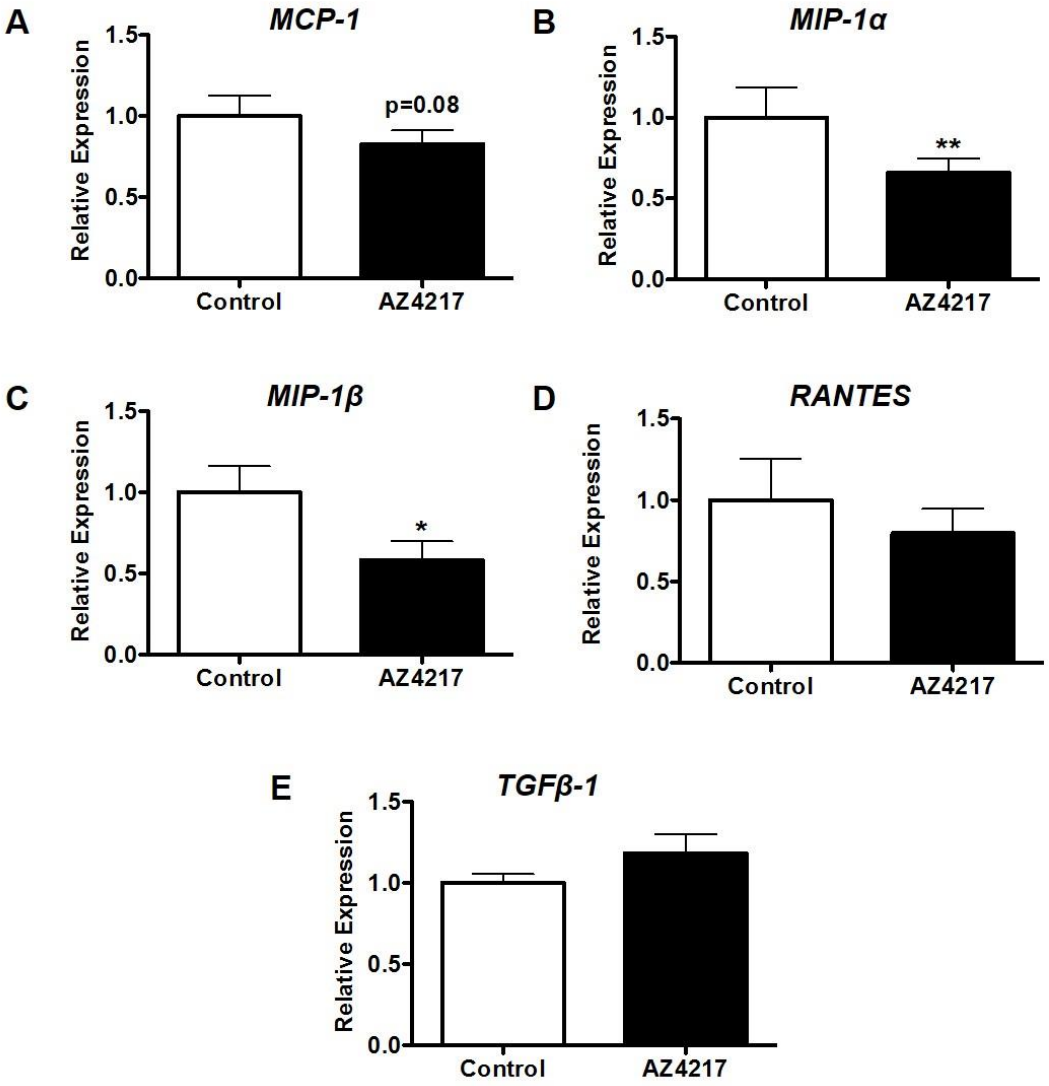

Figure 3.15 AZ4217 treatment significantly reduces *MIP-1α* and *MIP-1β* expression in white adipose tissue, but does not alter expression of other chemokines.

Histograms showing relative mRNA expression of chemokines (A) *MCP-1*, (B) *MIP-1α*, (C) *MIP-1β*, (D) *RANTES*, and pro-inflammatory cytokine (E) *TGFβ-1* in white adipose tissue. (A) AZ4217 treatment causes a non-significant reduction in *MCP-1* ($p=0.08$, n=5-9) and causes a significant reduction in (B) *MIP-1α* ($p<0.01$, n=5-9) and (C) *MIP-1β* ($p<0.05$, n=5-6) but has no significant effect on (A) *MCP-1* (n=5-9), (D) *Rantes* (n=4-8) or (E) *TGFβ-1* (n=7-9) expression.

3.3.6 Treatment with a structurally different BACE1 inhibitor does not mimic AZ4217 treatment

A second structurally different BACE1 inhibitor was examined, AZ3839, and the same metabolic measurements recorded as previously discussed (section 3.3.1). DIO mice were treated with AZ3839 (43mg/kg; Starting body weight: 49.56 ± 2.72g; n=5) or vehicle (Gluconic acid; Starting body weight: 49.94 ± 2.41g; n=5) (control mice) via oral gavage for up to 28 days, No change in body weight was observed following AZ3839 treatment (Figure 3.16A), which was associated with no observed difference in cumulative food intake between groups (Figure 3.16B). As BACE1 inhibition (with AZ4217 and peripheral Merck-3) reduces leptin levels, and as previously mentioned, the beneficial effects of inhibiting BACE1 may be dependent on reducing leptin levels, the circulating levels were measured in serum from AZ3839 treated mice. AZ3839 did not affect leptin levels in comparison to controls (Figure 3.16C), which suggests AZ3839 is not reducing leptin levels sufficiently and therefore not allowing for the subsequent reduction in body weight. As described in the AZ4217 study (section 3.3.1.2), the diabetic phenotype of these mice was examined. AZ3839 treatment had no effect on glucose clearance relative to control mice (Figure 3.17A and B) and did not alter fasting blood glucose levels (Figure 3.17C), consistent with no change in body weight. Blood glucose levels were also unaltered with AZ3839 treatment during all time points (15-120 minutes) of an ITT (Figure 3.17D). Collectively these results show AZ3839 was not effective in improving the impaired metabolic state of DIO mice and in mimicking the phenotype of AZ4217 treated mice, peripheral Merck-3 treated mice and *BACE1*$^{-/-}$ mice.

3.3.7 Central inhibition of BACE1 *in vivo* reduces body weight and improves glucose homeostasis in diet-induced obese mice

Peripheral treatment of AZ4217 produced many, but not all, of the outcomes observed in *BACE1*$^{-/-}$ mice and mice treated with peripheral Merck-3 (Meakin et al. 2012, unpublished data), whereas peripheral AZ3839 treatment appeared to have no effect on body weight and glucose homeostasis. One issue regarding this reduced and lack of effectiveness of peripherally applied compounds were their ability to cross the BBB sufficiently to reach levels that would reduce BACE1 activity and drive central actions. This led us to question how much of the outcomes associated with reduced BACE1 are owing to central rather

than peripheral actions. DIO mice were treated with Merck-3 (10mg/kg; 28 days; Starting body weight: 47.65 ± 1.37g; n=10) or vehicle (DMSO/PBS; Starting body weight: 48.69 ± 1.48g; n=9) through central administration directly into the brain. for 28 days, and the metabolic measurements carried out for the AZ4217 study, as previously described (section 3.3.1), were performed to compare the effects of central and peripheral BACE1 inhibition.

3.3.7.1 Central inhibition of BACE1 reduces body weight in diet-induced obese mice

Central treatment with Merck-3 caused a significant reduction in percentage body weight over the course of the study in comparison to vehicle treated (control) mice (Control; 0.6% vs. Merck-3; -7.6%, n=7-9, Figure 3.18A), although body weight began to rebound towards the end of the study. At the end of the study, there was still an overall decrease in body weight (Control; -1.17 ± 0.51g vs. Merck-3; -3.60 ± 0.76g, $p<0.05$, n=7-9, Figure 3.18B). It could not be determined if this reduction in body weight was due to a reduction in adiposity as these mice could not be placed in the Echo MRI scanner due to the ICV brain infusion kit implanted. In an attempt to address this issue, circulating leptin levels in the serum of these mice (obtained at the end of the study) were measured. There was a trend towards a reduction in circulating leptin levels in central Merck-3 treated mice (Figure 3.18), however this was not a significant effect. This may be due to the loss of body weight in central Merck-3 treated mice recovering towards the end of the study.

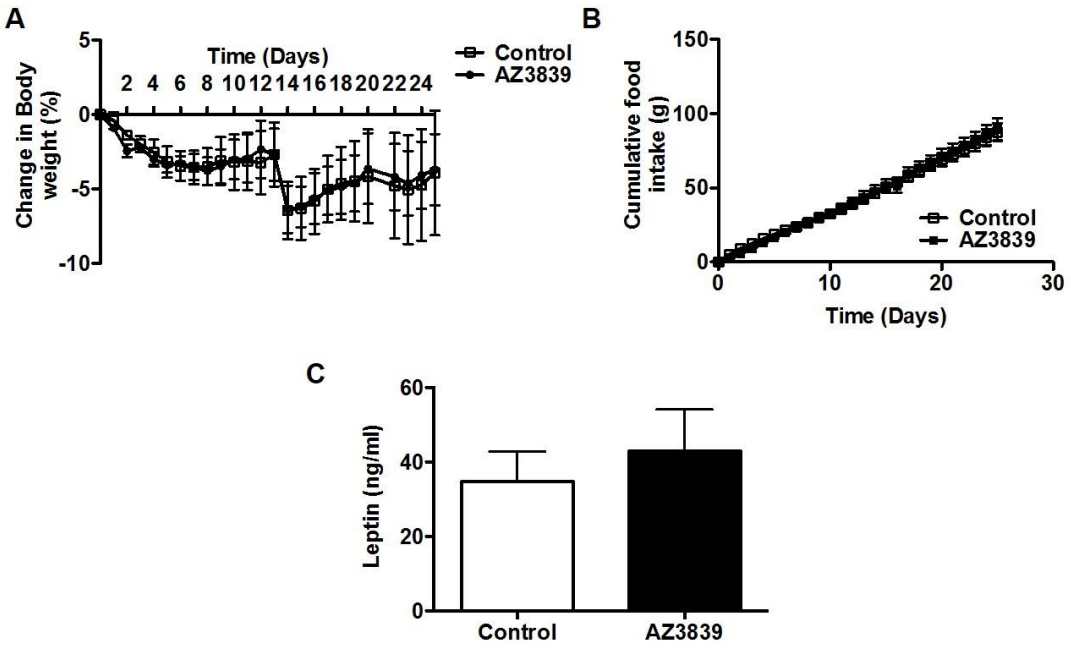

Figure 3.16 Treatment of diet-induced obese mice with AZ3839 for 28 days does not affect body weight or circulating leptin levels.

(A) Treatment with AZ3839 causes no change in percentage body weight over the course of 28 days (n=5). (B) Cumulative food intake is unchanged with AZ3839 treatment throughout the study (n=5). (C) AZ3839 treatment causes no significant difference in circulating serum leptin levels (n=5).

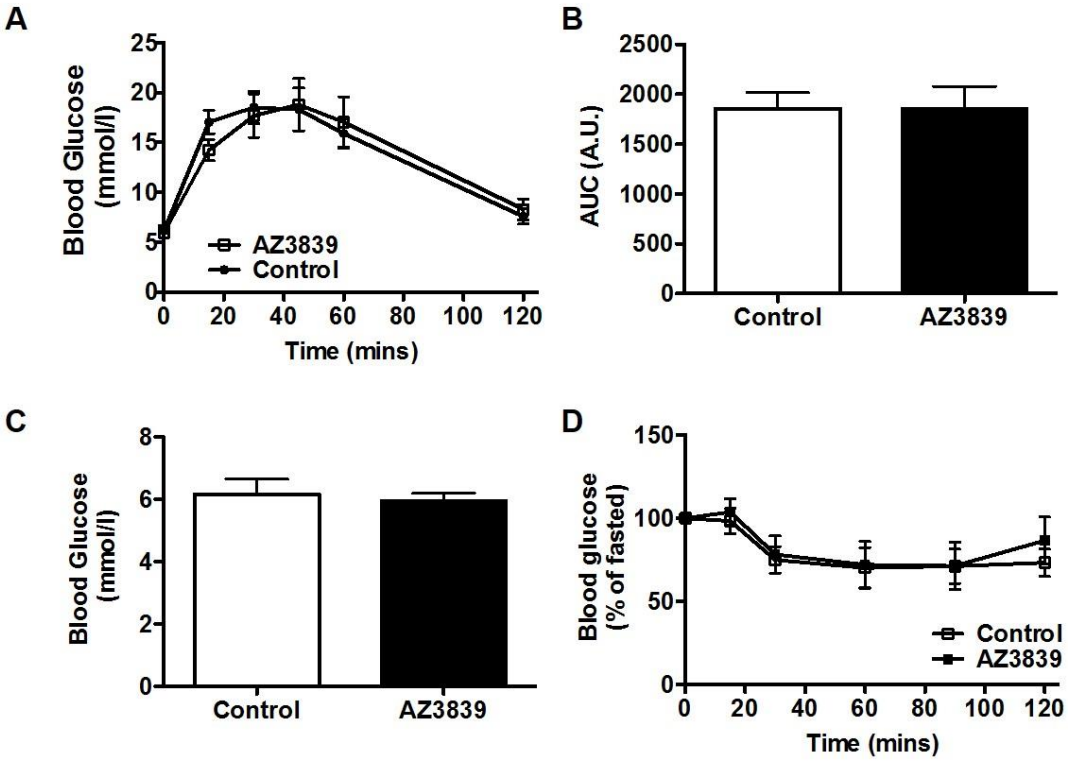

Figure 3.17 Treatment of diet-induced obese mice with AZ3839 for 28 days does not alter glucose homeostasis.

(A) Glucose tolerance test profile showing AZ3839 treatment does not affect glucose disposal (n=5). (B) Quantification of area under the curve (AUC) for glucose responses shown in (A). (C) Treatment with AZ3839 does not affect fasted blood glucose levels (n=5). (D) Insulin tolerance test profile shows there is no significant effect of AZ3839 treatment on insulin sensitivity in comparison to controls (n=5).

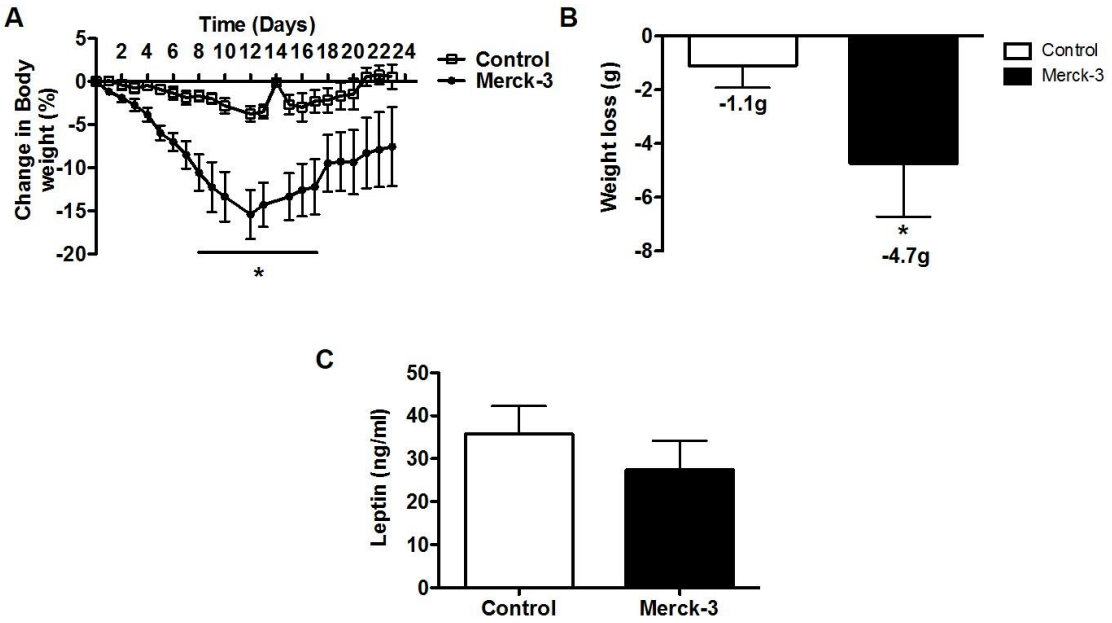

Figure 3.18 Central treatment of diet-induced obese mice with Merck-3 for 28 days significantly reduces body weight, but does not alter circulating leptin levels.

(A) Central Merck-3 treatment causes a significant reduction in percentage body weight from day 7 to day 17 of treatment ($p<0.05$, n=7-9). (B) Actual weight loss, at the end of the study, is significantly reduced in mice treated centrally with Merck-3 ($p<0.05$, n=7-9). (C) Histogram of circulating plasma leptin levels displays no significant effect with central Merck-3 treatment (n=8).
Data collection was carried out in collaboration with Dr. Paul J Meakin and Karolina Parmionova (Masters Student).

As with AZ4217 treatment, changes in food consumption was examined. There was no difference in cumulative food intake between central Merck-3 treated mice and control mice (Figure 3.19A), demonstrating both groups of mice consume the same over the course of the study. Therefore, changes in total food intake is not responsible for the observed reduction in body weight. Central Merck-3 treatment caused a significant increase in relative food intake (in relation to body weight) by day 16 of treatment, (Control; 0.09 ± 0.00 vs. 0.11 ± 0.01, $p<0.05$, n=7-8, Figure 3.19B), although no change was observed on day 1 of the study. By day 24 of treatment this effect was absent, with no significant difference displayed between central Merck-3 treated mice and control mice. These data suggest at the point in the study where loss in body weight is greatest central Merck-3 treated mice may be hyperphagic in relation to body weight.

3.3.7.2 Central inhibition of BACE1 improves glucose homeostasis in diet-induced obese mice

The diabetic phenotype of these mice was investigated by carrying out glucose tolerance (day 14) and insulin tolerance (day 21) tests. Following an overnight fast there was an increase in glucose clearance with Merck-3 treatment in comparison to control mice (AUC: control; 1299 ± 81.76 vs. Merck-3; 1020 ± 66.91, $p<0.05$, n=7-8, Figure 3.20A and B), while fasting blood glucose levels were unaltered (Figure 3.20C).

Following a four hour fast an ITT was carried out and central Merck-3 treatment caused no difference in blood glucose levels throughout the test (15-120 minutes) (Figure 3.21A). Circulating insulin levels were also measured in the serum of these mice following an overnight fast, at the end of the study (day 28). A trend towards a reduction in circulating insulin levels was found in central Merck-3 treated mice in comparison to control mice, however this was not a significant effect (Figure 3.21B). Taken together these data show central treatment with Merck-3 results in improved glucose tolerance, an effect observed at day 14 when weight loss in these animals is at its greatest. However, central Merck-3 treatment does not affect insulin sensitivity, mimicking the effects of AZ4217 treatment.

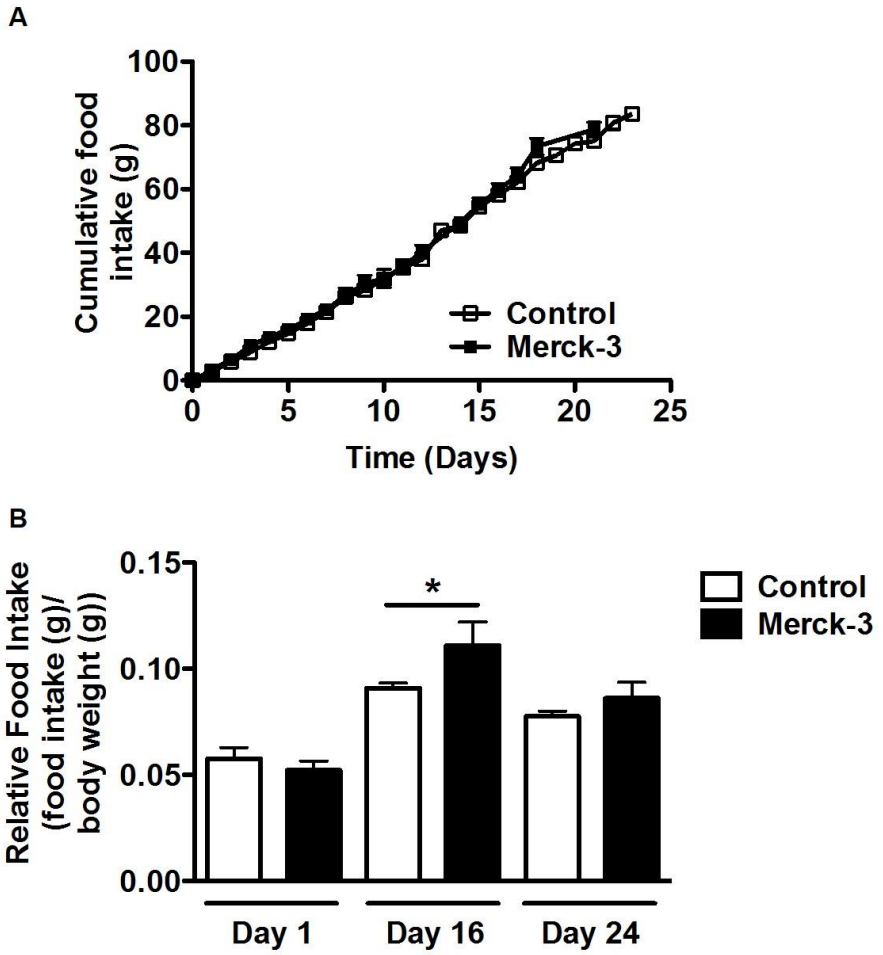

Figure 3.19 Central treatment of diet-induced obese mice with Merck-3 for 28 days does not affect food intake, however increases relative food intake.

(A) Cumulative food intake was unchanged with central Merck-3 treatment (n=7-9). (B) Relative food intake, described as a ratio between food intake and body weight, was significantly increased at day 16 of the study, but had no effect at day 1 or day 24 ($p<0.05$, n=9-10).

Data collection was carried out in collaboration with Dr. Paul J Meakin and Karolina Parmionova (Masters Student).

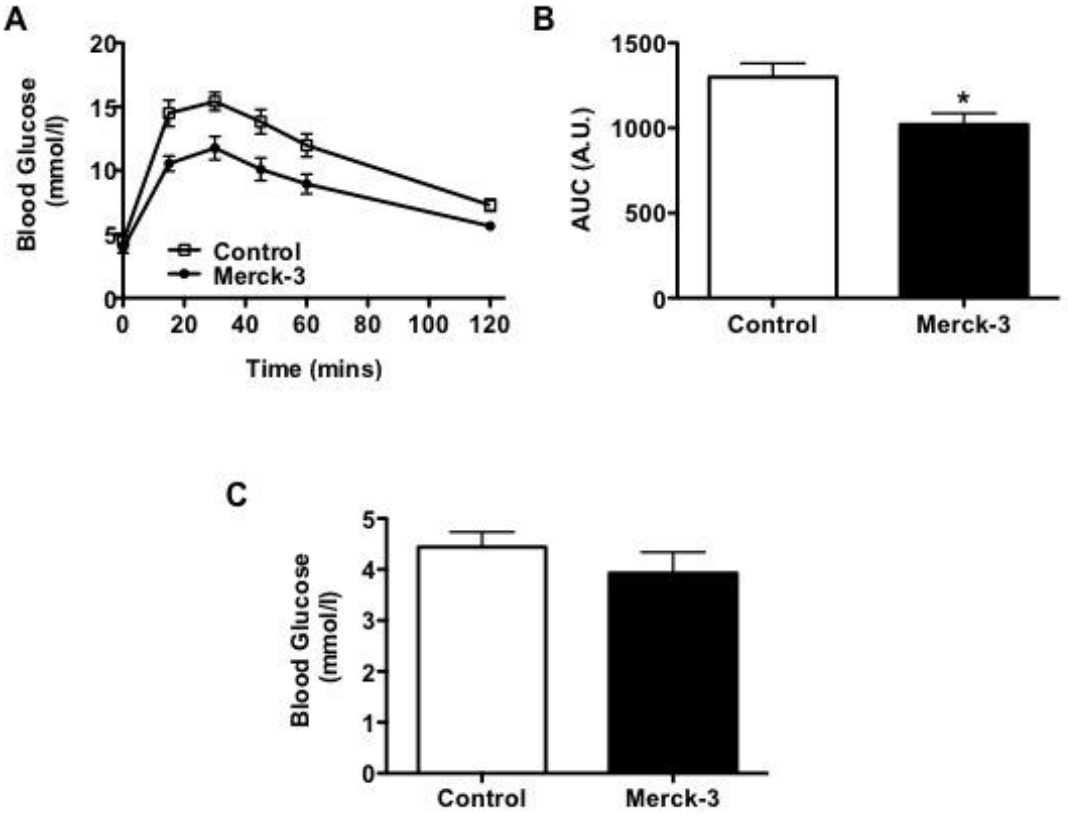

Figure 3.20 Central treatment of diet-induced obese mice with Merck-3 for 28 days improves glucose homeostasis.

(A) Glucose tolerance test profile showing central Merck-3 treatment improves glucose disposal. (B) Quantification of the area under the curve (AUC) for the glucose responses shown in (A), demonstrating a significant reduction in glucose disposal with central Merck-3 treatment ($p<0.05$, n=7-8). (C) Central Merck-3 treatment does not affect fasted blood glucose levels (n=7-9).
Data collection was carried out in collaboration with Dr. Paul J Meakin and Karolina Parmionova (Masters Student).

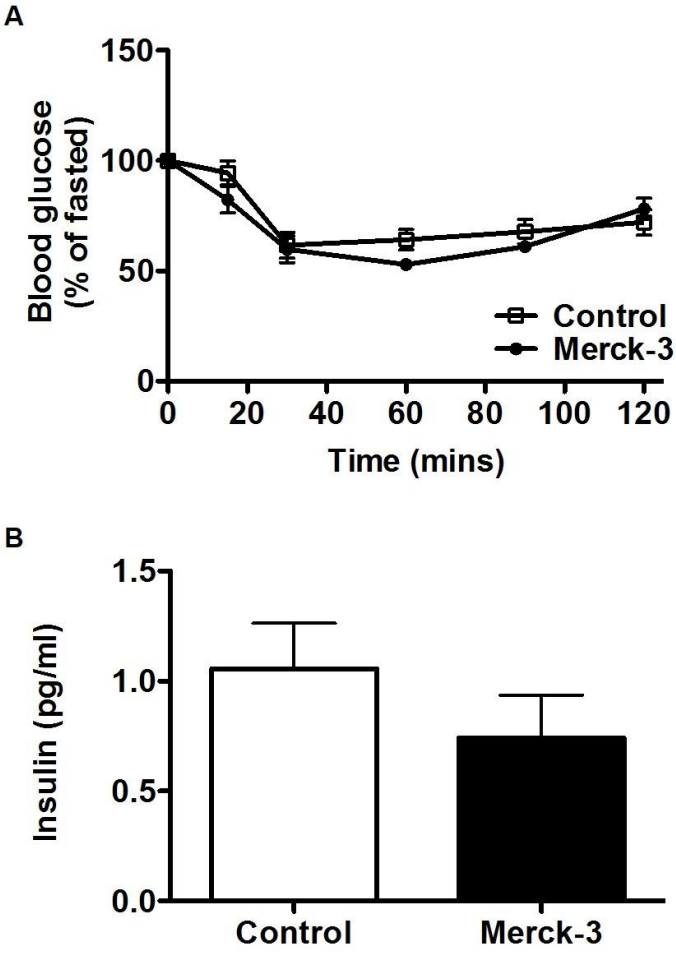

Figure 3.21 Central treatment of diet-induced obese mice with Merck-3 for 28 days does not alter insulin sensitivity.

(A) Insulin tolerance test profile displaying no significant effect of central Merck-3 treatment on insulin sensitivity (n=9-10). (B) Central Merck-3 treatment caused no significant effect on circulating serum insulin levels (n=7-10).
Data collection was carried out in collaboration with Dr. Paul J Meakin and Karolina Parmionova (Masters Student).

3.3.7.3 Central inhibition of BACE1 alters splenic weight, but does not impact other organs

Upon termination of the study tissue weights of spleen, heart, liver and brain were measured in all mice as an indication of the health of these tissues and as a crude measure of lean mass. Central Merck-3 treatment caused an increase in actual splenic size and spleen weight represented as a percentage of total body weight, compared to control mice (Actual weight: Control; 0.12 ± 0.01g vs. Merck-3; 0.18 ± 0.01g, % of body weight: Control; 0.27 ± 0.02% vs. Merck-3; 0.43 ± 0.05%, $p<0.01$, n=7-9, Figure 3.22A and B). However, no effect was observed on heart, liver or brain weights. Taken together these data show central BACE1 inhibition only affects splenic weight and does not impact other organ size or weights.

3.3.8 Central inhibition of BACE1 modifies white adipose tissue leptin expression in diet-induced obese mice

Having observed a reduction in body weight and a trend towards a reduction in circulating leptin levels following central Merck-3 treatment, the relative expression of *leptin* in WAT was examined. Central Merck-3 treatment resulted in decreased *leptin* in comparison to control mice (Control; 1.00 ± 0.14 vs. Merck-3; 0.52 ± 0.14, $p<0.05$, n=8, Figure 3.23A). *ObRb* relative levels were unaltered between Merck-3 treated mice and controls (Figure 3.23B), demonstrating, although there is a reduction in *leptin* levels, receptor expression remains the same. Collectively, these data show that, although circulating leptin levels are not significantly reduced central BACE1 inhibition is reducing leptin WAT expression, which is consistent with results from genetic and pharmacological reduction in BACE1 (unpublished data, section 3.3.2).

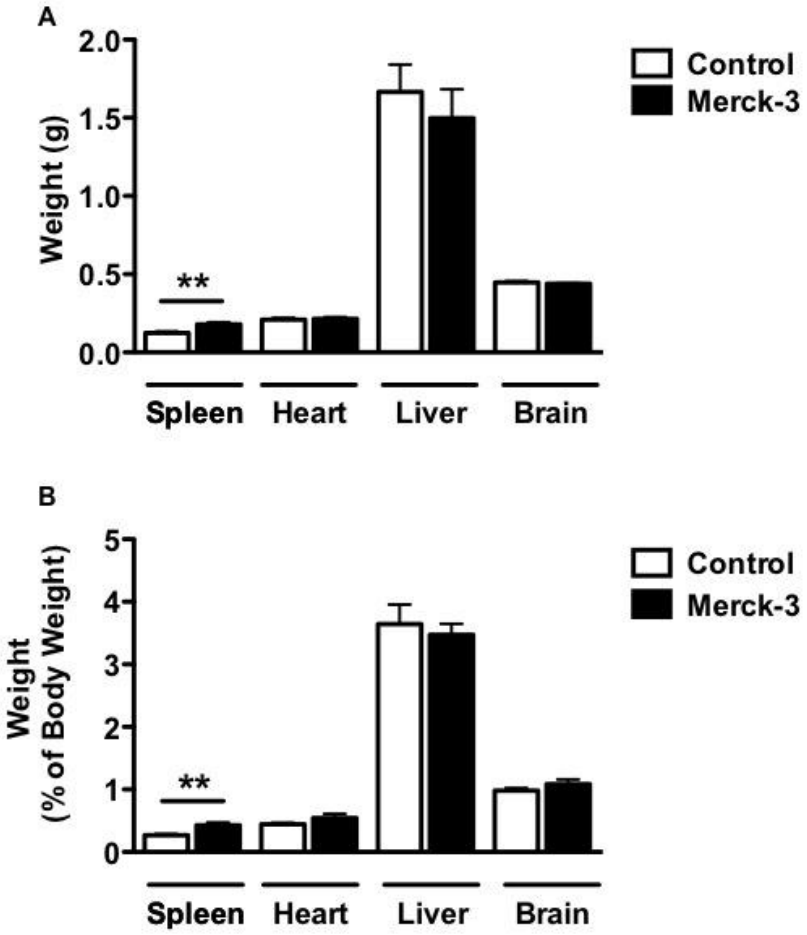

Figure 3.22 Central treatment of diet-induced obese with Merck-3 mice alters spleen weight but does not impact other organs.

(A) Central treatment with Merck-3 results in a significant increase in spleen weight ($p<0.01$) but has no effect on heart, liver or brain weights (n=7-9). (B) Actual weights represented as a percentage of total body weights.

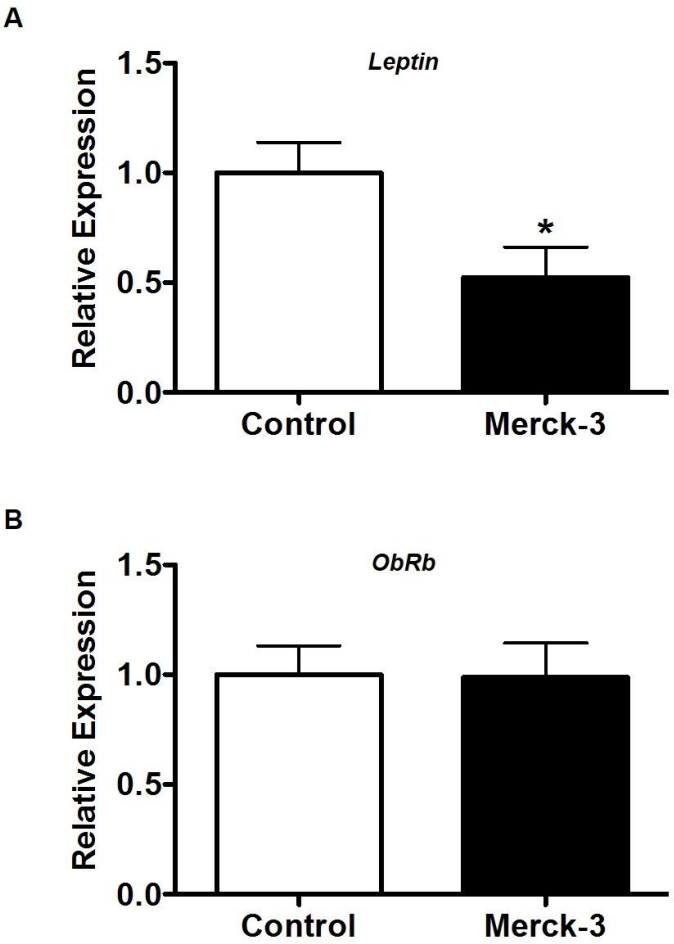

Figure 3.23 Central Merck-3 treatment significantly reduces *leptin* mRNA expression in white adipose tissue.

Histograms showing (A) *leptin* and (B) the long form of the leptin receptor (*ObRb*) in white adipose tissue. (A) Central Merck-3 treatment causes a significant reduction in *leptin* ($p<0.05$, n=8), however causes no significant effect on (B) *ObRb* (n=7-8).
Data collection was carried out in collaboration with David Allsop (PhD Student).

3.3.9 Central inhibition of BACE1 alters hypothalamic leptin signalling in diet-induced obese mice

As with peripheral AZ4217 treatment, the expression of key neuropeptides involved in leptin signalling were examined in the hypothalamus (section 3.3.3) to assess the direct effect of leptin signalling. Central Merck-3 treatment reduced *CART* expression in comparison to controls (Control; 1.00 ± 0.11 vs. Merck-3; 0.80 ± 0.08, $p<0.05$, n=7-8, Figure 3.24B), however had no significant effect on *POMC* expression (Figure 3.24A), although a trend towards an increase in comparison to controls was observed. Central Merck-3 treatment did not affect *NPY* or *AgRP* expression (Figure 3.24C and D), however resulted in a non-significant increase in the ratios of both *NPY/POMC* and *AgRP/POMC* (*NPY/POMC*: p=0.08, Figure 3.24E and F). Taken together these data indicate that central Merck-3 treatment may alter hypothalamic leptin signalling through reduced anorexigenic *CART* expression and promotion of orexigenic signalling.

Central Merck-3 treatment had no effect on the negative regulator of leptin signalling *SOCS3* expression (Figure 3.25A). Unexpectedly, central Merck-3 treatment resulted in a slight, but significant, increase in the negative regulator *PTP1B* levels in comparison to control mice (Control; 1.00 ± 0.05 vs. Merck-3; 1.16 ± 0.06, $p<0.05$, n=7-9,Figure 3.25B), an effect not observed with peripheral BACE1 inhibition. Collectively these data demonstrate central Merck-3 administration does not largely impact the negative regulation of hypothalamic leptin signalling, and therefore alterations in hypothalamic leptin signalling may not be directly responsible for the observed effects. However, measurements of actual leptin sensitivity in these animals has not been tested.

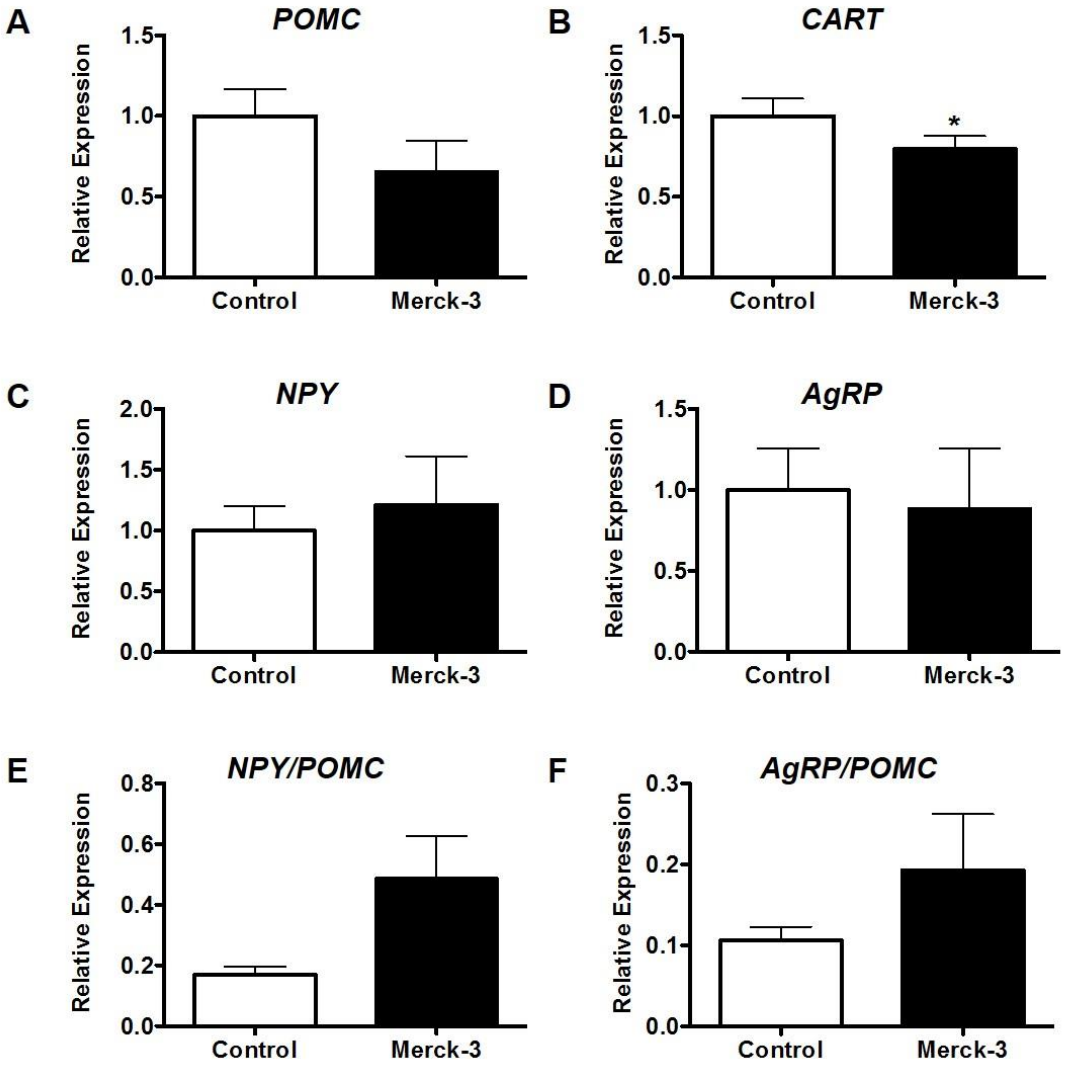

Figure 3.24 Central Merck-3 treatment reduces anorexigenic neuropeptide expression and promotes orexigenic signalling in the hypothalamus.

Histograms showing relative mRNA expression of (A) *POMC*, (B) *CART*, (C) *NPY*, (D) *AgRP*, (E) *NPY/POMC* and (F) *AgRP/POMC* in the hypothalamus. (A and B) Central Merck-3 treatment causes a trend towards a reduction in hypothalamic *POMC* mRNA expression (n=7-9) and a significant reduction in *CART* mRNA expression ($p<0.05$, n=7-8). (C and D) Central Merck-3 treatment had no significant effect on orexigenic neuropeptides *NPY* (n=7-9) or *AgRP* (n=7-8). (E and F) Representative hypothalamic ratios of *NPY/POMC* (n=7-9) and *AgRP/POMC* (n=6-9) display a slight, but non-significant, increase.Data collection was carried out in collaboration with Karolina Parmionova (Masters Student).

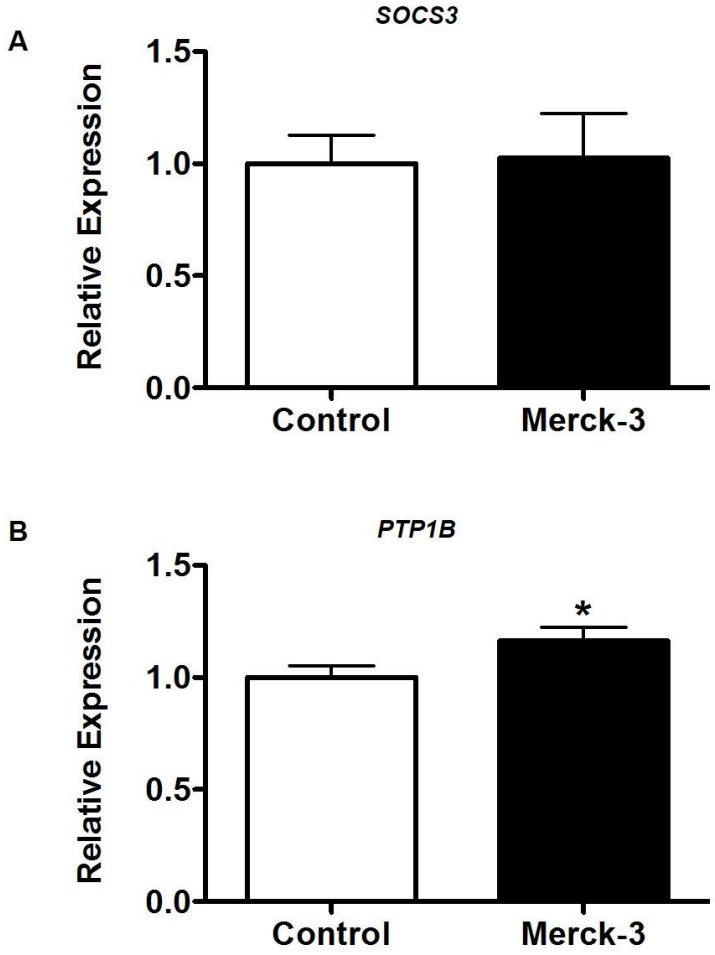

Figure 3.25 Central Merck-3 treatment significantly increases *PTP1B* gene expression, but does not alter *SOCS3* expression in the hypothalamus.

Histograms showing relative mRNA expression of (A) *SOCS3* and (B) *PTP1B* in the hypothalamus. (A) Central Merck-3 treatment has no significant effect on *SOCS3* (n=7-9). (B) Central Merck-3 treatment causes a significant increase in hypothalamic *PTP1B* expression ($p<0.05$, n=7-9).

3.3.10 Central inhibition of BACE1 alters thermogenic programming in diet-induced obese mice

Having observed central Merck-3 largely mimicking the *in-vivo* effects of peripheral BACE1 inhibition, which may be due in part to alterations in thermogenic programming, the expression of genes involved in thermogenesis were also examined. In BAT, central Merck-3 treatment did not alter *UCP1* expression levels compared to control mice (Figure 3.26A), although other markers indicating up-regulation of thermogenic programming in BAT were elevated following central Merck-3 treatment. *PGC1α* was significantly increased (Control; 1.00 ± 0.12 vs. Merck-3; 2.00 ± 0.38, $p<0.05$, n=9, Figure 3.26B), *DIO2* displayed a non-significant increase ($p=0.07$, Figure 3.26C) and *Prdm16* displayed a trend towards an increase (Figure 3.26D). These data show, although *UCP1* expression is not altered, other genes involved in thermogenic programming are upregulated following central Merck-3 treatment, indicating thermogenesis may be initiated; an effect not observed following peripheral AZ4217 treatment.

The skeletal muscle of central Merck-3 treated mice was also examined, but unlike AZ4217 treatment, central Merck-3 treatment caused an unexpected decrease in *UCP2* levels in skeletal muscle (Control; 1.00 ± 0.31 vs. Merck-3; 0.65 ± 0.15, $p=0.06$, n=7-8, Figure 3.27A). However, no change in *UCP3* mRNA levels was observed (Figure 3.27B). These data are consistent with the lack of strong evidence for increasing thermogenesis in BAT or muscle.

Having observed increased expression of genes involved in thermogenesis in BAT, the presence of increased energy expenditure via 'browning' of WAT was examined. In WAT central Merck-3 treatment displayed a trend towards a small increase in *UCP1* expression (Figure 3.28A), however did not alter *PGC1α*, *DIO2* or *Prdm16* expression in comparison to control mice (Figure 3.28C, D and E). These data indicate that central Merck-3 does not affect enhanced thermogenesis in WAT. Although there is an effect on BAT, collectively these data suggest increased thermogenesis may not be the main factor driving the improved metabolic phenotype caused by central inhibition of BACE1.

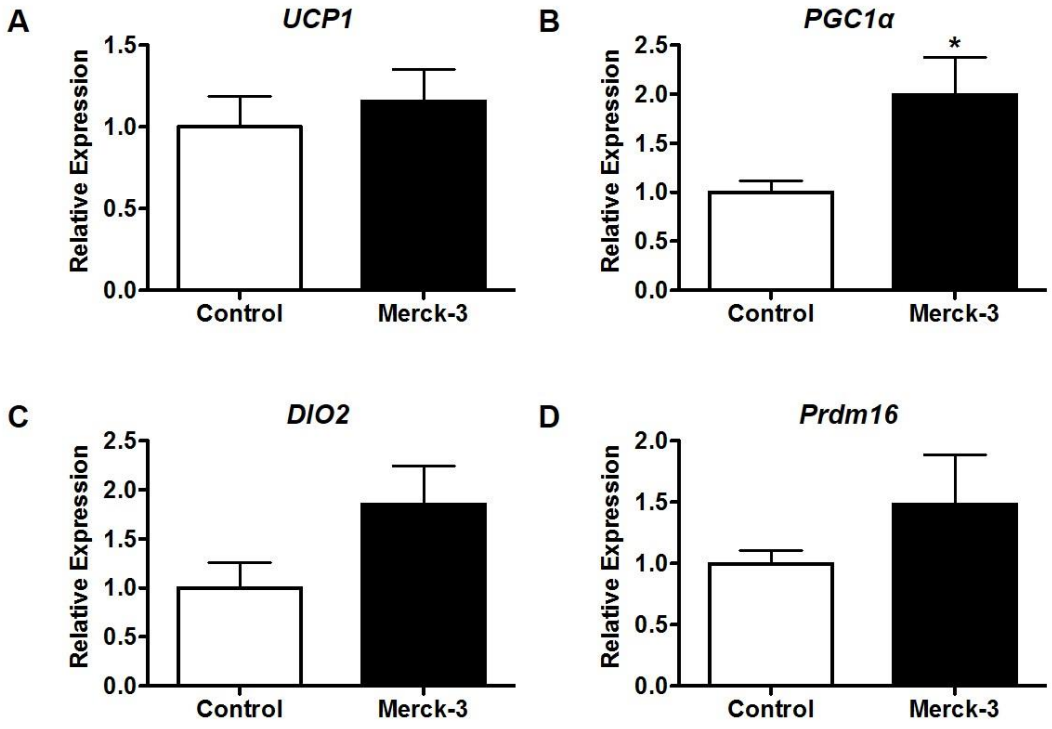

Figure 3.26 Central Merck-3 treatment significantly increases *PGC1α* but does not alter other markers of thermogenic programming in brown adipose tissue.

Histograms showing relative mRNA expression of (A) *UCP1*, (B) *PGC1α*, (C) *DIO2* and (D) *Prdm16* in brown adipose tissue. (A) Central Merck-3 treatment causes no significant effect on (A) *UCP1* (n=8). (B) Central Merck-3 treatment causes a significant increase in *PGC1α* ($p<0.05$, n=9) relative expression and a non-significant trend towards an increase in (C) *DIO2* ($p=0.07$, n=8) and (D) *Prdm16* (n=9) relative expression.
Data collection was carried out in collaboration with Dr. Gemma Montagut.

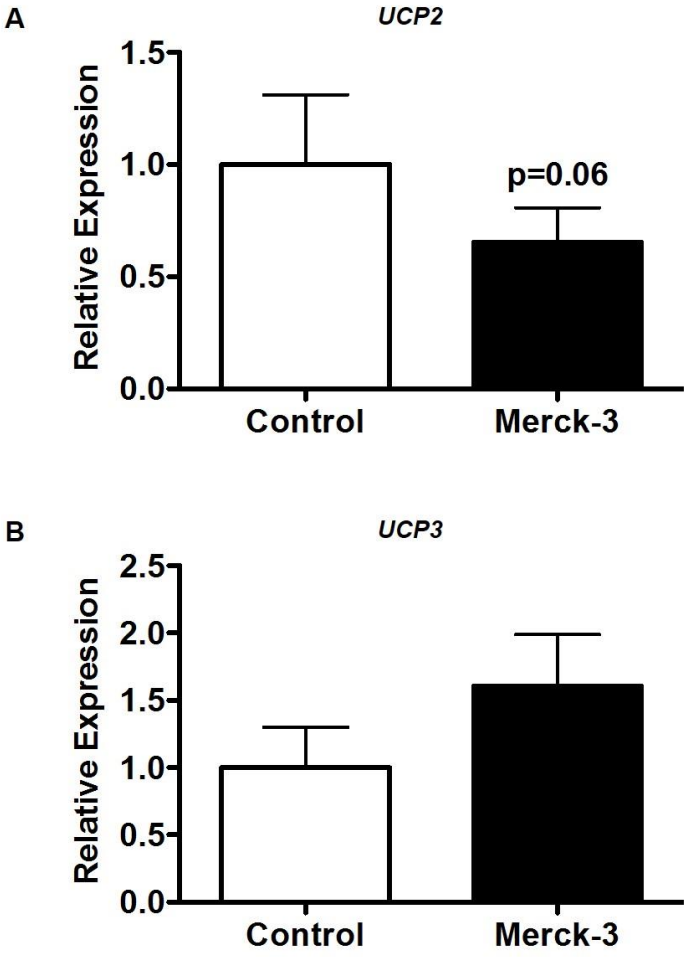

Figure 3.27 Central Merck-3 treatment alters *UCP2* expression, but not *UCP3*, in skeletal muscle.

Histograms showing relative mRNA expression of (A) *UCP2* and (B) *UCP2* in skeletal muscle. Central Merck-3 treatment causes a decrease in (A) *UCP2* expression (p=0.06, n=7-8), however has no effect on (B) *UCP3* expression (n=8).
Data collection was carried out in collaboration with Christopher McGinley (DCAT Summer Project Studentship).

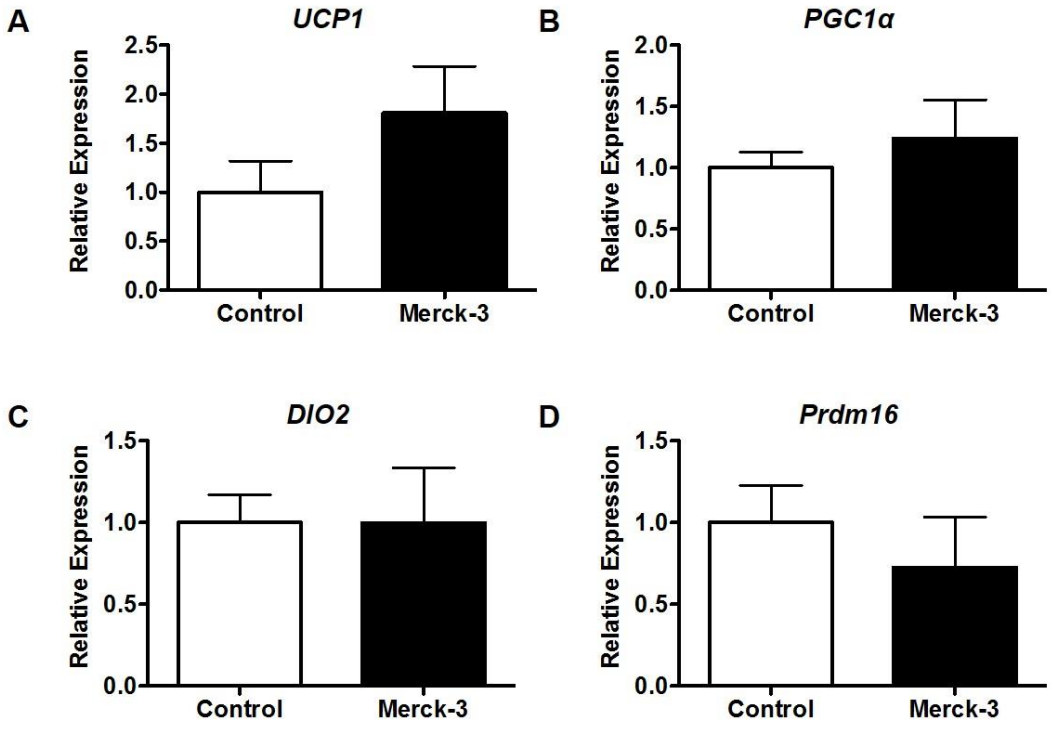

Figure 3.28 Central Merck-3 treatment does not alter thermogenic programming in white adipose tissue.

Histograms showing relative mRNA expression of (A) *UCP1*, (B) *PGC1α*, (C) *DIO2* and (D) *Prdm16* in white adipose tissue. (A) Central Merck-3 treatment causes a trend towards an increase in *UCP1* (n=7-8) relative expression. (B-D) Central Merck-3 treatment causes no significant effect on (B) *PGC1α* (n=8), (C) *DIO2* (n=8) or (D) *Prdm16* (n=8) relative expression.
Data collection was carried out in collaboration with Dr. Gemma Montagut.

3.3.11 Central inhibition of BACE1 modifies high-fat diet-mediated inflammatory programming in diet-induced obese mice

Having observed that peripheral inhibition of BACE1 (AZ4217 treatment) reduced WAT inflammation we next examined whether central inhibition would cause the same effect. In the hypothalamus pro inflammatory cytokines, markers of the inflammasome and total macrophage expression were measured, as described previously for the AZ4217 study (section 3.3.5). In the hypothalamus central Merck-3 treatment caused no effect on *TNFα* expression (Figure 3.29A) however reduced *IL-6* expression (Control; 1.00 ± 0.12 vs. Merck-3; 0.80 ± 0.07, $p<0.05$, n=7-9, Figure 3.29B) compared to control mice. *IL-1β*, *NLRP3* and *Caspase 1* levels were reduced following central Merck-3 treatment relative to DIO controls (*IL-1β*: Control; 1.00 ± 0.16 vs. Merck-3; 0.63 ± 0.12, $p<0.05$, *NLRP3*: Control; 1.00 ± 0.14 vs. Merck-3; 0.68 ± 0.04, $p<0.001$, *Caspase 1*: Control; 1.00 ± 0.11 vs. Merck-3; 0.69 ± 0.10, $p<0.05$, n=7-9, Figure 3.29C, D and E), however *F4/80* expression, as an indication of total macrophage levels, was not altered (Figure 3.29F). Taken together these data show central Merck-3 treatment reduces hypothalamic inflammation through a large reduction in *IL-1β* and markers of the inflammasome, suggesting reduced central inflammatory programming may drive a proportion of the *in-vivo* changes observed in our mice.

In WAT pro- and anti-inflammatory cytokines, previously described for AZ4217 treatment (section 3.3.5), as well as *F4/80* expression were measured. Central Merck-3 treatment drove a reduction in *NOS2* expression (Control; 1.00 ± 0.10 vs. Merck-3; 0.67 ± 0.13, $p<0.05$, n=7-8, Figure 3.30A), but did not alter *IFNγ*, *IL-1β* or *TNFα* compared to controls (Figure 3.30B, C and D). Interestingly, central Merck-3 treatment caused a trend towards an increase in *IL-6* expression compared to control mice (Control; 1.00 ± 0.10 vs. Merck-3; 1.76 ± 0.36, $p=0.07$, n=8, Figure 3.30E). Central Merck-3 treatment also drove a large increase in anti-inflammatory cytokines *IL-10*, *YM-1* and *Arg-1* compared to control mice (*IL-10*: Control;1.00 ± 0.27 vs. Merck-3; 1.43 ± 0.15, $p<0.05$, *YM-1*: Control; 1.00 ± 0.13 vs. Merck-3; 2.69 ± 0.63, $p<0.05$, *Arg-1*: Control; 1.00 ± 0.15 vs. Merck-3; 1.69 ± 0.21, $p<0.05$, n=6-8, Figure 3.30F, G and H), and a slight trend towards an increase in *F4/80* expression compared to control mice ($p=0.07$, Figure 3.30I). Collectively these data, in particular the large increase in anti-inflammatory cytokines, suggests central BACE1 inhibition is modifying inflammatory programming in WAT.

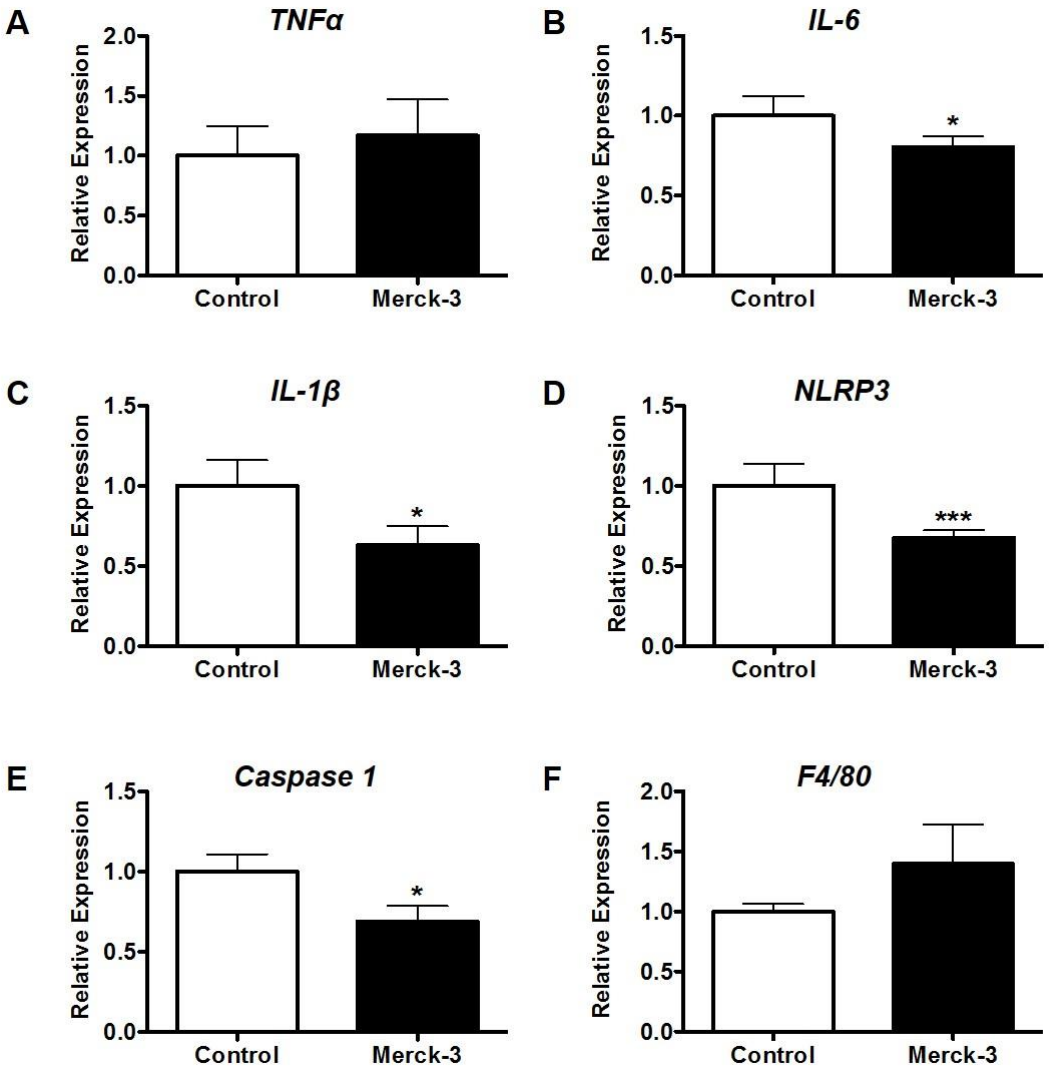

Figure 3.29 Central Merck-3 treatment significantly reduces pro-inflammatory cytokines and markers of the inflammasome, but does not affect *F4/80* expression in the hypothalamus.

Histograms showing relative mRNA expression of pro-inflammatory cytokines (A) *TNFα* , (B) *IL-6*, (C) *IL-1β*, markers of the inflammasome (D) *NLRP3*, (E) *Caspase 1* and macrophage marker (F) *F4/80* in the hypothalamus.(A) Central Merck-3 treatment causes no significant effect on *TNFα* expression (n=7-9). (B) Central Merck-3 treatment causes a significant reduction in (B) *IL-6* expression ($p<0.05$, n=7-9).(C) Central Merck-3 treatment causes a significant reduction in *IL-1β* expression ($p=0.05$, n=7-9, and a significant reduction in other markers of the inflammasome (D) *NLRP3* ($p<0.001$, n=7-9) and (E) *Caspase 1* ($p<0.05$, n=7-8) expression. (F) Central Merck-3 treatment results in a non-significant trend towards an increase in total macrophage number measured by *F4/80* expression (n=7-9).
Data collection was carried out in collaboration with Dr. Paul J Meakin and Karolina Parmionova (Masters Student).

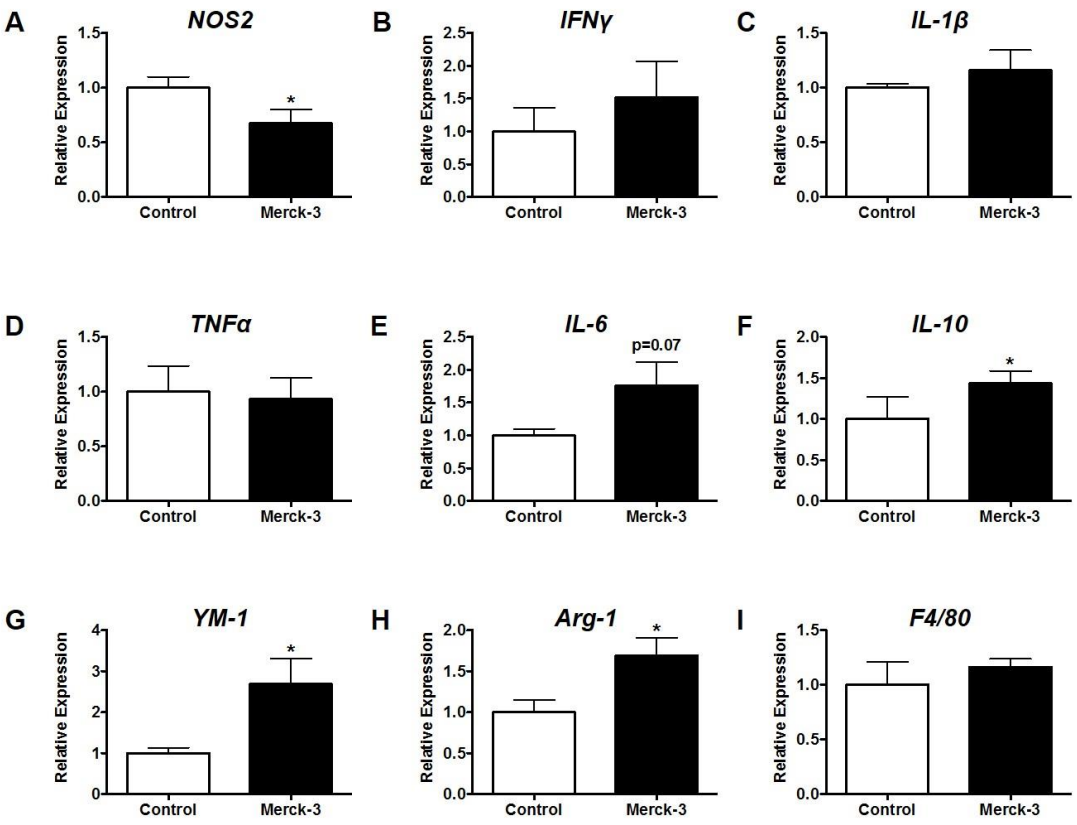

Figure 3.30 Central Merck-3 treatment increases anti-inflammatory signalling in white adipose tissue.

Histograms showing relative mRNA expression of pro-inflammatory cytokines (A) *NOS2*, (B) *IFNγ*, (C) *IL-1β*, (D) *TNFα*, (E) *IL-6*, anti-inflammatory cytokines (F) *IL-10*, (G) *YM-1*, (H) *Arg-1* and macrophage marker (I) *F4/80* in white adipose tissue.(A) Central Merck-3 treatment causes a significant reduction in *NOS2* expression ($p<0.05$, n=7-8). (B-D) Central Merck-3 treatment caused no significant effect on pro-inflammatory cytokines *IFNγ*, *IL-1β* and *TNFα* expression (n=8), although showed a trend towards an increase in (E) *IL-6* ($p=0.07$, n=8) expression. (F-H) Central Merck-3 treatment caused a significant increase in anti-inflammatory cytokines *IL-10* ($p<0.05$, n=7-8), *YM-1* ($p<0.05$, n=8) and *Arg-1* ($p<0.05$, n=6-8). (I) Total number of macrophages are unchanged, indicated by (I) *F4/80* expression (n=8).
Data collection was carried out in collaboration with David Allsop (PhD Student).

Macrophage infiltration of WAT was also examined via measuring levels of chemotactic cytokines; *MCP-1*, *MIP-1α* and *MIP-1β*, and *RANTES*, as previously described for AZ4217 treatment (section 3.3.5). Central Merck-3 treatment had no effect on *MCP-1*, *MIP-1α* or *RANTES* (Figure 3.31A, B and D), and raised *MIP-1β* levels (Control; 1.00 ± 0.10 vs. Merck-3; 1.75 ± 0.29, $p<0.05$, n=7-8, Figure 3.31C) relative to controls. *TGFβ-1* levels were also unaltered following Merck-3 treatment, compared to control mice (Figure 3.31E). These data suggest that central Merck-3 treatment does not affect chemokine expression, and therefore macrophage migration and/or infiltration of WAT.

Taken together these data (supported by results from *BACE1*$^{-/-}$ mice and mice treated with peripheral Merck-3 (unpublished data)) demonstrate that BACE1 may play a role in HFD mediated inflammatory programming, with central inhibition of BACE1 reducing inflammation both centrally (hypothalamus) and peripherally (WAT), and this could drive, in part, the improved obese/diabetic phenotype of mice with reduced BACE1 levels.

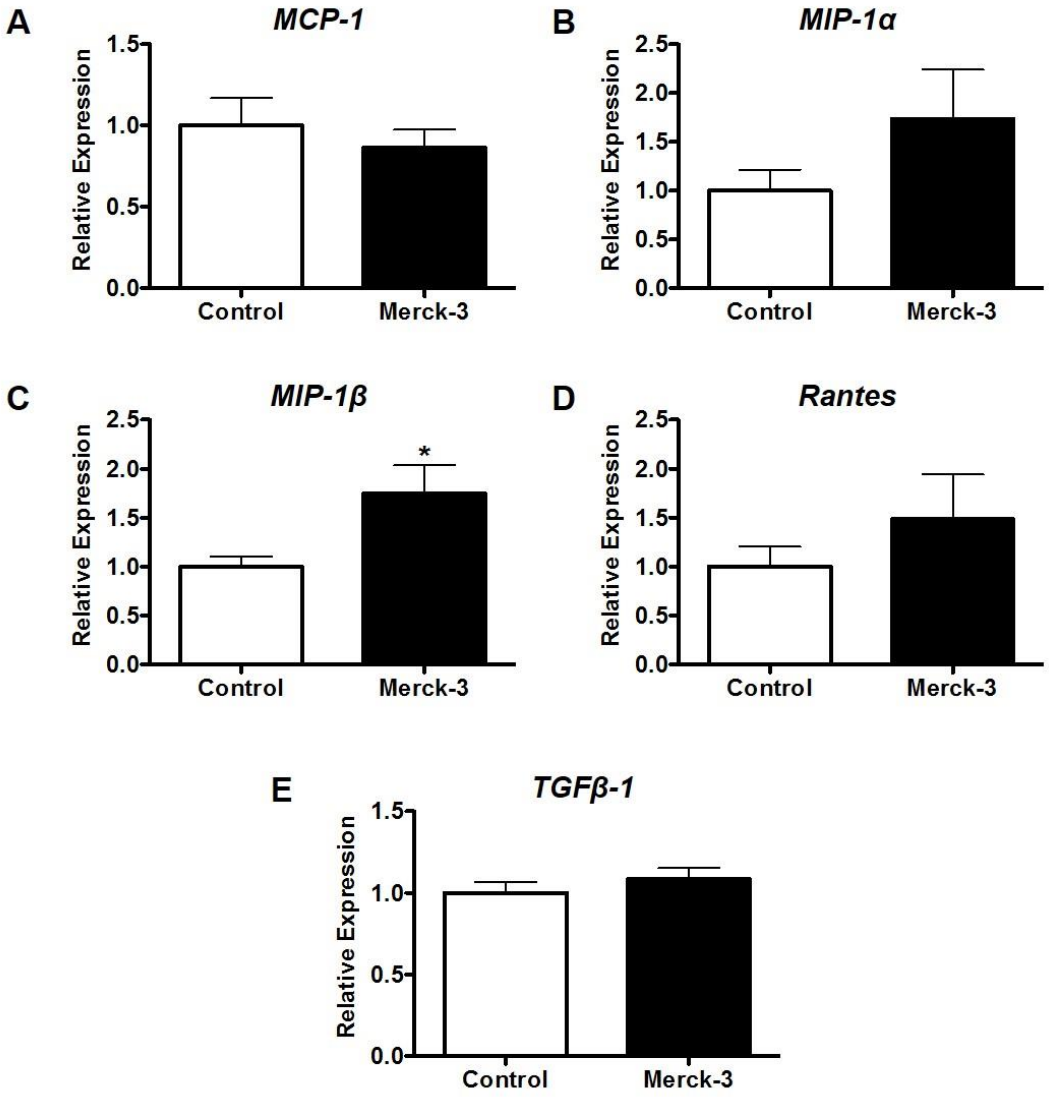

Figure 3.31 Central Merck-3 treatment significantly increases *MIP-1β* expression in white adipose tissue, but does not alter the expression of other chemokines.

Histograms showing relative mRNA expression of chemokines (A) *MCP-1*, (B) *MIP-1α*, (C) *MIP-1β*, (D) *Rantes*, and (E) *TGFβ-1* in white adipose tissue. (A and B) Central Merck-3 treatment does not cause a significant effect on *MCP-1* (n=7-8), or *MIP-1α* (n=6-8) expression. (C) Central Merck-3 treatment causes a significant increase in *MIP-1β* expression ($p<0.05$, n=7-8). (D and E) Central Merck-3 treatment causes no significant effect on *Rantes* (n=7-8) or (E) *TGFβ-1* (n=7-8) expression.
Data collection was carried out in collaboration with David Allsop (PhD Student).

3.4 Discussion

3.4.1 Summary

Within this chapter we set out to investigate the effects of treating DIO mice with BACE1 inhibitors and comparing the results to the previously reported metabolic phenotype of the *BACE1*$^{-/-}$ mouse. The results from these studies are summarised in Table 3.1. Overall, we found both peripherally and centrally inhibiting BACE1 (using AZ4217 and Merck-3) improved all metabolic outcomes in DIO mice (excluding insulin sensitivity), however AZ3839 had no effect. Through studies utilising real-time PCR, to examine changes in gene expression, we found both peripheral and central BACE1 inhibition alters the expression of genes involved in hypothalamic leptin signalling, and may promote orexigenic signalling. Real-time PCR studies demonstrated no clear effect on thermogenesis following peripheral and central BACE1 inhibition, with a lack of consistent changes in the expression of genes involved in thermogenic programming. Lastly, both peripheral and central BACE1 inhibition altered a degree of high-fat diet driven inflammation, through changes in gene expression of cytokines and chemokines in both the hypothalamus and WAT, generally driving a reduction in pro-inflammatory cytokine expression following treatment. These results, and the potential underlying mechanisms, will be further discussed in the following sections.

Metabolic Outcome	***BACE1*$^{-/-}$**	**AZ4217**	**AZ3839**	**Merck-3 (central infusion)**
Body weight	↓	↓	-	↓
Fat mass	↓	↓	-	/
Food intake	-	-	-	-
Leptin levels	↓	↓	-	↓
Glucose tolerance	↑	↑	-	↑
Insulin sensitivity	-	-	-	-

Table 3.1 Summary of results for metabolic outcomes measured during inhibitor studies and previously reported *BACE1*$^{-/-}$ studies.

Symbols as follows: ↓, reduced. ↑, improved. -, unchanged. /, could not be measured.

3.4.2 Pharmacological inhibition of BACE1 improves an obese/diabetic phenotype

Herein we have demonstrated that pharmacological inhibition of BACE1 (with peripheral AZ4217 and central Merck-3 treatment) in DIO mice improves an obese/diabetic phenotype. This was observed through improvements in a variety of metabolic markers and the results mimic the effects of genetically reducing BACE1 (Meakin et al. 2012) or pharmacologically inhibiting BACE1 with Merck-3 administered peripherally (unpublished data). Overall, the weight loss and glucose homeostasis effects measured in the *BACE1*$^{-/-}$ mouse are emulated with both peripheral and central inhibition of BACE1, shown by a large reduction in body weight, specifically due to a reduction in fat mass in AZ4217 treated mice (this could not be measured in centrally treated mice), over the course of treatment. Unlike AZ4217 treatment, it was observed that with central Merck-3 treatment there was a rebound in body weight after day 14 of treatment, where treated animals began to slowly re-gain weight. This may be due to compensatory mechanisms being initiated as the reduction in body weight following initial administration of the drug was dramatic and these mice lost more weight in the first two weeks of the study than those treated peripherally. A re-bound in body weight is often observed following rapid and large weight loss regimes in humans (Blomain et al. 2013). As mentioned, the compound utilised in the central inhibitor experiments has previously been tested peripherally (unpublished data) and in the current studies we utilised the same dose. Sankaranarayanan and colleagues reported that Merck-3 poorly penetrates the BBB (Sankaranarayanan, Price, Wu, M. Crouthamel, et al. 2008) when administered peripherally. In contrast to these results, our lab found that Merck-3 does enter the brain, reaching concentrations of 250pmol/g (wet brain) (unpublished data). Therefore, when Merck-3 is delivered directly into the lateral ventricle the central concentration may be very high, causing a rapid and dramatic loss of body weight, and so engaging alternative compensatory weight-gain mechanisms. Future studies would be required to examine the amount of Merck-3 that is present in the brain, following central administration, using mass spectrometry of brain samples from treated mice to determine if the concentration is indeed far higher than when Merck-3 is administered peripherally.

In line with the correlation between circulating levels of leptin and fat mass (Maffei et al. 1995) we also observe a large reduction in plasma leptin levels in AZ4217 treated mice. This suggests inhibition of BACE1 is causing a reduction in the high circulating levels of

leptin which develop in obesity (Considine et al. 1996), and as a result is reversing the resulting leptin resistance. It has formerly been reported that *BACE1*$^{-/-}$ mice also display increased leptin sensitivity, even when challenged with a HFD (unpublished data), supporting the concept that a reduced degree of adiposity or resistance to diet-induced obesity is the result of increased hypothalamic leptin sensitivity. Interestingly, these effects are dependent on leptin. In the genetically obese *ob/ob* and *db/db* mouse models BACE1 inhibition does not elicit beneficial effects (unpublished data), demonstrating that reduction of BACE1 not only increases leptin sensitivity, but requires intact leptin signalling to produce metabolic effects. The requirement for intact leptin signalling is suggestive of a centrally acting mechanism driving the observed effects as the signalling form of the leptin receptor is predominantly expressed in the hypothalamus (Fei et al. 1997; Lee et al. 1996), and the hypothalamus, primarily the ARC, is the main site of leptin resistance (Enriori et al. 2007). Unfortunately, we do not observe a significant reduction in leptin levels in centrally treated mice, although there is a trend towards a reduction, which may be due to the observed re-bound in body weight. Leptin levels were measured at the end of the study when the mice had re-gained weight, thus there is likely an associated rise in leptin levels. It would be beneficial to measure leptin levels when mice have been treated centrally with a lower dose of Merck-3, or alternatively if the duration of the study was modified to a time point where mice were maintaining steady weight loss (i.e terminate the study at day 14). Additionally, it is important to highlight that in all studies we have not definitively measured leptin sensitivity. It is necessary to examine changes in food intake and body weight and/or pSTAT3 in response to exogenous leptin treatment following short-term treatment with peripherally administered Merck-3, to give a precise assessment of the effect of BACE1 inhibition on leptin sensitivity. A measure of leptin sensitivity has been carried out in *BACE1*$^{-/-}$ mice (unpublished data) by continuous daily injections of leptin to attain plasma levels higher than observed for DIO. Interestingly, *BACE1*$^{-/-}$ mice do not develop obesity when challenged with a HFD, demonstrating that not only is intact leptin signalling required for the effects of BACE1 inhibition, but there is a reciprocal requirement of a minimum level of BACE1 to cause the development of leptin resistance.

In models of obesity a reduction in body weight can often be linked to a concomitant reduction in food intake. Within our studies we observed that BACE1 inhibition (central and peripheral) does not alter food intake, thus mice are not consuming less to account for their reduced body weight. Conversely, we observed that these mice have relative

hyperphagia in relation to body weight. This is an effect observed at the end of the study in AZ4217 treated mice, and at day 16 for central Merck-3 treated mice, indicative of the point at which weight loss is greatest. Moreover, *BACE1*$^{-/-}$ mice also display hyperphagia in response to fasting, in comparison to WT littermates (unpublished data). As no change in daily food intake is observed when BACE1 is reduced, however mice are relatively hyperphagic, we assume the loss of body weight is caused by increased energy expenditure. In support of this, *BACE1*$^{-/-}$ mice reportedly have an increased resting metabolic rate (Meakin et al. 2012), a result also observed in mice treated peripherally with Merck-3, however no change in locomotor activity is observed (unpublished data). Unfortunately, these measurements could not be attained in the BACE1 inhibitor treated mice described in these studies due to technical issues; therefore no change in actual energy expenditure can be definitively concluded. As all metabolic changes found in these mice mimic those recorded in peripheral Merck-3 treated and *BACE1*$^{-/-}$ mice, it can be hypothesised that AZ4217 and central Merck-3 treatment will also cause increased resting metabolic rate with no alterations in locomotor activity. Taken together, it is hypothesised that mice treated with a BACE1 inhibitor are not exercising more and consequently the increased energy expenditure may be by means of upregulated thermogenic programming.

Within this chapter we have shown that inhibition of BACE1 (peripheral and central) improves glucose homeostasis, through increased glucose disposal and fasted blood glucose levels during a GTT. These data suggest increased glucose uptake by peripheral tissues (Hamilton et al. 2014) and reversal of impaired glucose handling observed in obese mouse models (Bray & York 1979; Winzell & Ahren 2004). Again, this was an effect which mimicked findings from *BACE1*$^{-/-}$ mice (Meakin et al. 2012) and peripheral Merck-3 treated mice (unpublished data). Furthermore, BACE1 overexpression *in vitro*, in skeletal muscle cells, has been shown to decrease glucose uptake (Hamilton et al. 2014). Only mild improvements in glucose homeostasis are observed in NC fed animals given Merck-3 peripherally (unpublished data), indicating this beneficial effect only occurs in an obese state when BACE1 levels are elevated. Noteworthy, is that we performed GTTs on day 14 of the studies, at which point central Merck-3 treated mice show the greatest reduction in body weight, therefore, it is unsurprising that we observe effects on glucose handling. In support of an improved diabetic phenotype, insulin sensitivity was also measured in these studies and only modest improvements were observed. This was not unique to our studies, as this is also observed with peripheral

Merck-3 treatment (unpublished data). Due to the retention of leptin sensitivity and improved glucose homeostasis it was hypothesised that BACE1 inhibition may also reverse insulin resistance, although this was not demonstrated in our studies. *BACE1*$^{-/-}$ mice show increased insulin sensitivity (Meakin et al. 2012) and BACE1 inhibition *in vitro,* on skeletal muscle cells, show enhanced insulin signalling (Hamilton et al. 2014). Therefore, a lack of effect in our study may be due to the length of treatment and possibly a longer period of inhibition would be required to evoke changes in insulin tolerance and serum insulin levels. As the development of insulin resistance can be considered, at least in part, to be due to central effects as insulin receptors are also present in the hypothalamus, it may be interesting to focus on central inhibitor studies to address this. Noteworthy, is that during central inhibitor studies the ITT was conducted during the re-bound of body weight and this may mask any changes so it would be beneficial to re-test insulin sensitivity with a lower dose of Merck-3 or before substantial weight is re-gained.

Interestingly, AZ3839 (a structurally different BACE1 inhibitor) did not induce the same metabolic effects as the previously tested compounds; causing no change in body weight, food intake, or glucose homeostasis in DIO mice. In addition, treatment of DIO mice with AZ3839 did not reduce circulating levels of leptin, which has been found to be one of the larger effects observed with BACE1 inhibition utilising other compounds. If it is assumed reducing BACE1 improves an obese phenotype by increasing leptin sensitivity and this effect is necessary to cause the resulting metabolic changes, AZ3839 may not reduce circulating leptin levels sufficiently to see any subsequent body weight and glucose tolerance changes. This inability of AZ3839 to replicate the effects of previously tested BACE1 inhibitors may be due to the route of administration, which was via oral gavage. Compounds administered through the oral route tend to have a slower onset of action and can have reduced absorption, mainly due to the first-pass effect of the liver which results in a reduced concentration of compound entering the general circulation (Turner et al. 2011). It is necessary to measure the concentration of AZ3839 centrally and in the plasma to further clarify this. Additionally, dose and/or route of delivery (i.e peripheral administration via osmotic minipump) of AZ3839 may need to be adjusted for further testing. It is important to note that the benefit and reason for utilising orally active compounds is to reflect the administration of the drug if it were to be transitioned to humans. Furthermore, we also do not have a measure, in any of our inhibitor studies, of the magnitude to which the compounds tested reduce BACE1 activity. It has been shown that following peripheral treatment with Merck-3 that BACE1 protein levels are reduced

in the hypothalamus and WAT (unpublished data) and it can be assumed the compounds tested in these experiments will elicit the same effects. However, it is necessary to reliably measure BACE1 activity and this could be achieved by measuring sAPPβ levels by ELISA. This would provide the knowledge of the magnitude in which BACE1 activity is reduced following treatment with a BACE1 inhibitor, and potentially demonstrate AZ3839 does not reduce BACE1 activity adequately. Due to time constraints and animal numbers repeated testing of AZ3839 could not be conducted, and as we have shown two structurally different compounds result in the same metabolic effects it was not deemed necessary to validate the effects of BACE1 inhibition further.

3.4.3 Inhibition of BACE1 alters hypothalamic leptin signalling

Data within this chapter demonstrate that inhibition of BACE1 not only reduces circulating serum leptin levels but also *leptin* and *ObRb* mRNA levels in WAT, supporting the notion that BACE1 inhibition is reversing diet-induced leptin resistance. These data suggest that BACE1 may directly affect adipocytes to alter transcription of leptin and the levels of protein made. Additionally, these data propose a role for leptin signalling and that inhibiting BACE1 may modify the hypothalamic circuits involved in retaining leptin responsiveness. This is consistent with an observed reduction in anorexigenic neuropeptides, and a concomitant trend towards an increase in orexigenic/anorexigenic transcript ratios in inhibitor treated mice (central and peripheral) which echoes results reported from peripheral Merck-3 treated animals (unpublished data). These data suggest that reducing BACE1 may promote orexigenic signalling in the hypothalamus, which is consistent with the relative hyperphagia exhibited in these mice and is also suggestive of altered energy expenditure.

In addition, negative regulators of leptin signalling are altered following inhibition of BACE1, providing a possible explanation for the observed reversal of leptin resistance. Notably, *SOCS3* mRNA is reduced following AZ4217 treatment, supportive of a reversal of leptin resistance as SOCS3 inhibits leptin signalling and is reported to be a mediator of leptin resistance (Bjorbak et al. 2000; Banks et al. 2000). Conversely, *PTP1B* transcript levels are unchanged with AZ4217 treatment. These effects were not observed following central inhibition of BACE1 with Merck-3, with no changes found in SOCS3 mRNA and unexpectedly *PTP1B* transcript levels were increased. PTP1B also inhibits leptin (and insulin) signalling and is increased centrally in high-fat fed animals (Zabolotny et al. 2002; White et al. 2009), so we would expect levels to decrease in our mice as leptin

sensitivity is enhanced. This is observed in *BACE1*$^{-/-}$ mice that display reduced PTP1B levels in comparison to WT littermates. Furthermore, following a HFD PTP1B levels are increased in WT littermates, however this response is diminished in *BACE1*$^{-/-}$ mice (unpublished data). The reported PTP1B expression in our studies is transcript levels only, therefore it is necessary to measure protein levels before assuming the increase in *PTP1B* in centrally treated mice, or lack of response in AZ4217 treated mice, is of physiological relevance. Accordingly, a role for PTP1B in re-sensitising BACE1 inhibitor treated mice to leptin should not be ruled out and future work investigating this, primarily through Western blotting for PTP1B in the hypothalamus of inhibitor treated mice should be conducted. Particularly owing to the fact neuronal PTP1B KO mice display a similar phenotype to our inhibitor treated mice and *BACE1*$^{-/-}$ mice (Bence et al. 2006). Conversely, we may conclude that although BACE1 inhibition reduces WAT *leptin* expression, and circulating leptin levels, a direct action on hypothalamic leptin signalling is not necessarily responsible for this outcome.

3.4.4 The effects of inhibition of BACE1 on thermogenic programming

As previously considered the relative hyperphagia, but lack of change in total food intake, observed in BACE1 inhibitor treated mice alludes to the fact there is increased energy expenditure. This is not due to changes in locomotor activity (measured in *BACE1*$^{-/-}$ mice and peripherally Merck-3 treated mice) and therefore it may be through heat loss. Markers of thermogenic programming (UCP1, PGC1α, DIO2 and Prdm16), are upregulated in BAT indicating switching on of thermogenesis, and can also be detected in WAT representing 'brite' adipocytes, indicative of enhanced thermogenesis (Seale et al. 2011; Cao et al. 2011). These markers were examined in the current study and interestingly we observed no change in thermogenic programming in both BAT and WAT of AZ4217 treated mice; opposing findings from *BACE1*$^{-/-}$ mice and peripheral Merck-3 treated mice. Only *PGC1α* transcript levels changed in both tissues and *Prdm16* showed reduced expression in WAT, suggestive of reduced adaptive thermogenesis in WAT as the upregulation of thermogenic genes in WAT is thought to be correlated with levels of Prdm16 (Seale et al. 2011). Central Merck-3 treated mice showed an upregulation in thermogenic genes (*PGC1α*, *DIO2* and *Prdm16*) in BAT which may indicate enhanced thermogenic programming, although *UCP1* levels were unchanged. These data suggest that central Merck-3 treatment alters thermogenic programming in BAT, indicative that

this mechanism is centrally driven. Furthermore, we hypothesise that this would be a more striking effect if tissue had been examined when weight loss was at its peak. Many centrally acting signals have been implicated in the regulation of BAT thermogenesis and the browning of WAT, including fibroblast growth factor 21 (FGF21), TGFβ and brain derived neurotrophic factor (BDNF) (Schulz & Tseng 2013), therefore it would be of interest to measure hypothalamic levels of these factors in inhibitor treated mice to examine their contribution to the enhanced adaptive thermogenesis. Thermogenic genes in WAT showed no changes in central Merck-3 treated mice although, as mentioned, this may be due to the time point at which the tissue was examined as there is a trend towards an increase in *UCP1* levels suggestive of browning of WAT occurring. Additionally, no change was observed in *UCP2* and *UCP3* gene expression in skeletal muscle from AZ4217 or central Merck-3 treated mice. Collectively, these data suggest that alterations in thermogenic programming may occur through a central mechanism with central Merck-3 treatment showing greater effects than AZ4217 treatment. Although, overall our results indicate that thermogenesis is unlikely to be the main factor driving reduced obesity in BACE1 inhibitor treated mice. This is contradictory to results from peripheral Merck-3 treated and *BACE1*$^{-/-}$ mice where *UCP1* expression in BAT, and *UCP2* and *UCP3* expression in muscle is enhanced, as well as an upregulation of thermogenic markers in WAT (unpublished data). However, AZ4217 is structurally different from Merck-3 and therefore unsurprisingly may act differently on target tissues. Additionally, the route of delivery of AZ4217 in our studies and Merck-3 from previous work are different, with AZ4217 delivered via oral gavage and Merck-3 through an osmotic minipump placed subcutaneously. Consequently, AZ4217 plasma and central levels may not be sufficient to reduce BACE1 adequately to reproduce all the effects observed with the concentration of Merck-3 utilised, which we believe is inhibiting BACE1 adequately. Taking this into consideration, as well as the fact increases in thermogenic genes in BAT, WAT and skeletal muscle are upregulated in *BACE1*$^{-/-}$ mice (Meakin et al. 2012, unpublished data), and more recent data establishing *BACE1*$^{-/-}$ mice have a higher body temperature (unpublished data) suggest, although increased thermogenesis may not be the mechanism whereby AZ4217 elicits its effects, it may still be a driving factor for the phenotype observed with reduced BACE1.

3.4.5 Inhibition of BACE1 alters inflammatory programming

We have shown that treatment with AZ4217 does not impact thermogenic programming, leaving the mechanism responsible for the improved metabolic phenotype undetermined.

Another contributor to leptin resistance is inflammation (Zhou & Rui 2013) which is associated with and caused by diet-induced obesity. As changes in leptin sensitivity, associated with reduced BACE1, are observed in the hypothalamus and leptin mRNA is reduced in WAT, in the present study, these tissues were examined regarding inflammatory status. Enhanced expression of pro-inflammatory cytokines can be observed as early as a few days post HFD in the hypothalamus (Thaler et al. 2012). In the present study mice have been fed a HFD for 20 weeks prior to BACE1 inhibitor treatment, therefore it is hypothesised that these mice will have increased pro-inflammatory cytokine expression. If this is assumed, this effect is attenuated with AZ4217 treatment which causes a large reduction in transcript levels of the pro-inflammatory cytokine *TNFα*. Although, other pro-inflammatory cytokines and markers of the inflammasome are unchanged. Collectively, these data indicate AZ4217 treatment does not impact hypothalamic inflammation. Peripheral inflammation, in WAT, has been found to be reduced in *BACE1*$^{-/-}$ mice and peripheral Merck-3 treated mice, through reduced expression of pro-inflammatory cytokines and raised expression of anti-inflammatory cytokines (unpublished data). Furthermore, *BACE1*$^{-/-}$ mice also demonstrate reduced immune cell number, notably macrophages. Alike the hypothalamus, *TNFα* transcript levels are reduced in WAT following AZ4217 treatment, as well as reduced *F4/80* mRNA levels utilised as an indication of total macrophage expression. However, all other pro-inflammatory cytokines examined remain unchanged, as do anti-inflammatory cytokines analysed, suggesting reduced peripheral inflammation is not the main contributor for the improved obese phenotype in these mice. Although no change in inflammatory programming is observed with AZ4217 treatment in both central and peripheral tissues, a reduction is seen in chemokine (*MCP-1*, *MIP-1α* and *MIP-1β*) expression in WAT which is suggestive of a reduction in the recruitment and infiltration of macrophages to the WAT (Surmi & Hasty 2010). This is supportive of the fact MIP-1α and MIP-1β in WAT are elevated in obesity (Surmi et al. 2010; Surmi & Hasty 2008) Further validation of the protein levels of both MIP-1α and MIP-1β are required, as the present data represent transcript expression only. Taken together, these data demonstrate moderate effects of AZ4217 treatment on peripheral HFD-induced inflammation and the accumulation of macrophages at peripheral tissue. As with the collected thermogenesis data, these results are not comparable to the effects observed in peripheral Merck-3 treated or *BACE1*$^{-/-}$ mice, presumably due to structural differences in AZ4217 and its efficacy of reducing BACE1 in central and peripheral tissues.

Our study revealed that central Merck-3 treatment diminished hypothalamic inflammation arising from diet-induced obesity, causing reductions in pro-inflammatory cytokines (*IL-6* and *IL-1β*) and markers of the inflammasome (*NLRP3* and *caspase 1*). An associated reduction in *NOS2* and a concomitant increase in anti-inflammatory cytokines (*IL-10*, *YM-1*, and *Arg-1*) is also observed in the WAT from central Merck-3 treated mice. Furthermore, upon termination of the study it was noted that spleen size from these mice was increased. An increased spleen is generally associated with inflammation and increased neutrophils within the circulation, thus we may observe a greater splenic mass due to the re-bound in weight resulting in an increase in inflammatory processing. Alternatively, this may be a physiological response and the greater splenic size could represent an increased number of immune cells, such as anti-inflammatory M2-like macrophages, that do not exacerbate the inflammatory state but are required to deal with chronic diet-induced inflammation. Taken together, these data demonstrate a drive towards reduced central and peripheral inflammation, which was not observed with AZ4217 treatment, however correlates with the reported inflammatory phenotype of *BACE1*$^{-/-}$ mice and peripheral Merck-3 treated mice. This indicates a central mechanism likely drives the altered inflammatory profile observed following reduced BACE1. To determine the mechanisms behind this further, it would be interesting to study the brains of inhibitor treated mice, utilising IF, staining for astrocytes and microglia as these cells are a central source of cytokines when activated in response to stress (Avila-Muñoz & Arias 2014; Choi et al. 2014). For example, in AD Aβ activates astrocytes and microglia resulting in the secretion of cytokines and exacerbation of the disease (Johnstone et al. 1999). We would hypothesise that BACE1 inhibition would reduce the number of activated microglia and astrocytes driven by chronic nutrient excess, thus reducing the secretion of cytokines. Additionally, of interest would be to co-stain for astrocytes and microglia with BACE1 to observe if BACE1 is expressed in these cell types in DIO mice, to determine if BACE1 acts directly on these cells to alter inflammatory processing. It may be hypothesised that BACE1 does elicit its effects through direct action on immune cells, as low BACE1 expression is observed *in vitro* in bone marrow derived macrophages (BMDMs), and this is elevated when BMDMs are stimulated with palmitate (modelling the effects of high-fat feeding *in vivo*) (unpublished data). To examine this further it would be of interest to remove BACE1 exclusively from immune cells using a conditional *BACE1*$^{-/-}$ mouse with loxed alleles crossed with a mouse line with cre expression specifically in immune cells. Furthermore, to investigate if

BACE1 is affecting the macrophages by interacting with other tissues it will also be necessary to remove BACE1 exclusively in WAT and more interestingly, as we assume a central mechanism is involved, in neurons, utilising the same cre lox technology.

In both central and peripheral tissues *F4/80* expression, utilised as a crude measurement of total macrophage expression, is unchanged with central Merck-3 treatment implying total numbers of macrophages are unaffected. However, to solidify this result a more direct measure would need to be carried out such as utilising flow cytometry to quantify absolute macrophage numbers, as F4/80 transcript levels do not represent actual macrophage numbers. This has been performed in *BACE1*$^{-/-}$ mice and peripheral Merck-3 treated mice, and both show reduced actual macrophage numbers (unpublished data). Unlike peripheral AZ4217 treatment, central inhibition of BACE1 did not alter chemokine levels (*MCP-1*, *MIP-1α*, *RANTES* and *TGFβ-1*) in WAT. Importantly, transcript levels of these chemokines, as with F4/80 expression, is only a guide measurement, and the levels of these transcripts will not demonstrate the actual ability of the macrophages to respond to chemotaxis signals. Of benefit would be to examine protein levels of these chemokines to determine if changes in transcript levels relate to functional changes. Furthermore, to definitively examine the effects of BACE1 on macrophage migration and chemotaxis we would need to employ *in vitro* models utilising migration chambers to study the ability of macrophages to migrate in the presence of high BACE1 levels or when BACE1 is reduced. Interesting future work would also be to examine ER stress markers in central and peripheral tissues, as diet-induced inflammation is associated with increased ER stress, and leptin resistance is particularly associated with central, hypothalamic ER stress (Zhou & Rui 2013; Ozcan et al. 2004). In addition, *BACE1*$^{-/-}$ mice reportedly show reduced expression of ER stress related genes in the hypothalamus even when exposed to a HFD (unpublished data). Therefore, we hypothesise BACE1 inhibition may reduce central ER stress associated with obesity, and this will contribute to the improved leptin sensitivity in BACE1 inhibitor treated DIO mice.

3.4.6 Concluding Remarks

The data presented within this chapter, with recent work from our lab, provide evidence that BACE1 inhibition could be a novel therapeutic strategy for the treatment of metabolic disease. We have shown that partial reduction of BACE1 improves an obese/diabetic phenotype in DIO mice by reducing body weight and improving glucose homeostasis.

The data presented herein implicate modifications in thermogenic and inflammatory programming to mediate the metabolic changes observed following BACE1 inhibition, and that this may be in large part due to a centrally acting mechanism. Further work is necessary to examine the precise mechanisms whereby BACE1 inhibition increases energy expenditure through thermogenesis and alters inflammatory processing to reduce diet-induced inflammation. It would be of benefit to test the metabolic effects of a clinically tested BACE1 inhibitor with the knowledge from this research allowing for future work to repurpose BACE1 inhibitors currently trialled for AD treatment for the treatment of obesity and T2DM.

Chapter 4

The role of APP processing on an obese and diabetic phenotype

4.1 Introduction

In the previous chapter it was demonstrated that inhibition of BACE1 improves an obese/diabetic phenotype, mimicking the effects observed utilising a previously tested BACE1 inhibitor and the phenotype of *BACE1*$^{-/-}$ mice. The data alluded to the notion that this improvement may be predominantly due to a centrally acting mechanism, affecting inflammation and/or thermogenic programming. However, as yet the precise mechanism is still unknown. This is a difficult concept to unpick as BACE1 has a number of substrates other than APP, and as yet many are unidentified (Vassar 2014). The majority of BACE1 substrates are type 1 transmembrane proteins and many have centrally acting roles (Hemming et al. 2009). Those identified include neureglin-1 type III (NRG1) which is involved in myelination (Hu et al. 2006), a neural cell adhesion molecule; CHL1, involved in axonal growth and ventricle development (Heyden et al. 2008) and Jagged 1 (JAG1) which is involved in notch signalling to control cell differentiation (Hu et al. 2013). In addition, substrates involved in immune cell function, primarily immune cell adhesion and activation, have also been described for BACE1. These include the type II transmembrane protein, TGN-resident β-galactoside α2,6-sialytransferase (ST6Gal1) (Kitazume et al. 2001) and P-selectin glycoprotein ligand-1 (PSGL-1) which is also a substrate for the α-secretase (Lichtenthaler et al. 2003), as well as the interleukin 1 receptor II (IL-1R2) proposed as a potential substrate (Kuhn et al. 2007). Owing to the number of BACE1 substrates and the various functions of each it is challenging to decipher the precise role of BACE1 and which substrate it cleaves to mediate metabolic actions.

The most characterised and studied substrate for BACE1, although it is in fact a relatively poor substrate, is APP. The majority of APP mutations giving rise to AD are due to increased BACE1-mediated APP processing (Vassar 2014; Jonsson et al. 2012). Thus, BACE1 may utilise APP as it's substrate in regards to its functions in energy homeostasis, and if so, this knowledge would allow for a better understanding of the role of BACE1 in energy metabolism. The FAD associated Swedish mutation K67ON/M671L is a double mutation of APP localised to the N-terminus of the β-secretase cleavage site (Mullan et al. 1992). This mutation strengthens APP as a substrate for BACE1, whereby BACE1 cleaves APP up to approximately 100-fold more efficiently than under normal circumstances, and accordingly results in increased Aβ levels (Vassar et al. 2009; Vassar 2004). This mutation demonstrates BACE1-mediated processing of APP is implicated in the development of AD.

Under normal circumstances APP is a stronger substrate for the ADAMs; identified as the α-secretase. As a result the non-amyloidogenic pathway exists as the dominant pathway in regards to APP processing and α-secretase cleavage of APP occurs far more readily than BACE1 cleavage. In fact, BACE1 and the α-secretase compete for APP as a substrate, and blockage of one pathway gives rise to enhanced processing down the opposing route (Yan et al. 1999; Postina et al. 2004). This balance, which favours α-secretase mediated processing of APP, is vital for cellular health, as sAPPα has been found to play physiological roles in synapse formation (Morimoto et al. 1998), neurite growth and neuronal survival (Araki et al. 1991). Furthermore, elevations in BACE1 lead to increased β-secretase cleavage, Aβ production and subsequently neuronal dysfunction and cell death (Hardy & Higgins 1992). Consequently, instances where the accessibility of BACE1 to utilise APP as a substrate over the α-secretase is detrimental, for example in the presence of high cholesterol (Marquer et al. 2011).

Cholesterol metabolism is closely linked with APP and associated with AD, in particular through the ApoE gene which is present in plaques and tangles (Strittmatter et al. 1993). Specifically, the E4 allele of the ApoE gene is associated with high cholesterol (Sing & Davignon 1985) and this allele is strongly linked to FAD (Strittmatter et al. 1993). However, when cholesterol levels are depleted in neurons levels of Aβ are reduced (Simons et al. 1998), and furthermore when cholesterol is reduced in cells overexpressing ADAM10 there is an increase in sAPPα (Kojro et al. 2001). Consequently, enhancing α-secretase cleavage is believed to beneficial in preventing AD progression. This is further supported by work showing overexpression of ADAM10; the predominant α-secretase in neurons (Kuhn et al. 2010), in mouse models of AD prevents plaque formation, whereas expression of a catalytically inactive form gives rise to plaque deposition (Postina et al. 2004). Furthermore, mutations in ADAM10 are found in families with late-onset AD and reportedly cause attenuation of α-secretase activity and reduced sAPPα, accompanied with increased Aβ levels (Kim et al. 2009). Therefore, the non-amyloidogenic pathway is crucial for precluding Aβ production and may be a target of therapeutic intervention for AD. However, how alterations in α-secretase affect energy homeostasis is unknown, and if BACE1-mediated APP processing is pivotal for the role of BACE1 in metabolism is yet to be defined.

In the present studies we aimed to investigate if disturbances in normal APP processing, resulting in elevated BACE1, would give rise to defects in energy metabolism. To do so, mice harbouring the double Swedish mutation implicated in FAD were challenged with

a HFD diet and various metabolic measurements taken. In addition, α-secretase activity was blocked in mice challenged with a HFD, and metabolic measurements examined. Both approaches alter the balance between non-amyloidogenic and amyloidogenic APP processing, causing increased BACE1-mediated APP processing. It was hypothesised that, if BACE1 is utilising APP as its substrate in regulating energy homeostasis, following increased BACE1 activity mice would demonstrate accelerated obesity and metabolic impairments associated with high-fat feeding. The knowledge from this research may provide information on the substrate BACE1 processes to contribute to energy metabolism and its overall role in energy homeostasis, as well as examining the role of α-secretase APP processing in the control of energy balance.

4.1.1 Objectives

- Examine if elevated BACE1 activity, using two models (overexpression of a human APP mutation and blocking α-secretase processing), will drive metabolic disease when challenged with a HFD measuring the following metabolic outcomes:
    - Changes in body weight and body composition
    - Changes in food intake
    - Changes in glucose homeostasis
    - Changes in insulin sensitivity
- Challenge mice overexpressing all isoforms of human APP containing the FAD associated Swedish mutation K67ON/M671L (*hAPPswe* mice) and littermates with a HFD for a period of 16 weeks
    - *hAPPswe* have approximately 2-3 fold increase in endogenous APP levels, increased β-secretase cleavage and Aβ levels, with a concomitant reduction in α-secretase cleavage (Lamb et al. 1997).
- Block α-secretase processing in mice challenged with a HFD using an ADAM10 inhibitor; GI254023X, for 28 days
    - ADAM10 is the predominant enzyme responsible for constitutive activity and basal α-secretase activity in neurons (Kuhn et al. 2010)GI254023X reportedly reduces sAPPα *in vitro* on SH-SY5Y cells (Tippmann et al. 2009) and *in vivo* in mice (Powers et al. 2012), and is selective for ADAM10 over other ADAM members.

4.2 Methods Summary

For *hAPPswe* studies, adult (8 weeks of age) *hAPPswe* mice and WT littermates were challenged with a 60% HFD. 60% HFD was utilised to attempt to accelerate a DIO phenotype. Animals were weighed weekly throughout the duration of the study, at the same time each week. Glucose tolerance tests were carried out during weeks 5 and 10, following an overnight fast, and insulin tolerance tests were carried out during weeks 6 and 11 following a four hour fast. An assessment of fat and lean mass was conducted at the beginning and end of the study. Throughout the study animals were maintained on the 60 % HFD. Following 16 days of high-fat feeding mice were fasted overnight and tissue harvested.

For ADAM10 inhibitor studies, WT adult (8 weeks of age) mice were placed on a 45% HFD for one week. Following one week of high-fat feeding animals were treated with an ADAM10 inhibitor; GI254023X (ADAM10i) via central infusion directly into the lateral ventricle for 28 days. Throughout the study body weight and food intake measurements were taken daily. Glucose tolerance tests were performed on day 14 and day 28 of the study, following an overnight fast, and an insulin tolerance test was performed on day 21 following a four hour fast. Throughout the study animals were maintained on the 45% HFD. Following 28 days of treatment mice were fasted overnight and tissue harvested.

4.3 Results

4.3.1 The effects of overexpressing *hAPPswe* in diet-induced obesity

Owing to the increased β-secretase cleavage, *hAPPswe* mice were utilised as a model of enhanced BACE1 activity in order to study the interaction between increased BACE1 activity and high-fat feeding. Due to reports of increased mortality in young homozygote mice, hemizygous mice were used in these studies. Hemizygous mice show a 7-8 fold increase in global $A\beta_{1-42}$, however they do not display amyloid pathology as early as homozygote mice (Lamb et al. 1999).

4.3.1.1 Overexpression of *hAPPswe* does not affect body weight gain on a high-fat diet

hAPPswe mice (Starting body weight: 22.87 ± 0.67g; n=7) and WT littermates (Starting body weight: 23.19 ± 0.48g; n=16) were challenged with a 60% HFD to accelerate diet-induced obesity. Mice were monitored over a 16 week period and body weight assessed by weighing mice weekly over the course of the study. *hAPPswe* mice did not exhibit any differences in body weight compared to WT littermates throughout the period of high-fat feeding; week 1 to 16, as presented by absolute (Figure 4.1A) and percentage change in body weight (Figure 4.1B). Taken together these data show *hAPPswe* overexpression does not result in exacerbated obesity when challenged with a HFD.

4.3.1.2 Overexpression of *hAPPswe* does not alter glucose homeostasis in diet-induced obesity

Although no change in body weight was observed when challenged with a HFD, the diabetic phenotype of *hAPPswe* mice was examined at 5-6 and 10-11 weeks of the study,

using glucose and insulin tolerance tests, to determine if a glucose-handling defect was present. At an early stage (5 weeks) no change in glucose disposal following an overnight fast was observed between *hAPPswe* mice and WT littermates (Figure 4.2A and B). At this time point there is also no impact on fasted blood glucose levels (Figure 4.2C). To determine whether this time point was too early to assess defects in glucose homeostasis a second glucose tolerance test, at a later stage (10 weeks), when a greater degree of obesity was achieved, was conducted. At 10 weeks there was still no difference in glucose disposal between *hAPPswe* mice and WT littermates (Figure 4.2D and E) or fasted blood glucose levels (Figure 4.2F); levels remained comparable to measurements taken at 5 weeks.

At both an early (week 6) and late (week 11) stage, following a four hour fast, no difference in blood glucose levels over all time points (15-120 minutes) of an ITT was observed between *hAPPswe* mice and WT littermates (Figure 4.3A and B). Taken together these data indicate *hAPPswe* overexpression does not alter glucose disposal or insulin sensitivity when challenged with a HFD and enhancing APP processing through the β-secretase route in this instance does not induce exacerbated metabolic syndrome.

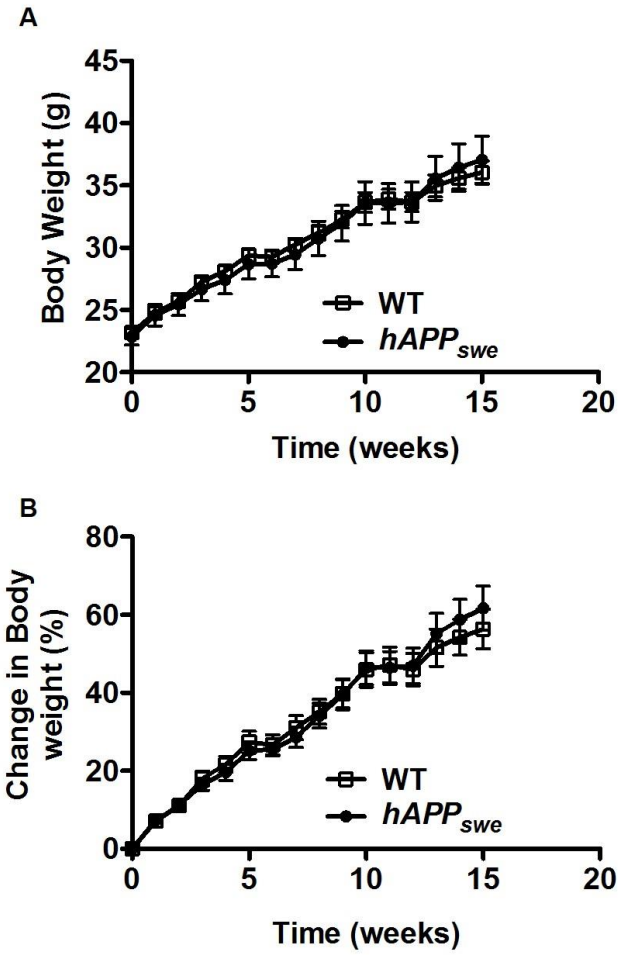

Figure 4.1 Overexpression of *hAPPswe* does not affect body weight gain in mice challenged with a high-fat diet.

(A) Overexpression of *hAPPswe* causes no significant effect in body weight change over the course of 16 weeks challenged with a high-fat diet (n=7-16). (B) Body weight gain represented as a percentage change in body weight, displaying no significant effect of *hAPPswe* overexpression.

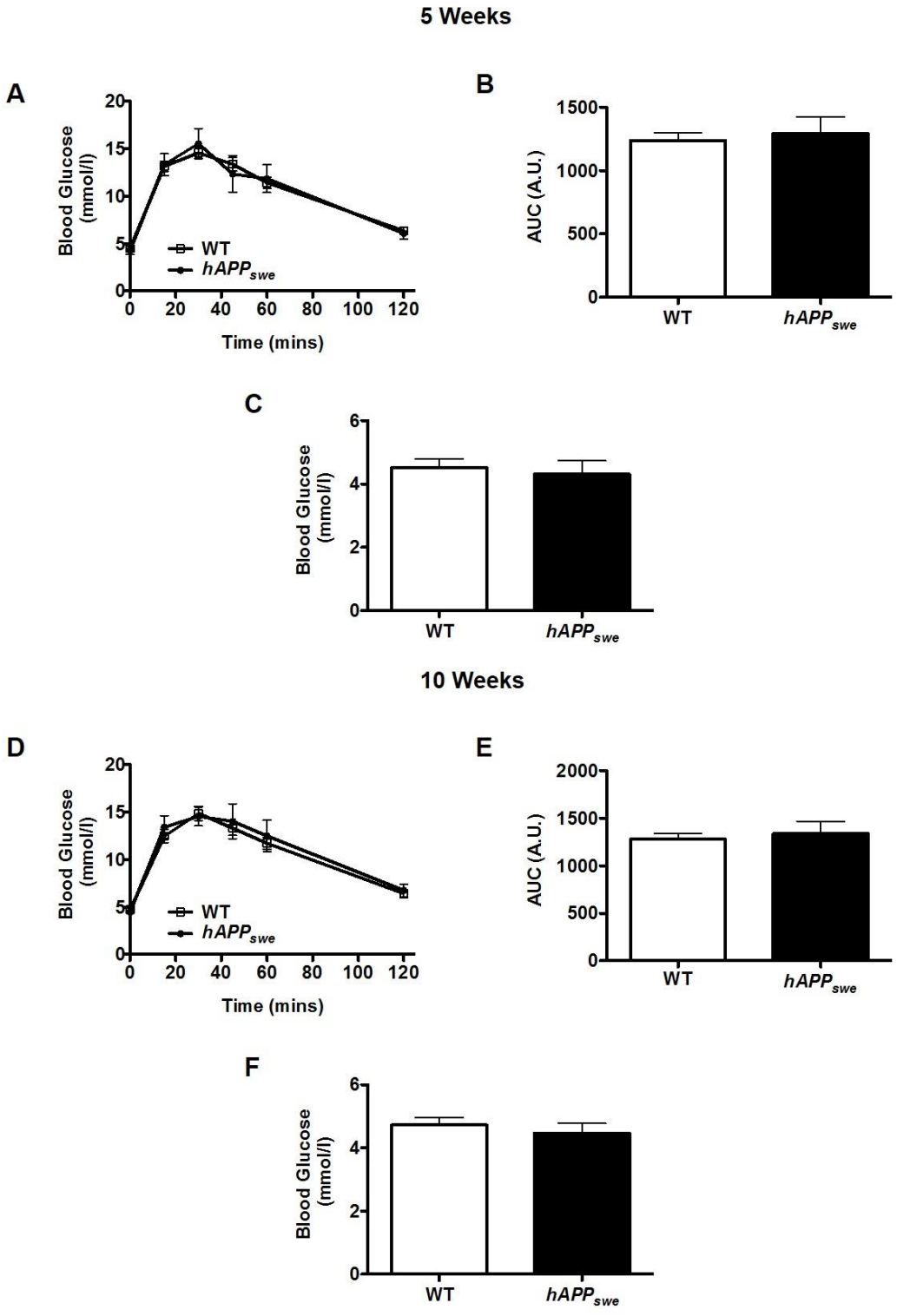

Figure 4.2 Overexpression of *hAPPswe* has no effect on glucose homeostasis in mice following 5 or 10 weeks on a high-fat diet.

(A and D) Glucose tolerance test profiles showing hAPPswe overexpression has no effect on glucose disposal following 5 or 10 weeks on a high-fat diet (n=7-16). (B and E) Quantification of area under the curve for glucose responses shown in (A and D), demonstrating no significant change in glucose disposal. (C and F) hAPPswe overexpression causes no significant effect on fasted blood glucose levels (n=7-16).

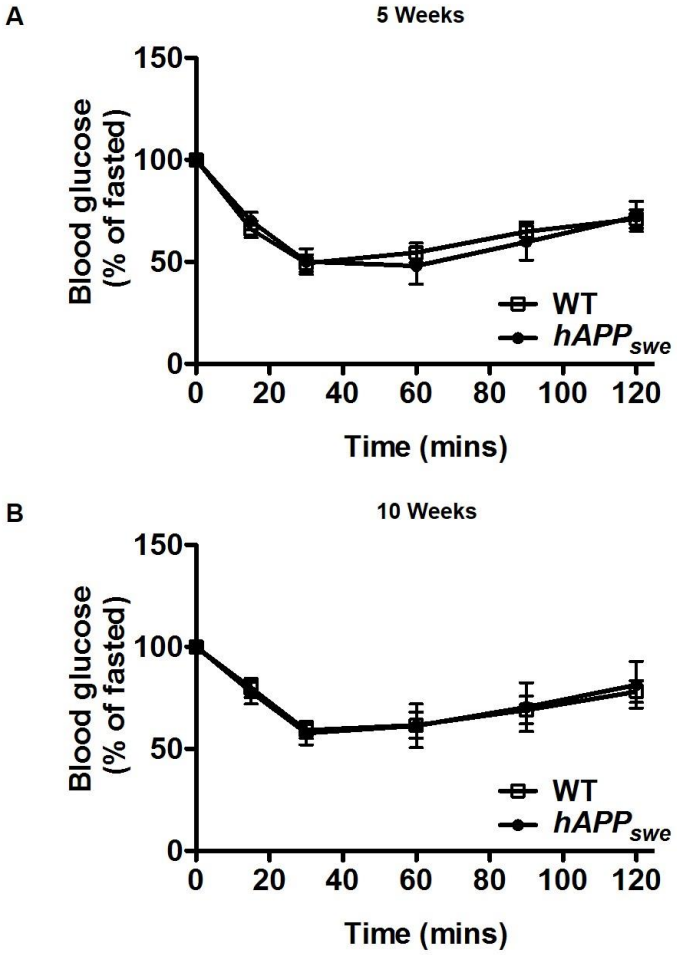

Figure 4.3 Overexpression of *hAPPswe* does not alter insulin sensitivity in mice challenged with a high-fat diet.

(A) Insulin tolerance test profile showing no significant difference in insulin sensitivity with *hAPPswe* overexpression following 6 weeks on a high-fat diet (n=7-15). (B) Insulin tolerance test profile showing there is still no significant effect on insulin sensitivity following 11 weeks on a high-fat diet (n=7-16).

4.3.1.3 Overexpression of *hAPPswe* does not impact organ weight following a high-fat diet

Although no *in-vivo* phenotype was observed in *hAPPswe* mice following high-fat feeding, upon termination of the study tissue weights of spleen, heart, liver and brain were collected to provide an indication of tissue health and a crude measure of lean mass. For all tissues, actual size was noted as well as organ weight as a percentage of total body weight. No effect was observed for the spleen, heart, liver or brain (Figure 4.4A and B) between *hAPPswe* mice and WT littermates. Taken together these data show hAPP overexpression does not affect organ weights.

4.3.2 The effects of inhibiting α-secretase APP processing on diet-induced obesity

Having observed no metabolic phenotype as a result of global overexpression of hAPP the effects of increasing BACE1 activity on energy homeostasis was yet to be examined. In the *hAPPswe* model upregulation of α-secretase activity still occurs through mouse APP processing and presumably to a degree through hAPP processing, so total sAPPα in the brains of these mice may still be relatively high. Therefore, selective reduction of α-secretase-mediated processing may provide a better model for studying the effects of increased BACE1 activity, sAPPβ and Aβ levels. Reduction of ADAM10 will result in reduced basal α-secretase-mediated processing and thus it is assumed this will cause a concomitant increase in BACE1-mediated processing of APP and production of sAPPβ. Consequently, we examined the effects of altering the balance of APP processing down the α-secretase versus the β-secretase pathway through central inhibition of ADAM10 activity in mice challenged with a HFD. It was hypothesised that this would result in a worsening of the metabolic phenotype associated with diet-induced obesity.

Age-matched, male WT mice were treated with a potent ADAM10 inhibitor; GI254023X (ADAM10i) or vehicle. Due to the large effect of central inhibition of BACE1 on energy homeostasis in DIO mice, mice in these studies were also treated through central administration directly into the lateral ventricle. Central administration of the compound or vehicle was delivered for 28 days, with the same metabolic measurements carried out during BACE1 inhibitor studies (section 3.2.1) performed to compare the effects of reducing and enhancing BACE1 activity.

4.3.2.1 Inhibition of ADAM10 does not significantly affect body weight gain following high-fat feeding

Central treatment with ADAM10i (10mg/kg; Starting body weight: 27.10 ± 0.37g; n=9) caused a slight, but non-significant, increase in percentage body weight over the course of the study in comparison to vehicle (DMSO/PBS; Starting body weight: 26.74 ± 0.46g; n=9) treated (control) mice (Figure 4.5A). Although this was a non-significant effect, actual change in body weight at the end of the study displayed a trend towards increased weight gain with central ADAM10i treatment (Figure 4.5B). It could not be determined if changes in adiposity were present in these animals, as the mice could not be placed in the Echo MRI scanner due to the ICV brain infusion kit implanted. Taken together, these data show central inhibition of ADAM10 results in a modest increase in body weight.

As with BACE1 inhibitor studies, changes in food consumption were examined. There was no difference in cumulative food intake over the course of the study between ADAM10i treated mice and control mice (Figure 4.5C), indicating that both groups of mice consume the same. Thus, a change in total food intake is not responsible for the slight change in body weight observed in ADAM10i treated mice. As the observed change in body weight is small, as expected relative food intake in relation to body weight of these mice was also unchanged (data not shown).

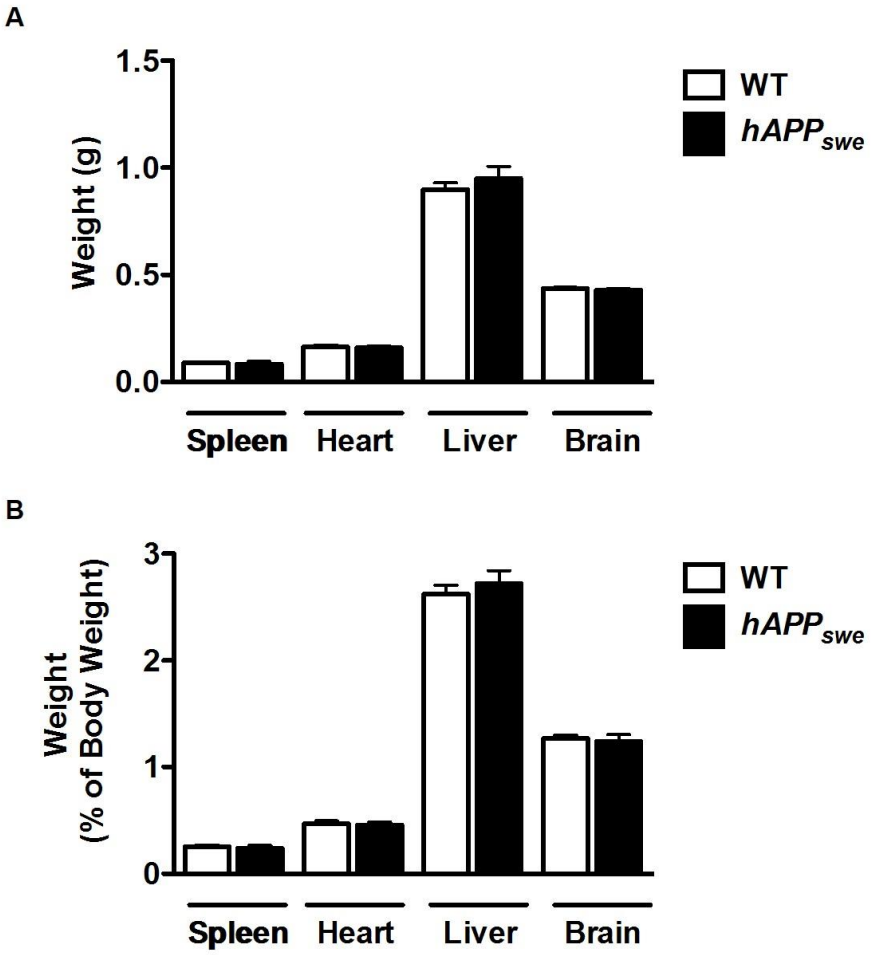

Figure 4.4 Overexpression of *hAPPswe* does not alter organ weights following high-fat feeding.

(A) Overexpression of *hAPPswe* has no significant effect on spleen, heart, liver or brain weights (n=7-16). (B) Actual weights represented as a percentage of total body weight.

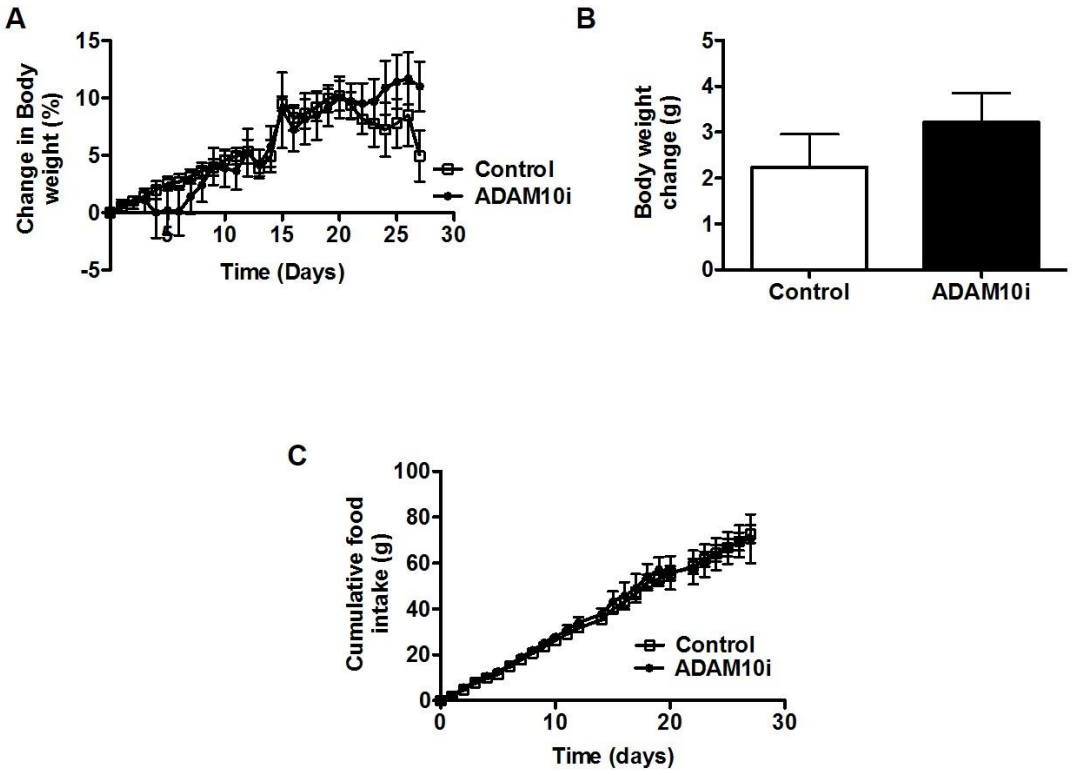

Figure 4.5 Central ADAM10i treatment for 28 days causes a modest increase in body weight but does not alter food intake following high-fat feeding.

(A) Central ADAM10i treatment causes a slight increase in percentage body weight over the course of the study (n=9). (B) Actual weight change from starting body weight, at the end of the study (day 27), shows a trend towards an increase in mice treated centrally with ADAM10i (n=8). (C) Cumulative food intake was unchanged with central ADAM10i treatment (n=8).
Data collection was carried out in collaboration with Dr. Paul J Meakin.

4.3.2.2 Inhibition of ADAM10 exacerbates a diabetic phenotype following high-fat feeding

The diabetic phenotype of these mice was also investigated by performing a GTT (day 14) and ITT (day 21). Following an overnight fast there was a small decrease in glucose clearance with ADAM10i treatment in comparison to control mice (AUC: control; 1429 ± 49.21 vs. ADAM10i; 1555 ± 47.66, p=0.09, n=8-9, Figure 4.6A and B), however fasting blood glucose levels were unaltered (Figure 4.6C). As a slight impairment in glucose handling was observed, although not significant, a second GTT on day 28 was carried out to assess if this was due to the length of treatment and/or the duration of high-fat feeding. By day 28, glucose tolerance was further compromised with ADAM10i treatment, displaying a trend towards impaired glucose homeostasis in comparison to control mice (AUC: control; 1368 ± 90.24 vs. ADAM10i; 1840 ± 194.6, p=0.06, n=3-4, Figure 4.6D and E). Again, fasting blood glucose levels in these mice were unaltered on day 28 (Figure 4.6F).

Following a four hour fast an ITT was carried out and ADAM10i treatment caused a significant impairment in insulin sensitivity 60 minutes into testing ($p<0.05$, n=8-9, Figure 4.7A). Taken together, these data show central treatment with ADAM10i results in impaired glucose tolerance, an effect observed at day 14 and further worsened at day 28, when weight gain is beginning to increase in comparison to control mice. Insulin sensitivity is also reduced following ADAM10i treatment, displaying an overall worsened diabetic phenotype and contrasting the effects of reducing BACE1 levels.

4.3.2.3 Inhibition of ADAM10 does not impact organ weights following a high-fat feeding

Upon termination of the study tissue weights of spleen, heart, liver and brain were measured in all mice, as an indication of the health of these tissues and as a crude measure of lean mass. For all tissues, actual size was measured as well as organ weight as a percentage of total body weight. ADAM10i treatment caused no effect on the spleen, heart or brain compared to control mice (Figure 4.8A and B), however ADAM10i treatment caused a significant increase in liver weight as a percentage of body weight (Control; 3.54 ± 0.12% vs. ADAM10i; 4.08 ± 0.05%, $p<0.01$, n=4-5, Figure 4.8). Taken together these data show ADAM10 inhibition does not affect raw organ weights.

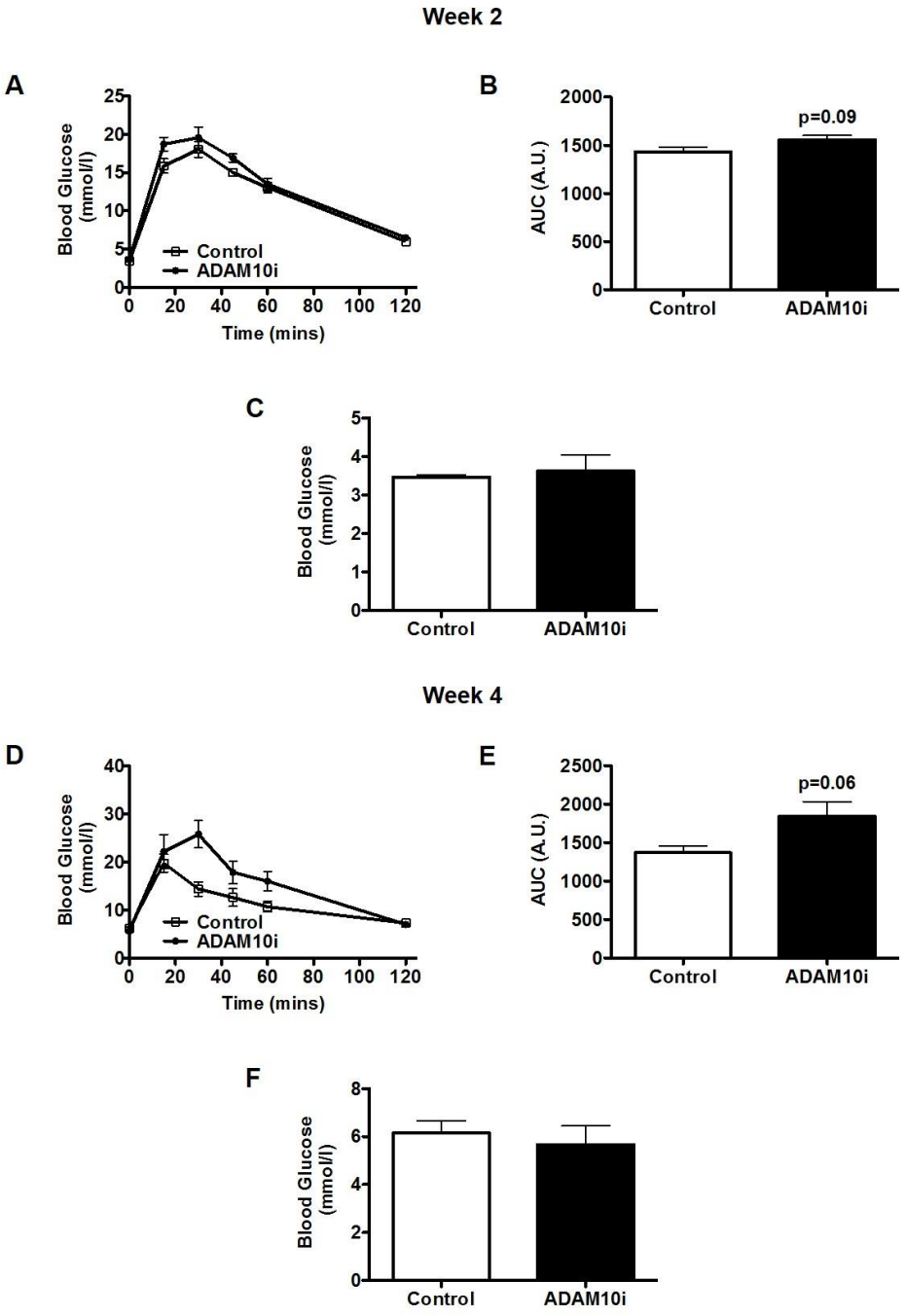

Figure 4.6 Central ADAM10i treatment impairs glucose homeostasis following 14 and 28 days on a high-fat feeding.

(A and D) Glucose tolerance test profiles showing central ADAM10i treatment impairs glucose disposal following 2 weeks (n=8-9) and 4 weeks (n=3-4) on a high-fat diet. (B and E) Quantification of area under the curve for glucose responses shown in (A and D), demonstrating an increase in glucose disposal with central ADAM10i treatment (Week 2; p=0.09, n=8-9, Week 4; p=0.06, n=3-4). (C and F) Central ADAM10i treatment causes no significant effect on fasted blood glucose levels at 2 weeks (n=8-9) or 4 weeks (n=3-4).

Data collection was carried out in collaboration with Dr. Paul J Meakin.

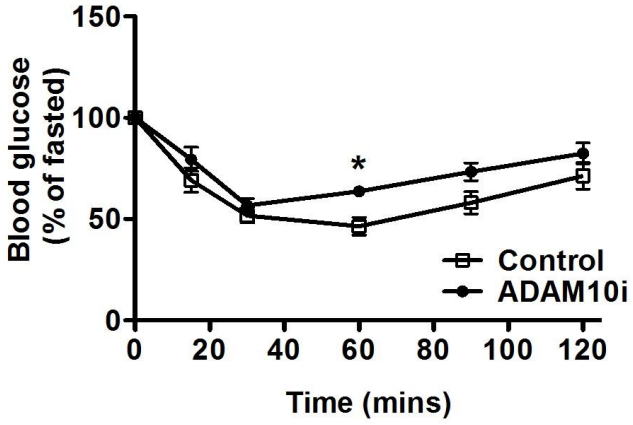

Figure 4.7 Central ADAM10i treatment impairs insulin sensitivity following 21 days on a high-fat diet.

Insulin tolerance test profile displaying significant effect of central ADAM10i treatment on insulin sensitivity at 60 minutes ($p<0.05$, n=8-9).
Data collection was carried out in collaboration with Dr. Paul J Meakin.

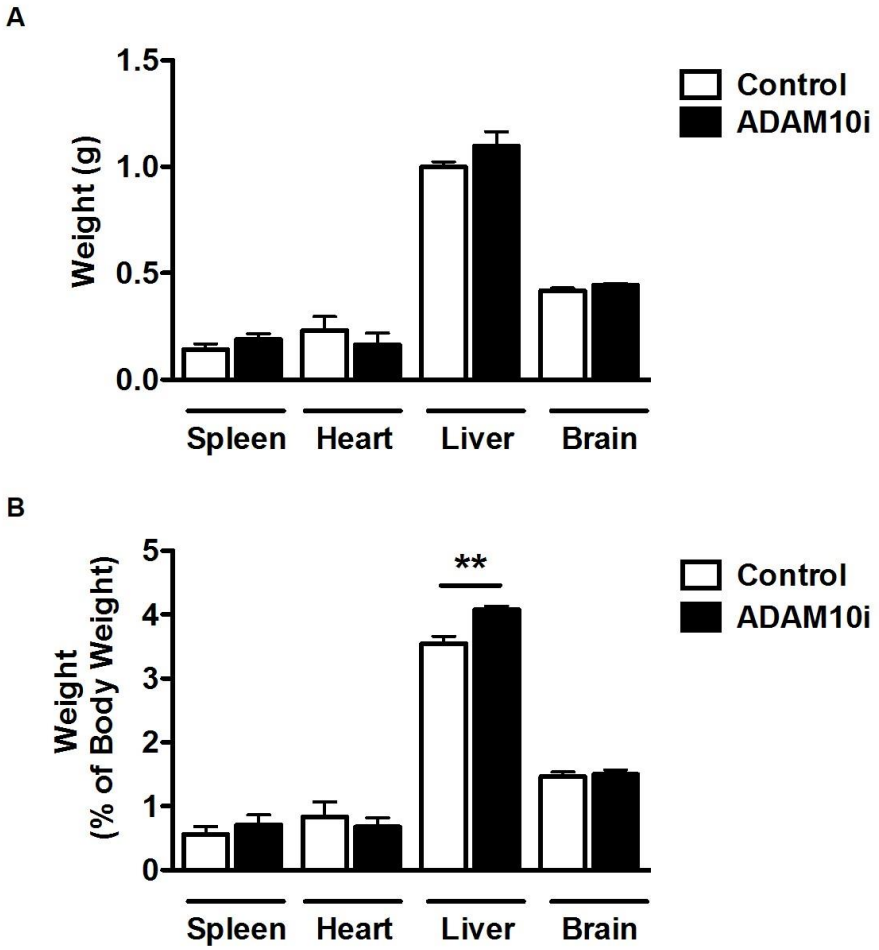

Figure 4.8 Central ADAM10i treatment for 28 days does not alter raw organ weights.

(A) Central ADAM10i treatment has no significant effect on spleen, heart, liver or brain raw weights. (B) Actual weights represented as a percentage of total body weight demonstrates increased liver weight with central ADAM10i treatment ($p<0.01$, n=4-5). Data collection was carried out in collaboration with Dr. Paul J Meakin.

4.4 Discussion

4.4.1 Summary

Within this chapter we set out to investigate if altering the balance between non-amyloidogenic and amyloidogenic APP processing to favour BACE1-mediated cleavage would drive an obese/diabetic phenotype. Herein, with the two models utilised we did not observe a drastic exacerbation of obesity when challenged with a HFD. *hAPPswe* mice did not differ from WT littermates in their responses to all metabolic outcomes measured when challenged with a HFD. However, ADAM10 inhibition in mice fed a HFD resulted in a modest increase in body weight and small impairments in glucose tolerance and insulin sensitivity. These results, and the potential underlying mechanisms, will be further discussed in the following sections.

4.4.2 Overexpression of *hAPPswe* does not worsen an obese/diabetic phenotype

In the previous chapter we demonstrated that a reduction in BACE1 improves an obese/diabetic phenotype through enhanced leptin sensitivity and reduced HFD-induced inflammation. To address if increasing BACE1 levels exacerbates an obese state we sought to alter the balance between α-secretase and BACE1-mediated APP processing. This was initially examined utilising an AD transgenic mouse model carrying the human APP_{swe} mutation that results in increased BACE1-cleavage of APP. It was hypothesised that *hAPPswe* mice would have increased body weight gain when challenged with a HFD and impaired glucose homeostasis owing to elevated BACE1 levels and consequently enhanced β-secretase cleavage of both native and human APP. However, in the present study, when challenged with a HFD no metabolic phenotype was observed in *hAPPswe* mice, as demonstrated by no change in body weight gain and glucose homeostasis (GTT and ITT) in comparison to littermate controls; opposing our hypothesis. These mice also showed no change in organ weight, indicative of a lack of inflammation and no change in lean mass.

The lack of phenotype observed in *hAPPswe* mice may be due to the AD model utilised which overexpresses human APP globally. Although the presence of the *hAPPswe* mutation results in more BACE1-mediated APP processing the mouse APP gene is still present and unaffected, thus α-secretase mediated APP processing still occurs. Mouse APP is processed favouring the α-secretase pathway which produces protective effects,

as sAPPα has neuroprotective functions (Araki et al. 1991; Meziane et al. 1998; Stein et al. 2004). Therefore, this may compensate for and mask the effects of the elevated BACE1-mediated processing. Moreover, sAPPα has been shown to act like an insulin sensitizer; stimulating glucose uptake and glucose oxidation in neuronal SH-SY5Y cells (John Findlay PhD Thesis) and primary cortical synaptosomes (Mattson et al. 1999), as well as in skeletal muscle (C_2C_{12}) cells (Hamilton et al. 2014). Furthermore, sAPPα may mediate some protective effects through activation of the PI3K pathway (Jimenez et al. 2011) which promotes cell survival. This is supported by data from our lab showing that the stimulatory effects of sAPPα on glucose uptake and oxidation are dependent on PI3K signalling (Hamilton et al. 2014, John Findlay PhD Thesis). Accordingly, if sAPPα is behaving as an insulin sensitizer through the PI3K pathway it is possible it may also act on the hypothalamus as a leptin sensitizer, as leptin also utilises the PI3K pathway. If this is the case, sAPPα may have the ability to re-sensitise hypothalamic neurons to leptin preventing leptin resistance associated with high-fat feeding. This could account for the lack of phenotype observed in our studies as the PI3K-dependent cell survival action of sAPPα may compensate for the effects of HFD, and delay the onset of metabolic dysfunction.

In the present studies, it would be interesting to examine sAPPβ and Aβ levels, as well as sAPPα levels, in our animals to measure the degree of which BACE1 activity is increased, as in our model BACE1 activity may not be elevated to the level at which other stressors cause. An additional stressor that elevates BACE1 levels may be required to observe significant effects. This is supported by data from our lab demonstrating that aged *hAPPswe* mice (>12 months old) show a non-significant increase in body weight and impaired glucose homeostasis, whereas no phenotype is observed when mice are fed a NC diet (unpublished data). In addition, work utilising a triple transgenic mouse model (3xTgAD) with mutations in APP, PS1 and tau show no initial change in body weight when challenged with a HFD however, show increased fat mass from 7 months onwards (Knight et al. 2014), indicative of an altered metabolic response to high-fat feeding. Aging is associated with elevated BACE1 levels and midlife obesity has been shown to be associated with increased AD risk (Fitzpatrick et al. 2009). Moreover, Mody *et al* found that ageing alone does not exacerbate obesity in AD transgenic models with a double transgenic (*APP/PSEN1*) mouse model and a single PS1 mutation mouse model both showing no change in body weight in comparison to WT littermates during the ageing process when fed a NC diet (Mody et al. 2011). This further supports the notion that a

greater enhancement of BACE1 may be required, through a combination of stresses, to elicit metabolic effects. In addition, Mody and colleagues found that *APP/PSEN1* mice were more susceptible to obesity, displaying greater body weight gain, following 8 weeks on a HFD, accompanied by impaired glucose homeostasis and insulin signalling, in comparison to mice with a single AD mutation and WT littermates (Mody et al. 2011). Cao *et al* also utilised double transgenic AD mice and found that replacing their water with sucrose-sweetened water, representing increased calorific intake, increased body weight, impaired glucose homeostasis and increased circulating insulin levels (Cao et al. 2007). These data suggest our mouse model may represent a mild AD model, which is supported by an absence of plaque pathology observed at 16 months (unpublished data). Therefore, it would be interesting to examine our mice further following a longer duration of high-fat feeding or utilising a more severe AD mouse model. In the models described, whereby double or triple mutations are incorporated and metabolic dysfunction is observed, it would be of interest to treat these mice with a BACE1 inhibitor (as previously carried out in chapter 3) or cross these mice with a *BACE1*$^{-/-}$ mouse to reduce BACE1 levels by 50%, and examine if the observed effects are BACE1 dependent. We would hypothesise that reducing BACE1 levels in these mice would reverse the obese phenotype, suggesting BACE1 is utilising APP as a substrate in regards to its metabolic actions.

Conversely, opposing the data described above, groups have shown that single mutation AD mouse models incorporating the same APP mutation as our mouse line do show metabolic defects following HFD (Kohjima et al. 2010; Ho et al. 2004). Kohjima and colleagues found mice with a single APP mutation (Tg2576 mice) are obese and insulin resistant, displaying increased body weight, fat mass, food intake and impaired glucose homeostasis and insulin sensitivity following 16 weeks on a HFD (Kohjima et al. 2010). In this study it was also found that Aβ levels were elevated at an earlier time point than previously reported for this mouse model and that this increase may be directly due to increased food intake and body weight. These data implicate Aβ as the potential driver for metabolic dysfunction, as opposed to sAPPβ. Noteworthy, is the fact Kohjima and colleagues conducted their GTT at 16 weeks, whereas we performed a GTT at only 10 weeks and consequently may be missing a defect. This is unlikely to be the sole reason for the lack of phenotype observed as Kohjima *et al* show clear body weight changes at 4 weeks and 12 weeks; effects we do not observe. The data from Ho *et al* also demonstrate that Tg2576 mice challenged with a HFD show increased circulating insulin levels, body

weight and fat mass, accompanied by impaired glucose homeostasis (Ho et al. 2004). Again, the time points slightly differ to our study whereby the effects observed by Ho and colleagues are demonstrated after 5 months on a HFD, whereas our studies where terminated at four months. Although the mutations in the Tg2576 mouse and the *hAPPswe* mouse are the same, the models differ slightly and this may account for the differences observed when challenged with a HFD. In the Tg2576 mouse the FAD mutation is driven by the hamster prion protein promoter (Elder et al. 2010) whereas in our model the mutation is driven by the mouse APP promoter. Furthermore, in Tg2576 mice expression of human APP is over five times higher than mouse APP expression and consequently plaque pathology can be observed from 11-13 months of age (Elder et al. 2010). Alternatively, the mouse model utilised in our studies reportedly overexpress human APP only 2-3 fold in relation to mouse APP levels and, as mentioned, do not develop plaques. This further supports the notion that our model may represent a relatively mild AD model. Nonetheless, our model itself may not be the sole reason we observe no altered metabolic phenotype and other factors within our study design may contribute.

The interesting observation from our study is that both groups (WT and *hAPPswe* mice) did not gain substantial weight when placed on the HFD. In previous studies we utilise DIO mice, considered to be obese when they reach a weight of over 40g which is achieved following approximately 20 weeks on a 45% HFD. Herein, we find neither group of mice achieve DIO status even when challenged with a 60% HFD for 16 weeks. A diet of 60% fat was utilised in these studies with the aim of inducing obesity at an earlier time point. This would suggest the diet has had a major effect on our study and it is possible that it is less palatable than the 45% diet and therefore mice are consuming less. Unfortunately, food intake could not be measured in these mice owing to the consistency of the 60% diet and the fact mice were group housed, thus we cannot definitively conclude if changes in food intake may account for the lack of weight gain. It would be more advantageous to repeat these studies utilising 45% HFD, which has been shown to induce diet-induced obesity by 20 weeks of high-fat feeding, and conduct the study for a longer duration.

4.4.3 Altering APP processing through inhibition of the α-secretase pathway on an obese/diabetic phenotype

Within this chapter we have shown that blockage of the α-secretase pathway may produce the opposite phenotype observed in BACE1 inhibitor treated mice (chapter 3), by

worsening an obese/diabetic phenotype. We demonstrated this through central ADAM10 inhibition causing a slight increase in body weight and impaired glucose and insulin tolerance over the course of treatment. These effects were somewhat mild which may be due to the dose and duration of the study, as the greatest effects occurred at the end of the study with a greater defect in glucose handling observed at day 28 in comparison to day 14, and impaired insulin tolerance observed at day 21. This correlates with changes in body weight, as inhibitor treated mice do not begin to gain weight faster than control mice until approximately day 20 of treatment, consequently the glucose handling defect may be a direct consequence of increased body weight. Of particular interest, is that between glucose tolerance tests the response of vehicle treated mice is unaltered, suggesting the compound is accelerating the effects of diet-induced obesity. This is supported by data showing that α-secretase inhibition *in vitro* on SH-SY5Y cells reduced glucose uptake, and over-expression of BACE1 caused the opposite effect (John Findlay PhD Thesis). Conversely, fasting blood glucose levels increase in both groups of mice suggesting basal glucose levels are a result of the diet and not the treatment. Alike BACE1 inhibitor treated mice, we observe no change in food intake, and therefore the mild increase in body weight is not owing to animals consuming more. Furthermore, these animals are not relatively hyperphagic suggesting that the neuronal circuitry controlling food intake is not altered following ADAM10 inhibition. Nonetheless, if the length of treatment was extended we would possibly observe more severe changes in body weight and consequently feeding behaviour. It is also necessary to measure circulating leptin levels in these mice, which we would have initially hypothesised to be elevated (indicative of leptin resistance), however owing to only mild effects on body weight this may not occur. Interestingly, insulin tolerance was affected in inhibitor treated mice at day 21 of treatment, before even mild changes in body weight are detected. This is intriguing as it suggests insulin resistance is occurring independently of body weight changes, and notably we do not observe changes in insulin tolerance following inhibition of BACE1 (section 3.2.1.2 and 3.2.7.2). This is supportive of the notion that ADAM10 inhibition is accelerating the effects of high-fat feeding, driving insulin resistance at a time point in which BACE1 inhibition cannot reverse this. The change in insulin tolerance with ADAM10 inhibition is still relatively mild, and may worsen as body weight changes occur. Additionally, due to time we could not measure circulating levels of insulin, although we would hypothesise that following central ADAM10i treatment plasma insulin levels will also be elevated, indicative of insulin resistance.

In addition to obesity another contributor to insulin resistance is chronic inflammation, and this may play a part in the impaired ITT and mild metabolic defects observed with ADAM10 inhibition. This is in keeping with our data suggesting BACE1 inhibition improves metabolic disease by reducing diet-induced inflammation (section 3.2.11). Owing to this, and with the knowledge that AD is associated with increased inflammation (Yang & Song 2013), we would hypothesise that treatment with an ADAM10i would cause upregulation in inflammatory mediators in both central and peripheral tissues. This is in keeping with the fact that known ADAM10 substrates include PGSL-1, which plays a role in immune cell function; specifically leukocyte recruitment and migration into tissues. (Lichtenthaler et al. 2003; Dislich & Lichtenthaler 2012). Therefore, blocking ADAM10 activity will also impact the appropriate response to inflammation and inflammatory processing. In support of this, Postina *et al* demonstrated that ADAM10 overexpression in AD mouse models not only reduces Aβ levels, but it does so through reduced inflammation (Postina et al. 2004). Unfortunately, due to time constraints, the inflammatory profile of these mice could not be examined. It would be beneficial to conduct the same experiments performed in BACE1 inhibitor studies measuring inflammatory markers in the hypothalamus and WAT predominantly, as well as measuring levels in the plasma and carrying out flow cytometry to assess actual macrophage numbers in tissues. Also of interest would be to examine ER stress markers, as ER stress is also implicated in insulin resistance (Ozcan et al. 2004; Ozcan et al. 2006; Miller et al. 2007), and we hypothesise that an upregulation of ER stress would be present in the hypothalamus and peripheral tissues of ADAM10i treated mice. In support of the hypothesis that ADAM10 inhibition will drive increased inflammation, we do observe a larger liver size as a percentage of body weight in ADAM10i treated mice in comparison to controls. This may be indicative of an increased number of immune cells and inflammation in this tissue. Interestingly, this was only observed in the liver with no changes detected in the spleen, and notably raw organ weights were unaltered. It is possible that at this early stage only the liver is markedly affected, and if we continued the study for a longer period of time we may see enhanced inflammatory processing associated with changes in the spleen and WAT, accompanied by increased body weight. This is supported by the knowledge that inflammation associated with insulin resistance, involving increased pro-inflammatory cytokines such as TNFα and IL-6, primarily affects the liver, as well as adipose tissue. In addition, ADAM10 has many substrates other than APP, of which not all give rise to neuroprotective effects, for example these include both

TNFα and IL-6 (Pruessmeyer & Ludwig 2009). This suggests that inhibiting ADAM10 may actually provide some protective effects in regards to inflammation and highlights the importance of other possible functions of ADAM10 and α-secretase activity. The complexity of additional substrates and functions needs to be addressed as their subsequent effects may account for the mild phenotype observed in our study.

The rationale behind blocking the α-secretase pathway through inhibition of ADAM10 was due to the fact ADAM10 is considered the predominant α-secretase responsible for constitutive activity (Kuhn et al. 2010). We inhibited ADAM10 centrally as this ADAM is present in neurons and is necessary for α-secretase activity in neurons (Marcinkiewicz & Seidah 2000). As mentioned, ADAM10 has many other substrates and functions, of which not all are fully defined, therefore when inhibiting ADAM10 in these studies we will also be affecting other substrates and these may influence the mild phenotype we observe. Amongst the known substrates of ADAM10 in the brain is Notch (Pruessmeyer & Ludwig 2009), and this is a major substrate indicated by the finding that ADAM10-deficient mice are embryonic lethal (Hartmann et al. 2002). In addition, other ADAMs also exist as the α-secretase (ADAM 9 and 17 being the most characterised), thus in the present study we have not exclusively abolished all α-secretase activity. This is supported by maintained α-activity, through ADAM9 and ADAM17, in ADAM10-deficient mice (Hartmann et al. 2002), demonstrating multiple ADAMs are required to fully regulate α-secretase activity. Taken together, this may account for the mild affects observed in our studies, as some degree of compensation of α-secretase activity may be occurring, particularly through ADAM17. ADAM17 is the ADAM which is capable of being regulated, therefore conditions such as high-fat feeding may induce ADAM17 causing increased α-secretase activity through this ADAM, although there is currently no evidence for this. Furthermore, other studies have shown that knock-down of ADAM10 only mildly elevates β-secretase activity and consequently Aβ levels (Kuhn et al. 2010). Therefore, in the present studies, through inhibition of ADAM10, we may not be causing a large increase in BACE1 activity and/or levels, comparable to those found with other stressors such as HFD, hypoxia, oxidative stress or age, and in turn are only producing a mild phenotype. If we inhibited all α-secretase activity this may give rise to a more severe obese/diabetic phenotype, yet owing to the neuroprotective functions and other substrates of the α-secretase this could be detrimental. Additionally, treatment with an ADAMi in a model where BACE1 levels are already high, for example in aged mice, may elicit a

worsened metabolic phenotype, and such experiments could be beneficial to conduct in the future.

Overall, the results reported in this chapter support our hypothesis that elevated BACE1 activity exacerbates metabolic syndrome when challenged with a HFD, as blockage of ADAM10-mediated processing should result in increased BACE1 cleavage. Within these studies, by altering the balance of APP processing in this way we cannot conclude whether the metabolic effects observed are due to sAPPβ or Aβ elevations directly. We would hypothesise that the reported effects are due to increased central Aβ levels, specifically targeting the hypothalamus; contributing to inflammation and exacerbating obesity and insulin resistance. This is supported by work showing that Aβ oligomers directly bind to hypothalamic neurons in culture and that central administration of Aβ oligomers induces hypothalamic inflammation, impaired glucose homeostasis and insulin resistance (Clarke et al. 2015). Importantly, we cannot say definitively that the proposed effects are solely due to Aβ in the brain. BACE1 is expressed throughout peripheral tissues, including the heart, liver, skeletal muscle and WAT, and furthermore BACE1 levels are elevated in response to stress (HFD) in a number of peripheral tissues (unpublished data). Therefore, although a large component of the suggested effects of Aβ may be due to central action there may also be direct effects on peripheral tissues. Recent work in our lab also implicates Aβ in metabolic dysfunction, supporting the work by Clarke *et al*, by showing that central infusion of mouse $A\beta_{42}$ worsens an obese/diabetic phenotype in mice challenged with a HFD, through increased body weight gain, and impaired glucose and insulin tolerance (unpublished data). Interestingly, Clark and colleagues demonstrated that following administration of Aβ oligomers hypothalamic inflammation was induced as early as four hours post injection, whereas impairments in glucose homeostasis were observed days following administration (Clarke et al. 2015). From this study it was concluded that the Aβ-induced inflammation, accompanied by hypothalamic ER stress, drove defects in glucose and insulin tolerance. This is supportive of our data demonstrating impaired glucose control during glucose and insulin tolerance tests prior to changes in body weight, suggestive that these effects are driven by inflammation and ER stress. This provides further emphasis on the requirement to measure cytokine levels and ER stress markers in our mice. Importantly, the phenotype observed following administration of Aβ oligomers by Clark *et al*, and our lab, mimic the phenotype we observe with ADAM10 inhibition, however they represent a far more severe phenotype, indicating Aβ is the driving factor for the metabolic dysfunction.

4.4.4 Concluding Remarks

The data presented in this chapter highlight a role for BACE1 in energy metabolism and that this may be through the cleavage of APP as a substrate. We have shown that altering the balance between non-amyloidogenic and amyloidogenic APP processing to favour increased BACE1 cleavage causes mild metabolic dysfunction associated with a HFD. This is due to reduced α-secretase activity causing increased BACE1 levels and/or activity, which will result in elevated levels of Aβ. Taken together, these data and recent work from our lab, show that increased Aβ can drive not only AD progression, but may contribute to the onset of obesity and diabetes. Furthermore, therapeutic intervention targeting Aβ, for instance through inhibition of BACE1 to reduce Aβ levels, may provide a novel treatment strategy for metabolic disease.

Chapter 5

The role of BACE1 in the hypothalamus

5.1 Introduction

Within both chapter 3 and chapter 4 we have demonstrated that reducing BACE1 activity in DIO mice improves an obese/diabetic phenotype and that alterations in α-secretase mediated APP processing exacerbates an obese/diabetic phenotype. However, the precise mechanism(s) responsible for these actions are yet to be defined. In particular, inhibition of BACE1 reduces the high circulating levels of leptin associated with DIO, potentially re-sensitising leptin resistant animals to the effects of leptin. Furthermore, these effects are leptin dependent as work from our lab has found treatment of genetically obese *ob/ob* and *db/db* mice with a BACE1 inhibitor causes no effect (unpublished data). Taken together, these data suggest that the mechanism whereby BACE1 alters energy homeostasis must involve intact leptin signalling. In addition, we have shown that central inhibition of BACE1 causes a dramatic effect on energy balance (section 3.2.7) thus this mechanism is likely centrally driven. Furthermore, BACE1 reduction does not alter food intake suggesting BACE1 may be acting through the hypothalamic circuitry involved in regulating leptin action on energy expenditure.

The main site of leptin action in the brain is the hypothalamus; predominantly the ARC. Within the ARC there is a dense population of leptin receptor-expressing neurons which mediate leptin action; the two main populations being POMC/CART-expressing neurons (Cowley et al. 2001) and NPY/AgRP-expressing neurons (Hâkansson et al. 1998). The accepted model is that leptin binds its receptor on these neurons activating POMC neurons whilst inhibiting NPY/AgRP neurons, to reduce food intake and increase energy expenditure (Coll & Yeo 2013). Synaptic inputs between these neurons play an important role in mediating these effects, as NPY neurons also directly inhibit POMC neurons through synaptic innervation from NPY itself or the inhibitory neurotransmitter GABA (Horvath 2005; Dietrich & Horvath 2013). Alterations in the synaptic inputs of first order ARC neurons are observed in *ob/ob* mice, where there are increased numbers of synapses on NPY neurons and a concomitant increase in inhibitory tone onto POMC neurons, with an associated reduction in the number of synapses on POMC neurons (Pinto et al. 2004). Interestingly, Pinto and colleagues found administration of leptin reversed this and altered the synaptic arrangement prior to any body weight or food intake changes, proposing that alterations in synaptic plasticity may account for the metabolic phenotype of *ob/ob* mice (Pinto et al. 2004). As a result, synaptic plasticity in the hypothalamus has received more attention recently. Hypothalamic circuits are known to show some plasticity through adult life, thus it is considered a potential mediator of the energy regulatory effects of leptin

(Horvath 2005). This is supported by studies examining synaptic inputs on first order ARC neurons following fasting and high-fat feeding. Horvath *et al* demonstrated that in DIO rats there is a reduction in the number of synapses on POMC neurons and increased inhibitory tone on these neurons, with the opposite observed in rats resistant to diet-induced obesity (Horvath et al. 2010). Subsequent studies showed that following fasting there is an increase in inhibitory postsynaptic currents (frequency and amplitude) in POMC neurons (Vong et al. 2011). In addition, work by Benani and colleagues found that following only one week of high-fat feeding mice show an upregulation of genes involved in synaptic plasticity exclusively in the ARC (Benani et al. 2012). This further supports the notion that synaptic plasticity may be involved in the regulation of leptin action at an early stage in the nutrient challenge, particularly through POMC and NPY/AgRP neurons. However, when leptin receptor expression is ablated from POMC neurons or AgRP neurons, only mild obese phenotypes are observed (Balthasar et al. 2004; Van De Wall et al. 2008). Although, when leptin receptor expression is knocked-out of both POMC- and AgRP-expressing neurons an additive affect is observed, with greater body mass and fat mass observed (Van De Wall et al. 2008). Furthermore, Berglund and colleagues demonstrated that when leptin receptor expression is ablated and only re-expressed in ARC POMC neurons, that this only partially recovers the obesity caused by complete leptin receptor ablation, and does not affect food intake (Berglund et al. 2012). This demonstrates that POMC/CART neurons and NPY/AgRP neurons play a small role in mediating the food intake and body weight effects of leptin, providing strong evidence that leptin receptors expressed elsewhere must also be crucial.

The signalling form of the leptin receptor, ObRb, is found in neuronal populations within the ARC which are distinct from POMC/CART and NPY/AgRP neurons. One such population are RIPCre neurons (Cui et al. 2004). Due to the localisation of these neurons in the ARC and their close proximity to POMC/CART neurons and NPY/AgRP neurons it is believed leptin will also act upon these neurons to elicit energy homeostatic effects. Furthermore, ObRb is found outwith the ARC, in the VMH, LH and DMH, as well as in extra-hypothalamic regions such as the brainstem. One hypothalamic region with abundant leptin receptor expression is the VMH, which is also key in facilitating control of energy balance. Within the VMH the predominant neuronal population are SF-1 neurons, and it has been shown that removal of the leptin receptor from these neurons causes a similar phenotype to that observed in mice with a lack of leptin receptor expression on POMC neurons (Dhillon et al. 2006). Therefore, SF-1 neurons also play a

role in mediating the effects of leptin. Interestingly, when ObRb expression is ablated from both SF-1 and POMC neurons there is again an additive effect; increased body weight, however no change in food intake (Dhillon et al. 2006). This demonstrates leptin action is dependent on various populations within the hypothalamus, which will project to and communicate with one another.

The phenotype of ObRb-expressing neurons and their mode of action differ throughout the hypothalamus. The two main neurotransmitters utilised by the CNS are the inhibitory neurotransmitter GABA and the excitatory neurotransmitter glutamate (Delgado 2013). Within the ARC the majority of ObRb-expressing neurons are GABAergic, and when the leptin receptor is removed from GABAergic neurons a very large increase in body weight and fat mass is observed, accompanied by hyperphagia (Vong et al. 2011). Conversely, when ObRb expression is absent in glutamatergic neurons only minimal effects are observed, which are likely produced via the VMH as SF-1 neurons are predominantly glutamatergic (Vong et al. 2011). Vong *et al* showed that specifically in the ARC the majority of AgRP neurons are co-localised with VGAT; a GABA transporter, however minimal co-localisation was observed between VGAT and POMC. Importantly, the ARC POMC neurons are surrounded by and in close apposition to the GABAergic neurons, suggestive of cross-talk between different populations of leptin responsive neurons. This is demonstrated by the aforementioned action of leptin on the GABAergic ARC neurons attenuating the inhibitory actions on POMC neurons (Vong et al. 2011; Cowley et al. 2001).

Leptin receptors are also expressed in extra-hypothalamic areas such as the NTS where the majority of leptin responsive neurons are excitatory, glutamatergic neurons (Vong et al. 2011). GABAergic leptin-responsive neurons within the ARC project to other hypothalamic areas as well as extra-hypothalamic sites which forms the neural circuitry crucial for regulating leptin action. Leptin receptor activation in ARC neurons alters the activity of the neurons leading to altered outputs to hypothalamic nuclei such as the PVN and LH, affecting catabolic and anabolic pathways involved in energy balance. The NTS is the major centre receiving signals from these catabolic and anabolic pathways. Signals from peripheral peptides also send input to the NTS via the vagus nerve and the sympathetic nervous system (SNS). The NTS integrates all these signals, along with other higher brain centres, to mediate desired outcomes, for example inhibition of food intake (Schwartz et al. 2000). Furthermore, ObRb-expressing neurons present in the NTS can also feed back onto catabolic neurons within the PVN. However, less is known regarding

the input and output signals generated by these neurons and the precise circuitry involved between the ARC and brainstem requires further research.

It has been alluded to that BACE may be involved in the neuronal circuitry regulating leptin function. However, how BACE1 affects these pathways is unknown. BACE1 expression in the brain has been extensively studied, in particular during the identification of BACE1 as the β-secretase, where it has been shown to be expressed across various regions in the brain including the cortex, hippocampus, thalamus, spinal cord and medulla (Vassar et al. 1999). Imaging studies have also indicated BACE1 is expressed throughout the brain of WT mice with strongest staining present in the hippocampus (Zhao et al. 2007). Within these areas it has been shown that BACE1 is predominantly expressed in neurons and not glia (Zhao et al. 2007; Hussain et al. 1999; Vassar et al. 1999). Owing to the role of BACE in AD the majority of studies focus on its expression in the hippocampus and the cortex, as these areas are the first affected during AD progression. The hypothalamus is less studied in regards to BACE1, although BACE2 has been shown to be expressed in the hypothalamus in contrast to its low expression across the rest of the brain (Vassar 2004). As a role has emerged for BACE1 in energy homeostasis it is likely BACE1 is present in the hypothalamus, potentially acting on leptin responsive neurons and their corresponding pathways, and this requires investigation to better understand the role of BACE1 in metabolism.

In the present studies the hypothalamic expression of BACE1 was investigated, primarily utilising immunofluorescence (IF) in WT mice brains, to determine where BACE1 is expressed and in which cell type(s). Various neuronal populations important in mediating the body weight and food intake actions of leptin were examined to observe the presence or absence of BACE1. The aim of these experiments was to determine the localisation of BACE1 expression in specific hypothalamic neuronal populations to enable further studies to be undertaken to ascertain the functions of BACE1 in energy homeostasis and how it alters metabolism.

5.1.1 Objectives

- Examine BACE1 expression in the hypothalamus and extra hypothalamic areas under normal conditions to investigate if BACE1 is implicated in the neuronal circuitry controlling energy homeostasis
- Use dual-labelling experiments to examine if BACE is co-expressed with the following cellular populations in the hypothalamus:
    - Leptin receptor-expressing neurons
    - First-order ARC neurons (POMC, NPY/AgRP and RIPCre neurons)
    - GABAergic and glutamatergic ARC neurons
    - VMH neurons (SF-1 and RIPCre neurons)
    - Astrocytes

5.2 Methods Summary

Whole brains from adult mice (>8 weeks of age) were fixed and processed for IF or FISH (as detailed in section 2.6). In brief, brains were sectioned at 30µm thickness and slices containing the hypothalamus selected. Sections were stained for BACE1 alone or co-stained with markers of different cellular populations and imaged using a confocal microscope. For cell counting experiments total cell numbers were counted, using Fiji Image Analysis Software, from a number of sections from different animals. The mean of the total cell count for each population, from all animals, was then calculated.

5.3 Results

5.3.1 BACE1 expression in the brain

BACE1 is shown to be expressed in the cortex and hippocampus of rodents and humans, primarily due to research focused on Alzheimer's disease, with other brain regions largely ignored. Thus, the expression of BACE1 in additional brain regions, in comparison to levels in the hippocampus and cortex, was investigated. Initially, using Western blotting and IF on WT adult mice, BACE1 protein levels were measured, in four main brain regions; the hippocampus, hypothalamus, cerebellum and cortex. BACE1 was detected in all four brain regions (Figure 5.1). BACE1 expression was highest in the cortex (mean=0.22 arbitrary units), and this expression was significantly greater than all other areas investigated ($p<0.01$, $n=6$, Figure 5.1A and B). Interestingly, the hippocampus exhibited lower BACE1 levels, which were comparable to those measured in the

cerebellum and hypothalamus. These data show, although the hippocampus is the most widely studied brain area in regards to BACE1, this area does not have the most abundant expression. To investigate the expression pattern of BACE1 in these areas further IF was carried out. Representative confocal images show BACE1 is expressed throughout areas of the hippocampus, hypothalamus, cerebellum and cortex, in line with the Western blotting data. The images demonstrate BACE1 expression is high in discrete groups of cells (Figure 5.1C). Note, BACE1 is expressed across the whole brain, in other regions outwith the hippocampus, hypothalamus, cerebellum and cortex, although there are also regions completely negative for BACE1 staining (data not shown). Taken together, these data show BACE1 is highly expressed in distinct groups of cells throughout the brain, and to a substantial level in brain regions out with the cortex and hippocampus, which may also have important functions in regards to the role of BACE1.

It has been reported that many BACE1 antibodies give non-specific signals, therefore to confirm the specificity of BACE1 expression in the brain, IF was carried out on sections from *BACE1*$^{-/-}$ mice and minimal staining was detected (Figure 5.2). This is supported by work from our lab that has tested this antibody on brain tissue from *BACE1*$^{-/-}$ mice using Western blotting (Meakin et al. 2012) and work from other groups testing this antibody on *BACE1*$^{-/-}$ mice utilising immunohistochemistry (Zhao et al. 2007); both reporting it is highly specific.

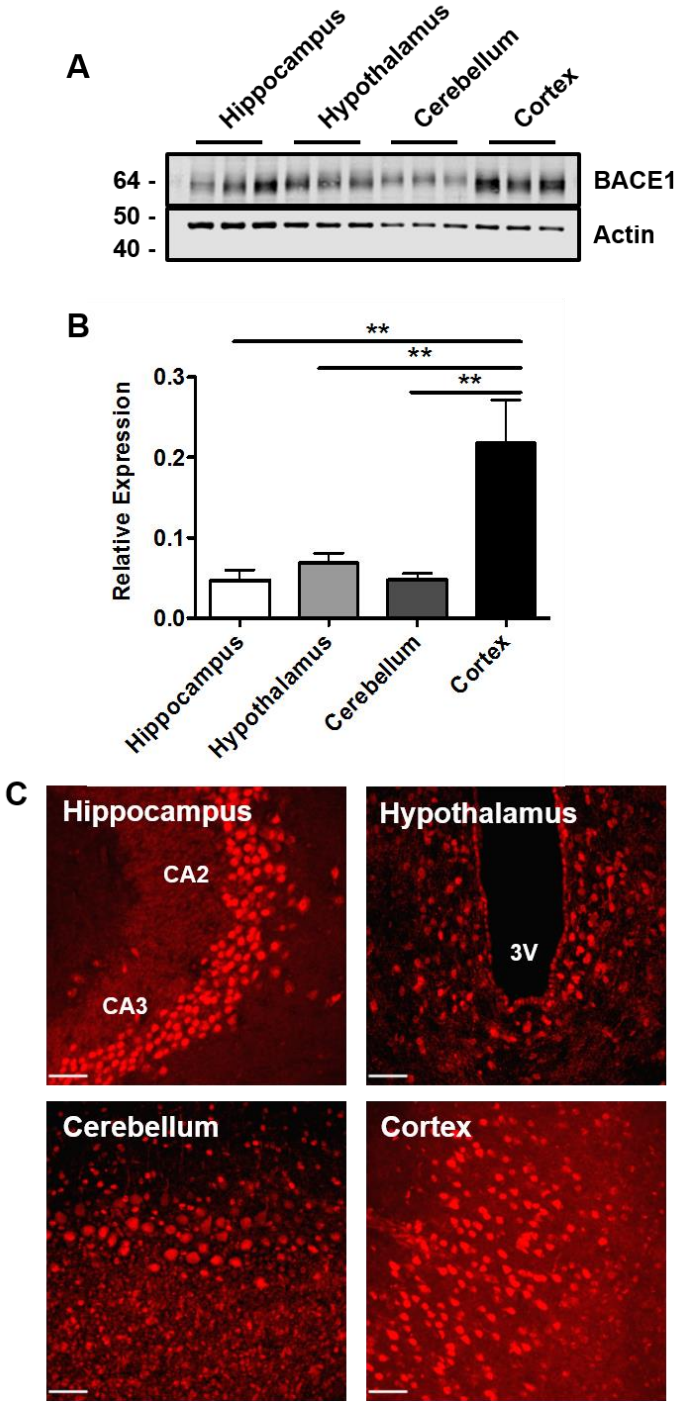

Figure 5.1 BACE1 protein expression in the brain.

(A) Representative Western blot showing BACE1 protein expression in different regions of the brain. Molecular mass is given in kDa on the left-hand side. (B) Densitometric analysis showing BACE1 is highly expressed in the cortex; significantly higher than in the hippocampus, hypothalamus and cerebellum ($p<0.01$, $n=9$). (C) Representative confocal images, taken at x40 magnification, demonstrating BACE1 protein expression in areas of the hippocampus, hypothalamus, cerebellum and cortex. 3V, third ventricle. CA2, CA2 field. CA3, CA3 field. All scale bars 50µm.

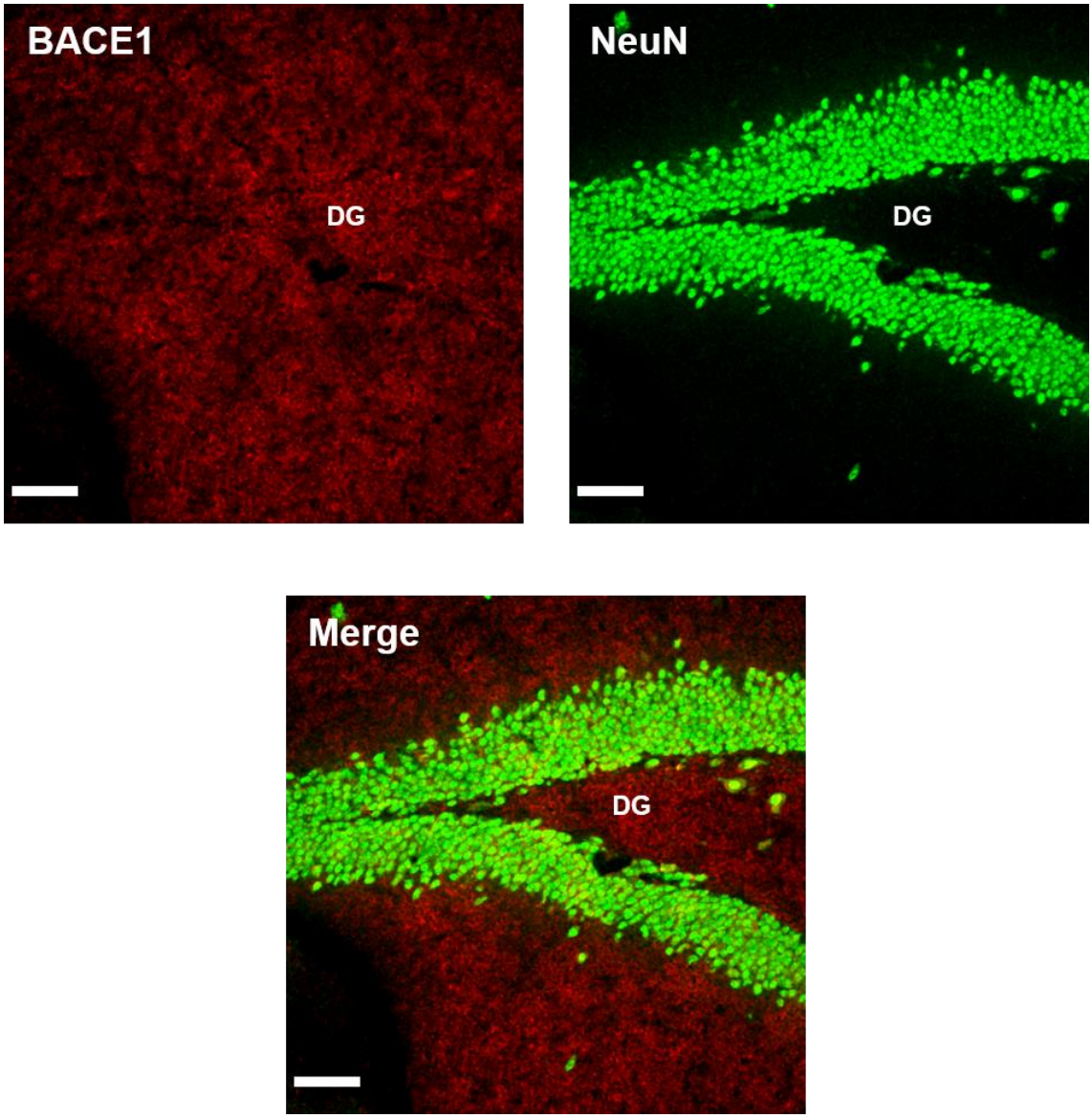

Figure 5.2 Specificity of BACE1 antibody staining in a *BACE1*$^{-/-}$ mouse brain.

Confocal images, taken at x40 magnification, showing BACE1 (red), neuronal marker NeuN (green) and merged channels within a region of the hippocampus from a *BACE1*$^{-/-}$ mouse. Representative images display minimal BACE1 staining. DG, dentate gyrus. All scale bars 50um.

5.3.2 BACE1 expression in the hypothalamus

Having previously discussed a role for BACE1 in energy metabolism and observing BACE1 protein in abundance in the hypothalamus; the central control centre for whole body energy metabolism, this area was examined in greater detail. The distribution of BACE1 protein throughout the hypothalamus was examined using IF on WT adult mice fed a NC diet. BACE1 was observed throughout the hypothalamus, within the DMH, LH, VMH and ARC (Figure 5.3). Throughout the hypothalamus the observed expression is not homogenous, BACE1 is present in discrete groups of cells (Figure 5.3 higher magnification images). These data show BACE1 is expressed in cells present in the key centres of the hypothalamus involved in the control of energy homeostasis, and consequently it is likely that these cells may contribute to the functional outputs associated with the effects of lowering or increasing BACE1 on whole body energy metabolism.

5.3.3 BACE1 is expressed in neurons throughout the hypothalamus

Having identified distinct populations of BACE1 positive cells throughout the hypothalamus the precise phenotype of these cells was investigated. As previously mentioned, in the hippocampus and cortex BACE1 is accepted to be predominantly expressed in neurons and not glia (Zhao et al. 2007; Hussain et al. 1999; Vassar et al. 1999), therefore initially the localisation of BACE1 to neurons in the hypothalamus was studied. This was examined using IF, with double-staining of BACE1 (red) and the neuronal marker, NeuN (green), on brain sections from WT adult mice fed a NC diet. The predominate focus is on the ARC, where representative confocal images display BACE1 is largely neuronal, determined by the majority of BACE1 positive cells co-localising with NeuN in this area, observed as yellow (Figure 5.4D).This finding was also observed in all other examined regions of the hypothalamus; the DMH, VMH and LH (Figure 5.4B-C), showing BACE1 is predominantly neuronal throughout the hypothalamus.

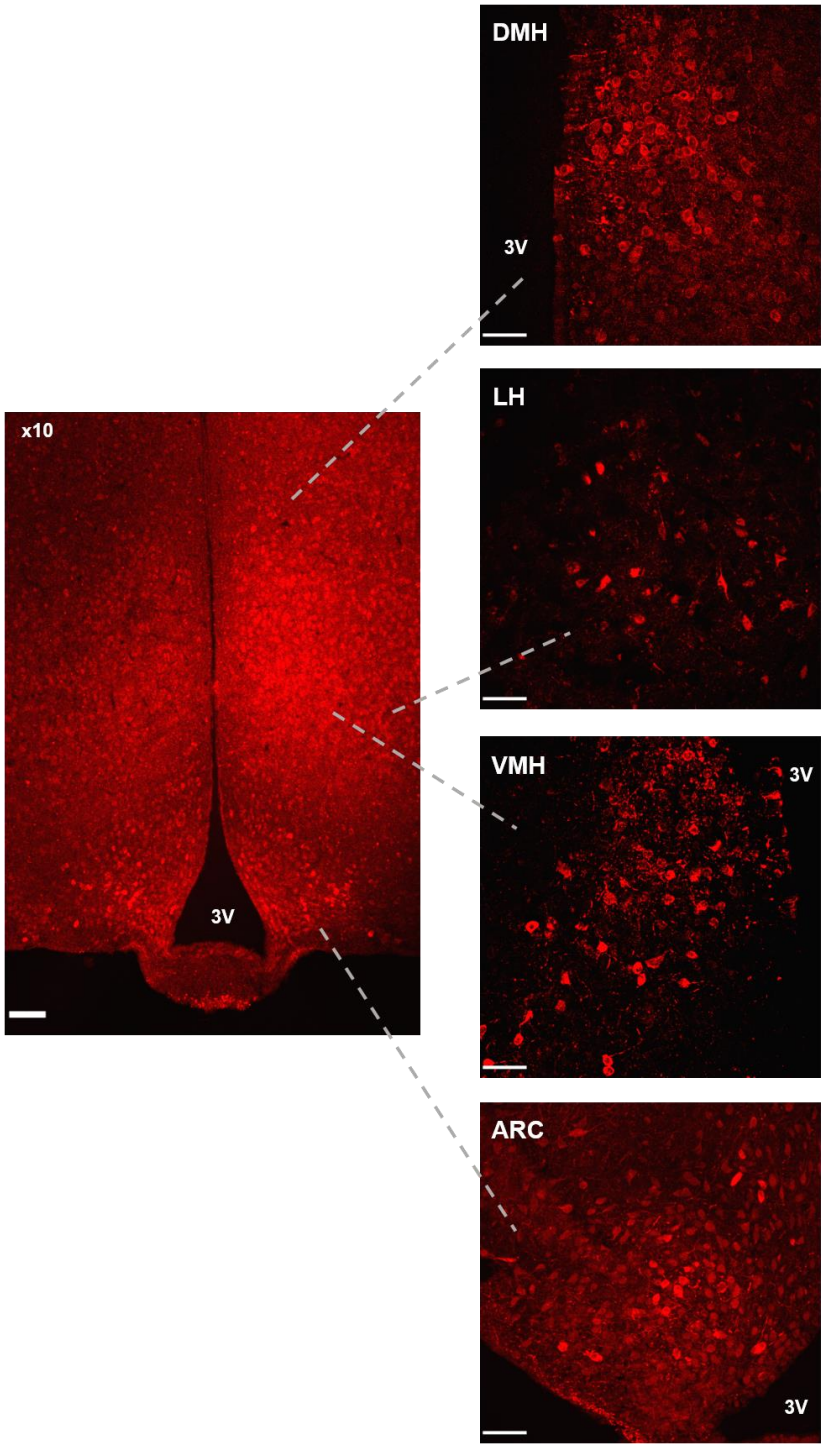

Figure 5.3 BACE1 is expressed throughout the hypothalamus.

Representative confocal images showing BACE1 protein expression within regions of the hypothalamus. Low magnification (x10) image demonstrates BACE1 expression throughout the whole hypothalamus. Higher magnification images (x40) show distinct BACE1 cells in the dorsmedial hypothalamus (DMH), lateral hypothalamus (LH), ventromedial hypothalamus (VMH) and arcuate nucleus (ARC). 3V, third ventricle. x10 magnification image scale bar 100µm. All x40 magnification images scale bars 50µm.

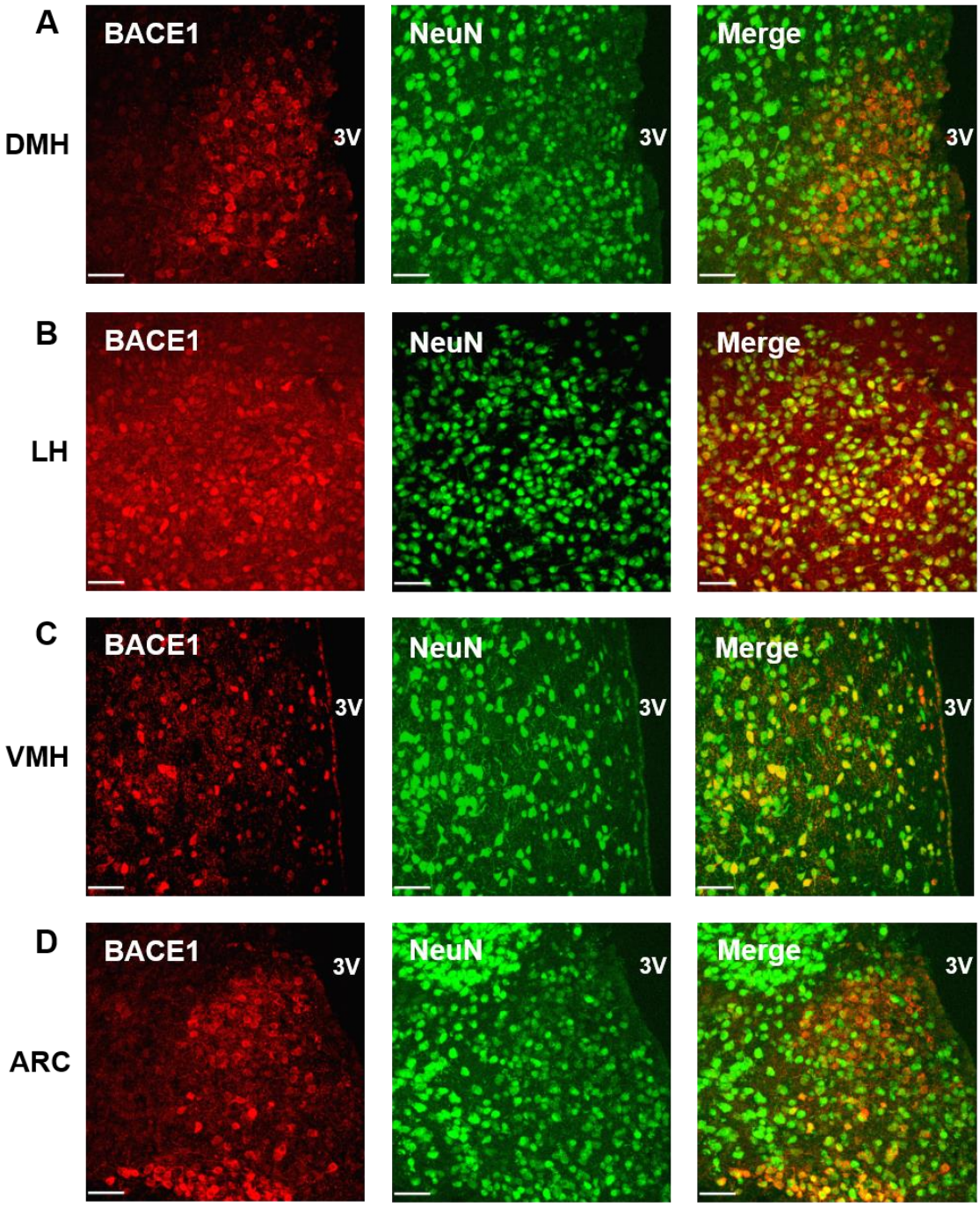

Figure 5.4 BACE1 is expressed in neurons throughout the hypothalamus.

Confocal images, taken at x40 magnification, showing BACE1 (red), neuronal marker NeuN (green) and merged channels within regions of the hypothalamus. Representative images from (A) the dorsomedial hypothalamus (DMH), (B) the lateral hypothalamus (LH), (C) the ventromedial hypothalamus (VMH) and (D) the arcuate nucleus (ARC). 3V, third ventricle.

5.3.4 BACE1 is not expressed in astrocytes throughout the hypothalamus

Although BACE1 was found to be predominantly neuronal, not all BACE1 positive cells were co-localised with the neuronal marker, NeuN, in the hypothalamus. In the hippocampus and cortex BACE1 is not reported to be present in astrocytes under normal conditions (Zhao et al. 2007; Hussain et al. 1999; Vassar et al. 1999), therefore whether this is also the case in the hypothalamus was investigated. This was achieved using IF with double-staining of BACE1 (red) and the astrocyte marker, GFAP (green), on brain sections from WT adult mice fed a NC diet. In the ARC, representative confocal images show BACE1 is not expressed in astrocytes, demonstrated by a lack of co-localisation (lack of yellow staining) of BACE1 positive cells and GFAP (Figure 5.5D). This finding was also observed in all other examined regions of the hypothalamus; the DMH, VMH and LH (Figure 5.5B-C), showing BACE1 is not astrocytic throughout the hypothalamus.

5.3.5 Leptin responsiveness of BACE1 neurons in the arcuate nucleus

5.3.5.1 BACE1 neurons express the leptin receptor

Leptin receptors are abundantly expressed in the ARC of the hypothalamus, with the long form of the leptin receptor (ObRb) required for leptin signalling (Tartaglia 1997). Having found BACE1 is abundantly expressed in the ARC and that BACE1 plays a role in leptin sensitivity and energy metabolism (chapter 3), the presence of ObRb in BACE1-positive neurons was investigated. Using IF brain sections from WT adult mice fed a NC diet were double-stained for BACE1 (red) and ObRb (green) in the ARC. Representative confocal images show a proportion of BACE1 neurons express ObRb, indicated by co-localisation of BACE1 and ObRb, observed as yellow (Figure 5.6A). However, not all BACE1-positive neurons express ObRb. Quantitative analysis of co-localised cells (counted across 4 images) found approximately 24% of BACE1-positive neurons express ObRb and furthermore 27% of detected ObRb-positive neurons are BACE1-positive neurons (Figure 5.6B). Taken together, these data show only a proportion of BACE1 neurons in the ARC express ObRb, and therefore only a proportion may be directly responsive to leptin.

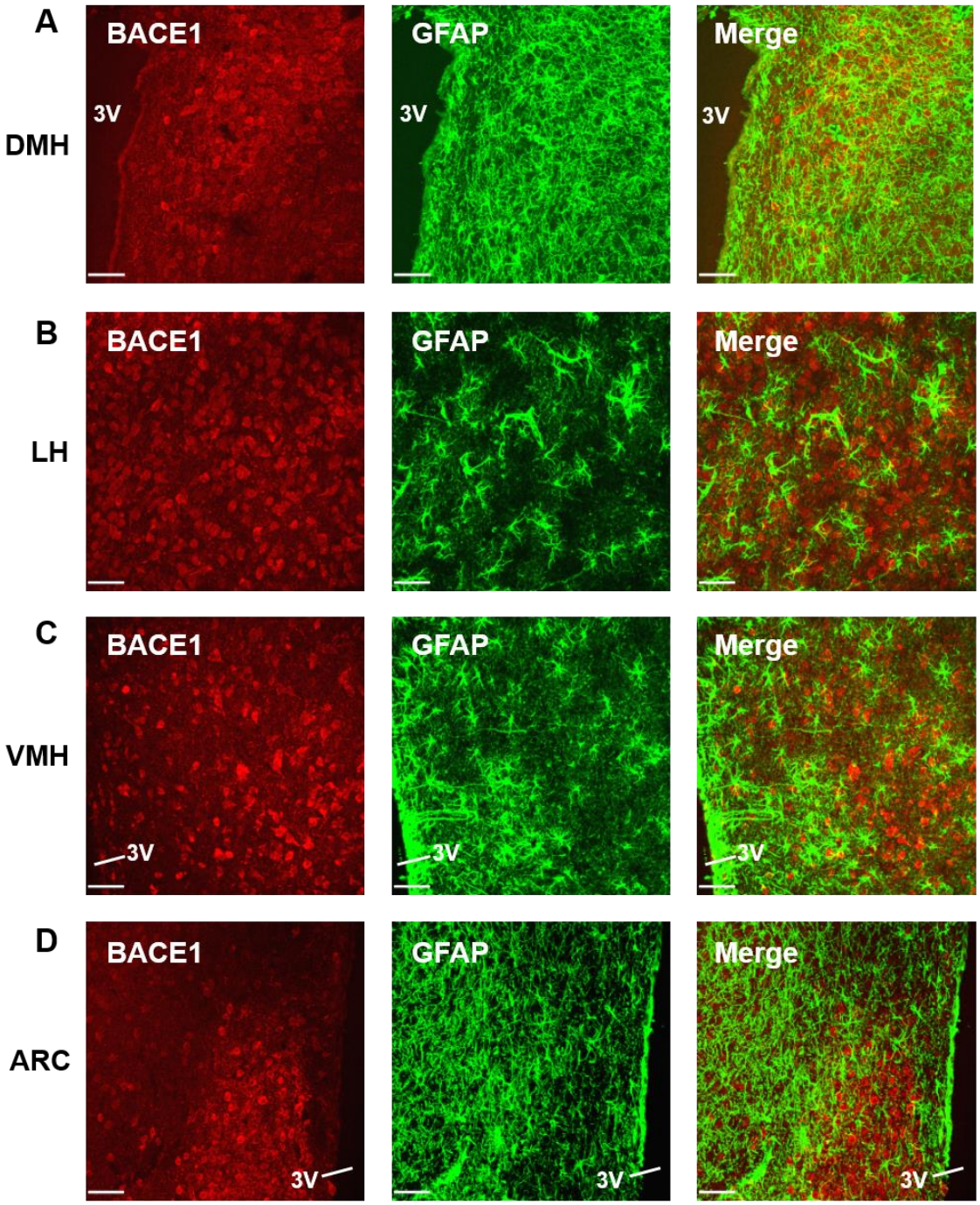

Figure 5.5 BACE1 is not expressed in astrocytes throughout the hypothalamus.

Confocal images, taken at x40 magnification, showing BACE1 (red), astrocytic marker GFAP (green) and merged channels within regions of the hypothalamus. Representative images from (A) the dorsomedial hypothalamus (DMH), (B) the lateral hypothalamus (LH), (C) the ventromedial hypothalamus (VMH) and (D) the arcuate nucleus (ARC). 3V, third ventricle. All scale bars 50µm.

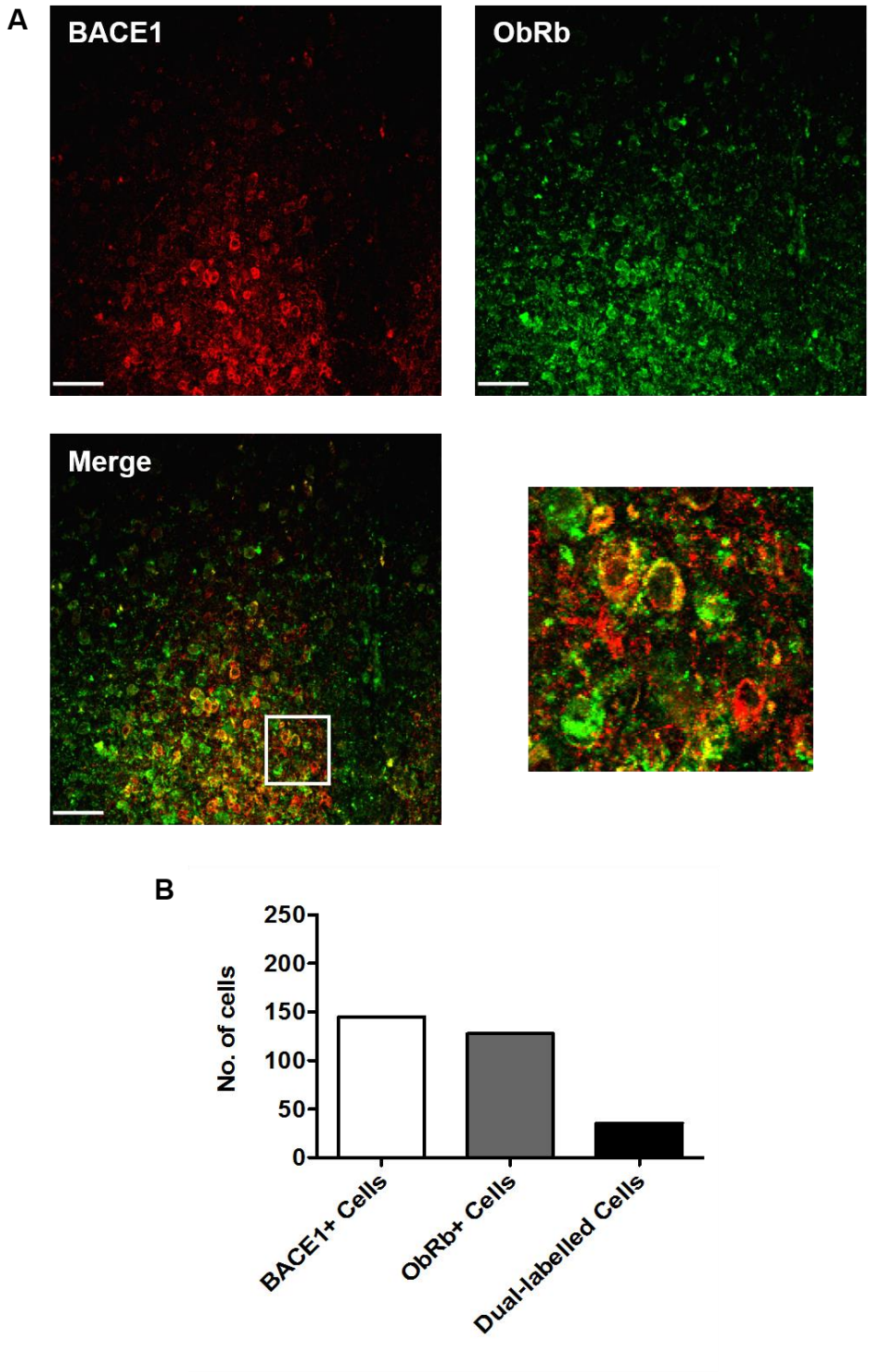

Figure 5.6 BACE1 neurons in the arcuate nucleus possess the long form of the leptin receptor.

(A) Representative confocal images, taken at x40 magnification, showing BACE1 (red), the long form of the leptin receptor (ObRb) (green) and merged channels in the arcuate nucleus. All scale bars 50µm. (B) Histogram displaying total number of BACE1+ cells, ObRb+ cells and dual-labelled cells per field of view, showing a proportion of BACE1 neurons express ObRb (4 fields of view, n=2).

5.3.5.2 BACE1 neurons are not directly responsive to leptin

Upon leptin binding to ObRb there is initiation of the JAK-STAT signalling pathway, which ultimately results in phosphorylation of STAT3 to drive transcription of POMC, whilst inhibiting NPY/AgRP. To further evaluate the effect of BACE1 on leptin signalling, whether the BACE1 neurons expressing ObRb in the ARC are directly responsive to leptin through this pathway was investigated. WT adult mice fed a NC diet were fasted overnight before an intraperitoneal (i.p) injection of leptin (4mg/kg) and sacrificed one hour post-leptin injection. IF was performed on brain sections, double-staining for BACE1 (red) and pSTAT3 (green). In a separate cohort of animals, saline was administered as a control, and minimal pSTAT3 staining was observed (Figure 5.7B). Representative confocal images show the vast majority of BACE1-positive neurons in the ARC do not respond to leptin treatment by increased pSTAT3, indicated by very low levels of co-localisation of BACE1 and p-STAT3 (lack of yellow staining) (Figure 5.7A). Quantitative analysis (counted across 6 images) confirms this by showing approximately only 1% of BACE1 neurons are co-localised with pSTAT3 and furthermore from the detected number of p-STAT3 cells approximately only 4% co-localise with BACE1-positive neurons (Figure 5.7B). These data suggest, although a proportion of BACE1 neurons express ObRb, these neurons may not be directly responsive to leptin and BACE1 may not directly affect leptin JAK2/STAT3 signalling in the ARC.

It has been reported that leptin reduces BACE1 expression and activity (Marwarhaet al. 2014), therefore the observed lack of co-localisation between BACE1- and pSTAT3-neurons may be due to a lack of detectable BACE1. To investigate if this is the case in the ARC, BACE1 staining on brain sections from leptin- and saline-treated mice (described above) were examined. Confocal images showed reduced BACE1 expression in the ARC of leptin treated animals in comparison to control mice (Figure 5.8). Quantitative analysis supports this, showing the actual number of BACE1-positive neurons detected is decreased in leptin treated mice (Control; ~95 cells vs. leptin; ~60 cells, counted across 6-7 images), (Figure 5.8B). Taken together, these data show BACE1 expression is reduced upon leptin stimulation, and therefore the number of BACE1-positive neurons present is diminished. Assuming BACE1 neurons which express ObRb are those which are reduced, this may account for the lack of co-localisation with p-STAT3 and the un-responsiveness to leptin.

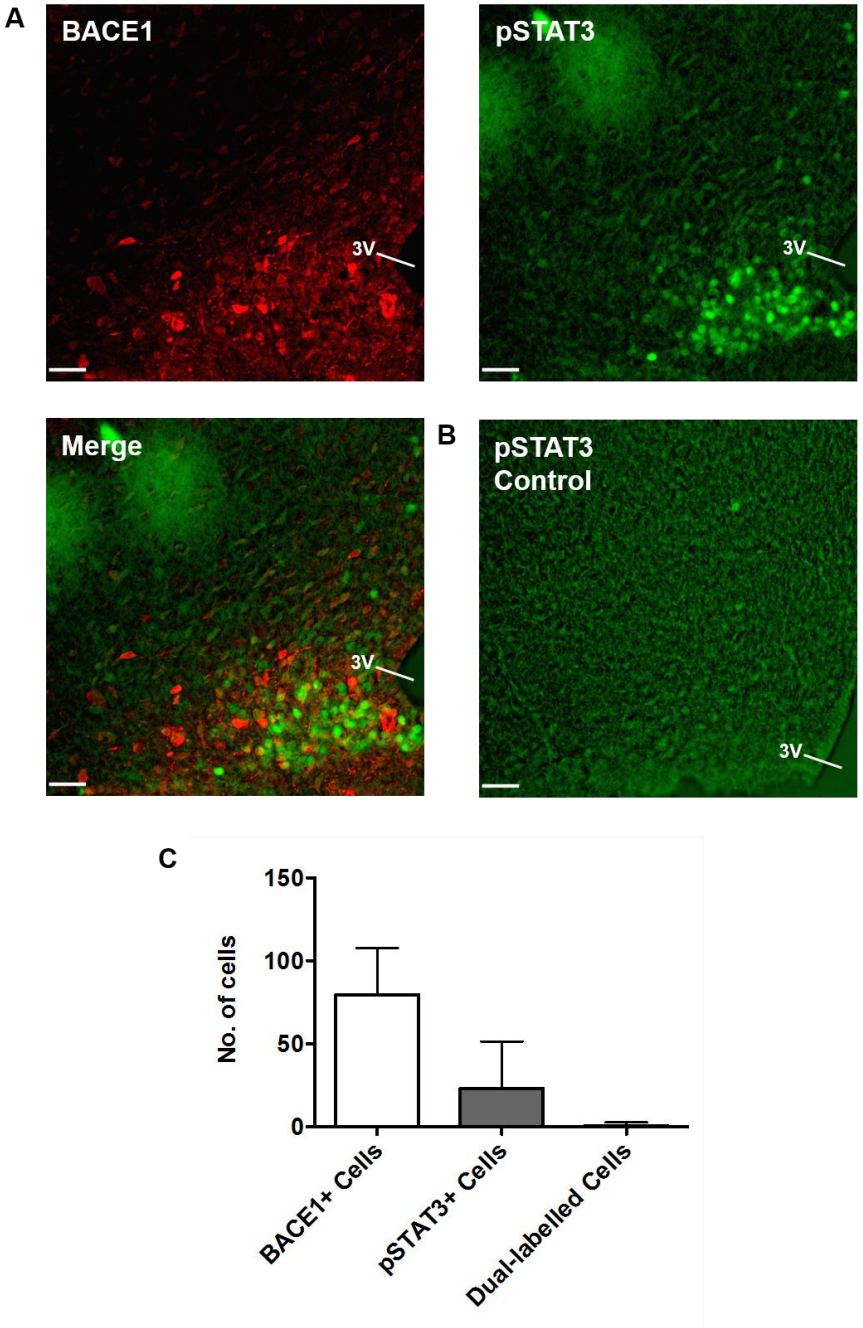

Figure 5.7 BACE1 is not co-localised with pSTAT3 in the arcuate nucleus following leptin treatment.

(A) Representative confocal images, taken at x40 magnification, showing BACE1 (red), pSTAT3 (green) and merged channels in the arcuate nucleus of wild-type mice one hour post intraperitoneal leptin (4m/kg) treatment. (B) Representative confocal image, taken at x40 magnification, showing minimal pSTAT3 staining in the arcuate nucleus following intraperitoneal saline (control) treatment. 3V, third ventricle. All scale bars 100µm. (C) Histogram displaying total number of BACE1+ cells, pSTAT3+ cells and dual-labelled cells per field of view, showing minimal co-localisation between BACE1 and pSTAT3 (6 fields of view, n=2-3).

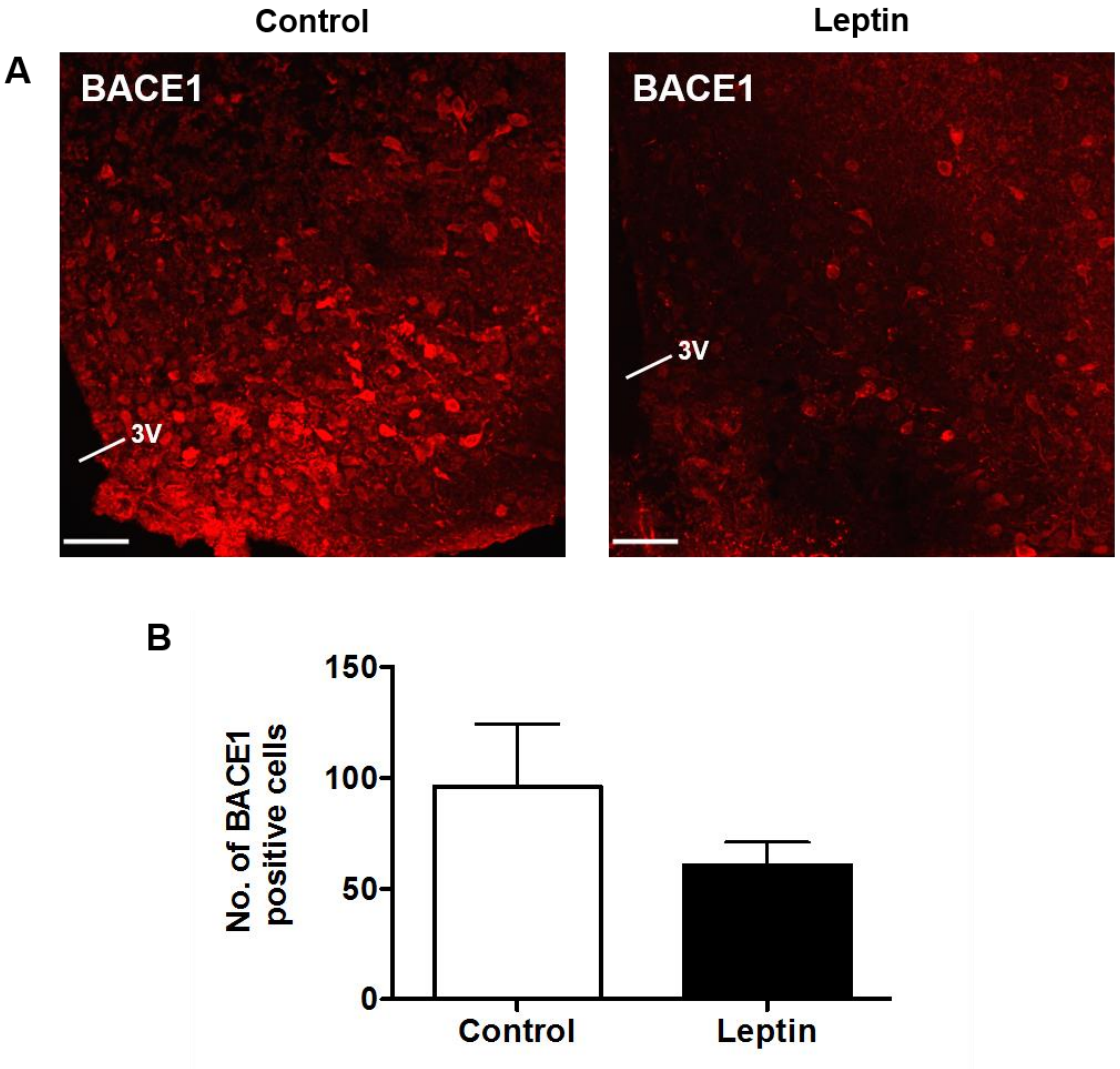

Figure 5.8 BACE1 expression is reduced in the arcuate nucleus following leptin treatment.

(A) Representative confocal images, taken at x40 magnification, showing BACE1 expression in the arcuate nucleus one hour post intraperitoneal leptin (4m/kg) treatment or saline (control) treatment. 3V, third ventricle. All scale bars 50µm. (B) Histogram displaying the total number of BACE1-positive cells per field of view, showing a reduced number of BACE1 neurons with leptin treatment (6-7 fields of view, n=2-3).

5.3.5.3 Leptin sensitivity in the absence of BACE1

Having observed no pSTAT3 response to leptin in BACE1-positive neurons it is undetermined whether BACE1 neurons in the ARC directly affect leptin signalling or whether BACE1-positive neurons are modified by leptin. To examine this levels of pSTAT3, following i.p leptin, were measured in *BACE1*$^{-/-}$ mice and age-matched WT mice fed a NC diet. Both *BACE*$^{-/-}$ and WT mice show induction of pSTAT3 in the ARC one hour post-i.p of leptin (4mg/kg) (Figure 5.9A). Minimal pSTAT3 staining was observed when saline was administered as a control (Figure 5.9B). Quantitative analysis shows there is a trend towards an increase in the number of pSTAT3 cells in *BACE1*$^{-/-}$ mice in comparison to WT mice (counted across 8 images), however this is not a significant difference (Figure 5.9B).

5.3.6 BACE1 expression in first order neurons in the arcuate nucleus

Having observed BACE1 protein abundantly expressed in the ARC, and that a proportion of these neurons may be involved in leptin signalling, next it was determined if BACE1 is present in first order neurons involved in this pathway. The two main neuronal populations in the ARC are anorexigenic POMC/CART neurons and orexigenic NPY/AgRP neurons (Funahashi et al. 2003). Leptin acts on both populations to induce food intake actions. As a proportion of BACE1 neurons express the leptin receptor, and reducing BACE1 activity alters body weight and fat mass (chapter 3), it was hypothesised that BACE1 may be present in these neurons and may evoke at least some of its actions on energy metabolism via these neuronal populations.

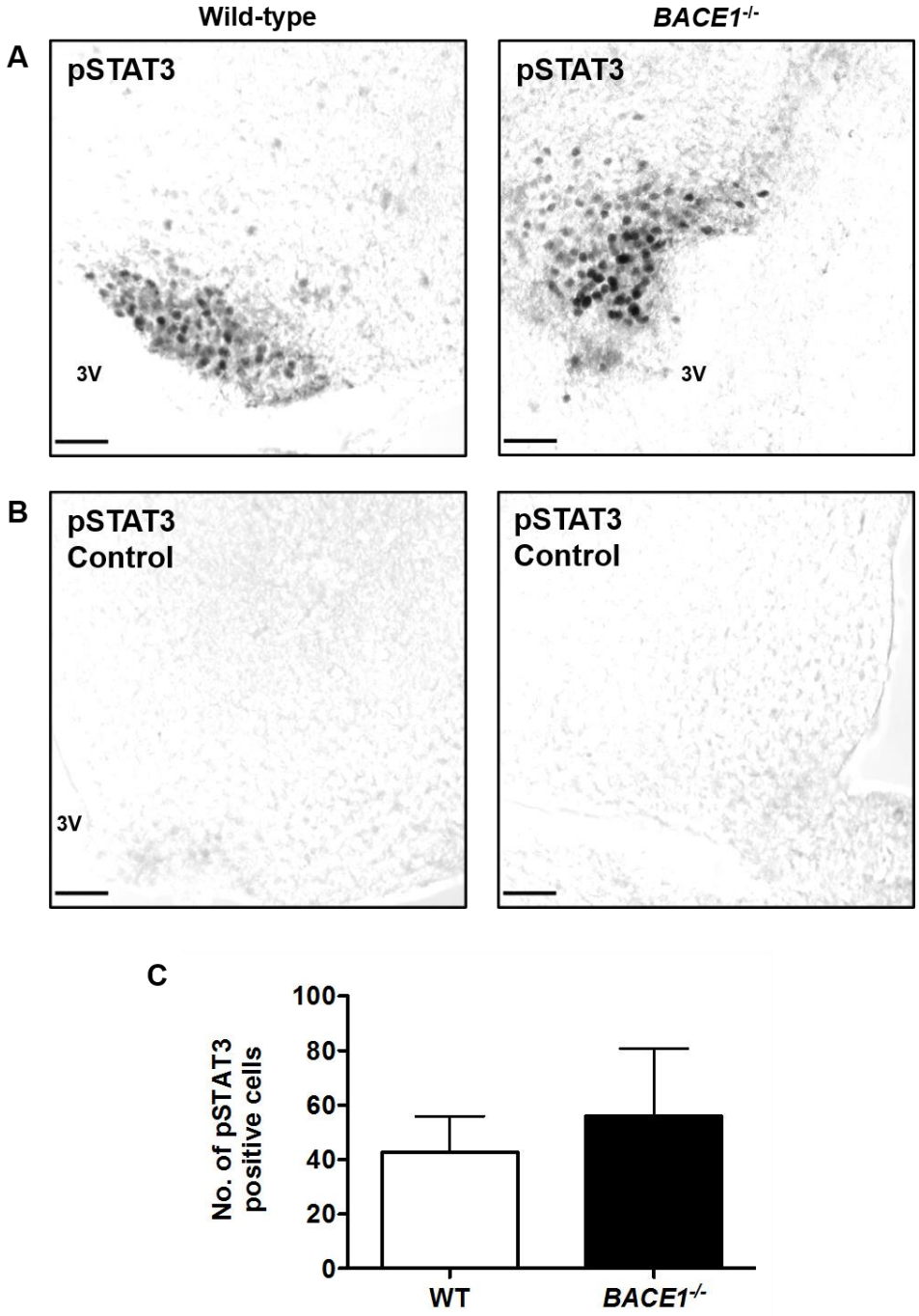

Figure 5.9 pSTAT3 expression is unaltered in the arcuate nucleus of *BACE1*$^{-/-}$ mice following leptin treatment.

(A) Representative confocal (bright-field) images, taken at x40 magnification, showing pSTAT3 expression in the arcuate nucleus one hour post intraperitoneal leptin (4mg/kg) treatment in wild-type and *BACE1*$^{-/-}$ mice. (B) Representative confocal images, taken at x40 magnification, showing minimal pSTAT3 staining in the arcuate nucleus following intraperitoneal saline (control) treatment in wild-type and *BACE1*$^{-/-}$ mice 3V, third ventricle. All scale bars 50µm. (B) Histogram displaying the total number of pSTAT3-positive cells per field of view (8 fields of view, n=3).

5.3.6.1 BACE1 is expressed in a small number of proopiomelanocortin neurons in the arcuate nucleus

Initially the presence of BACE1 and the ARC anorexigenic neuropeptide population was examined. As neuropeptides are constantly being transported along the axons of neurons visualisation in the cell body with classic IF (using antibodies) can be difficult, as antibodies have a tendency only to pick up nerve fibres, therefore IF on POMC-GFP tissue, and IF carried out following fluorescent *in-situ* hybridisation (FISH) were utilised to visualise POMC in WT adult mouse brain. Sections were double stained with BACE1 (red) to determine if BACE1 is present in POMC-expressing neurons (green). Using both FISH and IF confocal images show a small number of BACE-positive neurons are co-localised with POMC-expressing neurons in the ARC, observed as yellow (Figure 5.10A and B). The majority of BACE1 neurons are not co-localised with POMC, however representative images show that many of the BACE1 neurons lie in very close apposition to POMC neurons, as deomstrated in the higher magnification boxed regions in Figure 5.10A and B. Quantitative analysis of BACE1 and POMC cells show approximately 5% of BACE1 neurons are co-localised with POMC-expressing neurons by the method of FISH (counted across 5 images) and IF (counted across 11 images) and 8% of POMC-expressing neurons are co-localised with BACE1-positive neurons (Figure 5.10C). Due to a lack of tissue and FISH probe the anorexigenic neuropeptide CART could not be examined, however in the ARC all POMC neurons co-express CART (Elmquist et al. 1999), therefore it is likely that BACE1 is also not co-localised with CART-expressing neurons in the ARC to a large extent (approximately 5-10%). Taken together, these data show BACE1 is expressed in a very small proportion of POMC-expressing neurons in the ARC, however POMC neuronal cell bodies and processes lie in close apposition to BACE1-positive neurons and vice versa, therefore BACE1 may not be acting directly via this neuronal population but may still be functionally connected to POMC/CART neurons in the ARC.

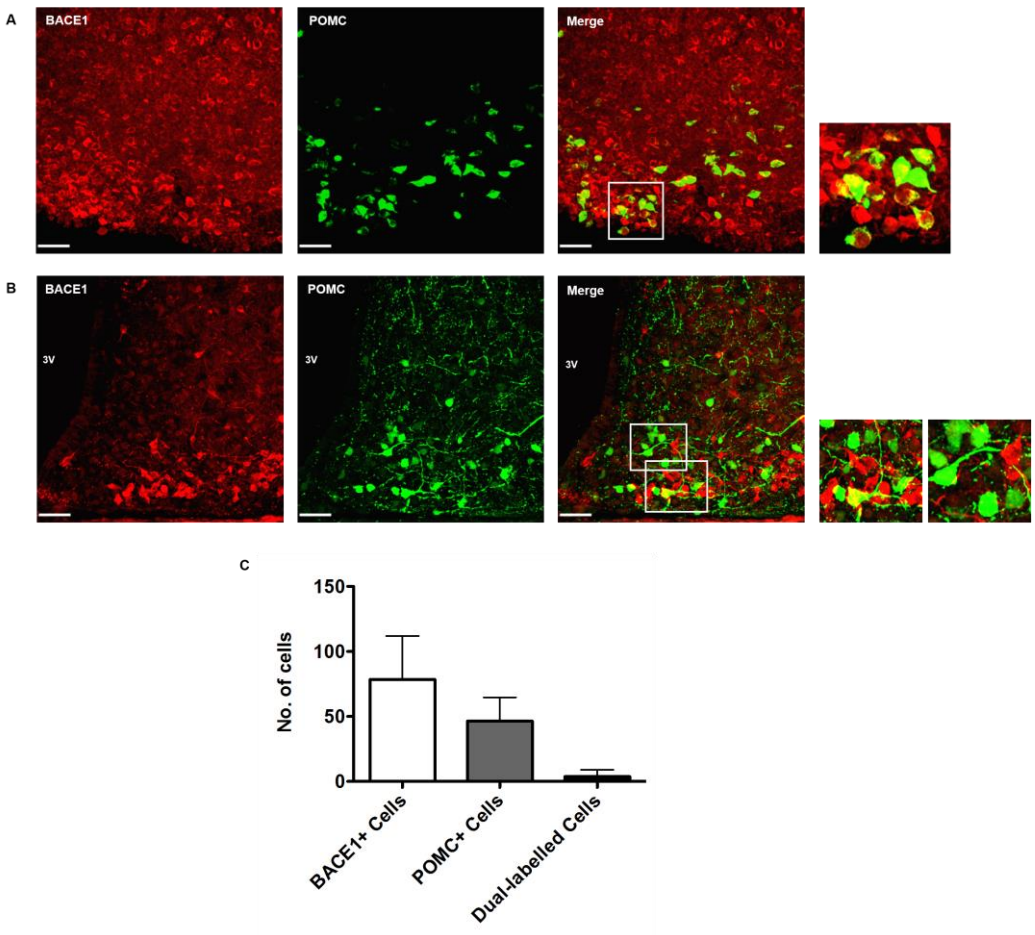

Figure 5.10 BACE1 is co-localised with POMC-expressing neurons in the arcuate nucleus.

Representative confocal images, taken at x40 magnification, showing BACE1 (red), POMC (green) and merged channels in the arcuate nucleus. (A) Fluorescent *in-situ* hybridisation (FISH) images showing BACE1 co-stained with POMC, demonstrating co-localisation between a small proportion of BACE1 and POMC neurons, highlighted with higher magnification boxed region.(B) POMC-GFP immunofluorescence (IF) images showing BACE1 co-stained with POMC demonstrating co-localisation between a small proportion of BACE1 and POMC neurons, highlighted with higher magnification boxed regions. 3V, third ventricle. All scale bars 50µm. (C) Histogram displaying total (FISH and IF) number of BACE1+ cells, POMC+ cells and dual-labelled cells per field of view, showing minimal co-localisation between BACE1 and POMC-positive (FISH: 5 fields of view, n=3, POMC-GFP: 11 fields of view, n=2).

5.3.6.2 BACE1 is expressed in neuropeptide-Y/agouti related peptide neurons in the arcuate nucleus

Next, the presence of BACE1 in the ARC orexigenic neuropeptide population was investigated. As with POMC, NPY was visualised using both FISH and IF on NPY-GFP tissue. Sections were double stained with BACE1 (red) to determine if BACE1 is co-localised with NPY-expressing neurons (green). Using both FISH-IF and NPY-GFP-IF, confocal images show a number of BACE-positive neurons are co-localised with NPY-expressing neurons in the ARC, observed as yellow (Figure 5.11A and B) and highlighted in higher magnification boxed regions. A large number of BACE1 neurons are not co-localised with NPY, however representative images show many BACE1 neurons, alike POMC-expressing neurons, are in close apposition to NPY neurons, highlighted by higher magnification boxed regions in NPY-GFP images (Figure 5.11B). Quantitative analysis of BACE1- and NPY-positive neurons, collectively for FISH-IF (counted across 6 images) and NPY-GFP-IF (counted across 8 images), shows approximately12% of BACE1 neurons are co-localised with NPY-expressing neurons and approximately 14% of NPY-expressing neurons co-localised with BACE1-positive neurons (Figure 5.11C). Due to a lack of tissue and FISH probe the orexigenic neuropeptide AgRP could not be examined, however all NPY-expressing neurons in the ARC co-express AgRP (Broberger et al. 1998), therefore it is likely that BACE1 is present in approximately 12% of AgRP-expressing neurons. Taken together, these data show BACE1 is expressed in a greater number of orexigenic neurons than anorexigenic neurons, and BACE1 may elicit some of its effects via this population. However a large number of BACE1-positive neurons are still distinct from NPY/AgRP-expressing neurons and, as observed with POMC neurons, these neuronal cell bodies and processes lie in close apposition to the NPY-expressing neurons and therefore BACE1-positive neurons may still act via NPY/AgRP neurons indirectly to affect energy homeostasis.

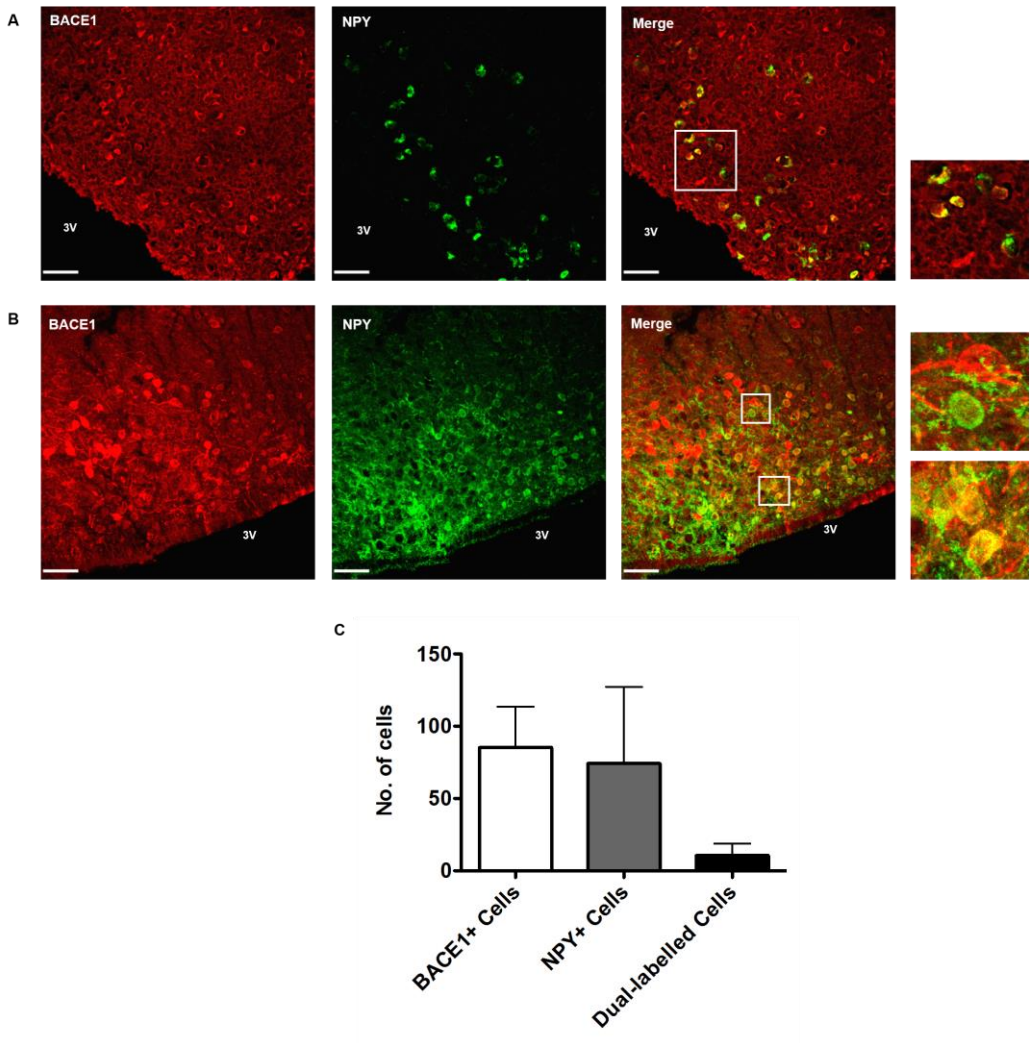

Figure 5.11 BACE1 is co-localised with NPY-expressing neurons in the arcuate nucleus.

Representative confocal images, taken at x40 magnification, showing BACE1 (red), NPY (green) and merged channels in the arcuate nucleus. (A) Fluorescent *in-situ* hybridisation (FISH) images showing BACE1 co-stained with NPY, demonstrating co-localisation between a small proportion of BACE1 and NPY neurons, highlighted with higher magnification boxed region. (B) NPY-GFP immunofluorescence (IF) images showing BACE1 co-stained with NPY demonstrating co-localisation between a small proportion of BACE1 and NPY neurons, highlighted with higher magnification boxed regions. 3V, third ventricle. All scale bars 50µm. (C) Histogram displaying total (FISH and IF) number of BACE1+ cells, NPY+ cells and dual-labelled cells per field of view, showing a small proportion of BACE1 neurons are co-localised with NPY neurons (FISH: 6 fields of view, n=3, NPY-GFP: 8 fields of view, n=3).

5.3.6.3 BACE1 is expressed in RIPCre neurons in the arcuate nucleus

Having shown BACE1 is present in a small number of POMC-, and NPY/AgRP-expressing neurons, a large proportion of ARC BACE1 neurons remain unidentified, which highlights the presence of non-POMC and non-NPY/AgRP first order neurons in the ARC. One identified population are RIPCre neurons, a small population which have Cre expression driven by the rat insulin-2 promoter (Song et al. 2010). These neurons have been implicated in the regulation of whole body energy homeostasis, are directly responsive to leptin and have shown to be in very close apposition (but distinct) to POMC- and NPY/AgRP-expressing neurons (Choudhury et al. 2005). Consequently, the presence of BACE1 in RIPCre neurons was examined. This was determined using IF, with double staining of BACE1 (red) and GFP (green), on sections from RIPCre-GFP mice. Confocal images show a large proportion of BACE1-positive neurons are co-localised with RIPCre neurons in the ARC, observed as yellow (Figure 5.12A) and highlighted in the higher magnification boxed region. Quantitative analysis (counted across 16 images) revealed the observed co-localisation is equal to approximately 58% of BACE1 neurons co-localised with RIPCre neurons, and furthermore 57% of detected RIPCre neurons co-localise with BACE1 Figure 5.12B). These data show that a large proportion of BACE1 neurons, indeed the majority detected in the ARC, are RIPCre neurons and therefore changes in hypothalamic BACE1 activity, resulting in altered energy homeostasis, may be mediated primarily via this neuronal population.

Owing to the majority of BACE1 neurons co-localising with RIPCre in the ARC, other hypothalamic nuclei known to express RIPCre neurons were examined. As described above, sections were double-stained for BACE1 (red) and GFP (green) on sections from RIPCre-GFP mice. Confocal images show a proportion of BACE1 neurons are also co-localised with RIPcre neurons in the DMH and VMH (Figure 5.13), however quantitative analysis was not performed.

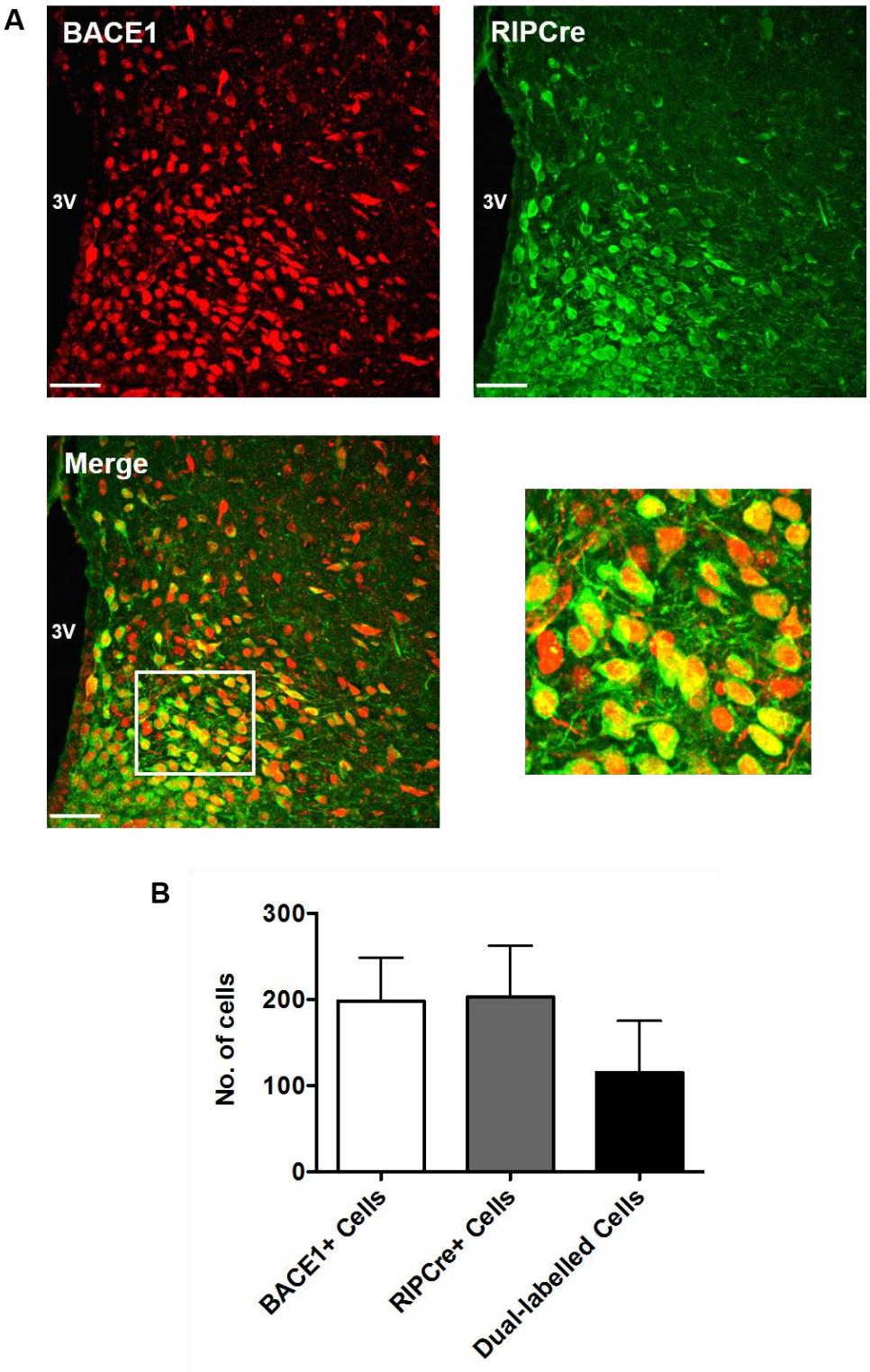

Figure 5.12 BACE1 is co-localised with RIPCre neurons in the arcuate nucleus.

(A) Representative confocal images, taken at x40 magnification, showing BACE1 (red), RIPCre (green) and merged channels in the arcuate nucleus. 3V, third ventricle. All scale bars 50µm. (B) Histogram displaying total number of BACE1+ cells, RIPCre+ cells and dual-labelled cells per field of view, showing a large number of BACE1 neurons are RIPCre neurons (16 fields of view, n=4).

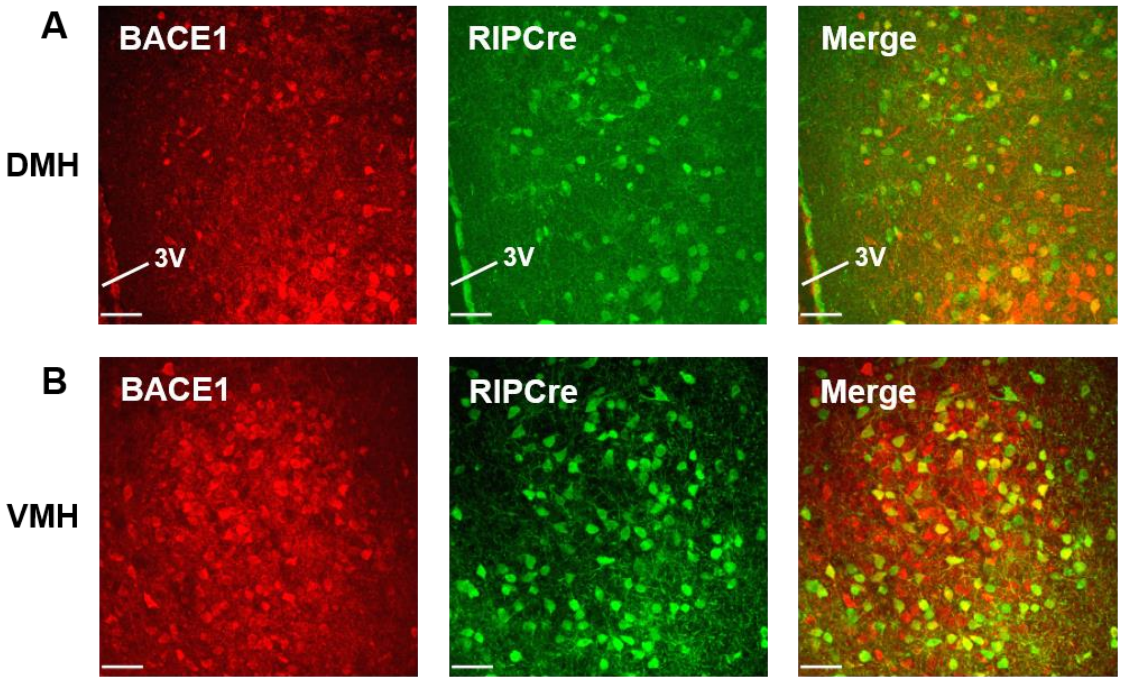

Figure 5.13 BACE1 is co-localised with RIPCre neurons in the ventromedial and dorsomedial hypothalamus.

Confocal images, taken at x40 magnification, showing BACE1 (red), RIPCre (green) and merged channels within regions of the hypothalamus outwith the arcuate nucleus. Representative images from (A) the dorsomedial hypothalamus (DMH) and (B) the ventromedial hypothalamus (VMH). 3V, third ventricle. All scale bars 50µm.

5.3.7 BACE1 neurons in the arcuate nucleus are a heterogeneous population of GABAergic and glutamatergic neurons

Having observed BACE1 is present in distinct neuronal populations in the ARC the precise phenotype of these neurons, i.e whether they are excitatory or inhibitory, was investigated. In the hypothalamus there is a mixed population of excitatory and inhibitory neurons, with these neurons releasing different neurotransmitters as well as responding to them. This is the case within the hypothalamus as a whole, but also within sub-populations of neurons. For example NPY/AgRP and POMC/CART neurons in the ARC receive both excitatory and inhibitory synaptic inputs (Delgado 2013). As demonstrated, BACE1 is present in a large proportion of RIPCre neurons and the main neurotransmitter utilised by these neurons is thought to be GABA. This is an important issue as RIPCre neurons in various hypothalamic centres will have distinct roles. The main inhibitory neurotransmitter in the hypothalamus, and the CNS overall, is GABA with the main excitatory neurotransmitter being glutamate (Delgado 2013). Therefore it was examined whether BACE1 positive neurons in the ARC were predominantly GABAergic or glutamatergic using IF on GAD67-GFP tissue and VGlut2-GFP tissue, double-staining sections for BACE1 (red) and GFP (green) to determine the phenotype in the ARC. GAD67 is an isoform of glutamate decarboxylase, an enzyme responsible for the synthesis of GABA (Buddhala et al. 2009) and therefore indicates GABAergic neurons. Using IF, confocal images show numerous BACE1-positive neurons are co-localised with GAD67 neurons in the ARC, observed as yellow and highlighted in higher magnification boxed regions (Figure 5.14A), indicating many BACE1 neurons are GABAergic in this area. However, a significant proportion of BACE1 neurons are not co-localised with GAD67 (Figure 5.14A). Quantitative analysis (counted across 19 images) shows 34% of BACE1 neurons are GAD67-positive and furthermore 36% of GAD67-positive neurons are co-localised with BACE1 (Figure 5.14B). VGlut2 is a vesicular glutamate transporter responsible for packaging glutamate into synaptic vesicles for release and is the dominant glutamate transporter present in the hypothalamus, indicative of glutamatergic, excitatory neurons in this area (Delgado 2013; Meister 2007). Representative confocal images show a proportion of BACE1-positive neurons are co-localised with VGlut2 neurons in the ARC, observed as yellow and highlighted in higher magnification boxed regions (Figure 5.15

A), demonstrating BACE1 neurons are also glutamatergic in this area. A proportion are not co-localised with VGlut2 (Figure 5.15A), supporting the finding of GABAergic-BACE1 neurons in the ARC. Quantitative analysis (counted across 17 images) shows 30% of BACE1 neurons are co-localised with VGlut2 and furthermore 29% of VGlut2-positive neurons are co-localised with BACE1 (Figure 5.15B). Taken together, these data show that BACE1 neurons are a heterogeneous population of GABAergic neurons and glutamatergic neurons within the ARC, and these will contribute different roles in the hypothalamic neuronal circuitry involved in maintaining energy homeostasis.

5.3.8 Extra-arcuate nucleus BACE1 expression

5.3.8.1 BACE1 is expressed in steroidogenic factor-1 neurons in the ventromedial hypothalamus

Although the ARC is a key site of leptin action, other hypothalamic regions are of importance in the regulation of energy homeostasis. Leptin receptors are present in areas such as the VMH, which is also involved in regulating leptin actions on body weight and food intake. Having found BACE1 is also expressed in neurons throughout this region, the phenotype of these neurons was investigated to determine whether BACE1 activity may influence leptin action via the VMH, as well as the ARC. The main neuronal population in the VMH are steroidogenic factor-1 neurons, which leptin directly acts upon to contributing to its body weight actions (Dhillon et al. 2006). Hence the presence of BACE1 in SF-1 neurons was examined. This was determined using IF, with double staining of BACE1 (red) and GFP (green), on sections from SF-1-GFP mice. Confocal images show BACE1-positive neurons are co-localised with SF-1 neurons in the VMH, observed as yellow (Figure 5.16A) and highlighted in the higher magnification boxed region. However, not all BACE1-positive neurons in the VMH are SF-1 neurons, confirmed by quantitative analysis (counted across 14 images) which shows 31% of BACE1 neurons are co-localised with SF-1 neurons, and 32% of detected SF-1 neurons are co-localised with BACE1 (Figure 5.16B). These data show a substantial proportion of BACE1 neurons are SF-1 neurons in the VMH and therefore BACE1 may act via this neuronal population to modify leptin action on body weight. However, there are a large proportion of unidentified VMH BACE1-positive neurons that may also be implicated in regulating energy homeostasis.

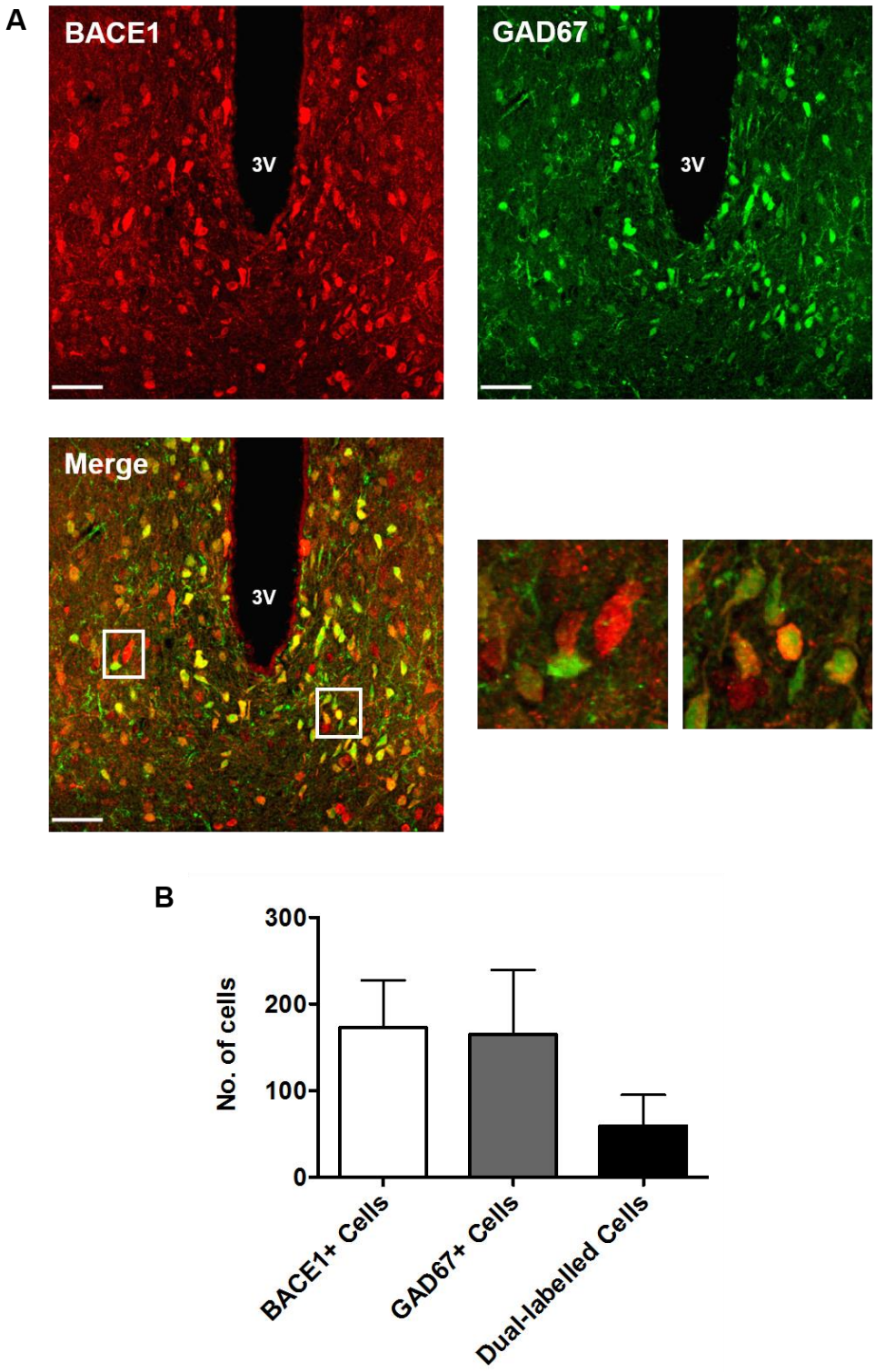

Figure 5.14 BACE1 neurons are GABAergic in the arcuate nucleus.

(A) Representative confocal images, taken at x40 magnification, showing BACE1 (red), GAD67 representing GABA neurons (green) and merged channels in the arcuate nucleus. 3V, third ventricle. All scale bars 50µm. (B) Histogram displaying total number of BACE1+ cells, GAD67+ cells and dual-labelled cells per field of view, showing a proportion of BACE1 neurons are GABAergic neurons (19 fields of view, n=3).
Data collection was carried out in collaboration with Karolina Parmionova (Masters Student).

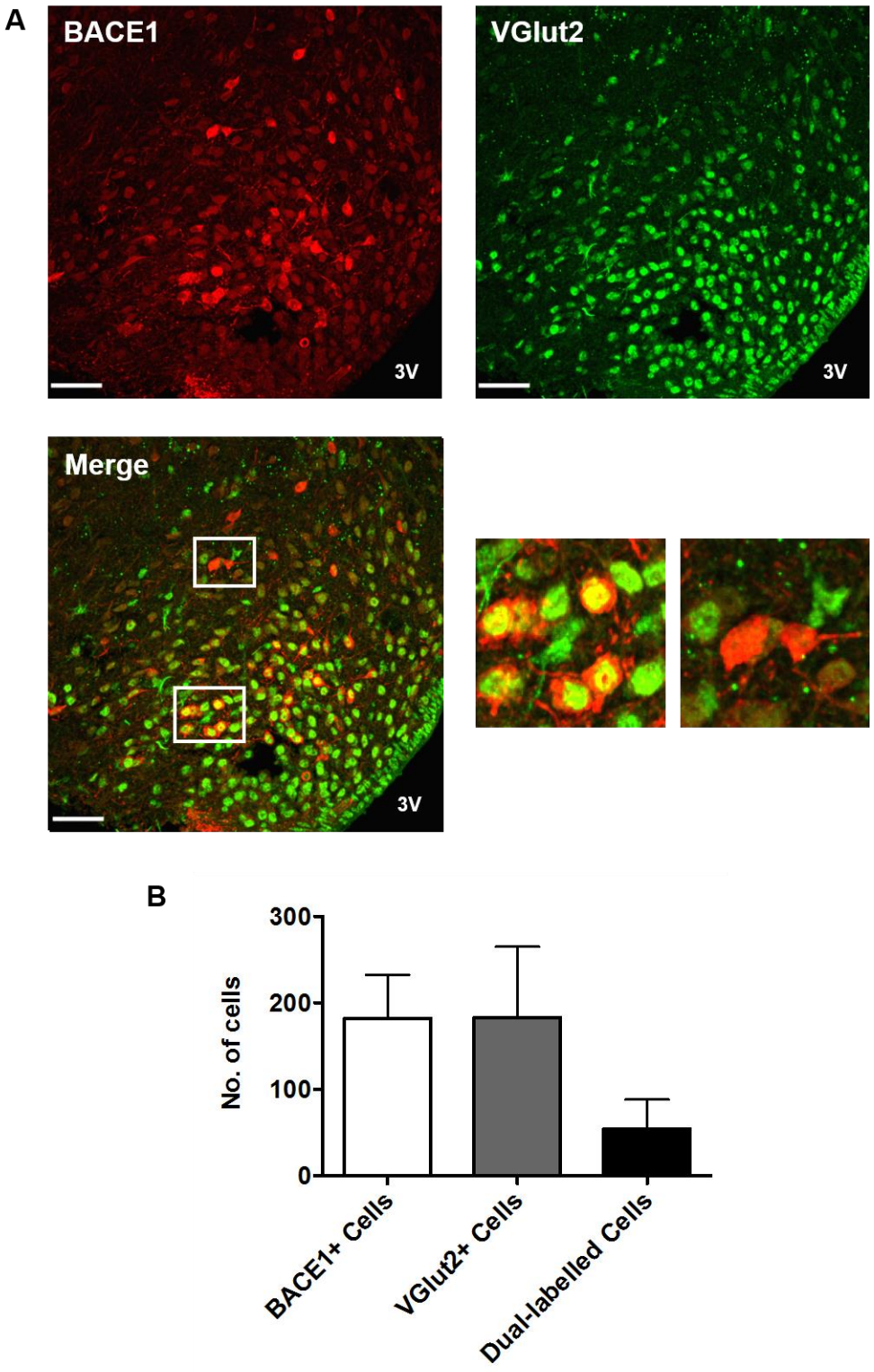

Figure 5.15 BACE1 neurons are glutamatergic in the arcuate nucleus.

(A) Representative confocal images, taken at x40 magnification, showing BACE1 (red), VGlut2 representing glutamatergic neurons (green) and merged channels in the arcuate nucleus. 3V, third ventricle. All scale bars 50µm. (B) Histogram displaying total number of BACE1+ cells, VGlut2+ cells and dual-labelled cells per field of view, showing a proportion of BACE1 neurons are glutamatergic neurons (17 fields of view, n=3).

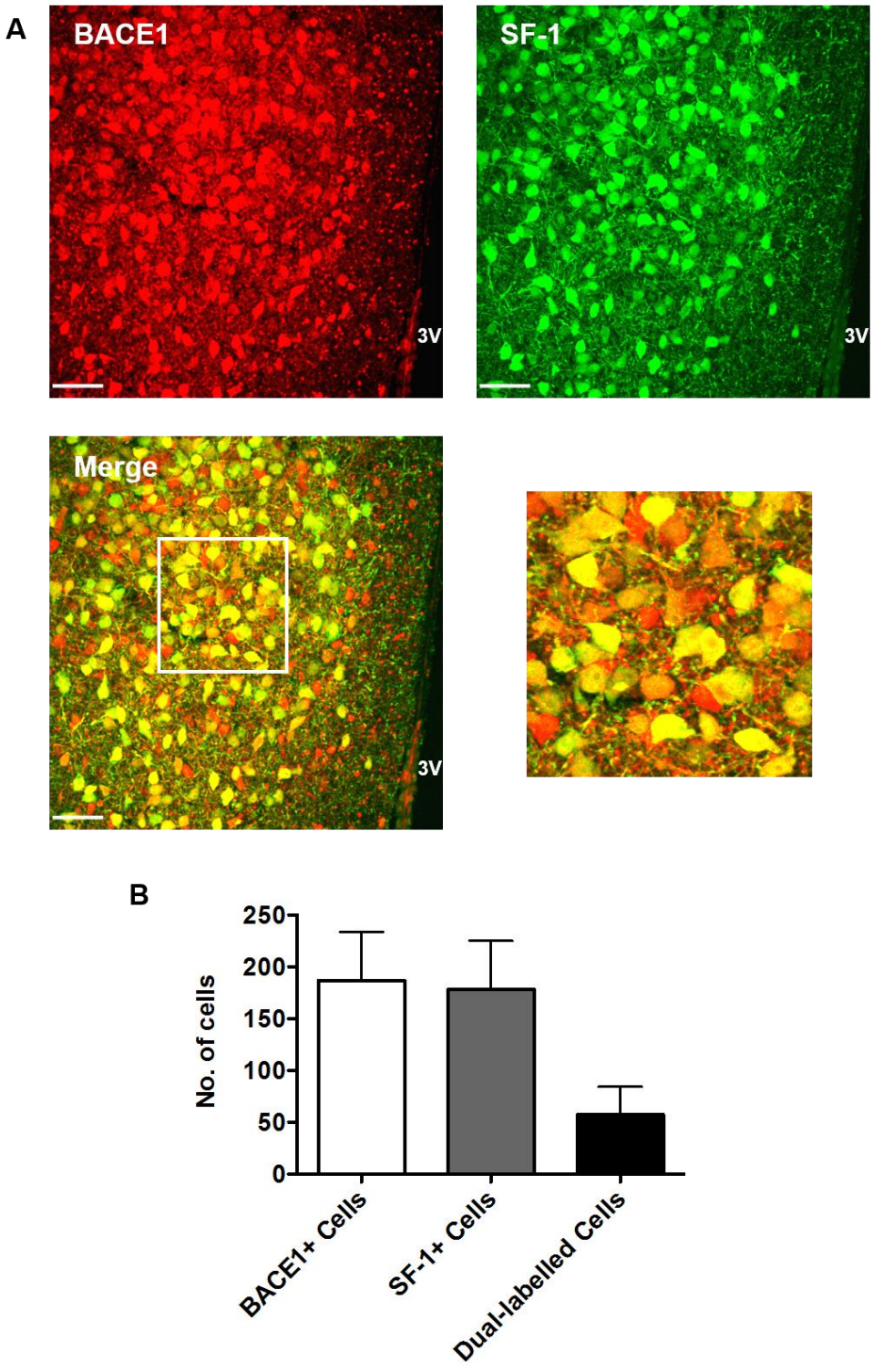

Figure 5.16 BACE1 is co-localised with SF-1 neurons in the ventromedial hypothalamus.

(A) Representative confocal images, taken at x40 magnification, showing BACE1 (red), SF-1 (green) and merged channels in the ventromedial hypothalamus. 3V, third ventricle. All scale bars 50µm. (B) Histogram displaying total number of BACE1+ cells, SF-1+ cells and dual-labelled cells per field of view, showing a proportion of BACE1 neurons are SF-1 neurons (14 fields of view, n=3).

5.3.8.2 BACE1 expression in the paraventricular nucleus

Having observed BACE1 expression in first order ARC neurons involved in energy metabolism, next it was investigated whether BACE1 is expressed in other hypothalamic areas involved in the hypothalamic circuitry. The PVN is a distinct hypothalamic region where many neurons project to and pathways converge. For example, NPY and POMC neurons from the ARC and orexin neurons from the LH both project directly to the PVN (Arora & Anubhuti 2006). Using IF, sections were double-stained for BACE1 and NeuN, to determine if BACE1 is present in neurons in the PVN. Representative confocal images show that BACE1 is expressed abundantly in this area, and is predominantly neuronal, demonstrated by the majority of BACE1 positive cells co-localising with NeuN, observed as yellow (Figure 5.17). These data show BACE1 is expressed in the PVN, and suggest that BACE1 may be involved in the neuronal circuits associated with PVN neurons that control energy balance.

5.3.9 BACE1 expression in the hindbrain

The hypothalamus connects to centres within the hindbrain such as the NTS, which has dense input from the hypothalamus as well as peripheral signals carried from the vagus nerve. NTS neurons project back to areas of the hypothalamus, such as the PVN forming neural circuitry which regulates feeding behaviour and energy expenditure (Schwartz et al. 2000). Having observed BACE1 neuronal expression within the ARC and PVN the presence of BACE1 neurons in the NTS was examined to investigate if BACE1 is involved in the CNS circuits controlling energy balance. In particular the NTS has a dense population of NPY neurons (Arora & Anubhuti 2006), therefore it was investigated if BACE1 was present in these neurons using IF on NPY-GFP tissue. Representative confocal images show BACE1 (red) is present in abundance in the NTS, and a proportion of neurons are co-localised with NPY neurons (green), observed as yellow and highlighted in the higher magnification boxed region (Figure 5.18A), demonstrating BACE1 neurons are also NPY-positive in the NTS. A large proportion are not co-localised with NPY, with quantitative analysis (counted across 6 images) showing only 11% of BACE1 neurons are co-localised with NPY, however a large proportion of NPY neurons (52%) are co-localised with BACE1 (Figure 5.18B). Taken together, these data show BACE1 is present in an area of the brainstem involved in receiving and projecting information involved in energy regulation, and a proportion of these neurons are NPY neurons. Therefore BACE1 may act via this neuronal population within the NTS and the neural circuits involved in regulating energy expenditure and food intake.

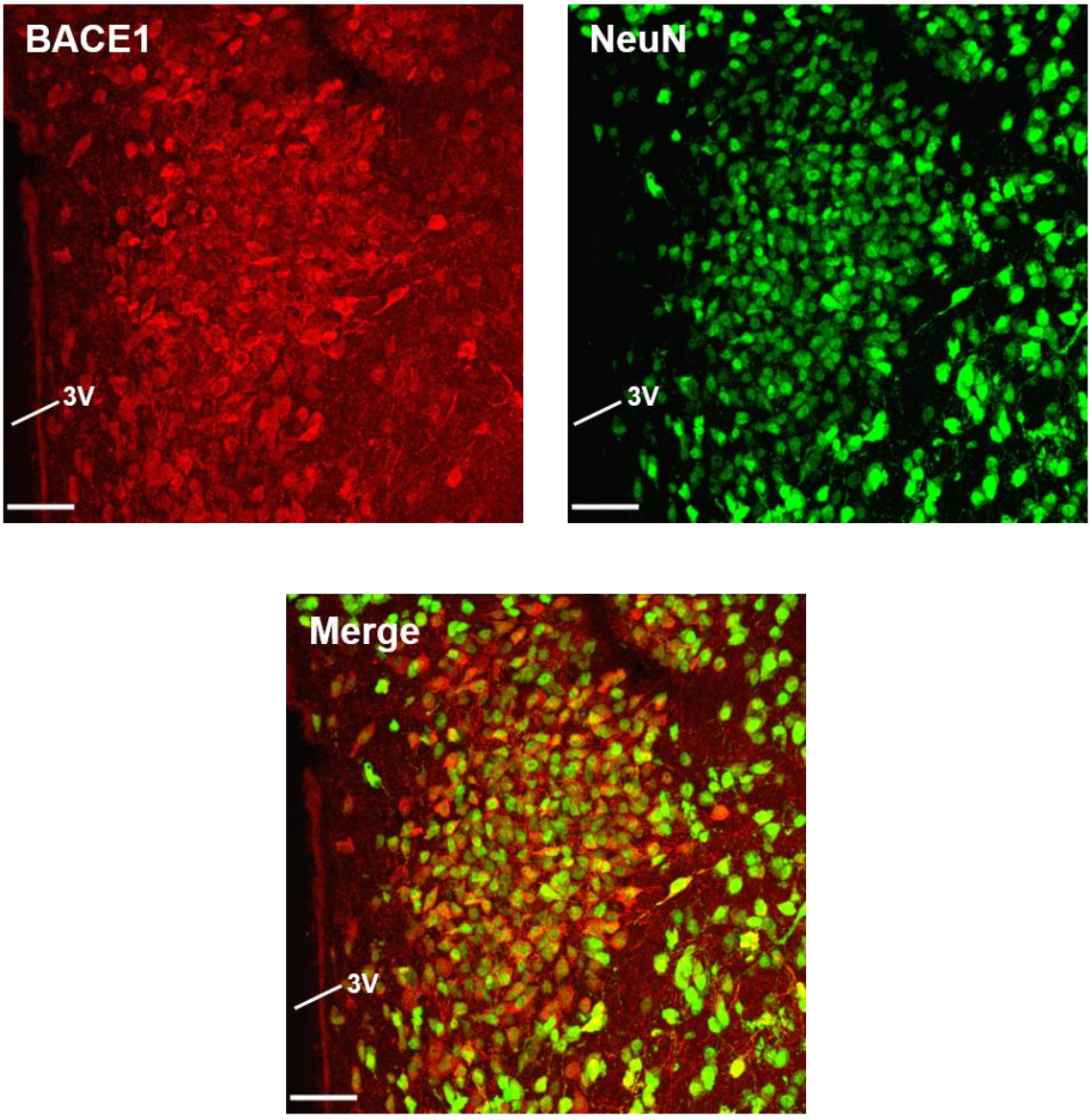

Figure 5.17 BACE1 is expressed in neurons in the paraventricular nucleus.

Representative confocal images, taken at x40 magnification, showing BACE1 (red), neuronal marker NeuN (green) and merged channels in the paraventricular nucleus. 3V, third ventricle. All scale bars 50µm.

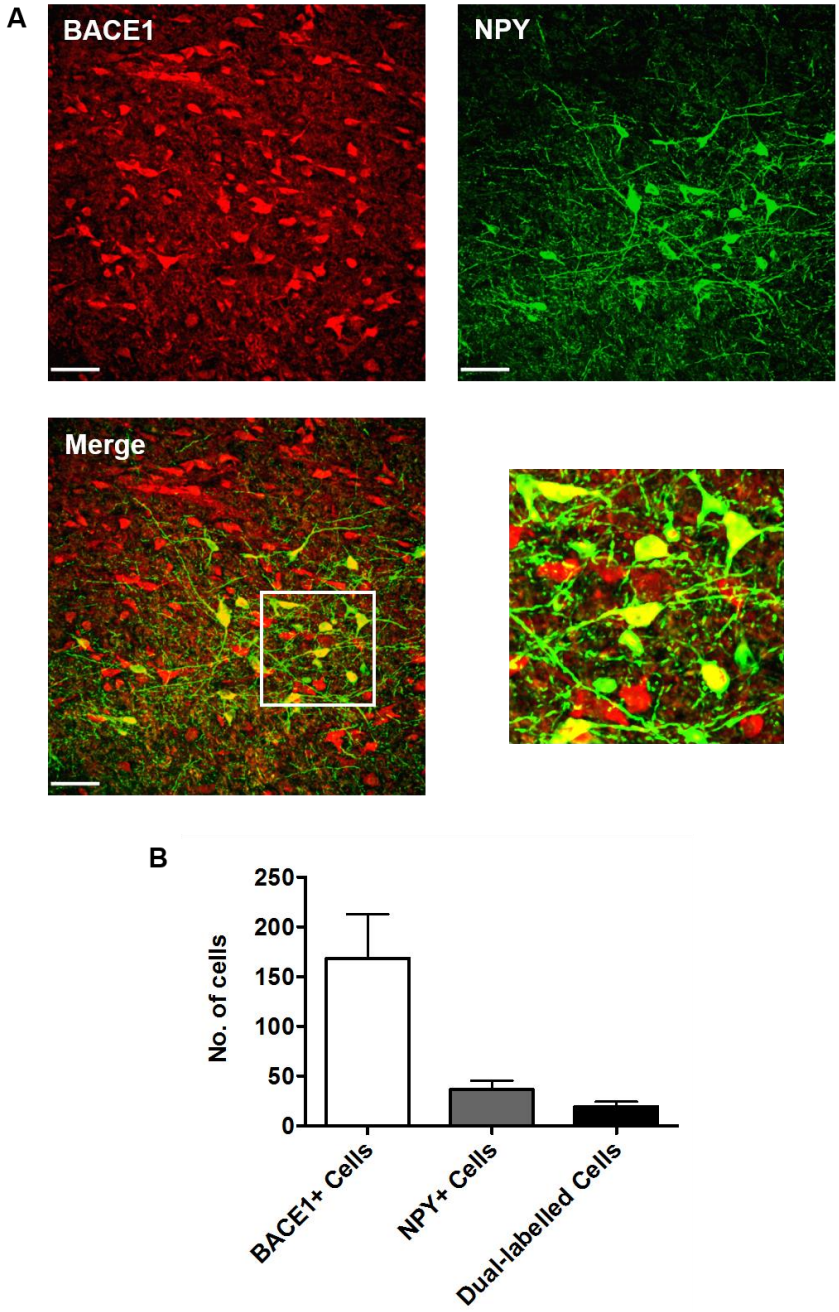

Figure 5.18 BACE1 is co-localised with NPY neurons in the nucleus tractus solitarius.

(A) Representative confocal images, taken at x40 magnification, showing BACE1 (red), NPY (green) and merged channels in the nucleus tractus solitarius (NTS). All scale bars 50µm. (B) Histogram displaying total number of BACE1+ cells, NPY+ cells and dual-labelled cells per field of view, showing a small proportion of BACE1 neurons are NPY neurons however a large proportion of NPY neurons are BACE1 positive (6 fields of view, n=3).

5.4 Discussion

5.4.1 Summary

Within this chapter we set out to investigate the expression of BACE1, particularly in the hypothalamus, and identify the cell populations it is expressed in to determine any implication in the neuronal circuitry controlling energy balance. Herein, we have found BACE1 is expressed throughout regions of the hypothalamus and the brainstem (the NTS); all areas involved in the neuronal pathways controlling whole body energy homeostasis. Specifically in the ARC, we demonstrated BACE1 is predominantly neuronal and a proportion of these neurons express the leptin receptor. In addition, we demonstrated BACE1 is expressed in a small population of first-order NPY neurons and a large population of RIPCre neurons, of which these neurons are a mixed population of both GABAergic and glutamatergic neurons. This large population of RIPCre-BACE1 neurons may be responsible for the role of BACE1 in metabolism. Furthermore, we found BACE1 is also expressed in RIPCre neurons in extra-ARC areas, such as the VMH, where BACE1 was also found to be present in SF-1 neurons. These results, and the potential implications, will be further discussed in the following sections.

5.4.2 BACE1 in the hypothalamus

Herein we have presented novel findings regarding BACE1 expression in the hypothalamus. The results show by using both Western blotting and IF that BACE1 is expressed throughout the hypothalamus, present in all nuclei shown to play a role in regulating energy balance. Interestingly, this expression was not uniform across the hypothalamus and BACE1 is present in distinct groups of cells throughout. This localised expression is suggestive of a functional output. In keeping with the literature describing BACE1 to be largely present in neurons and not glia (Zhao et al. 2007; Hussain et al. 1999; Vassar et al. 1999), we found throughout all hypothalamic nuclei BACE1 is predominantly expressed in neurons. This was anticipated prior to co-staining experiments as morphologically the BACE1-positive cells do not resemble astrocytes and tend to bear resemblance to neuronal cell bodies. An overall observation from these data is the localisation of BACE1 staining within neurons; it can be observed on processes and within the cell body, however in some instances there is strong staining in the nuclei.

In regards to a lack of BACE1 expression observed in glia, it is noteworthy that these data were generated from healthy, WT mice fed a NC diet *ad libitum*. In some instances

BACE1 has been shown to be present in astrocytes following stress conditions. Blasko *et al* found that following modelling of traumatic brain injury in rodents, elevated levels of BACE1 were present in astrocytes, shown by co-localisation of BACE1 and the astrocyte marker GFAP, in the hippocampus and cortex (Blasko et al. 2004). This stress-related switch in BACE1-cell type could also occur in the hypothalamus. For example, BACE1 is mainly neuronal under normal conditions, whereas under stress conditions such as HFD, there may be an upregulation within astrocytes. BACE1 has already shown to be increased in the hypothalamus following HFD (unpublished data), thus it would be of interest to examine if BACE1 expression changes at a cellular level in the hypothalamus in response to high-fat feeding. This could be achieved in the future using IF, co-staining for BACE1 and the cell specific markers described, on WT mice fed a HFD for a period of 20 weeks to induce obesity associated with central leptin resistance.

Interestingly, under normal conditions not all hypothalamic BACE1 is neuronal as we found a small proportion of BACE1-positive neurons that are not co-localised with the neuronal marker NeuN, thus an unidentified population of cells which express BACE1 exists. It can be assumed that we are not missing co-localisation with neurons as NeuN has been shown to specifically mark almost all neuronal nuclei in the brain, with the exception of a few populations outwith the hypothalamus (Mullen et al. 1992). Therefore, the BACE1-positive cells detected must be a separate cell type, such as oligodendrocytes, microglia and/or tanycytes and ependymal cells. It is possible BACE1 would be present in these cell as oligodendrocytes are involved in the formation of myelin and BACE1 may be required in this process as *BACE1*$^{-/-}$ mice have reportedly thinner myelin sheath (Hu et al. 2006). Similarly, we have shown BACE1 may play a role in inflammatory programming, with BACE1 inhibition reducing central HFD-associated inflammation (section 3.2.11). Consequently, BACE1 may be present in microglia, including resident microglia, perivascular macrophages and blood-borne immune cells. In addition, tanycytes and ependymal cells line the third ventricle and we observe this staining pattern with our BACE1-positive staining. Moreover, tanycyte processes extend to hypothalamic nuclei controlling food intake and energy expenditure and may play a role in the control of energy balance (Bolborea & Dale 2013), thus BACE1 may also be present in this cellular population To clarify this further experiments are required, utilising IF and co-staining for BACE1 and markers of oligodendrocytes, microglia and tancytyes, both under normal conditions and following HFD to observe if BACE1 is upregulated in non-neuronal cell types under stress conditions.

5.4.3 Leptin responsiveness of BACE1 neurons

Having observed that pharmacological reduction of BACE1 appears to alter leptin sensitivity (chapter 3) and *BACE1*$^{-/-}$ mice are more leptin sensitive than WT littermates (unpublished data), we hypothesised that BACE1 directly affects leptin-responsive neurons in the hypothalamus and alters leptin signalling. Utilising IF and confocal microscopy it was found that approximately 30% of BACE1-positive neurons express ObRb, suggestive that only a proportion are responsive to leptin. Notably, there are other receptors present in the ARC which also play an important role in energy expenditure, food intake and inflammatory processing and it may be that BACE1 still alters energy metabolism via alternative receptors. Examples include serotonin and its receptors 5-HT_{2c}R and 5-HT_{1B}R which are present in the ARC and play a role in regulating energy balance (Sohn et al. 2013). Studies on 5-HT_{2c}R and 5-HT_{1B}R deficient mice support this as both mouse models display hyperphagia, obesity and impaired glucose tolerance (Tecott et al. 1995; Bouwknecht et al. 2001). Interestingly, serotonin acts like leptin in the ARC as 5-HT_{2c}R activates POMC neurons whilst and 5-HT_{1B}R inhibits NPY/AgRP neurons (Sohn et al. 2013). Additionally, 5-HT_{2c}R activates POMC neurons which are completely distinct from those activated by leptin (Sohn et al. 2011). These data demonstrate there are neuronal populations key in regulating food intake and body weight which do not possess the leptin receptor, and it may be that BACE1-positive neurons in the ARC express 5-HT_{2c}R. Similarly, insulin receptors are present in the ARC, and as previously discussed a proportion of these are co-expressed with POMC neurons (Benoit et al. 2002). As insulin and leptin signalling converge, and BACE1 also affects insulin; with *BACE1*$^{-/-}$ mice displaying reduced circulating insulin levels and improved insulin sensitivity (Meakin et al. 2012), BACE1 may also be co-expressed in neurons with the insulin receptor. Many other receptor subtypes also exist in the ARC, such as the OX_1R isoform of the orexin receptor which is thought to play a role in satiety signalling, as well as the ghrelin receptor which is also expressed in the ARC (Arora & Anubhuti 2006). Thus, there are a number of receptors present in the ARC which BACE1-positive neurons may express, and further experiments using IF and co-staining for these receptors and BACE1 would be required to examine which/ if any of these receptors may be expressed by BACE1 ARC neurons. Further examination of these neurons could also be conducted utilising electrophysiological measurements to determine the functional and electrical properties of these neurons.

It is assumed that neurons within the ARC expressing ObRb are first order neurons that directly respond to leptin and project to second order neurons in other hypothalamic regions. However, we show that following leptin treatment BACE1-positive neurons do not co-localise with pSTAT3, indicative of a lack of leptin responsiveness, disputing our hypothesis. One potential reason for this is the observed reduction in BACE1 expression in the ARC following leptin treatment, which is a finding reported previously in the literature in other brain areas highly expressing BACE1 (Marwarha et al. 2010; Marwarha et al. 2014). The precise mechanism whereby leptin causes this presumable degradation of BACE1 is unknown, although this is likely to be a physiological process as it occurs rapidly with the effects observed in our studies one hour post-leptin treatment. In these studies we used a 4mg/kg dose of leptin which others have reportedly used for leptin-induced pSTAT3 stimulations (Vong et al. 2011), although this could be deemed a high dose as many groups observe a pSTAT3 leptin response with lower doses, such as 2mg/kg (Enriori et al. 2007; Zabolotny et al. 2002). The reduction in BACE1 expression following leptin treatment could therefore be an acute effect due to a high dose of leptin and it would be of interest to conduct the same experiments at a lower, sub-maximal dose (for example 1-2mg/kg) to attempt to overcome this effect. In addition, it would be intriguing to conduct these experiments on high-fat fed mice, as the associated leptin resistance may cause the BACE1 in the ObRb-positive neurons to no longer become degraded. As previously mentioned *BACE1*$^{-/-}$ mice have improved leptin sensitivity and they also show elevated basal pSTAT3 levels (unpublished data), however we find no significant difference in the number of pSTAT3-positive cells following leptin treatment in *BACE1*$^{-/-}$ mice compared to WT littermates. Again, this could be due to the dose administered and we are possibly observing maximal activation in which case no large difference would be observed. Noteworthy, is that this was examined in mice fed a NC diet and the changes may be mild, therefore the effect may be masked due to the high dose of leptin. Of benefit would be to conduct the same experiments in mice challenged with a HFD, as this may elicit a greater effect. The high levels of BACE1 as a result of high-fat feeding may result in reduced pSTAT3 signalling, an effect avoided in *BACE1*$^{-/-}$ mice.

Alternatively, Marwarha and colleagues demonstrated that in SH-SY5Y cells the attenuation of BACE1 expression caused by leptin is due to increased sirtuin 1 (SIRT1) expression (Marwarha et al. 2014). SIRT1 is a deactylase enzyme which regulates metabolism through involvement in many processes including stress responses, oxidative metabolism and cell apoptosis and differentiation (Haigis & Sinclair 2010). Marwarha *et*

al suggested the leptin-induced reduction of BACE1 occurs due to SIRT1 inhibiting NF-κB signalling, which is also implicated in the regulation of BACE1, presenting the notion of a leptin-SIRT1-NF-κB pathway controlling BACE1 regulation (Marwarha et al. 2014). This also associates SIRT1 with BACE1 and its role in energy metabolism, which is possible as SIRT1 is involved in calorie restriction and also plays a role in the neuronal response to stress (Duan 2013). Furthermore, in SH-SY5Y cells over-expression of BACE1 reduces SIRT1 protein levels (John Findlay PhD Thesis). Owing to this it would be interesting to examine if SIRT1 changes following inhibition of BACE1 and if SIRT1 is highly expressed in the hypothalamus and co-expressed in BACE1-positive neurons, to determine if this is responsible for mediating some of our findings.

Notably, leptin treatment did not completely diminish BACE1 expression which is in keeping with only a proportion of BACE1-positive neurons in the ARC expressing ObRb. In line with our original hypothesis that BACE1-ObRb-expressing neurons are leptin responsive, it may be that these neurons are those that the expression of BACE1 has been reduced therefore the pSTAT3 response is merely being missed. To counteract this issue we could utilise FISH to stain for BACE1 mRNA, assuming the protein is being degraded, and therefore in the presence of all BACE1-expressing neurons observe pSTAT3 co-localisation. However, Marwarha and colleagues did note a reduction in BACE mRNA expression, as well as protein, following leptin treatment (Marwarha et al. 2014), thus this technique may not be feasible. In addition, we did not examine BACE1 expression following leptin treatment in areas outwith the ARC, away from the dense site of ObRb expression. If BACE1 is only reduced in areas where ObRb is expressed this further supports our hypothesis that only BACE1 neurons that express the leptin receptor, and thus are directly responsive to leptin, are diminished following leptin treatment.

Importantly, the lack of co-localisation with pSTAT3 may not be conclusive of a lack of leptin responsiveness as not all leptin outputs are via pSTAT3. The PI3K pathway is also required for mediating the actions of leptin and BACE1 may conduct its role on energy metabolism through this signalling cascade. To investigate this further co-staining of BACE1 and downstream targets of PI3K; pPKB or PIP3, following leptin treatment could be performed in the future. It can be hypothesised that BACE1-positive neurons in the ARC are co-localised with PIP3 and/or pPKB and thus BACE1 is acting via this pathway to affect leptin outcomes. BACE1 may act through this pathway in particular affecting the downstream target FoxO1, which mediates the anorectic effects of leptin. FoxO1 is also important in mediating responses to oxidative stress (Nakae et al. 2008), and is

implicated in the progression of insulin resistance, potentially through activation of inflammatory signalling (Fan et al. 2010), therefore also potentially contributing to AD progression (Manolopoulos et al. 2010). Taken together, high levels of BACE1 may be associated with impaired hypothalamic (and possibly other brain areas) FoxO1 signalling, exacerbating metabolic syndrome, as well as AD, and this is an area worth further investigation.

5.4.4 BACE1 and first order arcuate neurons

Within this chapter we have shown BACE1 is present in less than 5% of POMC/CART neurons and approximately 10% of NPY/AgRP neurons in the ARC. This is somewhat unsurprising as we showed that BACE1 inhibition did not evoke large effects on food intake (section 3.2.1.1 and 3.2.7.1). Of interest is the slightly greater number of BACE1-positive neurons that are co-expressed with NPY/AgRP neurons, as this would suggest a potential role of BACE1 in fasting. In support of this, our data show *BACE1*$^{-/-}$ mice become hyperphagic following a period of fasting (unpublished data) and DIO mice treated with a BACE1 inhibitor display an increased ratio of orexigenic/anorexigenic neuropeptide mRNA expression (unpublished data, section 3.2.3 and 3.2.9), reversing the suppression which occurs following HFD. Future experiments will be required to examine the expression and co-localisation pattern of BACE1 with POMC/CART and NPY/AgRP neurons in the fasted state, as all data presented in this chapter are from mice fed a NC diet *ad libitum*, as well as during the course of re-feeding after an overnight fast. Following an overnight fast NPY/AgRP transcript expression is increased and POMC/CART expression is reduced, and this expression pattern becomes switched during re-feeding (Mizuno et al. 1998; Swart et al. 2002), thus BACE1 expression in these neurons may also change over the course of fasting and re-feeding.

Imaging studies described in this chapter to examine first order ARC neurons only looked at POMC and NPY expression specifically. As mentioned, within the ARC almost all POMC neurons co-express CART (Elmquist et al. 1999) and all NPY neurons co-express AgRP (Broberger et al. 1998), allowing the assumption that BACE1 is present in approximately 5% of CART neurons and 15% of AgRP neurons. However, this can only be assumed to be the case within the ARC, as for instance CART is expressed elsewhere in the hypothalamus such as the PVN and DMH, as well as also found in extra-hypothalamic sites. Although BACE1 did not co-localise largely with POMC/CART or NPY/AgRP neurons in the ARC, the staining pattern reveals that BACE1-positive

neurons are situated in very close apposition to these first order neurons. In particular, BACE1 and POMC cell bodies and processes can be observed lying very close to each other, suggestive that although BACE1 is not present in POMC neurons the two populations may communicate in some way. To examine this further the utilisation of additional techniques are required, such as electrophysiology. Our results indicate, by the appearance of the staining, that the contact between BACE1 and POMC, and NPY/AgRP neurons, may be through synaptic input as it appears that BACE1 may be present at the synapse. This raises an interesting point as synaptic plasticity within the hypothalamus is receiving more attention recently as a potential mechanism in the regulation of energy homeostasis (Horvath 2005; Dietrich & Horvath 2013). Unfortunately, confocal microscopes do not have the adequate resolution to accurately detect synapses, thus we cannot definitively conclude that BACE1 is indeed synaptic and this would require electron microscopy and primary neuronal cultures for more precision. However, if we assume due to the position of the BACE1 neurons in respect to POMC and NPY/AgRP neurons, that BACE1 is making synaptic contacts this would be in line with research demonstrating that synaptic innervation of these first order neurons is important for their response to leptin and thus body weight and food intake actions (Horvath 2005; Dietrich & Horvath 2013). Synaptic plasticity occurs in the hypothalamus and is thought to be involved in the regulation of energy balance indicated by Pinto and colleagues work which showed alterations in the ratio of inhibitory to excitatory synaptic inputs onto NPY/AgRP neurons, displaying an increased number of synapses and excitatory tone on NPY neurons, in *ob/ob* mice (Pinto et al. 2004). This work showed leptin has the ability to ‘re-wire’ synaptic inputs by normalising this ratio and increasing the number of synapses on POMC whilst reducing the number on NPY neurons (Pinto et al. 2004). Of interest is that the leptin-induced rearrangement in synaptic densities occurs prior to body weight or food intake effects providing further evidence for the role of synaptic plasticity in regulating whole body energy homeostasis. Our findings provide potential evidence for BACE1 to be involved in this process.

Within the ARC it has been shown that NPY directly inhibits POMC through synaptic innervation from NPY/AgRP neurons or through GABA input (Cowley et al. 2001). Although we find BACE1 is not highly expressed in POMC and NPY/AgRP neurons we do observe BACE1 is present in approximately 35% of GABA neurons, therefore BACE1 may be acting upon these neurons via GABA release. The ARC contains a heterogeneous population of both GABAergic and glutamatergic neurons (Vong et al. 2011), which

supports our findings of BACE1 also co-expressing with VGlut2 in approximately 30% of neurons in the ARC. GABAergic neurons are the major population in the ARC and all NPY/AgRP are considered to be GABAergic whereas few POMC are believed to be GABAergic (Vong et al. 2011). Although, this finding is not supported by other groups with studies showing approximately 50% of POMC neurons express the GABA synthesising enzyme, GAD67, in mice (Wittmann et al. 2013). Regardless, of interest is the finding that leptin acts to decrease inhibitory postsynaptic currents on POMC neurons through leptin receptor action on presynaptic GABAergic neurons and that these leptin-responsive neurons described are not NPY/AgRP neurons (Vong et al. 2011). This suggests there are GABAergic neurons independent of NPY/AgRP neurons in the ARC, which is supported by the phenotype of the BACE1-postive neurons we observe in our studies, and significantly it is these neurons that impact synaptic inputs onto POMC neurons. Furthermore, leptin induces anti-obesity effects largely by modulating first order GABA neurons causing inhibition of other local first order neurons such as POMC. Our findings indicate that BACE1 neurons in the ARC, although not present in the majority of POMC and NPY/AgRP neurons, may regulate energy homeostasis via synaptic contact onto neurons in the melanocortin system (Figure 5.19).

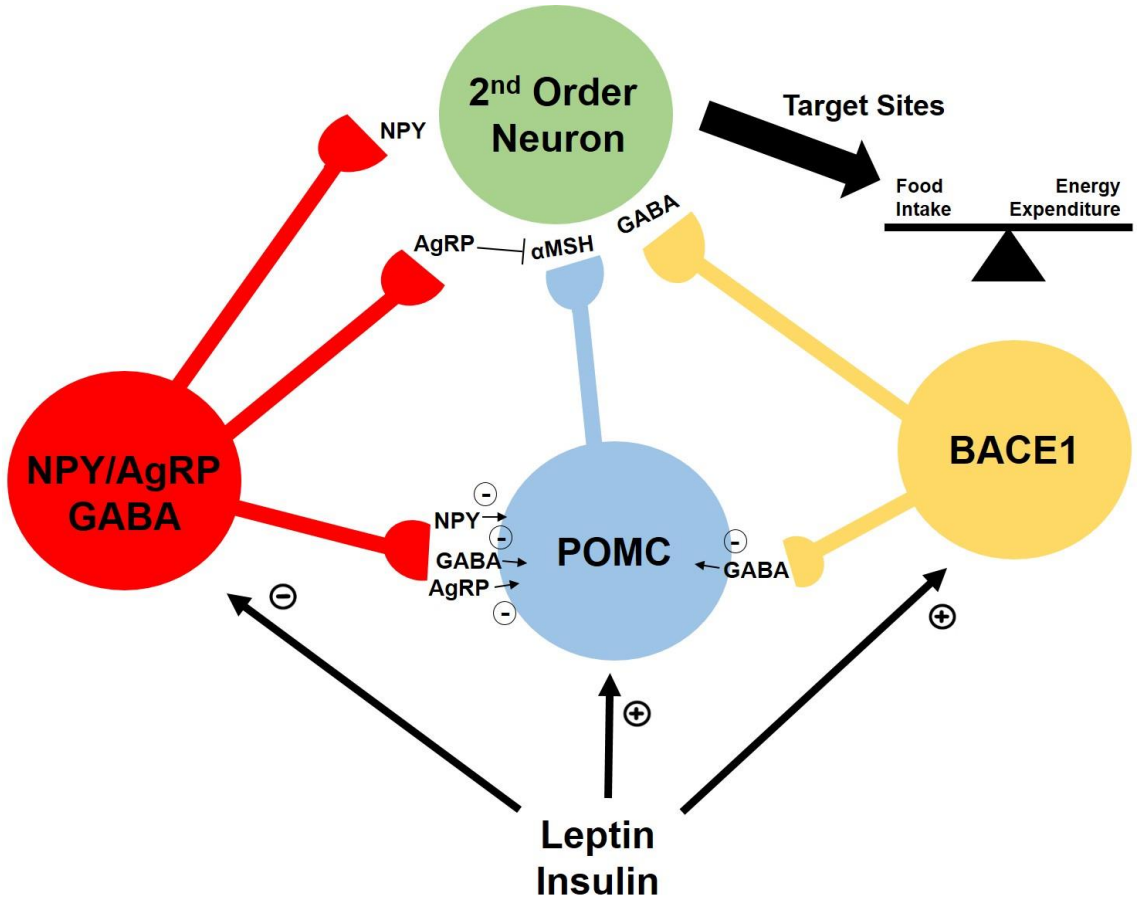

Figure 5.19 Schematic diagram showing the potential interaction of BACE1-positive ARC neurons in the current two neuron model of energy balance control.

Adiposity signals insulin and leptin act on ARC first order neurons to inhibit NPY/AgRP neurons and activate POMC neurons. POMC neurons release α-MSH which acts on second order neurons and AgRP acts to inhibit this action. GABAergic NPY/AgRP neurons can also innervate POMC neurons through synaptic GABA, NPY and AgRP release, directly inhibiting POMC action. The present data suggest that BACE1-positive ARC neurons also respond to peripheral signals and make synaptic contacts with POMC neurons. First order ARC neurons (BACE1-positive, POMC and NPY/AgRP neurons) project to second order neurons to influence food intake and energy expenditure, maintaining energy balance.
Figure adapted from Ashford Lab teaching material.

The notion discussed above is further supported by our finding that a large proportion of BACE1 neurons are RIPCre neurons in the ARC, as these neurons are distinct from POMC and NPY/AgRP neurons (Choudhury et al. 2005) and the majority are described to be GABAergic (Kong et al. 2012). Importantly, Kong and colleagues described that GABAergic RIPCre neurons are crucial for regulating energy expenditure, however not through alterations in food intake, but through increased BAT thermogenesis (Kong et al. 2012). This is supportive of our data showing BACE1 inhibition does not elicit major

effects regarding feeding behaviour and BACE1 is not largely expressed in neurons controlling food intake (POMC neurons), however following genetic or pharmacological removal of BACE1 we observe upregulation of thermogenic genes in WAT and BAT (unpublished data, section 3.2.10). Taken together, these data suggest BACE1 may be acting via RIPCre neurons to alter energy expenditure through BAT thermogenic programming.

Our data also demonstrate a reduction in inflammatory processing following pharmacological reduction of BACE1 (section 3.2.11), both centrally and peripherally, proposing a role for BACE1 in regulating inflammatory processes. Interestingly, this may also be due to the high expression of BACE1 observed in RIPCre neurons, as RIPCre neurons have also been implicated in the control of systemic inflammation. When *Pten*, which encodes a phosphatase that negatively regulates PI3K, is ablated from RIPCre neurons an anti-inflammatory pathway is activated whereby a phenotypic switch from a pro-inflammatory macrophage M1-like state to an anti-inflammatory macrophage M2-like state occurs in peripheral tissues (Wang et al. 2014). In addition, Wang *et al* demonstrated that this reduced pro- and enhanced anti-inflammatory state in *Pten*-RIPCre deficient mice results in protection from diet-induced obesity (Wang et al. 2014). The proposed mechanisms whereby RIPCre mediates the aforementioned role in energy expenditure and this role in systemic inflammation occur through central circuitry. In both cases it is hypothesised that ARC RIPCre neurons activate second order neurons in the PVN which project to the brainstem, notably the NTS, to mediate effects likely via the SNS (Kong et al. 2012; Wang et al. 2014). In particular, regarding energy expenditure effects, this is believed to occur via GABAergic ARC neurons and the projections to the NTS will further stimulate BAT function (Kong et al. 2012). With this in mind, our results show BACE1 is present in the ARC, of which a large proportion are GABAergic and RIPCre positive, furthermore we have also showed BACE1 is present in neurons in the PVN and the NTS, thus BACE1 fits into this proposed circuitry. Moreover, as discussed we also observe changes in thermogenic genes in BAT from BACE1 inhibitor treated mice and *BACE1*$^{-/-}$ mice (section 3.2.10, unpublished data), indicating BACE1 action on BAT. In regards to the role in systemic inflammation, the proposed mechanism indicates that in addition to activation of neurons in the NTS there is also projections from the PVN to the dorsal vagal motor nucleus (DVM), also within the brainstem. This controls vagal autonomic outflow and results in activation of an anti-inflammatory reflex causing the phenotypic switch of classically activated macrophages to an M2 state (Wang et al. 2014).

In our studies the expression of BACE1 in other regions of the brainstem (outwith the NTS) was not examined and it would be of interest to investigate this as at present it has not been shown if BACE1 is expressed in the DVM. As we show BACE1 is expressed in all other areas implicated in this circuitry, we would hypothesise BACE1 is also present in neurons within the DVM since, as mentioned, we also observe increased anti-inflammatory programming in both *BACE1*$^{-/-}$ mice and BACE1 inhibitor treated mice.

Taken together, we hypothesise that BACE1/RIPCre GABAergic neurons in the ARC act upon second order neurons in the PVN, which may also be BACE1-positive. These second order neurons project to neurons in the NTS regulating thermogenic and inflammatory programming in peripheral tissues, and these NTS neurons may also be BACE1-positive (Figure 5.20). This suggests that in instances where BACE1 is elevated, such as during diet-induced obesity, this will impair the described neuronal circuitry resulting in reduced energy expenditure and increased inflammation; exacerbating metabolic dysfunction and causing a vicious cycle to occur. Crucial future work to investigate this theory further would be to knock-out BACE1 exclusively in RIPCre neurons utilising a conditional *BACE1*$^{-/-}$ mouse with loxed alleles and crossing this with RIPCre transgenic mouse. The expected result would be that mice with BACE1 deletion from RIPCre neurons would be protected from diet-induced obesity, display increased energy expenditure and reduced systemic inflammation, demonstrating an overall improved metabolic phenotype.

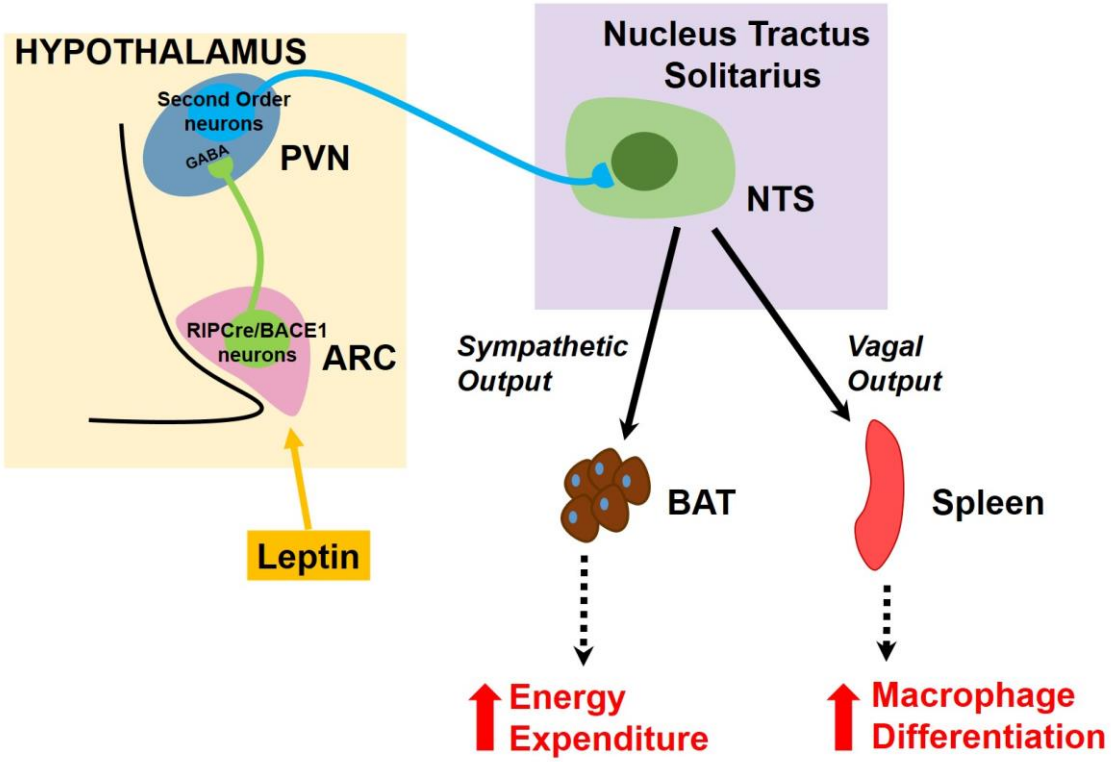

Figure 5.20 Schematic diagram showing BACE1-positive ARC neurons and the proposed neuronal pathway regulating energy expenditure and inflammatory processing.

The present data show a high proportion of BACE1-positive ARC neurons are GABAergic RIPcre neurons. These neurons respond to leptin and innervate second order neurons in the PVN through GABA release. Second order neurons in the PVN project to the NTS which stimulates energy expenditure in BAT through sympathetic output and macrophage differentiation in the spleen through vagal output to promote anti-inflammatory signalling.
Figure adapted from (Kong et al. 2012)

5.4.5 BACE1 expression outwith the arcuate nucleus

The role of BACE1 in energy metabolism may not be entirely mediated by RIPCre neurons as we have established BACE1 is expressed in other areas of the hypothalamus, which also regulate whole body energy homeostasis. The VMH plays a key role in energy homeostasis, involving control of glucose homeostasis and energy expenditure. We have shown BACE1 is co-localised with RIPCre neurons in this area, as well as the DMH, however less is known regarding the functions of RIPCre neurons within these nuclei, with focus remaining on the ARC. We have shown that throughout the VMH BACE1 is co-expressed with approximately 30% of SF-1 neurons, which are the predominant population in the VMH. Still, other genes are expressed throughout the VMH and may

represent distinct populations of neurons such as brain derived neurotrophic factor (BDNF), pituitary adenylate cyclase activating polypeptide (PACAP), and cerebellin 1 (Choi et al. 2013). Additionally, localised to the ventrolateral region of the VMH the estrogen receptor α (ERα), neuronal nitric oxide synthase, somatostatin and CKK also exist (McClellan et al. 2006). This supports our data which shows not all BACE1 neurons in the VMH are SF-1 neurons. These additional neuropeptides and transcription factors present in the VMH are also likely to play a role in metabolism, supported by findings that a lack of BDNF mRNA (Liao et al. 2012) or ERα (Musatov et al. 2007) expression in the VMH results in obesity and hyperphagia in mice. Furthermore, PACAP is also implicated in the control of energy balance with work demonstrating PACAP exerts anorexigenic effects in mice, and that PACAP neurons in the VMH are responsive to leptin and required for leptin action (Hawke et al. 2009). Future experiments would be required to examine if BACE1-positive neurons in the VMH, those in particular that may be distinct from some SF-1 neurons, co-express BDNF, ERα and PACAP to further unpick the role of BACE1 in the VMH.

SF-1 neurons are primarily involved in regulating glucose homeostasis and appropriately responding to glucose (Tong et al. 2007), proposing a role for BACE1 in the modulation of glucose homeostasis. Recent data from our lab supports this concept showing *in vitro*, utilising a hypothalamic (GT1-7) cell line, that BACE1 levels are sensitive to changes in glucose, with recurrent hypoglycaemia increasing BACE1 protein levels (John Findlay PhD Thesis). To investigate this further *in vivo* BACE1 could be ablated exclusively in SF-1 neurons, again utilising a conditional *BACE1*$^{-/-}$ mouse with floxed alleles and crossing this with a SF-1 transgenic mouse. Additionally, SF-1 neurons are also involved in regulating leptin action on energy expenditure. Studies show that global deletion of the leptin receptor or leptin receptor ablation on SF-1 neurons impairs the thermogenic response to high-fat feeding and reduces energy expenditure (Kim et al. 2011; Dhillon et al. 2006). This is in keeping with the proposed mechanism, whereby BACE1 may be primarily affecting thermogenesis and energy expenditure, however it may do so not only via RIPCre neurons but also SF-1 neurons. Interestingly, leptin action on SF-1 neurons may also occur through PI3K mediated mechanisms involving FoxO1, which we have proposed to be the case for BACE1 ARC neurons that do not appear to signal through pSTAT3 in response to leptin. When FoxO1 is ablated from SF-1 neurons, mice are lean, display increased energy expenditure and are more insulin and leptin sensitive (Kim et al. 2012). These data further support our findings that BACE1 neurons may respond to leptin

and alter energy balance through the PI3K pathway. Furthermore, when *Ptpn1*, the gene encoding the negative regulator of leptin and insulin signalling PTP1B, is knocked out of SF-1 neurons this causes obesity, impaired sympathetic output and reduced energy expenditure (Chiappini et al. 2014). Interestingly, these effects are only observed when mice are fed a HFD with no changes on body weight observed when mice are fed a NC diet, suggesting the additional stress of high-fat feeding is required which may be associated with increased BACE1 levels in SF-1 neurons, further exacerbating an obese phenotype and impairing neuronal function. In support of this is data from our lab showing PTP1B levels are reduced in *BACE1*$^{-/-}$ mice fed a HFD. The mechanism whereby BACE1 regulates energy metabolism in SF-1 neurons is unknown, as the precise connections SF-1 neurons make is not yet defined. In particular, other glucose-sensing neurons and how they interact with SF-1 neurons in the VMH is still to be investigated, however it can be assumed that these neurons will also connect to the brainstem due to their effects on glucose tolerance and in particular they will likely project to the NTS owing to their role in sympathetic output and energy expenditure.

Within this chapter we demonstrated BACE1 is expressed in the NTS and thus may be implicated in sympathetic output to peripheral tissues, notably BAT. However, the characterisation of BACE1 in the NTS was not examined, and we cannot definitively conclude a role for BACE1 in this area. It would be of interest to trace BACE1 neuronal projections to achieve a better understanding of the circuitry BACE1 is involved in. This could be achieved using electrophysiological measurements or through injection of fluorescent beads and channelrhodopsin 2-assisted circuit mapping (Atasoy et al. 2008) as utilised by Kong *et al* in the investigation of RIPCre neuronal projections (Kong et al. 2012). In addition, measurements of sympathetic activity in *BACE1*$^{-/-}$ mice and BACE1 inhibitor treated mice could be ascertained by measuring noradrenaline levels in the serum, to indicate whether BACE1 may indeed be implicated in altered SNS activity. Our results show that approximately 10% of BACE1 neurons in the NTS are NPY neurons, thus a large population are unidentified. Interestingly, approximately half of the NPY neurons we observed in the NTS co-express BACE1, suggesting BACE1 may be involved in the NPY-central circuitry regulating feeding behaviour. As the NTS receives and inputs many signals from hypothalamic areas, extra-hypothalamic areas and the periphery it is more complex to pin down the role BACE1 plays in this area. Further experiments examining co-expression of BACE1 with other known NTS neuronal populations, such as catecholaminergic neurons, CART and POMC neurons and proglucagon-expressing

neurons in this area is required (Sobrino Crespo et al. 2014). However, the important finding from our results is that BACE1 is present in the NTS, and therefore it may have a role in the neuronal circuitry the NTS is involved in.

The NTS receives an abundance of projections from the PVN, where, as previously discussed, we also find BACE1 to be expressed. As with other areas of the hypothalamus we find BACE1 is predominantly neuronal in the PVN and thus we can assume BACE1 is present in second order hypothalamic neurons. However, we did not examine the precise neuronal population BACE1 is co-localised with in the PVN. As mentioned, two main populations of second order neurons in the PVN are CRH- and TRH-releasing neurons, and it would be of interest to examine if BACE1 co-expresses with these populations. Another population of benefit to investigate in the PVN are tyrosine hydroxylase-expressing neurons. Tyrosine hydroxylase (TH) is an enzyme involved in the synthesis of catecholamines, and TH-releasing neurons have recently been shown to be targets of ARC NPY neurons and the relationship between the two may affect sympathetic tone on BAT impacting thermogenesis and energy expenditure (Shi et al. 2013). As we have proposed a mechanism whereby BACE1 may alter these processes, this is another potential pathway in which this may occur and examining co-expression of BACE1 and TH in the PVN and also measuring TH levels in our *BACE1*$^{-/-}$ and BACE1 inhibitor treated mice would be of interest to carry out in the future.

Further examination of BACE1 expression is also necessary in the LH and the DMH. In both areas we have shown that BACE1 is expressed and is predominantly neuronal, however the precise populations are as yet unidentified. Owing to their involvement in satiety and their projections to the ARC and NTS, orexin LH neurons would be of great interest to examine. If BACE1 is expressed in orexin neurons in the LH this would be another potential mechanism whereby BACE1 alters energy balance, and interestingly this would also implicate BACE1 in sleep and wakefulness, as orexin neurons play a major role in regulating these processes (Arora & Anubhuti 2006; Inutsuka & Yamanaka 2013). The role of BACE 1 in these processes is unknown and would be a novel area to examine. Firstly, it would be of interest to observe if BACE is present in the SCN; the control centre of circadian rhythms, as orexin receptors are found here and these neurons receive input from the SCN (Inutsuka & Yamanaka 2013). This could be achieved using IF on WT mice and we hypothesis that BACE1 would be co-expressed with LH neurons, and in turn in neurons of the SCN, as alterations in circadian rhythms are associated with diabetes and obesity (Scheer et al. 2009), and this could be due in part to increasing levels

of BACE1 altering the neuronal function of these neurons. In regards to obesity and the diet-induced response to thermogenesis, the DMH is crucial for further investigation. In particular NPY neurons in the DMH have been described to be important for regulating energy balance, as knocking down NPY expression in the DMH improves an obese phenotype by increasing energy expenditure and directly increasing thermogenic programming in BAT (Chao et al. 2011). Therefore, ARC NPY neurons may differ in their functions to DMH NPY neurons and it would be interesting to examine if BACE1 is expressed in NPY neurons in the DMH and to what extent, as this would further implicate BACE1 in the neuronal circuitry impacting energy expenditure and thermogenic programming.

5.4.6 Concluding Remarks

Collectively, the data presented in this chapter provide novel findings into the expression of BACE1 in the hypothalamus and more specifically the neuronal circuitry regulating energy balance. BACE1 was found to be expressed throughout hypothalamic nuclei controlling energy balance and within distinct neuronal populations involved in this control. Further investigation is required to examine BACE1 expression, particularly its role in RIPCre neurons, but also to investigate the potential of other novel populations of BACE1-positive neurons in the hypothalamus. The knowledge from this research implicates a role for BACE1 in the CNS neuronal circuitry controlling energy metabolism and allows for further work to investigate the functionality of this role as well as additional roles of BACE1 activity in the control or modulation of whole body energy homeostasis.

Chapter 6

Final Conclusions

6.1 The role of BACE1 in obesity and T2DM

At present, obesity and T2DM represent major public health problems, with the prevalence of both dramatically on the rise. It is estimated that 13% of the adult population worldwide are considered obese, a risk factor that is closely associated with T2DM (www.who.int). This is extremely worrying owing to the number of comorbidities connected with both T2DM and obesity, including cardiovascular disease and AD.

Of particular interest is the recent association of increased risk of AD to obesity and T2DM, with the diseases sharing many common features, including inflammation and insulin resistance. The link between AD, T2DM and obesity implicates BACE1, a protein whose expression levels and/or activity increase in response to stress conditions, such as factors associated with T2DM and obesity. The elevation in BACE1 activity and/or levels in response to stressors results in increased Aβ production, which is observed in obese mouse models (Julien et al. 2010). Elevations in Aβ protein levels are considered the primary causative factor for the progression of AD. According to the amyloid cascade hypothesis increased levels of Aβ gives rise to various cellular events, ultimately resulting in neuronal dysfunction and cell death (J. A. Hardy & Higgins 1992). The discovery of the Icelandic mutation that occurs adjacent to the BACE1 cleavage site, which actually reduces BACE1 activity, further supports the amyloid cascade hypothesis as this mutation causes reduced Aβ load and lifelong protection from AD. As a result, focus has been placed on BACE1 as a target for the treatment of AD, however owing to its association with obesity and T2DM it may also be a novel target for metabolic disease. In support of this it has been shown that *BACE1*$^{-/-}$ mice have an improved metabolic phenotype in comparison to WT littermates; *BACE1*$^{-/-}$ mice are resistant to DIO and display improved glucose homeostasis and insulin sensitivity (Meakin et al. 2012). Furthermore, pharmacological inhibition of BACE1 in skeletal muscle cells *in vitro* increases glucose uptake and oxidation (Hamilton et al. 2014). The same is observed in a neuronal (SH-SY5Y) cell line and in addition overexpression of BACE1 in these cells causes decreased glucose uptake and oxidation (John Findlay PhD Thesis). Taken together, these data implicate BACE1 in the control of energy metabolism. For this reason, the data presented in this thesis sought to investigate BACE1 as a therapeutic target for metabolic disease, with the overall goal to allow for advancements in the treatment of obesity and T2DM.

6.2 The pharmacological inhibition of BACE1 as a potential treatment for metabolic disease

The data presented in the current studies strongly suggest BACE1 inhibitors may provide a potential therapeutic strategy for the treatment of obesity and T2DM. Currently, treatment of these diseases emphasises altering lifestyle factors as the most desirable course of action. Reducing calorific intake and increasing energy expenditure are encouraged as both can reverse insulin and leptin resistance. However, due to the increasing prevalence of obesity and associated T2DM this strategy is clearly proving ineffective.

At present there are two alternative approaches for the treatment of obesity; oral medication or surgery. Gastric bypass surgery is considered the only effective treatment, resulting in maintained weight loss in the majority of patients, although it is only an option for cases of morbid obesity (BMI >40) (Arora & Anubhuti 2006; Adan 2013). Therefore, focus is placed upon anti-obesity agents. Early research believed thyroid hormones could be effective as anti-obesity agents, through increasing resting metabolic rate and energy expenditure, resulting in reduced body weight (Adan 2013). However, many side effects were associated with this treatment, such as hyperthyroidism, and as a result focus turned to 'noradrenergic' and 'serotonergic' agents. Noradrenergics, such as phenteramine, block noradrenaline uptake, acting to suppress appetite, and serotonergic agents, such as fenfluramine and dexfenfluramine, affect serotonin uptake and release. Other, once approved anti-obesity agents include sibutramine which acts to inhibit reuptake of noradrenaline, serotonin and dopamine (Arora & Anubhuti 2006; Rolls et al. 1998), and rimonabant; an antagonist of the endocannabinoid receptor, CB_1 (Adan 2013). Unfortunately, although many agents, such as the aforementioned, have undergone trials for the treatment of obesity and have proven to be effective in causing weight loss, most have been withdrawn due to severe side effects (Wong et al. 2012; Adan 2013). However, 2,4-dinitrophenol (DNP), which has been known for decades to cause rapid weight loss through enhancing basal metabolic rate and fat burning, is still currently available despite high risks of severe side effects and increasing reports of fatalities (Grundlingh et al. 2011). Thus, orlistat, an inhibitor of pancreatic lipase, is the only currently available and approved anti-obesity drug, acting to reduce efficiency of fat absorption (Padwal & Majumdar 2007) Although orlistat is widely prescribed, its weight loss effects are relatively mild and it is also associated with many gastrointestinal side effects (Li et al.

2005). As a result, newer drugs are also being researched and in the pipeline for obesity treatment, including lorcaserin; a serotonin receptor agonist, qsymia; a combination therapy of phenteramine and tipiramate (an anticonvulsant), and contrave; a combination therapy of a dopamine reuptake inhibitor (bupropion) and an opiod antagonist (naltrexone) (Wong et al. 2012; Adan 2013). However, associated side-effects are also emerging for these more recently approved compounds, including heart valve problems and psychiatric risks. A GLP-1 receptor agonist, liraglutide, has been also recently accepted as an anti-obesity agent, which was previously licensed as a treatment for T2DM (Adan 2013), although the mechanism for the body weight reducing effects of liraglutide are unknown. Alternatively, targeting of inflammatory processing may also present a potential therapeutic target due to the close association between inflammation, obesity and insulin resistance. In support of this, the use of an inhibitor of NF-κB β-subunit (IKK-β); salicylate, improves insulin resistance (Fleischman et al. 2008). In addition, anti-inflammatory cytokines such as IL-10 act as insulin sensitizers, further supporting the interference of inflammatory signalling as a potential treatment of obesity and associated insulin resistance (Zeyda & Stulnig 2009a).

Importantly, owing to the various complications and side effects of current drugs there is still a need to develop small molecule compounds which target the components involved in the development of leptin and insulin resistance to provide effective treatments for obesity and T2DM. The issue surrounding many of the current treatments being researched is that they target one pathway and therefore may become ineffective due to redundant pathways compensating for weight loss. Additionally, as found with many of the compounds that have been withdrawn, targeting neurotransmitters will also have non-satiety effects. Another key issue to be considered is the difficulty in maintaining weight loss, which may be due to a compensatory reduction in resting metabolic rate causing increased fat storage. Therefore, alternative strategies are required such as targeting energy expenditure and the natural control pathways (neuronal and hormonal) that regulate metabolic rate and processes such as thermogenesis. Additionally, other processes driving the progression of obesity and insulin resistance, predominantly inflammation and ER stress, should also be investigated. The data presented in this thesis have shown that BACE1 inhibition improves an obese/diabetic phenotype mainly through altered thermogenic and inflammatory programming. We hypothesise that BACE1 inhibitors cause a reduction in body weight by increasing energy expenditure through upregulation of thermogenic genes in WAT and BAT, and our data indicate reduced

central and peripheral inflammation. These results suggest that BACE1 inhibitors as novel anti-obesity agents may be more effective than currently available compounds. BACE1 inhibitors currently under clinical trials for AD would be of benefit to determine if they can elicit the same metabolic effects in humans produced in the present studies. This would allow for further research investigating the comparison between currently researched anti-obesity agents with BACE1 inhibitors and potentially broaden research trialling BACE1 inhibitors for AD to the treatment of metabolic disease in humans.

6.3 The role of BACE1 in the hypothalamic neuronal circuitry controlling energy balance

In an attempt to better understand the role of BACE1 in energy metabolism we turned our attention to the hypothalamus; deemed the control centre for the regulation of energy homeostasis. This control is reliant on intact neuronal circuitry and leptin signalling; disruption of this circuitry results in obesity, as demonstrated in the genetic *ob/ob* and *db/db* mouse models (Zhang et al. 1994; Chen et al. 1996). Such models demonstrate the requirement to preserve leptin signalling for regulating energy homeostasis, however during DIO there is a state of leptin resistance causing impaired leptin action (Considine et al. 1996). Distinct hypothalamic nuclei are involved in this control, although the ARC is the main site of leptin action and as a consequence is the main site of leptin resistance (Enriori et al. 2007).

The current neuronal hypothesis of leptin action in the ARC involves POMC and NPY/AgRP neurons. In brief, following binding of the long form of its receptor, leptin activates POMC/CART neurons and inhibits NPY/AgRP neurons, ultimately resulting in reduced food intake and increased energy expenditure (Cowley et al. 2001; Schwartz et al. 2000; Bates & Myers 2003). Latterly, this model has been deemed too simplistic as when the leptin receptor is removed from these neurons only mild obesity is observed (Balthasar et al. 2004; Van De Wall et al. 2008), thus other first order ARC neurons must play a role. In support of this, in the present studies we observe BACE1-positive neurons in the ARC, which are distinct from POMC and NPY/AgRP neurons. A small percentage of ARC BACE1-positive cells are POMC (~5%) and NPY/AgRP (~10%) therefore BACE1 may still influence food intake and energy expenditure pathways through these neuronal populations. We demonstrated that approximately 50% of the non-POMC/NPY/AgRP BACE1-positive neurons in the ARC are RIPCre GABAergic neurons, which are a relatively novel neuronal population implicated in the regulation of

thermogenic and inflammatory processes (Kong et al. 2012; Wang et al. 2014). Our data further supports this through finding that BACE1 inhibition may be acting to increase thermogenesis in BAT whilst inhibiting central and peripheral inflammation. RIPcre neurons have been described to be in close, though distinct, apposition to POMC and NPY/AgRP neurons (Choudhury et al. 2005), which is in keeping with our findings that BACE1-positive cells appear very close to contacting POMC neurons. Furthermore, BACE/RIPcre neurons express leptin receptors and as a result are considered responsive to leptin, likely through the PI3K pathway, as the data presented in the current study demonstrate a lack of evidence for pSTAT3 activation in BACE1-positive ARC neurons. These findings suggest leptin is not acting upon these neurons through the JAK-STAT signalling pathway and proposes activation of PI3K and possibly FoxO1, to be implicated, although this is yet to be tested. Owing to the co-localisation between BACE1-positive neurons and RIPCre neurons, and the positioning of these neurons in relation to POMC and NPY/AgRP neurons, allows us to hypothesis that it is more likely that a third neuronal population is crucial in the current two ARC neuronal model. This suggests leptin signals not only POMC and NPY/AgRP neurons but also BACE1/RIPCre neurons that will independently send projections to second order neurons in the PVN. In addition, within this proposed 'three-neuron model' it may be that BACE1/RIPcre neurons also inhibit POMC neurons indirectly from leptin signalling. This is observed with NPY/AgRP neurons that directly inhibit POMC through synaptic innervation by GABA and NPY release (Cowley et al. 2001). To fully investigate this concept it would be necessary to conduct further experiments using electrophysiological techniques, utilising a fluorescent BACE1 and/or RIPCre mouse model. A fluorescent BACE1 mouse model would be of particular interest, as there remains a population of BACE1-positive neurons in the ARC which are undefined and may represent alternative ARC populations such as dopaminergic or cholinergic neurons. This mouse model, as well as utilising more novel techniques such as DREADD (designer receptors exclusively activated by designer drugs) would allow these neurons to be investigated in further detail. DREADD technology, based upon mutated human muscarinic receptors which have a high efficacy for a pharmacologically inert ligand, allow for targeting of specific neuronal populations using viral vectors or over-expressing transgenic mouse models (Alexander et al. 2009). This technology permits direct activation and modulation of specific neurons, as demonstrated by Krashes *et al* investigating AgRP neuronal activation on feeding behaviour (Krashes et al. 2011), and Kong *et al* examining the effects on energy

expenditure through RIPCre neuronal activation (Kong et al. 2012). Utilising this technique, particularly fusing the DREADD with a fluorescent protein such as mCherry, would allow for the direct activation of BACE1-positive neurons and for their functional role to be investigated through examining their electrical properties.

The VMH is also crucial for the control of energy homeostasis and was the first site recognised to be important in this regulation (King 2006). The predominant neuronal population present in the VMH are SF-1 neurons, which are directly responsive to leptin; when the leptin receptor is ablated from these neurons an obese phenotype is observed (Dhillon et al. 2006). This obese phenotype resembles that of POMC ARC neurons, demonstrating the ARC is not the only site important for leptin action, and SF-1 neurons in the VMH are also required for leptin action. We find abundant BACE1-positive neurons within the VMH, of which approximately 30% are SF-1 neurons, implicating a role for BACE1 in leptin action in the VMH. In addition to the body weight and food intake actions of leptin on the VMH, this nuclei is crucial for the regulation of glucose homeostasis and mediating the counter-regulatory response (CRR) to hypoglycaemia. This was first demonstrated by Borg *et al* who demonstrated that following VMH damage rats show a blunted CRR, through reduced glucagon, adrenaline and noradrenaline release (Borg et al. 1994). As a result, neurons in the VMH are considered glucose-sensing neurons, and play a role in triggering the release of CRR hormones in response to hypoglycaemia. SF-1 neurons represent glucose-sensing neurons and are involved in mediating the appropriate response to glucose. Work by Tong *et al* demonstrated that when VGlut2 is knocked-out of SF-1 neurons there is blunting of the CRR to hypoglycaemia (Tong et al. 2007). Taken together, with our findings that BACE1 is present in SF-1 neurons, these data suggest that BACE1 may play an important role in glucose homeostasis, in particular the response to hypoglycaemia. This is supported by the knowledge that BACE1 levels are sensitive to hypoglycaemia, as there is a large increase in BACE1 protein levels observed following recurrent episodes of hypoglycaemia in a hypothalamic cell line (John Findlay PhD Thesis). Moreover, our data shows that in DIO mice BACE1 inhibition improves glucose homeostasis and enhanced BACE1 cleavage (through ADAM10 inhibition) causes defective glucose homeostasis, demonstrating a clear role for BACE1 in the regulation of glucose homeostasis, as well as whole body energy homeostasis. Importantly, we show there are BACE1-positive neurons in the VMH that are undefined, but which may represent additional VMH populations, also implicated in the control of energy balance, such as

BDNF-expressing and PACAP-expressing neurons, although further investigation would be necessary to examine this.

The neuronal circuitry principally controlling energy balance involves first order ARC neurons integrating peripheral signals and projecting to other hypothalamic nuclei, namely the PVN and LH. From here, second order neurons input this information to the brainstem, principally the NTS, as well as the DVC, where signals are integrated and outputs generated through the SNS and vagus nerve (Schwartz et al. 2000). As we conclude BACE1-positive neurons represent another population of first order ARC neurons we hypothesise these neurons will also project to second order neurons. To definitively conclude this it would be necessary to conduct studies using neuronal tracing with anterograde labelling and electrophysiology. This would again require the use of a fluorescently tagged BACE1 mouse model, so that BACE1-positive cells could be identified, patched and injected with a dye to follow the processes and determine where the neurons synapse. It would be of particular interest to examine if the second order neurons that project to the brainstem are also BACE1-positive neurons and furthermore if the NTS neurons, which receive inputs and integrate the signals, are also BACE1-positive. As we observe BACE1 present in all areas involved in the CNS circuitry described, and due to the number of BACE1 positive cells observed, particularly in the NTS, this is likely to be the case. These data strongly implicate BACE1 in the control of the neuronal circuitry regulating energy homeostasis.

6.4 Physiological relevance

The current data implicate BACE1 in the hypothalamic neuronal circuitry controlling energy balance, however the specific role under normal conditions is not yet known. As BACE1 has been shown to respond to various cellular stressors, it may sense and respond to acute stress within hypothalamic neurons allowing for preservation of neuronal activity. Conversely, under chronic stress conditions when BACE1 levels and/or activity remain elevated, for example following high-fat feeding, it is hypothesised that this will lead to dysfunction of the neuronal circuitry due to a loss of sensitivity and activity of the neurons. Specifically within RIPCre neurons, when BACE1 becomes elevated this may result in impairment of the circuitry to the PVN and NTS causing down-regulation of thermogenic programming and increased inflammatory processing; exacerbating metabolic disease.

A component of this dysregulation of neuronal circuits may be due to elevated Aβ generated from BACE1 cleavage. This is supported by our data that demonstrate that altering APP processing, through blockage of α-secretase activity, exacerbates an obese/diabetic phenotype. Data showing administration of Aβ oligomers cause the same effect, but produces a more severe phenotype, further supporting this concept. (Clarke et al. 2015). Additionally, recent work in our lab has supported this by centrally infusing mouse $A\beta_{1-42}$ in mice fed a HFD and demonstrating a large effect on the worsening of an obese state (unpublished data). High levels of Aβ, as a result of elevated BACE1 levels and/or activity, will activate microglia and astrocytes causing production of cytokines contributing to increased inflammation (Johnstone et al. 1999). This is further supported by the knowledge that Aβ may act as a danger-associated molecular pattern (DAMP) which activates inflammasomes causing increased inflammatory processing (Heneka et al. 2014). DAMPs trigger inflammation in brain cells through activation of inflammasomes, which are multi-molecular protein complexes found within cells (Guo et al. 2015). The inflammasomes activate inflammation via IL-β cleavage and pro-inflammatory cytokine release, predominantly through pro-caspase 1 cleavage and caspase-1 release from the inflammasome (Guo et al. 2015). Inappropriate inflammasome activity, for example enhanced activation, is implicated in metabolic disease through elevated IL-1β and pro-inflammatory cytokines strongly associating with ER stress and insulin resistance. Therefore, Aβ may be specifically activating inflammasomes within microglia resulting in elevated inflammation. This enhanced inflammatory processing drives increased levels of soluble Aβ oligomers, which may act as secondary DAMPs to independently elevate pro-inflammatory cytokines further (Clark & Vissel 2015). This exacerbation of inflammatory processing, connected to ER stress and insulin resistance, will in turn worsen metabolic dysfunction.

In the brain there is evidence of the packaging and release of Aβ directly from hippocampal neurons through elevated synaptic activity (Cirrito et al. 2005; Cirrito et al. 2008). Moreover, this release of Aβ following enhanced neuronal activity has the ability to directly alter synaptic transmission, through reducing the number of synapses on other neurons (Kamenetz et al. 2003). This may also occur in the hypothalamus, where following elevation in BACE1, Aβ may be packaged and released from hypothalamic neurons (stimulating inflammasomes), which would likely activate astrocytes and microglia, driving inflammation, ER stress and insulin resistance, and moreover, may reduce synapses on neighbouring POMC and NPY/AgRP neurons. Loss of neighbouring

synapses would lead to disruption and further dysfunction of the hypothalamic neuronal circuitry controlling energy balance. Conversely, Kamenetz *et al* demonstrated that rodent Aβ, which is not believed to have amyloidogenic properties, also alters synaptic transmission following neuronal activation, which in turn reduces neuronal activation (Kamenetz et al. 2003). These data suggest that Aβ, under normal circumstances, may have a physiological function where it forms a negative feedback loop controlling neuronal activity and function. This may also occur in the hypothalamus and is supportive of our hypothesis that BACE1 under normal circumstances may act to respond to stress and reduce neuronal activity to preserve functionality of neurons and alter energy balance, acting as a protective mechanism. In regards to chronic stress and prolonged elevation of BACE1 and associated Aβ levels, the current hypothesis suggests that BACE1 inhibitors will reduce BACE1 levels and/or activity in hypothalamic neurons and re-sensitise the neuronal circuits controlling energy balance to peripheral signals such as leptin. Specifically, in RIPCre neurons re-sensitising these cells to leptin would result in increased energy expenditure, reversing leptin resistance and targeting body weight, and reducing chronic inflammation, improving insulin resistance. Additionally, in SF-1 neurons re-sensitising these neurons to glucose through reduced BACE1 levels may improve and maintain glucose homeostasis, in particular the appropriate response to hypoglycaemia.

The data presented within this thesis describe BACE1 as a novel component of the central neuronal circuitry controlling energy balance. This knowledge, accompanied by recent findings, implicate BACE1 in the regulation of energy homeostasis, whereby long-lasting elevations in BACE1 worsen metabolic disease through impaired thermogenic programming and increased chronic inflammation; as a result of defective neuronal activity. Furthermore, reducing BACE1 activity may provide a therapeutic strategy for the treatment of obesity and T2DM, in which inhibition restores neuronal activity and function to allow for the regulation of energy balance. This leaves open the field for future studies to investigate the functional properties of BACE1-positive hypothalamic neurons to help determine the precise role of BACE1 in energy metabolism.

Chapter 7

References

Adan, R.A.H., 2013. Mechanisms underlying current and future anti-obesity drugs. *Trends in neurosciences*, 36(2), pp.133–40.

Ahima, R.S. et al., 1996. Role of leptin in the neuroendocrine response to fasting. *Nature*, 382(6588), pp.250–2.

Air, E.L. et al., 2002. Small molecule insulin mimetics reduce food intake and body weight and prevent development of obesity. *Nature medicine*, 8(2), pp.179–183.

Alexander, G.M. et al., 2009. Remote control of neuronal activity in transgenic mice expressing evolved G protein-coupled receptors. *Neuron*, 63(1), pp.27–39.

Allinson, T.M.J. et al., 2003. ADAMs family members as amyloid precursor protein alpha-secretases. *Journal of neuroscience research*, 74(3), pp.342–352.

Al-Qassab, H. et al., 2009. Dominant role of the p110beta isoform of PI3K over p110alpha in energy homeostasis regulation by POMC and AgRP neurons. *Cell metabolism*, 10(5), pp.343–354.

Alzheimer, A. et al., 1995. An English translation of Alzheimer's 1907 paper, "uber eine eigenartige erkankung der hirnrinde." *Clinical Anatomy*, 8(6), pp.429–431.

Araki, E. et al., 1994. Alternative pathway of insulin signalling in mice with targeted disruption of the IRS-1 gene. *Nature*, 372(6502), pp.186–190.

Araki, W. et al., 1991. Trophic effect of beta-amyloid precursor protein on cerebral cortical neurons in culture. *Biochemical and Biophysical Research Communications*, 181(1), pp.265–271.

Ariyasu, H. et al., 2001. Stomach is a major source of circulating ghrelin, and feeding state determines plasma ghrelin-like immunoreactivity levels in humans. *Journal of Clinical Endocrinology and Metabolism*, 86(10), pp.4753–4758.

Arora, S. & Anubhuti, 2006. Role of neuropeptides in appetite regulation and obesity - A review. *Neuropeptides*, 40(6), pp.375–401.

Atasoy, D. et al., 2008. A FLEX switch targets Channelrhodopsin-2 to multiple cell types for imaging and long-range circuit mapping. *The Journal of neuroscience*, 28(28), pp.7025–3.

Atasoy, D. et al., 2012. Deconstruction of a neural circuit for hunger. *Nature*, 488(7410), pp.172–177.

Avila-Muñoz, E. & Arias, C., 2014. When astrocytes become harmful: Functional and inflammatory responses that contribute to Alzheimer's disease. *Ageing Research Reviews*, 18, pp.29–40.

Bagdade, J.D., Bierman, E.L. & Porte Jr., D., 1967. The significance of basal insulin levels in the evaluation of the insulin response to glucose in diabetic and nondiabetic subjects. *Journal of Clinical Investigation*, 46, pp.1549–1557.

Balthasar, N. et al., 2005. Divergence of melanocortin pathways in the control of food intake and energy expenditure. *Cell*, 123(3), pp.493–505.

Balthasar, N. et al., 2004. Leptin receptor signaling in POMC neurons is required for normal body weight homeostasis. *Neuron*, 42(6), pp.983–91.

Banks, A.S. et al., 2000. Activation of downstream signals by the long form of the leptin receptor. *J Biol Chem*, 275(19), pp.14563–14572. Available at.

Banks, A.S. et al., 2000. Activation of Downstream Signals by the Long Form of the Leptin Receptor, 275(19), pp.14563–14572.

Banks, W.A., 2001. Anorectic effects of circulating cytokines: Role of the vascular blood-brain barrier. *Nutrition*, 17(5), pp.434–437.

Banno, R. et al., 2010. PTP1B and SHP2 in POMC neurons reciprocally regulate energy balance in mice. *Journal of Clinical Investigation*, 120(3), pp.720–734.

Bates, S.H. et al., 2003. STAT3 signalling is required for leptin regulation of energy balance but not reproduction. *Nature*, 421(6925), pp.856–859.

Bates, S.H. & Myers, M.G., 2003. The role of leptin receptor signaling in feeding and neuroendocrine function. *Trends in Endocrinology and Metabolism*, 14(10), pp.447–452.

Batterham, R.L. et al., 2003. Inhibition of food intake in obese subjects by peptide YY3-36. *The New England journal of medicine*, 349(10), pp.941–948.

Benani, A. et al., 2012. Food Intake Adaptation to Dietary Fat Involves PSA-Dependent Rewiring of the Arcuate Melanocortin System in Mice. *Journal of Neuroscience*, 32(35), pp.11970–11979.

Bence, K.K. et al., 2006. Neuronal PTP1B regulates body weight, adiposity and leptin action. *Nature medicine*, 12(8), pp.917–924.

Benjannet, S. et al., 2001. Post-translational processing of β-secretase (β -amyloid-converting enzyme) and its ectodomain shedding: The pro- and transmembrane/cytosolic domains affect its cellular activity and amyloid-β production. *Journal of Biological Chemistry*, 276(14), pp.10879–10887.

Bennett, B.D. et al., 2000. A furin-like convertase mediates propeptide cleavage of BACE, the Alzheimer's β-secretase. *Journal of Biological Chemistry*, 275(48), pp.37712–37717.

Bennett, B.D. et al., 2000. Expression analysis of BACE2 in brain and peripheral tissues. *Journal of Biological Chemistry*, 275(27), pp.20647–20651.

Benoit, S.C. et al., 2002. The catabolic action of insulin in the brain is mediated by melanocortins. *The Journal of neuroscience*, 22(20), pp.9048–9052.

Berglund, E.D. et al., 2012. Direct leptin action on POMC neurons regulates glucose homeostasis and hepatic insulin sensitivity in mice. *The Journal of Clinical Investigation*, 122(3), pp.1000–1009.

Biessels, G.J. et al., 2006. Risk of dementia in diabetes mellitus : a systematic review. *The Lancet Neurology*, 5(1), pp.64–74.

Billington, C.J. et al., 1991. Effects of intracerebroventricular injection of neuropeptide Y on energy metabolism. *The American journal of physiology*, 260(2 Pt 2), pp.R321–R327.

Billington, C.J. et al., 1994. Neuropeptide Y in hypothalamic paraventricular nucleus: a center coordinating energy metabolism. *The American journal of physiology*, 266(6 Pt 2), pp.R1765–R1770.

Bjorbaek, C. et al., 1998. Identification of SOCS-3 as a potential mediator of central leptin resistance. *Molecular Cell*, 1(4), pp.619–625.

Bjørbæk, C. et al., 1999. The role of SOCS-3 in leptin signaling and leptin resistance. *Journal of Biological Chemistry*, 274(42), pp.30059–30065.

Bjorbak, C. et al., 2000. SOCS3 mediates feedback inhibition of the leptin receptor via Tyr985. *The Journal of biological chemistry*, 275(51), pp.40649–57.

Black, R.A. et al., 1997. A metalloproteinase disintegrin that releases tumour-necrosis factor-alpha from cells. *Nature*, 385(6618), pp.729–733.

Blacker, M. et al., 2002. Effect of tumor necrosis factor-alpha converting enzyme (TACE) and metalloprotease inhibitor on amyloid precursor protein metabolism in human neurons. *Journal of neurochemistry*, 83(6), pp.1349–1357.

Blasko, I. et al., 2004. Experimental traumatic brain injury in rats stimulates the expression, production and activity of Alzheimer's disease β-secretase (BACE-1). *Journal of Neural Transmission*, 111(4), pp.523–536.

Blomain, E.S. et al., 2013. Mechanisms of Weight Regain following Weight Loss. *ISRN obesity*, 2013, p.210524.

Bolborea, M. & Dale, N., 2013. Hypothalamic tanycytes: Potential roles in the control of feeding and energy balance. *Trends in Neurosciences*, 36(2), pp.91–100.

Borg, W.P. et al., 1994. Ventromedial hypothalamic lesions in rats suppress counterregulatory responses to gypoglycemia. *The Journal of Clinical Investigation*, 93(4), pp.1677–1682.

Bouwknecht, J.A. et al., 2001. Male and female 5-HT1B receptor knockout mice have higher body weights than wildtypes. *Physiology & Behavior*, 74(4-5), pp.507–516.

Bradford, M., 1976. A Rapid and Sensitive Method for the Quantitation of Microgram Quantities of Protein Utilizing the Principle of Protein-Dye Binding. *Analytical Biochemistry*, 72(1-2), pp.248–254.

Bray, G. a & York, D. a, 1979. Hypothalamic and genetic obesity in experimental animals: an autonomic and endocrine hypothesis. *Physiological reviews*, 59(3), pp.719–809.

Broberger, C. et al., 1998. Hypocretin/orexin- and melanin-concentrating hormone-expressing cells form distinct populations in the rodent lateral hypothalamus: Relationship to the neuropeptide Y and agouti gene-related protein systems. *Journal of Comparative Neurology*, 402(4), pp.460–474.

Buddhala, C., Hsu, C.C. & Wu, J.Y., 2009. A novel mechanism for GABA synthesis and packaging into synaptic vesicles. *Neurochemistry International*, 55(1-3), pp.9–12.

Burks, D.J. et al., 2000. IRS-2 pathways integrate female reproduction and energy homeostasis. *Nature*, 407(6802), pp.377–382.

Butler, A.A. et al., 2000. A unique metabolic syndrome causes obesity in the melanocortin-3 receptor-deficient mouse. *Endocrinology*, 141(9), pp.3518–3521.

Cai, H.B. et al., 2001. BACE1 is the major beta-secretase for generation of A beta peptides by neurons. *Nature Neuroscience*, 4(3), pp.233–234.

Campfield, L.A. et al., 1995. Recombinant mouse OB protein- evidence for a peripheral signal linking adiposity and central neural networks. *Science*, 269(5223), pp.546–549.

Cao, D. et al., 2007. Intake of sucrose-sweetened water induces insulin resistance and exacerbates memory deficits and amyloidosis in a transgenic mouse model of Alzheimer disease. *Journal of Biological Chemistry*, 282(50), pp.36275–36282.

Cao, L. et al., 2011. White to brown fat phenotypic switch induced by genetic and environmental activation of a hypothalamic-adipocyte axis. *Cell Metabolism*, 14(3), pp.324–338.

Capell, A. et al., 2000. Maturation and pro-peptide cleavage of β-secretase. *Journal of Biological Chemistry*, 275(40), pp.30849–30854.

Caruso, C. et al., 2010. The role of adipose tissue and adipokines in obesity-related inflammatory diseases. *Mediators of Inflammation*, 2010.

Challis, B.G. et al., 2003. Acute effects of PYY3-36 on food intake and hypothalamic neuropeptide expression in the mouse. *Biochemical and Biophysical Research Communications*, 311(4), pp.915–919.

Chao, P.-T. et al., 2011. Knockdown of NPY expression in the dorsomedial hypothalamus promotes development of brown adipocytes and prevents diet-induced obesity. *Cell metabolism*, 13(5), pp.573–83.

Charlwood, J. et al., 2001. Characterization of the Glycosylation Profiles of Alzheimer's β-Secretase Protein Asp-2 Expressed in a Variety of Cell Lines. *Journal of Biological Chemistry*, 276(20), pp.16739–16748.

Chen, G.X. et al., 1996. Disappearance of body fat in normal rats induced by adenovirus-mediated leptin gene therapy. *Proceedings of the National Academy of Sciences of the United States of America*, 93(25), pp.14795–14799.

Chen, H. et al., 1996. Evidence that the diabetes gene encodes the leptin receptor: Identification of a mutation in the leptin receptor gene in db/db mice. *Cell*, 84, pp.491–495.

Chernoff, J., 1999. Protein tyrosine phosphatases as negative regulators of mitogenic signaling. *Journal of cellular physiology*, 180(2), pp.173–181.

Chiappini, F. et al., 2014. Ventromedial hypothalamus-specific Ptpn1 deletion exacerbates diet-induced obesity in female mice. *The Journal of clinical investigation*, 124(9), pp.1–12.

Choi, S.S. et al., 2014. Human astrocytes: Secretome profiles of cytokines and chemokines. *PLoS ONE*, 9(4).

Choi, Y.H. et al., 2013. Revisiting the ventral medial nucleus of the hypothalamus: The roles of SF-1 neurons in energy homeostasis. *Frontiers in Neuroscience*, 7(71), pp.1–9.

Choi, Y.H. et al., 2002. TRH decreases food intake and increases water intake and body temperature in rats. *Physiology and Behavior*, 77(1), pp.1–4.

Chou, T.C. et al., 2003. Critical role of dorsomedial hypothalamic nucleus in a wide range of behavioral circadian rhythms. *The Journal of neuroscience*, 23(33), pp.10691–10702.

Choudhury, A.I. et al., 2005. The role of insulin receptor substrate 2 in hypothalamic and beta cell function. *The Journal of Clinical Investigation*, 115(4), pp.940–950.

Cirrito, J.R. et al., 2008. Endocytosis Is Required for Synaptic Activity-Dependent Release of Amyloid-β In Vivo. *Neuron*, 58(1), pp.42–51.

Cirrito, J.R. et al., 2005. Synaptic activity regulates interstitial fluid amyloid-?? levels in vivo. *Neuron*, 48(6), pp.913–922.

Citron, M., 2004. Beta-secretase inhibition for the treatment of Alzheimer's disease--promise and challenge. *Trends in pharmacological sciences*, 25(2), pp.92–7.

Clark, I. a & Vissel, B., 2015. Alzheimer's disease: Amyloid beta not a primary initiator, but one of the secondary DAMPs. *British Journal of Pharmacology*,

Clarke, J.R. et al., 2015. Alzheimer-associated A b oligomers impact the central nervous system to induce peripheral metabolic deregulation. , 7(2), pp.190–210.

Colciaghi, F. et al., 2002. α-Secretase ADAM10 as well as αAPPs is reduced in platelets and CSF of Alzheimer disease patients. *Molecular medicine*, 8(2), pp.67–74.

Coll, A.P. & Yeo, G.S.H., 2013. The hypothalamus and metabolism: integrating signals to control energy and glucose homeostasis. *Current opinion in pharmacology*, 13(6), pp.970–6.

Considine, R.V. et al., 1996. Serum immunoreactive leptin concentrations in normal-weight and obese humans. *New England Journal of Medicine*, 334(5), pp.292–295.

Considine, R.V. et al., 1996. Serum immunoreactive-leptin concentrations in normal-weight and obese humans. *The New England journal of medicine*, 334(5), pp.292–5.

Coppari, R. et al., 2005. The hypothalamic arcuate nucleus: A key site for mediating leptin's effects on glucose homeostasis and locomotor activity. *Cell Metabolism*, 1(1), pp.63–72.

Costantini, C. et al., 2007. A reversible form of lysine acetylation in the ER and Golgi lumen controls the molecular stabilization of BACE1. *The Biochemical journal*, 407(3), pp.383–395.

Covey, S.D. et al., 2006. The pancreatic β cell is a key site for mediating the effects of leptin on glucose homeostasis. *Cell Metabolism*, 4(4), pp.291–302.

Cowley, M.A. et al., 2001. Leptin activates anorexigenic POMC neurons through a neural network in the arcuate nucleus. *Nature*, 411(6836), pp.480–484.

Creemers, J.W.M. et al., 2001. Processing of β-Secretase by Furin and Other Members of the Proprotein Convertase Family. *Journal of Biological Chemistry*, 276(6), pp.4211–4217.

Cui, Y. et al., 2004. Essential Role of STAT3 in Body Weight and Glucose Homeostasis Essential Role of STAT3 in Body Weight and Glucose Homeostasis. *Molecular and cellular biology*, 24(1), pp.258–269.

Delgado, T.C., 2013. Glutamate and GABA in Appetite Regulation. *Frontiers in endocrinology*, 4(August), p.103.

Dhillon, H. et al., 2006. Leptin directly activates SF1 neurons in the VMH, and this action by leptin is required for normal body-weight homeostasis. *Neuron*, 49(2), pp.191–203.

Dietrich, M.O. & Horvath, T.L., 2013. Hypothalamic control of energy balance: insights into the role of synaptic plasticity. *Trends Neurosci*, 36(2), pp.65–73.

Dislich, B. & Lichtenthaler, S.F., 2012. The membrane-bound aspartyl protease BACE1: Molecular and functional properties in Alzheimer's disease and beyond. *Frontiers in Physiology*, 3 FEB.

Dominguez, D. et al., 2005. Phenotypic and biochemical analyses of BACE1- and BACE2-deficient mice. *The Journal of biological chemistry*, 280(35), pp.30797–806.

Donato Jr., J., Frazao, R. & Elias, C.F., 2010. The PI3K signaling pathway mediates the biological effects of leptin. *Arquivos Brasileiros De Endocrinologia E Metabologia*, 54(7), pp.591–602.

Douglass, J. et al., 1995. PCR differential display identifies a rat brain mRNA that is transcriptionally regulated by cocaine and amphetamine. *The Journal of neuroscience*, 15(3 Pt 2), pp.2471–2481.

Dresner, a et al., 1999. Effects of free fatty acids on glucose transport and IRS-1-associated phosphatidylinositol 3-kinase activity. *The Journal of clinical investigation*, 103(2), pp.253–259.

Duan, W., 2013. Sirtuins: From metabolic regulation to brain aging. *Frontiers in Aging Neuroscience*, 5(JUL), pp.1–13.

Dunbar, J. et al., 2005. Hypothalamic agouti-related protein immunoreactivity in food-restricted, obese, and insulin-treated animals: Evidence for glia cell localization. *Experimental Neurology*, 191(1), pp.184–192.

Eketjäll, S. et al., 2013. AZ-4217: a high potency BACE inhibitor displaying acute central efficacy in different in vivo models and reduced amyloid deposition in Tg2576 mice. *The Journal of neuroscience*, 33(24), pp.10075–84.

Elchebly, M. et al., 1999. Increased insulin sensitivity and obesity resistance in mice lacking the protein tyrosine phosphatase-1B gene. *Science*, 283(5407), pp.1544–1548.

Elder, G.A. et al., 2010. Transgenic Mouse Models of Alzheimer's Disease. *The Mount Sinai journal of medicine, New York*, 77(2), pp.69–81.

El-Haschimi, K. et al., 2000. Two defects contribute to hypothalamic leptin resistance in mice with diet-induced obesity. *The Journal of Clinical Investigation*, 105(12), pp.1827–1832.

Elias, C.F. et al., 1998. Chemically defined projections linking the Mediobasal Hypothalamus and the Lateral Hypothalamic Area. *The Journal of Comparative Neurology*, 402(4), pp.442–459.

Elmquist, J.K. et al., 1998. Leptin activates distinct projections from the dorsomedial and ventromedial hypothalamic nuclei. *Proceedings of the National Academy of Sciences of the United States of America*, 95(2), pp.741–746.

Elmquist, J.K. et al., 1999. From lesions to leptin: hypothalamic control of food intake and body weight. *Neuron*, 22(2), pp.221–232.

Enriori, P.J. et al., 2007. Diet-induced obesity causes severe but reversible leptin resistance in arcuate melanocortin neurons. *Cell Metabolism*, 5(3), pp.181–194.

Erickson, J.C. et al., 1996. Sensitivity to leptin and susceptibility to seizures of mice lacking neuropeptide Y. *Nature*, 381(6581), pp.415–421.

Fan, W. et al., 2010. FoxO1 regulates Tlr4 inflammatory pathway signalling in macrophages. *The EMBO journal*, 29(24), pp.4223–4236.

Farooqi, I.S. et al., 2000. Dominant and recessive inheritance of morbid obesity associated with melanocortin 4 receptor deficiency. *The Journal of clinical investigation*, 106(2), pp.271–279.

Farooqi, I.S. et al., 1999. Effects of recombinant leptin therapy in a child with congenital leptin deficiency. *New England Journal of Medicine*, 341(12), pp.879–884.

Farris, W. et al., 2003. Insulin-degrading enzyme regulates the levels of insulin, amyloid beta-protein, and the beta-amyloid precursor protein intracellular domain in vivo. *Proceedings of the National Academy of Sciences of the United States of America*, 100(7), pp.4162–4167.

Fei, H. et al., 1997. Anatomic localization of alternatively spliced leptin receptors (Ob-R) in mouse brain and other tissues. *Proceedings of the National Academy of Sciences of the United States of America*, 94(13), pp.7001–7005.

Fekete, C. et al., 2000. alpha-Melanocyte-stimulating hormone is contained in nerve terminals innervating thyrotropin-releasing hormone-synthesizing neurons in the hypothalamic paraventricular nucleus and prevents fasting-induced suppression of prothyrotropin-releasing hormone ge. *The Journal of neuroscience : the official journal of the Society for Neuroscience*, 20(4), pp.1550–1558.

Fekete, C. et al., 2001. Neuropeptide Y has a central inhibitory action on the hypothalamic-pituitary-thyroid axis. *Endocrinology*, 142(6), pp.2606–2613.

Fitzpatrick, A.L. et al., 2009. Midlife and late-life obesity and the risk of dementia: cardiovascular health study. *Archives of Neurology*, 66(3), pp.336–342.

Fleischman, A. et al., 2008. Salsalate improves glycemia and inflammatory parameters in obese young adults. *Diabetes Care*, 31(2), pp.289–294.

Flier, J.S. & Maratos-Flier, E., 1998. Obesity and the Hypothalamus: Novel Peptides for New Pathways. *Cell*, 92(4), pp.437–440.

Francis, R. et al., 2002. aph-1 and pen-2 are required for Notch pathway signaling, gamma-secretase cleavage of betaAPP, and presenilin protein accumulation. *Developmental cell*, 3(1), pp.85–97.

Fukumoto, H. & Cheung, B., 2002. β-Secretase protein and activity are increased in the neocortex in Alzheimer disease. *Archives of Neurology*, 59(9), pp.1381-1389.

Funahashi, H. et al., 2003. Hypothalamic neuronal networks and feeding-related peptides involved in the regulation of feeding. *Anatomical science international / Japanese Association of Anatomists*, 78(3), pp.123–138.

Funahashi, H. et al., 2000. Morphological evidence for neural interactions between leptin and orexin in the hypothalamus. *Regulatory Peptides*, 92(1-3), pp.31–35.

Glenner, G.G. & Wong, C.W., 1984. Alzheimer's disease: initial report of the purification and characterization of a novel cerebrovascular amyloid protein. *Biochemical and Biophysical Research Communications*, 120(3), pp.885–89.

Gold, R., 1973. Hypothalamic obesity: the myth of the ventromedial nucleus. *Science*, 182, pp.482–490.

Gorospe, E.C. & Dave, J.K., 2007. The risk of dementia with increased body mass index. *Age and ageing*, 36(1), pp.23–9.

Gregor, M.F. & Hotamisligil, G.S., 2011. Inflammatory mechanisms in obesity. *Annual review of immunology*, 29, pp.415–445.

Grundke-Iqbal, I. et al., 1986. Abnormal phosphorylation of the microtubule-associated protein tau (tau) in Alzheimer cytoskeletal pathology. *Proceedings of the National Academy of Sciences of the United States of America*, 83(13), pp.4913–4917.

Grundlingh, J. et al., 2011. 2,4-Dinitrophenol (DNP): A Weight Loss Agent with Significant Acute Toxicity and Risk of Death. *Journal of Medical Toxicology*, 7(3), pp.205–212.

Guo, H. et al., 2015. Inflammasomes: mechanism of action, role in disease, and therapeutics. *Nature Medicine*, 21(7), pp.677–687.

Hahn, T.M. et al., 1998. Coexpression of Agrp and NPY in fasting-activated hypothalamic neurons. *Nature Neuroscience*, 1(4)pp.271-272.

Haigis, M.C. & Sinclair, D. a, 2010. Mammalian Sirtuins: Biological Insights and Disease Relevance. *Molecular Biology*, (5), pp.253–295.

Hâkansson, M.L. et al., 1998. Leptin receptor immunoreactivity in chemically defined target neurons of the hypothalamus. *The Journal of neuroscience*, 18(1), pp.559–572.

Halaas, J.L. et al., 1997. Physiological response to long-term peripheral and central leptin infusion in lean and obese mice. *Proceedings of the National Academy of Sciences of the United States of America*, 94(16), pp.8878–8883.

Halaas, J.L. et al., 1995. Weight-reducing effects of th plasma-protein encoded by the obese gene. *Science*, 269(5223), pp.543–546.

Hamilton, D.L. et al., 2014. Altered amyloid precursor protein processing regulates glucose uptake and oxidation in cultured rodent myotubes. *Diabetologia*, 57(8), pp.1684–1692.

Haniu, M. et al., 2000. Characterization of Alzheimer's beta-secretase protein BACE - A pepsin family member with unusual properties. *Journal of Biological Chemistry*, 275(28), pp.21099–21106.

Harada, H. et al., 2006. Beta-site APP cleaving enzyme 1 (BACE1) is increased in remaining neurons in Alzheimer's disease brains. *Neuroscience Research*, 54(1), pp.24–29.

Hardy, J. & Higgins, G., 1992. Alzheimer's disease: the amyloid cascade hypothesis. *Science*, 256(5054), pp.184–185.

Hardy, J.A. & Higgins, G.A., 1992. Alzheimer's Disease- The amyloid cascade hypothesis. *Science*, 256(5054), pp.184–185.

Harris, R.B. et al., 1998. A leptin dose-response study in obese (ob/ob) and lean (+/?) mice. *Endocrinology*, 139(1), pp.8–19.

Harrison, S.M. et al., 2003. BACE1 (β-secretase) transgenic and knockout mice: identification of neurochemical deficits and behavioral changes. *Molecular and Cellular Neuroscience*, 24(3), pp.646–655.

Hartmann, D. et al., 2002. The disintegrin/metalloprotease ADAM 10 is essential for Notch signalling but not for alpha-secretase activity in fibroblasts. *Human molecular genetics*, 11(21), pp.2615–2624.

Hawke, Z. et al., 2009. PACAP neurons in the hypothalamic ventromedial nucleus are targets of central leptin signaling. *The Journal of neuroscience*, 29(47), pp.14828–14835.

Van Heek, M. et al., 1997. Diet-induced obese mice develop peripheral, but not central, resistance to leptin. *The Journal of clinical investigation*, 99(3), pp.385–90.

Heide, L.P. et al., 2006. Insulin signaling in the central nervous system : Learning to survive. *Progress in Neurobiology*, 79(4), pp.205–221.

Hemming, M.L. et al., 2009. Identification of β-secretase (BACE1) substrates using quantitative proteomics. *PLoS ONE*, 4(12).

Heneka, M.T. et al., 2014. Innate immune activation in neurodegenerative disease. *Nature reviews. Immunology*, 14(7), pp.463–77.

Heyden, a. et al., 2008. Abnormal axonal guidance and brain anatomy in mouse mutants for the cell recognition molecules close homolog of L1 and NgCAM-related cell adhesion molecule. *Neuroscience*, 155(1), pp.221–233.

Heymsfield, S.B. et al., 1999. Recombinant leptin for weight loss in obese and lean adults - A randomized, controlled, dose-escalation trial. *Jama-Journal of the American Medical Association*, 282(16), pp.1568–1575.

Hill, J.W. et al., 2008. Acute effects of leptin require PI3K signaling in hypothalamic proopiomelanocortin neurons in mice. *Journal of Clinical Investigation*, 118(5), pp.1796–1805.

Ho, L. et al., 2004. Diet-induced insulin resistance promotes amyloidosis in a transgenic mouse model of Alzheimer's disease. *Faseb Journal*, 18(7), pp.902–904.

Horvath, T.L. et al., 2010. Synaptic input organization of the melanocortin system predicts diet-induced hypothalamic reactive gliosis and obesity. *Proceedings of the National Academy of Sciences of the United States of America*, 107(33), pp.14875–14880.

Horvath, T.L., 2005. The hardship of obesity: a soft-wired hypothalamus. *Nature neuroscience*, 8(5), pp.561–565.

Howard, L. et al., 1996. Molecular cloning of MADM: a catalytically active mammalian disintegrin-metalloprotease expressed in various cell types. *The Biochemical journal*, 317 (Pt 1, pp.45–50.

Hu, X. et al., 2006. Bace1 modulates myelination in the central and peripheral nervous system. *Nature Neuroscience*, 9(12), pp.1520–1525.

Hu, X. et al., 2013. BACE1 regulates hippocampal astrogenesis via the Jagged1-Notch pathway. *Cell Reports*, 4(1), pp.40–49.

Huse, J.T. et al., 2000. Maturation and endosomal targeting of beta-site amyloid precursor protein-cleaving enzyme - The Alzheimer's disease beta-secretase. *Journal of Biological Chemistry*, 275(43), pp.33729–33737.

Hussain, I. et al., 2000. ASP1 (BACE2) cleaves the amyloid precursor protein at the beta-secretase site. *Molecular and cellular neurosciences*, 16(5), pp.609–619.

Hussain, I. et al., 1999. Identification of a novel aspartic protease (Asp 2) as beta-secretase. *Molecular and Cellular Neuroscience*, 14(6), pp.419–427.

Huszar, D. et al., 1997. Targeted disruption of the melanocortin-4 receptor results in obesity in mice. *Cell*, 88(1), pp.131–141.

Inutsuka, A. & Yamanaka, A., 2013. The physiological role of orexin/hypocretin neurons in the regulation of sleep/wakefulness and neuroendocrine functions. *Frontiers in Endocrinology*, 4(MAR), pp.1–10.

Iqbal, K. et al., 2005. Tau pathology in Alzheimer disease and other tauopathies. *Biochimica et Biophysica Acta - Molecular Basis of Disease*, 1739, pp.198–210.

Janson, J. et al., 2004. Increased Risk of Type 2 Diabetes in Alzheimer Disease. *Diabetes*, 53(2), pp.474-481.

Jeppsson, F. et al., 2012. Discovery of AZD3839, a potent and selective BACE1 inhibitor clinical candidate for the treatment of alzheimer disease. *Journal of Biological Chemistry*, 287(49), pp.41245–41257.

Jimenez, S. et al., 2011. Age-dependent accumulation of soluble amyloid beta (Abeta) oligomers reverses the neuroprotective effect of soluble amyloid precursor protein-alpha (sAPP(alpha)) by modulating phosphatidylinositol 3-kinase (PI3K)/Akt-GSK-3beta pathway in Alzheimer mouse m. *The Journal of biological chemistry*, 286(21), pp.18414–18425.

Johnstone, M. et al., 1999. A central role for astrocytes in the inflammatory response to beta-amyloid; chemokines, cytokines and reactive oxygen species are produced. *Journal of neuroimmunology*, 93(1-2), pp.182–193.

Jonsson, T. et al., 2012. A mutation in APP protects against Alzheimer's disease and age-related cognitive decline. *Nature*, 488(7409), pp.96–99.

Julien, C. et al., 2010. High-fat diet aggravates amyloid-beta and tau pathologies in the 3xTg-AD mouse model. *Neurobiology of aging*, 31(9), pp.1516–31.

Kamenetz, F. et al., 2003. APP Processing and Synaptic Function. *Neuron*, 37(6), pp.925–937.

Kang, J. et al., 1987. The precursor of Alzhiemer's disease amyloid A4 proteing resembles a cell-surface receptor. *Nature*, 325(6106), pp.733–736.

Kellerer, M. et al., 1997. Leptin activates PI-3 kinase in C2C12 myotubes via janus kinase-2 (JAK-2) and insulin receptor substrate-2 (IRS-2) dependent pathways. *Diabetologia*, 40(11), pp.1358–1362.

Kim, K.W. et al., 2012. FOXO1 in the ventromedial hypothalamus regulates energy balance. *Journal of Clinical Investigation*, 122(7), pp.2578–2589.

Kim, K.W. et al., 2011. Steroidogenic factor 1 directs programs regulating diet-induced thermogenesis and leptin action in the ventral medial hypothalamic nucleus. *Proceedings of the National Academy of Sciences of the United States of America*, 108(26), pp.10673–10678.

Kim, M. et al., 2009. Potential late-onset Alzheimer's disease-associated mutations in the ADAM10 gene attenuate α-secretase activity. *Human Molecular Genetics*, 18(20), pp.3987–3996.

Kim, M.-S. et al., 2006. Role of hypothalamic Foxo1 in the regulation of food intake and energy homeostasis. *Nature neuroscience*, 9(7), pp.901–906.

Kim, Y.B. et al., 2000. In vivo administration of leptin activates signal transduction directly in insulin-sensitive tissues: Overlapping but distinct pathways from insulin. *Endocrinology*, 141(7), pp.2328–2339.

King, B.M., 2006. The rise, fall, and resurrection of the ventromedial hypothalamus in the regulation of feeding behavior and body weight. *Physiology and Behavior*, 87(2), pp.221–244.

Kirchgessner, a L. & Liu, M., 1999. Orexin synthesis and response in the gut. *Neuron*, 24(4), pp.941–951.

Kitazume, S. et al., 2001. Alzheimer's beta-secretase, beta-site amyloid precursor protein-cleaving enzyme, is responsible for cleavage secretion of a Golgi-resident sialyltransferase. *Proceedings of the National Academy of Sciences of the United States of America*, 98(24), pp.13554–13559.

Kloek, C. et al., 2002. Regulation of Jak kinases by intracellular leptin receptor sequences. *The Journal of biological chemistry*, 277(44), pp.41547–55.

Knight, E.M. et al., 2014. High-fat diet-induced memory impairment in triple-transgenic Alzheimer's disease (3xTgAD) mice isindependent of changes in amyloid and tau pathology. *Neurobiology of Aging*, 35(8), pp.1821–1832.

Kohjima, M., Sun, Y. & Chan, L., 2010. Increased food intake leads to obesity and insulin resistance in the Tg2576 Alzheimer's disease mouse model. *Endocrinology*, 151(4), pp.1532–1540.

Kojro, E. et al., 2001. Low cholesterol stimulates the nonamyloidogenic pathway by its effect on the alpha -secretase ADAM 10. *Proceedings of the National Academy of Sciences of the United States of America*, 98(10), pp.5815–5820.

Kong, D. et al., 2012. GABAergic RIP-Cre neurons in the arcuate nucleus selectively regulate energy expenditure. *Cell*, 151(3), pp.645–657.

Kopke, E. et al., 1993. Microtubule-associated protein tau. Abnormal phosphorylation of a non- paired helical filament pool in Alzheimer disease. *Journal of Biological Chemistry*, 268(32), pp.24374–24384.

Krashes, M.J. et al., 2011. Rapid, reversible activation of AgRP neurons drives feeding behaviour in mice. *Journal of Clinical Investigation*, 121(4), pp.1424–1428.

Krude, H. et al., 1998. Severe early-onset obesity, adrenal insufficiency and red hair pigmentation caused by POMC mutations in humans. *Nature genetics*, 19(2), pp.155–157.

Kuhn, P.H. et al., 2007. Regulated intramembrane proteolysis of the interleukin-1 receptor II by α-, β-, and γ-secretase. *Journal of Biological Chemistry*, 282(16), pp.11982–11995.

Kuhn, P.-H. et al., 2010. ADAM10 is the physiologically relevant, constitutive alpha-secretase of the amyloid precursor protein in primary neurons. *The EMBO journal*, 29(17), pp.3020–3032.

Kushi, a et al., 1998. Obesity and mild hyperinsulinemia found in neuropeptide Y-Y1 receptor-deficient mice. *Proceedings of the National Academy of Sciences of the United States of America*, 95(26), pp.15659–15664.

Kwon, H.Y. et al., 1994. Molecular structure and chromosomal mapping of the human homolog of the agouti gene. *Proceedings of the National Academy of Sciences of the United States of America*, 91(21), pp.9760–9764.

Laird, F.M. et al., 2005. BACE1, a major determinant of selective vulnerability of the brain to amyloid-beta amyloidogenesis, is essential for cognitive, emotional, and synaptic functions. *The Journal of neuroscience*, 25(50), pp.11693–709.

Lamb, B.T. et al., 1997. Altered metabolism of familial Alzheimer ' s disease-linked amyloid precursor protein variants in yeast artificial chromosome transgenic mice. *Human Molecular Genetics*, 6(9), pp.1535–1541.

Lamb, B.T. et al., 1999. Amyloid production and deposition in mutant amyloid precursor protein and presenilin-1 yeast artificial chromosome transgenic mice. *Nature Neuroscience*, 2(8), pp.695–697.

Lammich, S. et al., 1999. Constitutive and regulated alpha-secretase cleavage of Alzheimer's amyloid precursor protein by a disintegrin metalloprotease. *Proceedings of the National Academy of Sciences of the United States of America*, 96(7), pp.3922–3927.

Lee, G.H. et al., 1996. Abnormal splicing of the leptin receptor in diabetic mice. *Nature*, 379(6566), pp.632–635.

Lee, Y.-H. et al., 2008. Amyloid precursor protein expression is upregulated in adipocytes in obesity. *Obesity*, 16(7), pp.1493–500.

Leshan, R.L., Bjo, M. & Rebecca, L., 2006. Leptin Receptor Signaling and Action in the Central Nervous System. *Obesity*, 14(August) Supplemental 5, pp.208S-212S.

Li, C. et al., 1998. Absence of Soluble Leptin Receptor in Plasma from db Pas / db Pas and Other db / db Mice. *Journal of Biological Chemistry*, 273(16), pp.10078–10082.

Li, C. et al., 2000. Corticotropin releasing hormone neurons in the paraventricular nucleus are direct targets for neuropeptide Y neurons in the arcuate nucleus: An anterograde tracing study. *Brain Research*, 854(1-2), pp.122–129.

Li, L. & Hölscher, C., 2007. Common pathological processes in Alzheimer disease and type 2 diabetes: a review. *Brain research reviews*, 56(2), pp.384–402.

Li, R. et al., 2004. Amyloid beta peptide load is correlated with increased beta-secretase activity in sporadic Alzheimer's disease patients. *Proceedings of the National Academy of Sciences of the United States of America*, 101(10), pp.3632-7.

Li, Z. et al., 2005. Meta-analysis: pharmacologic treatment of obesity. *Annals of Internal Medicine*, 142(7), pp.532–46.

Liao, G. et al., 2012. Dendritically targetd Bdnf mRNA is essential for energy balance and response to leptin. *Nature Medicine*, 18(4), pp.564–571.

Lichtenthaler, S.F. et al., 2003. The cell adhesion protein P-selectin glycoprotein ligand-1 is a substrate for the aspartyl protease BACE1. *Journal of Biological Chemistry*, 278(49), pp.48713–48719.

Lin, X. et al., 2000. Human aspartic protease memapsin 2 cleaves the beta-secretase site of beta-amyloid precursor protein. *Proceedings of the National Academy of Sciences of the United States of America*, 97(4), pp.1456–1460.

Loh, K. et al., 2011. Elevated hypothalamic TCPTP in obesity contributes to cellular leptin resistance. *Cell Metabolism*, 14(5), pp.684–699.

Lu, D. et al., 1994. Agouti protein is an antagonist of the melanocyte-stimulating-hormone receptor. *Nature*, 371(6500), pp.799–802.

Luchsinger, J. & Gustafson, D., 2009. Adiposity, type 2 diabetes, and Alzheimer's disease. *Journal of Alzheimer's Disease*, 16(4), pp.693–704.

Luo, Y. et al., 2001. Mice deficient in BACE1, the Alzheimer's beta-secretase, have normal phenotype and abolished beta-amyloid generation. *Nature Neuroscience*, 4(3), pp.231–232.

Maffei, M. et al., 1995. Leptin levels in human and rodent: measurement of plasma leptin and ob RNA in obese and weight-reduced subjects. *Nature medicine*, 1(11), pp.1155–1161.

Majdic, G. et al., 2002. Knockout mice lacking steroidogenic factor 1 are a novel genetic model of hypothalamic obesity . *Endocrinology* , 143 (0013-7227 (Print)), pp.607–614.

Manolopoulos, K.N. et al., 2010. Linking Alzheimer's disease to insulin resistance: the FoxO response to oxidative stress. *Molecular psychiatry*, 15(11), pp.1046–1052.

Marcinkiewicz, M. & Seidah, N.G., 2000. Coordinated expression of beta-amyloid precursor protein and the putative beta-secretase BACE and alpha-secretase ADAM10 in mouse and human brain. *Journal of neurochemistry*, 75(5), pp.2133–2143.

Marquer, C. et al., 2011. Local cholesterol increase triggers amyloid precursor protein-Bace1 clustering in lipid rafts and rapid endocytosis. *The FASEB journal*, 25(4), pp.1295–1305.

Martin, R.L. et al., 2000. Leptin resistance is associated with hypothalamic leptin receptor mRNA and protein downregulation. *Metabolism: clinical and experimental*, 49(11), pp.1479–1484.

Marwarha, G. et al., 2014. Leptin attenuates BACE1 expression and amyloid-beta genesis via the activation of SIRT1 signaling pathway. *Biochim et Biophysica Acta*, 1842(9), pp.1587–1595.

Marwarha, G. et al., 2014. Leptin attenuates BACE1 expression and amyloid-β genesis via the activation of SIRT1 signaling pathway. *Biochimica et Biophysica Acta*, 1842(9), pp.1587–95.

Marwarha, G. et al., 2010. Leptin reduces the accumulation of Abeta and phosphorylated tau induced by 27-hydroxycholesterol in rabbit organotypic slices. *Journal of Alzheimer's Disease*, 19(3), pp.1007–1019.

Marwarha, G. et al., 2010. β-Amyloid regulates leptin expression and tau phosphorylation through the mTORC1 signaling pathway. *Journal of neurochemistry*, 115(2), pp.373–84.

Masters, C.L. et al., 1985. Amyloid plaque core protein in Alzheimer disease and Down syndrome. *Proceedings of the National Academy of Sciences of the United States of America*, 82(12), pp.4245–4249.

Mattson, M.P. et al., 1999. Secreted form of amyloid precursor protein enhances basal glucose and glutamate transport and protects against oxidative impairment of

glucose and glutamate transport in synaptosomes by a cyclic GMP-mediated mechanism. *Journal of Neurochemistry*, 73(2), pp.532–537.

McClellan, K.M. et al., 2006. Development of the ventromedial nucleus of the hypothalamus. *Frontiers in Neuroendocrinology*, 27(2), pp.193–209.

McConlogue, L. et al., 2007. Partial reduction of BACE1 has dramatic effects on Alzheimer plaque and synaptic pathology in APP Transgenic Mice. *The Journal of biological chemistry*, 282(36), pp.26326–34.

Meakin, P.J. et al., 2012. Reduction in BACE1 decreases body weight, protects against diet-induced obesity and enhances insulin sensitivity in mice. *Biochemical Journal*, 441(1), pp.285–296.

Meister, B., 2007. Neurotransmitters in key neurons of the hypothalamus that regulate feeding behavior and body weight. *Physiology & behavior*, 92(1-2), pp.263–71.

Meziane, H. et al., 1998. Memory-enhancing effects of secreted forms of the beta-amyloid precursor protein in normal and amnestic mice. *Proceedings of the National Academy of Sciences of the United States of America*, 95(21), pp.12683–12688.

Miller, R.S., Diaczok, D. & Cooke, D.W., 2007. Repression of GLUT4 expression by the endoplasmic reticulum stress response in 3T3-L1 adipocytes. *Biochemical and Biophysical Research Communications*, 1(362), pp.188–192.

Millington, G.W., 2007. The role of proopiomelanocortin (POMC) neurones in feeding behaviour. *Nutrition & metabolism*, 4, p.18.

Mittendorfer, B. et al., 2011. Recombinant Human Leptin Treatment Does not Improve insulin action in obese subjects with T2D. *Diabetes*, 60(5), pp.1–4.

Mizuno, T.M. et al., 1998. Hypothalamic pro-opiomelanocortin mRNA is reduced by fasting in ob/ob and db/db mice, but is stimulated by leptin. *Diabetes*, 47(2), pp.294–297.

Mody, N. et al., 2011. Susceptibility to diet-induced obesity and glucose intolerance in the APP SWE/PSEN1 A246E mouse model of Alzheimer's disease is associated with increased brain levels of protein tyrosine phosphatase 1B (PTP1B) and retinol-binding protein 4 (RBP4), and basal phosphorylation of S6 ribosomal protein. *Diabetologia*, 54(8), pp.2143–2151.

Mori, H. et al., 2004. Socs3 deficiency in the brain elevates leptin sensitivity and confers resistance to diet-induced obesity. *Nature medicine*, 10(7), pp.739–743.

Morimoto, T. et al., 1998. Involvement of amyloid precursor protein in functional synapse formation in cultured hippocampal neurons. *Journal of neuroscience research*, 51(2), pp.185–195.

Mullan, M. et al., 1992. A pathogenic mutation for probable Alzheimer's disease in the APP gene at the N-terminus of beta-amyloid. *Nature genetics*, 1(5), pp.345–347.

Mullen, R.J. et al., 1992. NeuN, a neuronal specific nuclear protein in vertebrates. *Development*, 116(1), pp.201–211.

Münzberg, H., Flier, J.S. & Bjørbæk, C., 2004. Region-specific leptin resistance within the hypothalamus of diet-induced obese mice. *Endocrinology*, 145(11), pp.4880–4889.

Münzberg, H. & Myers, M.G., 2005. Molecular and anatomical determinants of central leptin resistance. *Nature neuroscience*, 8(5), pp.566–570.

Musatov, S. et al., 2007. Silencing of estrogen receptor alpha in the ventromedial nucleus of hypothalamus leads to metabolic syndrome. *Proceedings of the National Academy of Sciences of the United States of America*, 104(7), pp.2501–2506.

Nakae, J. et al., 2008. The FoxO transcription factors and metabolic regulation. *FEBS Letters*, 582(1), pp.54–67.

Neary, N.M. et al., 2004. Appetite regulation: From the gut to the hypothalamus. *Clinical Endocrinology*, 60(2), pp.153–160.

Nillni, E. a., 2007. Minireview: Regulation of prohormone convertases in hypothalamic neurons: Implications for prothyrotropin-releasing hormone and proopiomelanocortin. *Endocrinology*, 148(9), pp.4191–4200.

Niswender, K.D. et al., 2001. Intracellular signalling. Key enzyme in leptin-induced anorexia. *Nature*, 413(6858), pp.794–795.

Niswender, K.D. & Schwartz, M.W., 2003. Insulin and leptin revisited: adiposity signals with overlapping physiological and intracellular signaling capabilities. *Frontiers in Neuroendocrinology*, 24(1), pp.1–10.

O'Brien, R.J. & Wong, P.C., 2011. Amyloid precursor protein processing and Alzheimer's disease. *Annual review of neuroscience*, 34, pp.185–204.

Olney, J.W., 1969. Brain lesions, obesity, and other disturbances in mice treated with monosodium glutamate. *Science (New York, N.Y.)*, 164(880), pp.719–721.

Olofsson, L.E. et al., 2013. Modulation of AgRP-neuronal function by SOCS3 as an initiating event in diet-induced hypothalamic leptin resistance. *Proceedings of the National Academy of Sciences of the United States of America*, 110(8), pp.E697–706.

Ozcan, U. et al., 2006. Chemical chaperones reduce ER stress and restore glucose homeostasis in a mouse model of type 2 diabetes. *Science*, 313(5790), pp.1137–1140.

Ozcan, U. et al., 2004. Endoplasmic reticulum stress links obesity, insulin action, and type 2 diabetes. *Science*, 306(5695), pp.457–461.

Padwal, R.S. & Majumdar, S.R., 2007. Drug treatments for obesity: orlistat, sibutramine, and rimonabant. *Lancet*, 369(9555), pp.71-7.

Parker, K.L. & Schimmer, B.P., 1997. Steroidogenic factor 1: a key determinant of endocrine development and function. *Endocrine reviews*, 18(3), pp.361–377.

Pastorino, L. et al., 2002. The carboxyl-terminus of BACE contains a sorting signal that regulates BACE trafficking but not the formation of total A(beta). *Molecular and cellular neurosciences*, 19(2), pp.175–185.

Patterson, C.M. et al., 2012. Leptin action via LepR-b Tyr1077 contributes to the control of energy balance and female reproduction. *Molecular Metabolism*, 1(1-2), pp.61–69.

Pinto, S. et al., 2004. Rapid rewiring of arcuate nucleus feeding circuits by leptin. *Science*, 304(5667), pp.110–115.

Plum, L. et al., 2009. The Obesity Susceptibility Gene Carboxypeptidase E Links FoxO1 Signaling in Hypothalamic Pro-opiomelanocortin Neurons with Regulation of Food Intake. *Nature Medicine*, 15(10), pp.1195–1201.

Porte, D., Baskin, D.G. & Schwartz, M.W., 2002. Leptin and insulin action in the central nervous system. *Nutrition reviews*, 60(10 Pt 2), pp.S20–S29; discussion S68–S84, 85–87.

Postina, R. et al., 2004. A disintegrin-metalloproteinase prevents amyloid plaque formation and hippocampal defects in an Alzheimer disease mouse model. *The Journal of clinical investigation*, 113(10), pp.1456–1464.

Powers, M.E. et al., 2012. ADAM10 mediates vascular injury induced by staphylococcus aureus alpha-hemolysin. *Journal of Infectious Diseases*, 206(3), pp.352–356.

Pritchard, L.E. et al., 2002. Pro-opiomelanocortin processing in the hypothalamus: Impact on melanocortin signalling and obesity. *Journal of Endocrinology*, 172(3), pp.411–421.

Pruessmeyer, J. & Ludwig, A., 2009. The good, the bad and the ugly substrates for ADAM10 and ADAM17 in brain pathology, inflammation and cancer. *Seminars in Cell and Developmental Biology*, 20(2), pp.164–174.

Qian, S. et al., 2002. Neither Agouti-Related Protein nor Neuropeptide Y Is Critically Required for the Regulation of Energy Homeostasis in Mice Neither Agouti-Related Protein nor Neuropeptide Y Is Critically Required for the Regulation of Energy Homeostasis in Mice. *Society*, 22(14), pp.5027–5035.

Qizilbash, N. et al., 2015. BMI and risk of dementia in two million people over two decades: a retrospective cohort study. *The Lancet Diabetes & Endocrinology*, 3(6), pp.431–436.

Qu, D. et al., 1996. A role for melanin-concentrating hormone in the central regulation of feeding behaviour. *Nature*, 380(6571), pp.243–247.

Reibmant, J. et al., 1991. Transforming growth factor beta 1 , a potent chemoattractant for human neutrophils, bypasses classic signal-transduction pathways. *Proceedings of the National Academy of Sciences of the United States of America*, 88(15), pp.6805–6809.

Roberds, S.L. et al., 2001. BACE knockout mice are healthy despite lacking the primary β -secretase activity in brain : implications for Alzheimer's disease therapeutics. *Human Molecular Genetics*, 10(12), pp.1317–1324.

Rolls, B.J. et al., 1998. Sibutramine reduces food intake in non-dieting women with obesity. *Obesity research*, 6(1), pp.1–11.

Rossi, J. et al., 2011. Melanocortin-4 receptors expressed by cholinergic neurons regulate energy balance and glucose homeostasis. *Cell Metabolism*, 13(2), pp.195–204.

Rossi, M. et al., 1998. A C-terminal fragment of Agouti-related protein increases feeding and antagonizes the effect of alpha-melanocyte stimulating hormone in vivo. *Endocrinology*, 139(10), pp.4428–4431.

Routh, V.H., 2010. Glucose sensing neurons in the ventromedial hypothalamus. *Sensors*, 10(10), pp.9002–9025.

Sainsbury, A. et al., 2002. Y4 receptor knockout rescues fertility in ob/ob mice. *Genes and Development*, 16(9), pp.1077–1088.

Sakurai, T. et al., 1998. Orexins and orexin receptors: A family of hypothalamic neuropeptides and G protein-coupled receptors that regulate feeding behavior. *Cell*, 92(4), pp.573–585.

Samad, F. et al., 1997. Elevated Expression of Transforming Growth Factor-beta in Adipose Tissue from Obese Mice. *Molecular Medicine*, 3(1), pp.37–48.

Sankaranarayanan, S. et al., 2008. In Vivo β-Secretase 1 Inhibition Leads to Brain Abeta Lowering and Increased α-Secretase Processing of Amyloid Precursor Protein without effect on Neuregulin-1. *Journal of Pharmacology and Experimental Therapeutics*, 324(3), pp.957-69.

Sathya, M. et al., 2012. BACE1 in Alzheimer's disease. *Clinica Chimica Acta*, 414, pp.171–178.

Savonenko, A. V et al., 2008. Alteration of BACE1-dependent NRG1/ErB4 signaling and schizophrenia-like phenotypes in BACE1-null mice. *Proceedings of the National Academy of Sciences of the United States of America*, 105(14), pp.10–15.

Sawchenko, P.E., 1998. Toward a new neurobiology of energy balance, appetite, and obesity: The anatomists weigh in. *Journal of Comparative Neurology*, 402(4), pp.435–441.

Scheer, F. a J.L. et al., 2009. Adverse metabolic and cardiovascular consequences of circadian misalignment. *Proceedings of the National Academy of Sciences of the United States of America*, 106(11), pp.4453–4458.

Schulz, T.J. & Tseng, Y.-H., 2013. Brown adipose tissue: development, metabolism and beyond. *The Biochemical journal*, 453(2), pp.167–78.

Schwartz, M.W. et al., 2000. Control of food intake. *Nature*, 404(6778), pp.661–671.

Schwartz, M.W. et al., 1997. Leptin increases hypothalamic pro-opiomelanocortin mRNA expression in the rostral arcuate nucleus. *Diabetes*, 46(12), pp.2119–2123.

Seale, P. et al., 2011. Prdm16 determines the thermogenic program of subcutaneous white adipose tissue in mice. *The Journal of clinical investigation*, 121(1), pp.96–105.

Selkoe, D.J., 1991. The Molecular of Alzheimer ' s Pathology Disease Review. *Neuron*, 6, pp.487–498.

Shi, H. et al., 2004. Suppressor of cytokine signaling 3 is a physiological regulator of adipocyte insulin signaling. *Journal of Biological Chemistry*, 279(33), pp.34733–34740.

Shi, Y.C. et al., 2013. Arcuate NPY controls sympathetic output and BAT function via a relay of tyrosine hydroxylase neurons in the PVN. *Cell Metabolism*, 17(2), pp.236–248.

Shimada, M. et al., 1998. Mice lacking melanin-concentrating hormone are hypophagic and lean. *Nature*, 396(6712), pp.670–674.

Simons, M. et al., 1998. Cholesterol depletion inhibits the generation of beta-amyloid in hippocampal neurons. *Proceedings of the National Academy of Sciences of the United States of America*, 95(11), pp.6460–6464.

Sing, C.F. & Davignon, J., 1985. Role of the apolipoprotein E polymorphism in determining normal plasma lipid and lipoprotein variation. *American journal of human genetics*, 37(2), pp.268–285.

Singer, O. et al., 2005. Targeting BACE1 with siRNAs ameliorates Alzheimer disease neuropathology in a transgenic model. *Nature neuroscience*, 8(10), pp.1343–9.

Sinha, S. et al., 1999. Purification and cloning of amyloid precursor protein beta-secretase from human brain. *Nature*, 402(6761), pp.537–540.

Sinha, S. & Lieberburg, I., 1999. Cellular mechanisms of beta-amyloid production and secretion. *Proceedings of the National Academy of Sciences of the United States of America*, 96(20), pp.11049–11053.

Sipols, A.J. et al., 1995. Effect of intracerebroventricular insulin infusion on diabetic hyperphagia and hypothalamic neuropeptide gene expression. *Diabetes*, 44(2), pp.147–151.

Skovronsky, D.M. et al., 2001. Neuronal localization of the TNFα converting enzyme (TACE) in brain tissue and its correlation to amyloid plaques. *Journal of Neurobiology*, 49(1), pp.40–46.

Small, C.J. et al., 2001. Effects of chronic central nervous system administration of agouti-related protein in pair-fed animals. *Diabetes*, 50(2), pp.248-54.

Sobrino Crespo, C. et al., 2014. Peptides and food intake. *Frontiers in Endocrinology*, 5(58), p.58.

Sohn, J.W. et al., 2011. Serotonin 2C receptor activates a distinct population of arcuate pro-opiomelanocortin neurons via TRPC channels. *Neuron*, 71(3), pp.488–497.

Sohn, J.W. et al., 2013. Neuronal circuits that regulate feeding behavior and metabolism. *Trends in neurosciences*, 36(9), pp.504–12.

Song, J. et al., 2010. Brain expression of Cre recombinase driven by pancreas-specific promoters. *Genesis*, 48(11), pp.628–634.

De Souza, C.T. et al., 2005. Consumption of a fat-rich diet activates a proinflammatory response and induces insulin resistance in the hypothalamus. *Endocrinology*, 146(10), pp.4192–4199.

Spiegelman, B.M. & Flier, J.S., 2001. Obesity and the regulation of energy balance. *Cell*, 104(4), pp.531–543.

Stanley, S. a. et al., 2001. Actions of cocaine- and amphetamine-regulated transcript (CART) peptide on regulation of appetite and hypothalamo-pituitary axes in vitro and in vivo in male rats. *Brain Research*, 893(1-2), pp.186–194.

Stein, T.D. et al., 2004. Neutralization of transthyretin reverses the neuroprotective effects of secreted amyloid precursor protein (APP) in APPSW mice resulting in tau phosphorylation and loss of hippocampal neurons: support for the amyloid hypothesis. *The Journal of neuroscience*, 24(35), pp.7707–7717.

Stellar, E., 1994. The physiology of motivation. *Pscyhological Review*, 101(2), pp.301–311.

Stockley, J.H. & O'Neill, C., 2008. Understanding BACE1: Essential protease for amyloid-β production in Alzheimer's disease. *Cellular and Molecular Life Sciences*, 65(20), pp.3265–3289.

Strittmatter, W.J. et al., 1993. Apolipoprotein E: high-avidity binding to beta-amyloid and increased frequency of type 4 allele in late-onset familial Alzheimer disease. *Proceedings of the National Academy of Sciences of the United States of America*, 90(5), pp.1977–1981.

Sun, X. et al., 2006. Increased BACE1 maturation contributes to the pathogenesis of Alzheimer's disease in Down syndrome. *The FASEB journal*, 20(9), pp.1361–1368.

Sun, X. et al., 2012. Regulation of β-site APP-cleaving enzyme 1 gene expression and its role in Alzheimer's disease. *Journal of neurochemistry*, 120 Suppl , pp.62–70.

Surmi, B.K. et al., 2010. Absence of macrophage inflammatory protein-1{alpha} does not impact macrophage accumulation in adipose tissue of diet-induced obese mice. *American journal of physiology. Endocrinology and Metabolism*, 299(3), pp.E437–E445.

Surmi, B.K. & Hasty, A.H., 2008. Macrophage infiltration into adipose tissue: initiation, propagation and remodeling. *Future Lipidology*, 3(5), pp.545–556.

Surmi, B.K. & Hasty, A.H., 2010. The role of chemokines in recruitment of immune cells to the artery wall and adipose tissue. *Vascular pharmacology*, 52(1-2), pp.27–36.

Sutton, G.M. et al., 2006. Diet-genotype interactions in the development of the obese, insulin-resistant phenotype of C57BL/6J mice lacking melanocortin-3 or -4 receptors. *Endocrinology*, 147(5), pp.2183–2196.

Swanson, L.W. & Sawchenko, P.E., 1983. Hypothalamic integration: organization of the paraventricular and supraoptic nuclei. *Annual review of neuroscience*, 6, pp.269–324.

Swart, I. et al., 2002. Hypothalamic NPY , AGRP , and POMC mRNA responses to leptin and refeeding in mice. *Regulatory, Integrative and Comparitive Physiology*, 283(5), pp.1020–1026.

Sweeney, G., 2002. Leptin signalling. *Cellular Signalling*, 14(8), pp.655–663.

Tamagno, E. et al., 2002. Oxidative stress increases expression and activity of BACE in NT2 neurons. *Neurobiology of disease*, 10(3), pp.279–288.

Tamamaki, N. et al., 2003. Green fluorescent protein expression and colocalization with calretinin, parvalbumin, and somatostatin in the GAD67-GFP knock-in mouse. *The Journal of comparative neurology*, 467(1), pp.60–79.

Tan, J. & Evin, G., 2012. β-Site APP-cleaving enzyme 1 trafficking and Alzheimer's disease pathogenesis. *Journal of Neurochemistry*, 120(6), pp.869–880.

Tanahashi, H. & Tabira, T., 2001. Three novel alternatively spliced isoforms of the human beta-site amyloid precursor protein cleaving enzyme (BACE) and their effect on amyloid beta-peptide production. *Neuroscience Letters*, 307(1), pp.9–12.

Tartaglia, L.A. et al., 1995. Identification and Expression Cloning of a Leptin Receptor, OB-R. *Cell*, 83(7), pp.1263–1271.

Tartaglia, L.A., 1997. The leptin receptor. *The Journal of biological chemistry*, 272(10), pp.6093–6.

Tecott, L.H. et al., 1995. Eating disorder and epilepsy in mice lacking 5-HT2c serotonin receptors. *Nature*, 374(6522), pp.542–546.

Tesco, G. et al., 2007. Depletion of GGA3 Stabilizes BACE and Enhances β-Secretase Activity. *Neuron*, 54(5), pp.721–737.

Thaler, J.P. et al., 2012. Obesity is associated with hypothalamic injury in rodents and humans. *Journal of Clinical Investigation*, 122(1), pp.153–162.

Tippmann, F. et al., 2009. Up-regulation of the alpha-secretase ADAM10 by retinoic acid receptors and acitretin. *The FASEB journal*, 23(6), pp.1643–1654.

Tong, Q. et al., 2007. Synaptic Glutamate Release by Ventromedial Hypothalamic Neurons Is Part of the Neurocircuitry that Prevents Hypoglycemia. *Cell Metabolism*, 5(5), pp.383–393.

Trivedi, P. et al., 1998. Distribution of orexin receptor mRNA in the rat brain. *FEBS letters*, 438(1-2), pp.71–75.

Tschöp, M. et al., 2000. Ghrelin induces adiposity in rodents. *Nature*, 407(6806), pp.908–913.

Turner, P. V et al., 2011. Administration of substances to laboratory animals: routes of administration and factors to consider. *Journal of the American Association for Laboratory Animal Science*, 50(5), pp.600–613.

Tyler, S.J. et al., 2002. α- and β-secretase: Profound changes in Alzheimer's disease. *Biochemical and Biophysical Research Communications*, 299(3), pp.373–376.

Uysal, K.T. et al., 1997. Protection from obesity-induced insulin resistance in mice lacking TNF-alpha function. *Nature*, 389(6651), pp.610–614.

Vandanmagsar, B. et al., 2011. The NALP3/NLRP3 Inflammasome Instigates Obesity-Induced Autoinflammation and Insulin Resistance. *Nature Medicine*, 17(2), pp.179–188.

Vassar, R., 2014. BACE1 inhibitor drugs in clinical trials for Alzheimer's disease. *Alzheimer's Research & Therapy*, 6, pp.1–14.

Vassar, R. et al., 1999. Beta-secretase cleavage of Alzheimer's amyloid precursor protein by the transmembrane aspartic protease BACE. *Science*, 286, pp.735–741.

Vassar, R., 2004. BACE1: the beta-secretase enzyme in Alzheimer's disease. *Journal of Molecular Neuorscience*, 23, pp.105–113.

Vassar, R. et al., 2009a. The beta-Secretase Enzyme BACE in Health and Alzheimer's Disease: Regulation, Cell Biology, Function, and Therapeutic Potential. *Journal of Neuroscience*, 29(41), pp.12787–12794.

Vassar, R. et al., 2009b. The beta-secretase enzyme BACE in health and Alzheimer's disease: regulation, cell biology, function, and therapeutic potential. *The Journal of neuroscience*, 29(41), pp.12787–94.

Vassar, R., 2001. The beta-secretase, BACE: a prime drug target for Alzheimer's disease. *Journal of molecular neuroscience*, 17(2), pp.157–170.

Velliquette, R.A. et al., 2005. Energy inhibition elevates beta-secretase levels and activity and is potentially amyloidogenic in APP transgenic mice: possible early events in Alzheimer's disease pathogenesis. *The Journal of neuroscience*, 25(47), pp.10874–83.

Velliquette, R.A. et al., 2005. Energy inhibition elevates beta-secretase levels and activity and is potentially amyloidogenic in APP transgenic mice: possible early events in Alzheimer's disease pathogenesis. *Journal of Neuroscience*, 25(47), pp.10874–10883.

Vong, L. et al., 2011. Leptin Action on GABAergic Neurons Prevents Obesity and Reduces Inhibitory Tone to POMC Neurons. *Neuron*, 71(1), pp.142–154.

Wahle, T. et al., 2005. GGA proteins regulate retrograde transport of BACE1 from endosomes to the trans-Golgi network. *Molecular and Cellular Neuroscience*, 29(3), pp.453–461.

Van De Wall, E. et al., 2008. Collective and individual functions of leptin receptor modulated neurons controlling metabolism and ingestion. *Endocrinology*, 149(4), pp.1773–1785.

Walter, J. et al., 2001. Phosphorylation Regulates Intracellular Trafficking of β-Secretase. *Journal of Biological Chemistry*, 276(18), pp.14634–14641.

Wang, J. et al., 2005. Caloric restriction attenuates beta-amyloid neuropathology in a mouse model of Alzheimer's disease. *The FASEB journal*, 19(6), pp.659–661.

Wang, L. et al., 2014. Pten deletion in RIP-Cre neurons protects against type 2 diabetes by activating the anti-inflammatory reflex. *Nature Medicine*, 20(5), pp.484–492.

Wang, Z. et al., 2000. Leptin resistance of adipocytes in obesity: role of suppressors of cytokine signaling. *Biochemical and biophysical research communications*, 277(1), pp.20–6.

Weisberg, S.P. et al., 2003. Obesity is associated with macrophage accumulation in adipose tissue. *Journal of Clinical Investigation*, 112(12), pp.1796–1808.

Wen, Y. et al., 2004. Increased β-secretase activity and expression in rats following transient cerebral ischemia. *Brain Research*, 1009(1-2), pp.1–8.

Weskamp, G. et al., 1996. MDC9, a widely expressed cellular disintegrin containing cytoplasmic SH3 ligand domains. *Journal of Cell Biology*, 132(4), pp.717–726.

Weskamp, G. et al., 2002. Mice lacking the metalloprotease-disintegrin MDC9 (ADAM9) have no evident major abnormalities during development or adult life. *Molecular and cellular biology*, 22(5), pp.1537–1544.

White, C.L. et al., 2009. HF diets increase hypothalamic PTP1B and induce leptin resistance through both leptin-dependent and -independent mechanisms. *American journal of physiology, Endocrinology and Metabolism*, 296(2), pp.E291–E299.

Williams, G. et al., 2000. The hypothalamus and the regulation of energy homeostasis: lifting the lid on a black box. *The Proceedings of the Nutrition Society*, 59(3), pp.385–396.

Wilsey, J. & Scarpace, P.J., 2004. Caloric restriction reverses the deficits in leptin receptor protein and leptin signaling capacity associated with diet-induced obesity: Role of leptin in the regulation of hypothalamic long-form leptin receptor expression. *Journal of Endocrinology*, 181(2), pp.297–306.

Winzell, M.S. & Ahren, B., 2004. The High-Fat Diet–Fed Mouse A model for Studying Mechanisms and Treatment of Impaired Glucose Tolerance and Type 2 Diabetes. *Diabetes*, 53, pp.215–219.

Wittmann, G. et al., 2013. Distinct glutamatergic and GABAergic subsets of hypothalamic pro-opiomelanocortin neurons revealed by in situ hybridization in male rats and mice. *The Journal of comparative neurology*, 521(14), pp.3287–302.

Wolfe, M.S., 2008. Inhibition and modulation of gamma-secretase for Alzheimer's disease. *Neurotherapeutics : the journal of the American Society for Experimental NeuroTherapeutics*, 5(3), pp.391–398.

Wolfe, M.S. et al., 1999. Two transmembrane aspartates in presenilin-1 required for presenilin endoproteolysis and gamma-secretase activity. *Nature*, 398(6727), pp.513–517.

Wong, D., Sullivan, K. & Heap, G., 2012. The pharmaceutical market for obesity therapies. *Nature Reviews Drug Discovery*, 11(9), pp.669–670.

Wunderlich, F.T. et al., 2008. Hepatic NF-kappa B essential modulator deficiency prevents obesity-induced insulin resistance but synergizes with high-fat feeding in tumorigenesis. *Proceedings of the National Academy of Sciences of the United States of America*, 105(4), pp.1297–1302.

Yamanaka, A. et al., 2000. Orexin-induced food intake involves neuropeptide Y pathway. *Brain Research*, 859(2), pp.404–409.

Yan, R. et al., 1999. Membrane-anchored aspartyl protease with Alzheimer's disease beta-secretase activity. *Nature*, 2558(1982), pp.533–537.

Yan, R. & Vassar, R., 2014. Targeting the β secretase BACE1 for Alzheimer's disease therapy. *The Lancet. Neurology*, 13(3), pp.319–29.

Yang, L.-B. et al., 2003. Elevated beta-secretase expression and enzymatic activity detected in sporadic Alzheimer disease. *Nature medicine*, 9(1), pp.3–4.

Yang, Y. & Song, W., 2013. Molecular links between Alzheimer's disease and diabetes mellitus. *Neuroscience*, 250, pp.140–50..

Yaswen, L. et al., 1999. Obesity in the mouse model of pro-opiomelanocortin deficiency responds to peripheral melanocortin. *Nature medicine*, 5(9), pp.1066–1070.

Yip, S.C. et al., 2010. PTP1B: a double agent in metabolism and oncogensis. *Changes*, 35(8), pp.442–449.

Yu, G. et al., 2000. Nicastrin modulates presenilin-mediated notch/glp-1 signal transduction and betaAPP processing. *Nature*, 407(6800), pp.48–54.

Yulyaningsih, E. et al., 2011. NPY receptors as potential targets for anti-obesity drug development. *British Journal of Pharmacology*, 163(6), pp.1170–1202.

Zabolotny, J.M. et al., 2002. PTP1B regulates leptin signal transduction in vivo. *Developmental Cell*, 2(4), pp.489–495.

Zelissen, P.M.J. et al., 2005. Effect of three treatment schedules of recombinant methyionyl human leptin on body weight in obese adults: a randomized, placebo-controlled trial. *Diabetes, obesity & metabolism*, 7(2), pp.755–761.

Zeyda, M. & Stulnig, T.M., 2009a. Obesity, Inflammation, and Insulin Resistance - A Mini-Review. *Gerontology*, 55(4), pp.379–386.

Zeyda, M. & Stulnig, T.M., 2009b. Obesity, inflammation, and insulin resistance--a mini-review. *Gerontology*, 55(4), pp.379–86.

Zhang, X. et al., 2007. Hypoxia-inducible factor 1alpha (HIF-1alpha)-mediated hypoxia increases BACE1 expression and beta-amyloid generation. *The Journal of biological chemistry*, 282(15), pp.10873–10880.

Zhang, Y. et al., 1994. Positional cloning of the mouse obese gene and its human homologue. *Nature*, 372(6505), pp.425–432.

Zhang, Z. et al., 2000. Presenilins are required for gamma-secretase cleavage of beta-APP and transmembrane cleavage of Notch-1. *Nature cell biology*, 2(7), pp.463–465.

Zhao, J. et al., 2007. Beta-site amyloid precursor protein cleaving enzyme 1 levels become elevated in neurons around amyloid plaques: implications for Alzheimer's disease pathogenesis. *The Journal of neuroscience*, 27, pp.3639–3649.

Zhou, Y. & Rui, L., 2013. Leptin signaling and leptin resistance. *Frontiers of Medicine*, pp.1–16.